The SseK effector proteins of *Salmonella* Typhimurium target host cell signaling proteins

Joshua Patrick Mark Newson

Submitted in total fulfilment of the requirements of the degree of

Doctor of Philosophy

August 2019

Department of Microbiology and Immunology

The Peter Doherty Institute for Infection and Immunity

The University of Melbourne

Australia

ABSTRACT

Pathogenic serovars of *Salmonella* are the causative agents of a variety of disease states, including typhoid fever, self-limiting gastroenteritis, and invasive bacteremia. To achieve infection, *Salmonella* relies on two type-three secretion systems (T3SS) to deliver distinct cohorts of effector proteins into host cells. These effector proteins interact with specific human proteins to subvert normal cellular processes, thus impairing the ability of host cells to respond to the invading bacteria. To date, more than 40 different effector proteins have been identified, though many remain poorly characterised. This thesis focused on the SseK family of effector proteins, which had a largely unknown molecular mechanism and role in *Salmonella* infection. The aim of this thesis was to identify the host proteins that are targeted by the SseK effectors in order to determine how these effectors contribute to *Salmonella* virulence.

The SseK effectors show strong sequence similarity to NleB1, a unique T3SS effector of enteropathogenic *E. coli*, which functions as an arginine glycosyltransferase and catalyses the addition of *N*-acetylglucosamine (GlcNAc) to arginine residues of the mammalian signaling adaptors FADD and TRADD. Based on strong sequence homology to NleB1, we predicted that the SseK effectors would similarly catalyse arginine glycosylation. Here, we determined that SseK1 and SseK3, but not SseK2, also function as arginine glycosyltransferases. We showed that these effectors catalyse arginine glycosylation of different host proteins and appear to play different roles during infection.

We developed a mass spectrometry-based strategy to enrich for arginine glycosylated peptides from host cells infected with *Salmonella* Typhimurium (*S.* Typhimurium). Using this approach, we identified the preferred substrate of SseK1 as the signaling adaptor TRADD, which participates in a range of innate immune signaling pathways. We also showed that overexpression of SseK1 broadens the range of glycosylated substrates, and that

SseK1 was capable of glycosylating both mammalian and bacterial proteins under these conditions. Further, we identified the site of glycosylation within TRADD, and using a mutagenesis approach we showed that SseK1 is also capable of glycosylating secondary sites within TRADD. Collectively, these data show that the preferred substrate of SseK1 is TRADD, and highlight the importance of studying effectors in the natural context of infection.

Next, we applied our strategy for enriching arginine glycosylated peptide to identify the substrates of SseK3. We identified the host signaling receptors TNFR1 and TRAILR as the preferred substrates of SseK3 during *S.* Typhimurium infection, and conducted a range of experiments to validate the glycosylation of these receptors and identify the specific residues that are modified. We also conducted preliminary analyses to explore the contribution of these glycosylation events to virulence *in vivo*.

Together, the data presented in this thesis demonstrate that the *S.* Typhimurium effectors SseK1 and SseK3 function as arginine glycosyltransferases that target different innate immune signaling proteins during infection. We showed that SseK1 prefers the adaptor protein TRADD while SseK3 targets the signaling receptors TNFR1 and TRAILR. These observations provide new mechanisms by which *Salmonella* may manipulate innate immune signaling during infection.

DECLARATION

This is to certify that:

i. This thesis comprises only my original work towards the PhD except where indicated in the Preface,

ii. Due acknowledgement has been made in the text to all other material used,

iii. This thesis is less than 100 000 words in length, exclusive of tables, maps, bibliographies, and appendices.

Joshua P M Newson
Department of Microbiology and Immunology
The Peter Doherty Institute for Infection and Immunity
The University of Melbourne
Australia

PREFACE

In accordance with the regulations of the University of Melbourne, I acknowledge that some of the work presented in this thesis was collaborative. Specifically:

In Chapter 3, *sseK123* mutants were constructed by Nathaniel Brown, as indicated in Table 2.1.2. Various plasmids expressing effector proteins or host proteins were constructed Cristina Giogha and Tania Wong, as indicated in Table 2.2. Mass spectrometry experiments were performed with the assistance of Laura Dagley and Andrew Webb.

In Chapter 4, arginine glycosylation enrichment and mass spectrometry experiments were performed with the assistance of Nichollas Scott. Various plasmids expressing effector proteins or host proteins were constructed Cristina Giogha and Tania Wong, as indicated in Table 2.2. Analysis of glycosylation of TRADD mutants was performed with the assistance of Nichollas Scott. Caspase-8 and IL-8 assays were performed with the assistance of Jaclyn Pearson.

In Chapter 5, arginine glycosylation enrichment and mass spectrometry experiments were performed with the assistance of Nichollas Scott. Various plasmids expressing effector proteins or host proteins were constructed Cristina Giogha and Tania Wong, as indicated in Table 2.2. Mass spectrometry analysis of *in vitro* glycosylation assays was performed with the assistance of Nichollas Scott. Various bacterial mutants were constructed by Nathaniel Brown, as indicated in Table 2.1.2. Caspase-8 and IL-8 assays were performed with the assistance of Jaclyn Pearson. Animal studies were performed with the assistance of Jaclyn Pearson and Nancy Wang.

The remainder of this thesis comprises only my original work.

PUBLICATIONS ARISING FROM THIS THESIS

This thesis contains material that is published or is currently in preparation for publication:

Newson JPM, Scott NE, Yeuk Wah Chung I, Wong Fok Lung T, Giogha C, Gan J, Wang N, Strugnell R, Brown NF, Cygler M, Pearson JS, Hartland EL (2019). *Salmonella* effectors SseK1 and SseK3 target death domain proteins in the TNF and TRAIL signaling pathways. *Mol Cell Proteomics*, Jun;18(6):1138-1156. doi: 10.1074/mcp.RA118.001093. Epub 2019 Mar 22.

ACKNOWLEDGMENTS

First, my lasting thanks to my primary supervisor Liz Hartland, for giving me the opportunity to join the lab and work on a project that held so many challenges and opportunities. Thanks also for support with funding, without which this work would not have been possible, and for supporting my trips to conferences nationally and overseas. Thanks also for your patience and support as I explored opportunities outside of my PhD, and a deep thanks for your continued support beyond our time together.

A deep thanks to my co-supervisor Jaclyn Pearson, who invested so much of herself professionally and personally in my PhD. Thanks for setting the example of excellence, which I have also strived to meet.

I thank the members of my PhD committee for their input, guidance, and patience. Thanks to Dick Strugnell, Sammy Bedoui, Hayley Newton, and Nancy Wang for their support throughout, particularly in the early years where the intellectual input was both needed and given.

Thanks to everyone from the Hartland lab for their help and support across the years. In particular, I thank Cristina Giogha and Tania Wong for all their work on this project and related projects, which has made this work possible. I thank Nichollas Scott for his transformative input in the area of mass spectrometry, which enabled a depth and scope to this project that would not otherwise have been possible. Thanks to Laura Dagley and Andrew Webb for their contributions in the early years of this work.

Thanks also to the many faces of the Department of Microbiology and Immunology, which made a difficult few years much easier to handle. In particular, thanks to Rebecca Whitsed, Karena Waller, Helen Cain, Odilia Wijburg, Hayley Newton, and Roy Robins-Browne.

Thanks to my friends outside the Department who were immensely welcoming, and without whom I would not have seen the completion of this thesis. Thanks to my family, without whom I would not have come to this point at all.

TABLE OF CONTENTS

Chapter One

Literature review

CHAPTER 1: Literature review

1.1 Introduction

Salmonella species are Gram-negative, facultative anaerobic, peritrichously flagellated bacilli of the family Enterobacteriaceae. Ancestrally, *Salmonella* is speculated to have diverged from the closely related *Escherichia coli* over 100 million years ago (1, 2). Contemporary phylogeny classifies the genus *Salmonella* into two distinct species. *Salmonella bongori* is typically associated with cold-blooded animals, and is rarely reported to cause disease in humans and other mammals (3). *Salmonella enterica* is the principal causative agent of salmonellosis, and is divided into six subspecies: *enterica* (I), *salamae* (II), *arizonae* (IIIa), *diarizonae* (IIIb), *houtenae* (IV), and *indica* (VI). *S. enterica* is further divided into more than 2500 serovars following the Kauffman-White scheme, which classifies *Salmonella* by variation in the somatic and flagellar surface antigens (4). Advances in whole genome sequencing of bacterial species has enabled the construction of more accurate phylogenies, and these approaches may replace serological-based phylogenies in future (5, 6).

Between serovars of *S. enterica*, there is considerable variation in host specificity, biochemical characteristics, virulence factors, and disease presentation in the host (7). Many serovars retain a broad host range and are proficient at colonisation and dissemination through multiple species, while some serovars exhibit host specificity and have undergone genomic reduction to better colonise a single host species (Figure 1.1) (8, 9). The diversity of *S. enterica* is reflected in the various disease states that arise in the infected host, and demonstrate the versatility of *Salmonella* in adapting to a broad range of evolutionary niches.

1.2 *Salmonella enterica*: disease, epidemiology, and treatment

Given the overwhelming variation in *Salmonellae* based on serological characteristics and genetic variation, the various *Salmonellae* are perhaps best considered by the disease they induce in the host. Throughout evolution, *S. enterica* has adapted to cause disease in a range of host species, and based on genetic factors of both the pathogen and the host will typically present with one of three disease states in humans, as described below.

1.2.1 *Salmonella* Typhi and enteric fever

Salmonella Typhi is a human-adapted serovar of *Salmonella enterica* that is transmitted through the fecal-oral route in contaminated food and water. Prior to the advent of classical microbiological techniques and the acceptance of the germ theory of disease, typhoid fever was conflated with other diseases characterised by acute fever and non-bloody diarrhoea, including typhus and tuberculosis. Typhoid fever became clearly defined after; (*i*) contaminated water sources were linked to transmission of the disease (10), (*ii*) the infectious microorganism was observed in the spleens of infected patients (11), and (*iii*) the microorganism was subsequently isolated and grown in pure culture (12).

Typhoid fever is characterised by a sustained high fever, with other symptoms ranging from abdominal pain, diarrhoea or constipation, characteristic rose spots on the chest and abdomen, and in severe cases a range of neuropsychological symptoms (13, 14). The closely related serovars *S.* Paratyphi A, B, and C cause similar symptoms in the infected host. These typhoidal serovars represent a serious burden of disease in the developing world, with an estimated 20 to 26 million infections occurring each year, resulting in approximately 200,000 to 600,000 deaths (15, 16). The true burden of disease is likely underreported (17), and obfuscated by infectious microorganisms that induce similar pathology in the host.

Humans represent the exclusive reservoir of the typhoidal serovars, and these bacteria have undergone significant genome degradation during host adaptation. Large numbers of genes that are functional in the related non-typhoidal *Salmonellae* are pseudogenes in *S.* Typhi (18, 19). These genes normally contribute to fimbrial adhesion, effector protein translocation, and bacterial motility (20), and so it is likely that pseudogenisation of these factors contributes to the unique pathology of the typhoidal serovars. Similarly, other host-adapted *Salmonellae* have undergone genome degradation, including the avian-adapted *S.* Gallinarum and *S.* Pullorum (21).

Typhoidal serovars infect the small intestine transiently and do not induce a strong inflammatory response during intestinal invasion (22), in contrast to non-typhoidal serovars. Upon gaining access to lymphoid tissue the bacteria replicate within mononuclear phagocytes. These cells provide a vector for the bacteria to spread systemically through mesenteric lymph nodes, resulting in colonisation of the liver, spleen, and gallbladder (9, 23, 24). Prolonged asymptomatic carriage can occur following convalescence, and biofilm formation on the gallbladder has been implicated as a mechanism by which infectious *S.* Typhi can continue to be shed for years after initial infection (25), contributing to the dissemination of the bacteria to new hosts.

S. Typhi possesses a number of virulence factors that are absent from the non-typhoidal serovars, and it is likely that these factors contribute to the unique virulence program of *S.* Typhi. The virulence (Vi) polysaccharide capsule is produced by *S.* Typhi (26), and functions in part to prevent recognition of surface components by host pathogen receptors and thus impede complement activation (27). Further, Vi capsule expression appears to interfere with neutrophil chemotaxis (28), providing a mechanism for bacterial immune evasion. More recently, a functional cytolethal distending toxin component was discovered in the genome of *S.* Typhi, and subsequently shown to be expressed following

internalisation of the bacteria into host cells (29, 30). Later studies demonstrated the complete holotoxin is comprised of three subunits that contribute to cell cycle arrest and cellular distension (31). Strikingly, direct administration of recombinant toxin can reproduce many symptoms of typhoid fever *in vivo* (31) and so the function of the typhoid toxin likely plays a key role in the progression of disease. Indeed, human patients in convalescence show high levels of toxin-specific antibodies in sera (32). A more complete understanding of how these unique virulence factors contribute to the intracellular activities of *S.* Typhi precedes the design of novel anti-virulence therapeutics and other treatment options.

Given the degree to which *S.* Typhi has become restricted to human hosts, vaccination represents a viable strategy for eliminating typhoid fever. A number of vaccines are available with various reported efficacy, while a range of newer vaccines are under development (19, 33). Ty21a is an orally-administered live attenuated vaccine, with an estimated average efficacy of 51% (34), while a parenterally-administered Vi polysaccharide vaccine is also available, with better indications ranging from 60% to 72% (33). A third vaccine currently under development utilises Vi polysaccharide conjugated to recombinant *Pseudomonas aeruginosa* exotoxin A, and this vaccine has shown considerable improvement in human trials (35). There are as yet no licenced vaccines against *S.* Paratyphi A, and little cross-protection is afforded by the current *S.* Typhi vaccines (9, 17)

Collectively, effective vaccination programs, the development of rapid diagnostics, and improved access to clean food and water in developing countries should enable great reductions in the incidence of typhoidal infections and potentially the elimination of endemic *S.* Typhi.

1.2.2 Non-typhoidal *Salmonella* serovars and gastroenteritis

In contrast to the host-adapted *Salmonella*, most serovars of *S. enterica* demonstrate a broad host-range, and are capable of colonising several host species. Collectively referred to as the non-typhoidal *Salmonella* (NTS), these bacteria represent a greater burden of disease globally relative to the typhoidal serovars, and cause a significant medical and economic impact across both the developing and developed world. NTS strains are estimated to cause approximately 90 million cases of human gastroenteritis annually, resulting in an estimated 150,000 deaths (36), though again these numbers are likely conflated with other diarrhoeal pathogens, including *Campylobacter* spp. and enteropathogenic *E. coli* (EPEC).

The original discovery of a non-typhoidal *Salmonella* occurred shortly after Gaffky isolated *S.* Typhi from a human patient (12). Salmon and Smith successfully isolated a bacillus from infected pigs suffering from hog cholera (37). Originally named *Bacillus choleraesuis*, the bacterium was later renamed in honour of Salmon as *Salmonella choleraesuis*, and the nomenclature of this genus has evolved over time through advances in serology and sequencing technology (38). Today, serovars *S.* Typhimurium and *S.* Enteritidis are recognised as the leading cause of human salmonellosis globally (39-42). These serovars typically colonise the gastrointestinal tract of a range of livestock animals, and shedding of the bacteria onto animal products or food crops causes frequent food-borne outbreaks in human populations (43). Controlling the dissemination of *Salmonella* in an agricultural setting is therefore a possible means of reducing the burden of human salmonellosis. *S.* Typhimurium is most often the model organism for studying *Salmonella* pathogenesis experimentally, particularly the derivative strains SL1344 and ATCC14028.

Infection by *S.* Typhimurium and other generalist serovars follows ingestion of live bacteria, which survive the acidity of the stomach and colonise the intestinal tract. The incubation period ranges from 6 to 72 hours, and typical symptoms include diarrhoea, fever,

nausea and abdominal pain (44). The infection is self-limiting and treatment therefore focuses on rehydration and bed rest. In some cases, infection can lead to chronic sequelae including irritable bowel syndrome, and a small percentage of convalescent patients become asymptomatic chronic carriers of *S. enterica* (45). In immunocompromised patients, these normally gut-restricted serovars are able to spread through circulating immune cells and achieve colonisation of systemic organs or induce bacteraemia (46, 47). These cases warrant antibiotic treatment, but for self-limiting gut infections there is no indication that antibiotic treatment effectively reduces the duration of disease (48), and there is some evidence that use of antibiotics prolongs the carriage of NTS (49).

Infection of the small intestine by NTS strains is characterised by a strong inflammatory response (50), and a large body of evidence has emerged to suggest that *Salmonella* deliberately induces a potent inflammatory response in order to disrupt resident microbiota and promote colonisation of *Salmonella* (51, 52). Further, *Salmonella* expresses an iron-scavenging siderophore (53) and a high-affinity zinc transporter (54) to overcome metal starvation responses induced by gut epithelial cells, and this confers a nutritional advantage over commensal gut bacteria. Similarly, *Salmonella* infection results in the induction of reactive oxygen and nitrogen species, altering the environment of the gut into an oxidative environment that is restrictive for resident anaerobic species, while also providing additional carbon sources for metabolism by *Salmonella* (55). These mechanisms demonstrate an elegant manipulation of the host immune response that enables *Salmonella* to proliferate within a highly competitive environment.

To achieve colonisation of the intestinal tract, *Salmonella* initially attaches to the apical surface of enterocytes lining the intestinal epithelium. Invasion into these non-phagocytic cells is mediated in part by the Rck and PagN invasins (56, 57), but is primarily achieved by induction of membrane ruffling to achieve bacterial uptake (50, 58, 59). This

bacterial-mediated endocytosis is largely mediated by the activity of effector proteins delivered through a type-three secretion system, described in detail below. *Salmonella* can also be taken up by microfold (M) cells which sample antigens present in the intestinal lumen, and be subsequently trafficked to lymphoid cells in Peyer's patches (60). A third means of ingress is uptake by dendritic cells, which extend protrusions through the epithelial monolayer to similarly sample the luminal contents (61). Egress from infected cells allows *Salmonella* to access the basolateral layer, where the bacteria can subsequently infect neighbouring epithelial cells, escape back to the lumen following disruption of tight junctions, or egress into the lamina propria to be taken up by a variety of phagocytic cells including macrophages, dendritic cells and polymorphonuclear cells (23, 50, 62, 63). Much of the interplay between *Salmonella* and the immune response is driven by potent inflammatory signaling that starts with cytokine release from infected epithelial cells, and leads to activation and recruitment of macrophages and a characteristic influx of neutrophils into the lumen of the intestine. Collectively, the disruption of epithelial integrity, potent inflammatory signaling, and influx of neutrophils is thought to largely contribute to the diarrhoeal symptoms characteristic of NTS infection (50, 64).

Many of these host cells represent intracellular niches that *Salmonella* actively remodel to promote bacterial replication. The intracellular activities of *Salmonella* were first suggested by Takeuchi and colleagues, who observed the bacteria become enveloped within a membrane following association with intestinal epithelial cells *in vivo* (65, 66), and later studies further characterised this vacuole as an intracellular niche for *Salmonella* (67-69). This *Salmonella*-containing vacuole (SCV) was subsequently associated with filament structures extending off the vacuole (70), and more recent research suggests this intracellular niche becomes a network of host membrane-derived tubules that extend throughout the cytoplasm of the infected host cell (71). Despite being classically understood as a vacuolar

pathogen, more recent research has characterised a population of *Salmonella* that escape the nascent SCV and hyper-replicate within the cytosol of the cell (72). Several studies have explored a process by which damaged SCVs cause release of *Salmonella* into the cytosol, which are then targeted by host autophagy machinery, though the consequences of these events are yet to be fully described (73-75). Advances in live-cell imaging and high-resolution microscopy will likely contribute to a greater understanding of the vacuolar and cytosolic activities of intracellular *Salmonella*.

There are currently no licenced vaccines against non-typhoidal *Salmonella* in humans, in part due to the broad antigenic variation between serovars. Given the primary reservoir of these serovars is food animals, vaccination of farm animals represents a viable strategy to reduce animal carriage of NTS and subsequent transmission to humans. A promising vaccine candidate currently under development relies on immunity generated against enriched *Salmonella* virulence factors (76). Other methods for controlling the animal reservoirs of NTS include irradiation of food products, antibiotic treatment, and selective culling of seropositive animals, though these approaches are not without disadvantages (48, 77).

While research into human and animal vaccines continues, the development of novel therapeutic approaches is better enabled by a deeper understanding of the interaction between *Salmonella* and the host. Research elucidating the mechanisms that enable *Salmonella* to manipulate immune signaling and therefore outcompete microbiota and establish infection may lead to new therapeutic approaches, while the intracellular activities of *Salmonella* may represent possible targets for antivirulence compounds.

1.2.3 Invasive non-typhoidal *Salmonella* and bacteremia

As described above, human infections of non-typhoidal *Salmonella* most commonly present as a self-limiting gastrointestinal infection, but can result in bloodstream infections in

patients who are immunocompromised (78). In contrast, these same serovars are primarily associated with bloodstream infections in populations across sub-Saharan Africa (79, 80). These infections are characterised by a febrile systemic illness, but diarrhoea is not commonly reported (81, 82), and so infections caused by these invasive non-typhoidal *Salmonella* (iNTS) are distinct from the classical presentation of gastroenteritis.

Infections caused by iNTS are now estimated to cause a greater burden of disease than that of the typhoidal serovars. Recent estimates place the number of iNTS infections at more than 3 million per year, with deaths caused by iNTS as high as 600 000 (80). The majority of these cases are reported across sub-Saharan Africa. (41, 80). Thus, iNTS is emerging as a greater public health issue than typhoid fever.

Primary risk factors for iNTS in African populations are malnutrition, sickle cell anaemia, malaria, and HIV infection. Indeed, an estimated 95% of adults presenting with iNTS in sub-Saharan Africa are also seropositive for HIV (81, 83). Several factors have been proposed to contribute to the deficiency of HIV-positive individuals to control *Salmonella* infection and thus present with invasive bacteremia. Depletion of epithelial-associated Th17 cells, dysregulated cytokine production during intracellular infection, and deficiencies in humoral immunity may collectively skew *Salmonella* infection from gastroenteritis to bacteremia (79, 84-86).

Serovars *S.* Typhimurium and *S.* Enteritidis are the serovars most frequently isolated from iNTS patients in sub-Saharan Africa, but smaller outbreaks of other serovars have been reported (41). Whole genome sequencing studies have revealed the majority of iNTS infections in sub-Saharan Africa are caused by a dominant regional sequence type of *S.* Typhimurium, termed ST313 (87, 88). Notably, ST313 possesses a partially degraded genome, similar to that observed in *S.* Typhi, prompting speculation that ST313 has undergone a similar process of host adaptation (87). The transmission of ST313 throughout

sub-Saharan Africa remains poorly defined, though the isolation of the bacterium from healthy persons suggests asymptomatic carriage contributes to the spread of disease (41, 86). Intriguingly, a recent report has demonstrated that ST313 is endemic to the United Kingdom but primarily causes gastroenteritis (89), suggesting the distribution of ST313 is wider than previously understood and that the confluence of disease and malnutrition in sub-Saharan Africa results in different outcomes during ST313 infection.

Ultimately, the emerging scope of iNTS infections globally represents both a unique insight into the ongoing evolution of a highly adaptive pathogen and a profound challenge for prevention and control of disease.

1.3 Genomic basis of *Salmonella* pathogenesis

All pathogenic serovars of *Salmonella* harbour virulence factors encoded on distinct pathogenicity islands distributed across the *Salmonella* genome. Termed *Salmonella* pathogenicity islands (SPI), these regions are hypothesised to have been acquired through horizontal gene transfer from other bacteria, based on the lower GC content relative to the rest of the bacterial chromosome (90). A subset of SPIs are conserved between serovars and are critical for pathogenesis, while others are less well distributed and appear to contribute to success in particular niches (91).

SPI-1 was first identified following observations that several genes involved in invasiveness were clustered on the *Salmonella* genome, and that this region was absent from the non-invasive *E. coli* K12 (92). Most genes in SPI-1 encode for the components of a type three secretion system (T3SS), as well as the cognate effector proteins and associated regulatory factors (93). The effector proteins translocated by the SPI-1 T3SS mediate entry into non-phagocytic cells through interactions with the actin cytoskeleton, and separately contribute to manipulation of inflammatory signaling (64, 94, 95), as described in detail

below. SPI-1 is highly conserved across *Salmonella* genomes, and is present in both *S. bongori* and *S. enterica* (96), which gives rise to the hypothesis that SPI-1 was acquired when *Salmonella* and *E. coli* diverged from a common ancestor (8, 97). SPI-1 mutants are attenuated for virulence when delivered orally in animal models but not when administered systemically (98), suggesting the primary function of SPI-1 is to enable colonization of the gut, presumably through conferring invasiveness.

SPI-2 was discovered after a signature-tagged mutagenesis screen revealed the importance of a number of undescribed genes for virulence in a mouse model of systemic infection (99). A number of these genes were observed to be homologous to genes encoding for components for the SPI-1 T3SS, and were found clustered together in a genomic island that is absent from the non-pathogenic *E. coli* K12 (100). Concurrently, another study also identified several genes based on homology to genes encoding T3SS components from other bacterial pathogens, and demonstrated that these were required for virulence in a mouse model of systemic infection (101). Further work described SPI-2 as two distinct genomic elements (102): a smaller region encoding for genes involved in tetrathionate respiration (103) and a larger region encoding for the structural components of a second T3SS along with associated regulators, chaperones, and effector proteins (104). Effector proteins translocated by the SPI-2 T3SS are thought to contribute collectively to the intracellular survival of *Salmonella* via a range of mechanisms, including subversion of host cell trafficking, stabilisation of the SCV, remodeling of the actin cytoskeleton, and manipulation of both innate and adaptive immune signaling (64, 105, 106). The functions of SPI-2 effectors and their contribution to *Salmonella* virulence are described more fully below. The region of SPI-2 encoding the T3SS is absent from *S. bongori* but well conserved across pathogenic *S. enterica*, (96, 107), providing a genomic basis for the difference in virulence potential between these species. While SPI-1 mutants are attenuated only when delivered

orally in murine models, SPI-2 mutants are deficient in both oral and systemic models of infection (99, 101), and so the ancestral acquisition of SPI-2 likely enabled *S. enterica* to cause systemic infections rather than remaining strictly localised to the gastrointestinal tract (8).

Later studies have described a number of other *Salmonella* pathogenicity islands distributed sporadically across pathogenic serovars (20, 90, 91). SPI-3 is a mosaic region comprised of a range of seemingly unrelated genes, including two genes encoding for a magnesium uptake system required to mitigate nutritional scarcity in the SCV, and other genes homologous to virulence factors from *Vibrio* spp. and enteropathogenic *E. coli* (108). SPI-4 encodes for a type I secretion system that translocates a non-fimbrial giant adhesin SiiE, which mediates initial contact between *Salmonella* and the host cell prior to invasion (109, 110). SPI-5 is a small pathogenicity island that encodes for the effector proteins SopB and PipB (111), while SPI-6 encodes for a type six secretion system (T6SS) that translocates toxins into neighbouring bacteria (112), enabling *Salmonella* to outcompete microbiota and efficiently colonise the gut (113). SPI-7 in *S.* Typhi encodes for the Vi antigen capsule polysaccharide which plays a critical role in the pathogenesis of typhoid fever (26-28). Many other *Salmonella* pathogenicity islands have been identified, though the function of their constituent genes and the contribution to virulence are still being elucidated (20). Ultimately, the acquisition of virulence factors across the evolutionary history of *Salmonella* has shaped the pathogenic potential of the various serovars as they have adapted to better suit different hosts and ecological niches.

1.4 Type III secretion systems of *Salmonella*

Type III secretion systems are macromolecular protein complexes that function to translocate effector proteins from the bacterial cytoplasm into host cells (114). A significant

body of research has emerged to demonstrate that a range of bacterial pathogens deploy a T3SS to influence host cells during infection, including *Salmonella, Yersinia, Pseudomonas,* and *Shigella* (114-116). Ancestrally, the T3SS is speculated to be derived from the flagellar secretion apparatus and recent evidence supporting this evolutionary process suggests the developing T3SS initially lost the capacity for motility but remained able to secrete bacterial proteins, while a later evolutionary event conferred the ability to actively inject bacterial proteins into target eukaryotic cells (115, 117). The acquisition of a translocation-competent T3SS endows a pathogenic bacterium with an exquisite level of influence over infected cells, and the virulence of many Gram-negative pathogens relies heavily on the activity of the T3SS (116, 118).

Structurally, the components of the T3SS are highly conserved across bacterial species, but the complement of effector proteins varies considerably between species (114, 116) and even within species (105), presumably to better suit the ecological niches available to a given species. As described above, pathogenic serovars of *Salmonella* typically carry the genomic elements SPI-1 and SPI-2, each encoding for a functionally distinct T3SS and an associated suite of regulators and effector proteins (93, 119). While encoded on different pathogenicity islands and comprised of distinct protein components, both T3SSs are structurally similar to each other and to T3SSs from other Gram-negative pathogens (116). The T3SS is comprised of a base structure that spans the bacterial envelope and a needle structure that extends off the bacterial surface, with an inner rod structure linking the needle to the base and a narrow channel traversing the entire complex that permits the translocation of substrate effector proteins (114, 116, 118, 120) (Figure 1.2A, B). The base structure is comprised of two rings associated with the inner membrane and two rings associated with the outer membrane, and these sets of rings are joined by a neck region (121). The proximal end of the needle complex is connected to an export apparatus that permits substrates through the

inner membrane and into the needle complex (122). This export apparatus is further associated with the cytoplasmic sorting platform, a large protein complex that interacts with substrate effectors and their cognate chaperones (123, 124) (Figure 1.2C). The distal end of the needle is capped with a tip complex (125), which enables secreted translocases to insert into the target cell membrane, and though the precise mechanism of translocase insertion remains to be defined (114, 116), this interaction ultimately completes the conduit from bacterial to host cell cytoplasm and enable effector translocation.

Salmonella is one of the few described Gram-negative pathogens that encodes for two T3SSs, and these secretion systems are functionally distinct and play different roles during infection. Transcriptional and environmental cues enable the appropriate temporal and spatial expression of the SPI-1 and SPI-2 T3SS. *Salmonella* expresses the SPI-1 T3SS while still in the gut lumen, and upon contact with host cells rapidly translocates an initial pool of effector proteins to mediate entry into the cell (126). In contrast, the SPI-2 T3SS is expressed during the intracellular stage of infection after the nascent SCV undergoes maturation, and translocates effectors across the SCV membrane into the host cell cytoplasm (127). The contributions of the T3SS are best understood in the context of effector protein function, and are described more fully below.

Many questions remain concerning the activity of the T3SS, including the mechanisms by which bacteria sense target cells and engage secretion machinery, the dynamics of the sorting platform as it organises and prioritises effector cargo, and the means by which energy is supplied to the T3SS (114, 116). Elucidating these details will not only deepen the understanding of host-pathogen interactions, but also enable the development of novel therapeutics and anti-virulence agents potentially effective against a range of Gram-negative pathogens.

1.5 Regulation of type III effector translocation

Salmonella relies on a complex network of regulatory factors to ensure the appropriate spatiotemporal expression of virulence factors during infection. Sensing of the extracellular environment and sequential induction of the SPI-1 and SPI-2 encoded T3SS ensures the invading bacterium efficiently translocates specific suites of effector proteins hierarchically to establish and maintain an intracellular niche, and to maximise transmission to new hosts.

Many virulence factors of *Salmonella* were acquired from other bacterial species through horizontal gene transfer (128). Horizontally acquired genes are subject to repression by the DNA-binding protein H-NS, which binds preferentially to AT-rich sequences of acquired genes and prevents interactions with RNA polymerase and so mitigates the deleterious effects of newly acquired genes (129-131). In *Salmonella*, H-NS binds to a large number of virulence genes including *hilA*, *hilD*, h*ilC*, and *rtsA*, which are transcription factors responsible for expression of the SPI-1 T3SS (132, 133). HilA is the master regulator of the structural components of the SPI-1 T3SS (134, 135) but also controls expression of InvF, another transcription factor that is required for expression of SPI-1 T3SS effectors and chaperones (136). HilA itself is regulated by HilD, HilC, and RtSA, which can also regulate expression of one another and of themselves, and thus SPI-1 gene expression is the product of a circuit of genes driven by positive feedback loops (137, 138).

Additionally, H-NS binds to genes encoding for components of the SPI-2 T3SS including *ssaB* and *ssaG* (139). Counter-silencing of H-NS and expression of the SPI-2 T3SS is, in part, dependent on the activity of a variety of two-component regulatory systems. These systems typically comprise a membrane-associated histidine kinase which senses a specific environmental factor, and a cytoplasmic response regulator that mediates transcription of target genes (140). In this manner, bacteria can sense their environment and adapt their

transcription profile in response, and many Gram-negative pathogens have incorporated an array of two-component systems to respond to diverse environmental cues (141).

In *Salmonella,* the PhoP-PhoQ two-component system senses a range of environmental stimuli including acidity, low Mg^{2+}, and cationic antimicrobial peptides (142-144). Therefore the PhoP-PhoQ system represents a means by which *Salmonella* can detect cues in the stomach and small intestine but also within the SCV during the intracellular stage of infection (128, 145). Detection of these stimuli prompts broad changes in gene expression, including the upregulation of several other two-component systems such as PmrA-PmrB and SsrA-SsrB (146, 147). The PmrA-PmrB system reportedly detects Fe^{3+} and Mg^{2+}, as well as mildly acidic conditions, and in response promotes a gene expression profile that modifies various components of lipolysaccharide in the bacterial cell wall, which may contribute to evasion of antimicrobial agents (148). Separately, the EnvZ-OmpR two-component system detects extracellular and intravacuolar osmolarity, and in response also upregulates the SsrA-SsrB two-component system (149, 150). Thus, the SsrA-SsrB system is regulated by both the PhoP-PhoQ and EnvZ-OmpR two-component systems.

The SsrA-SsrB system ultimately controls expression of the SPI-2 T3SS, and is therefore essential for intracellular survival of *Salmonella* (151). SsrB binds to the promoter regions of genes in the SPI-2 regulon, including components of the SPI-2 T3SS and its substrate effectors encoded both within the SPI-2 genomic island and elsewhere on the genome (151). SsrB can also function as an anti-silencer of H-NS, similarly enabling expression of silenced SPI-2 regulon genes (139). Further, the SPI-1 transcription factor HilD also upregulates SPI-2 gene expression (152), while SsrB in turn represses both HilD and HilA to downregulate SPI-1 expression (153), and so intravacuolar *Salmonella* appear to cease expression of the SPI-1 T3SS and rely on the SPI-2 T3SS to replicate intracellularly.

Thus, the expression of the SPI-1 and SPI-2 T3SS and the substrate effector proteins are subject to an incredibly sophisticated program of genetic regulation based on environmental cues, and this enables *Salmonella* to engage in the metabolically expensive activity of effector translocation only in the appropriate spatiotemporal context.

1.6 Type III effectors and *Salmonella* pathogenesis

Both the SPI-1 and SPI-2 T3SS have an associated suite of effector proteins that are translocated into the host cell. Typically, particular effectors are translocated exclusively through one of the two T3SSs, but there is evidence for some effectors suggesting they are secreted by both T3SSs (154, 155). To date, more than 40 effectors have been identified in the pangenome of sequenced *S. enterica* serovars, and while some have defined roles in pathogenesis, many remain poorly characterised (64, 105, 156). A summary of known effectors along with their biochemical activity and contributions to virulence is presented in Table 1.1, while each effector is described in the context of *Salmonella* pathogenesis below.

1.6.1 SPI-1 T3SS translocated effectors

The effectors translocated by the SPI-1 T3SS are relatively well understood, and collectively enable *Salmonella* to invade non-phagocytic cells, stimulate a potent localised immune response in the intestinal lumen, and initiate the biogenesis of the SCV (50, 156). Some of these effectors play multiple roles in the early stages of infection, and distinct domains within these effectors are responsible for different functions. At least ten effectors are translocated exclusively through the SPI-1 T3SS, while another four are reportedly substrates of both the SPI-1 and SPI-2 T3SS (64).

1.6.1.1 Host cell invasion and cytoskeletal remodeling

Translocation of the first cohort of effector proteins follows insertion of the translocases SipB and SipC into the host cell membrane, a process that is poorly understood but likely results in pore formation and completion of the protein channel that spans the T3SS (157, 158). SipD is also secreted by the T3SS during initial contact, and acts in cooperation with SipB and SipC to establish the translocase complex. Deletion of *sipB, sipC* or *sipD* causes deficiency in intimate attachment of *Salmonella* to host cells and similarly a deficiency in effector translocation (125, 159). Additionally, SipC induces nucleation of actin and bundles actin filaments leading to cytoskeletal arrangements at the site of invasion, and so plays a dual role in the early stage of infection (160). The actin manipulation of SipC is potentiated by SipA, an effector that binds directly to actin and inhibits depolymerisation of actin filaments at the site of *Salmonella* invasion (161, 162).

While SipA and SipC bind actin directly, a subset of SPI-1 effectors act indirectly to manipulate the actin cytoskeleton and achieve membrane ruffling and subsequent uptake of *Salmonella*. SopB is a phosphoinositide phosphatase that activates SH3-containing guanine nucleotide exchange factor (SGEF), which in turn activates RhoG and thus drives Rho family GTPase-mediated actin rearrangement (163), while SopD acts cooperatively with SopB by promoting membrane fission and macropinosome formation (164). Similarly, SopE and SopE2 mimic guanine nucleotide exchange factors (GEFs) to activate the Rho GTPases Cdc42 and Rac-1 (165, 166). This leads to stimulation of N-WASP and WAVE2 and subsequent recruitment of the Arp2/3 complex, which results in the cytoskeletal rearrangements that produce membrane ruffling and formation of invaginations that engulf the bacterium (167, 168). Mutants deficient in *sopB, sopE*, and *sopE2* are unable to induce membrane ruffling and cannot invade effectively (169).

Strikingly, *Salmonella* deploys another SPI-1 effector to assist in restoration of normal actin architecture following invasion. SptP possesses a GTPase activation (GAP) domain which deactivates Cdc42 and Rac-1, promoting reversal of the cytoskeletal changes induced by SopE and SopE2 (170). Further, SopE is rapidly degraded following translocation while SptP has a longer half-life in the host cell (171), thus providing a mechanism for *Salmonella* to achieve temporally appropriate restoration of the host cell following invasion.

1.6.1.2 Manipulation of inflammatory signaling

Several of the SPI-1 effectors involved in host cell invasion also stimulate innate immune signaling, either as a consequence of activating pathways necessary for invasion or by directly acting on host signaling proteins. Activation of Cdc42 and Rac-1 by SopE, SopE2, and SopB triggers induction of mitogen-activated protein kinase (MAPK) pathways, including the JNK, p38, and ERK pathways (172). This subsequently induces activation of the transcription factors NF-κB and AP-1, which ultimately leads to production of pro-inflammatory cytokines including interleukin-8 (IL-8) (163). IL-8 functions as a potent chemoattractant for neutrophils which migrate into the lumen of the small intestine and contribute to the inflammatory causes of diarrhoea (173, 174). SopE, SopE2, SopB, and SipA also contribute to disruption of epithelial tight junctions, further enabling transmigration of neutrophils into the lumen (175). SipA also functions to promote neutrophil transmigration by a signal transduction cascade that activates protein kinase Cα (176, 177) leading to the secretion of the chemoattractant hepoxillin A3 (178). Similarly, SopA is an E3 ubiquitin ligase that mimics the host HECT E3 ligase to induce neutrophil transmigration (179). Separately, SipB directly binds and activates caspase 1 and induces the secretion of the pro-inflammatory cytokine IL-1β (180), while SopB promotes the secretion of cellular chloride ions, which further contributes to diarrhoea (181). SspH1 is an effector translocated by both

the SPI-1 and SPI-2 T3SS, and functions as an E3 ubiquitin ligase to inhibit NF-κB activation and subsequent IL-8 secretion (155, 182, 183). Collectively, these effectors drive a strong localised innate immune response that contributes to the ability of *Salmonella* to outcompete resident commensal bacteria and produce the symptoms of diarrhoea, thereby driving both colonisation and transmission.

Conversely, several SPI-1 effectors function to inhibit inflammatory signaling through enzymatic modification of host immune proteins. SptP inhibits the activation of MAPK pathway through an N-terminal domain with GAP activity and a C-terminal domain with tyrosine phosphatase activity (184, 185). SpvC is a SPI-1 effector with phosphothreonine lyase activity that inhibits the JNK, ERK, and p38 MAP kinases (186, 187). AvrA is an acetyltransferase that targets MAPK kinases to inhibit JNK and NF-κB signaling (188), and also functions to stabilise tight junctions and alleviate inflammation (189, 190). Thus, manipulation of host innate immunity is not limited to stimulation of signaling pathways, and *Salmonella* likely deploys SPI-1 effectors in a hierarchical or temporal manner to achieve the appropriate program of immune signaling.

1.6.1.3 SCV biogenesis

Several SPI-1 effectors contribute to the early stages of SCV formation and maturation. Immediately following engulfment into the host cell, the bacterium resides in a spacious phagosome that transiently acquires early endosomal markers including Rab5 and Rab11, transferrin receptor, and early endosomal antigen 1 (EEA1) (191, 192). Both SopB and SopE are involved in recruitment of Rab5 to the nascent SCV, which subsequently binds Vps34 to generate PI(3)P and recruits EEA1 (193-195). SopB further promotes recruitment of sorting nexin-1 (SNX-1) and therefore contributes to diversion of SCV trafficking from the endosomal pathway (196). SipA is also recruited to the cytoplasmic face of the SCV, where it

acts to promote relocation of the SCV to the perinuclear region in cooperation with SifA, an effector of the SPI-2 T3SS (197). GtgE proteolytically cleaves Rab29, Rab32, and Rab38, and this activity appears to be important for intracellular replication within the SCV (198, 199). Further maturation and trafficking of the SCV is mediated by the effector cohort of the SPI-2 T3SS, as described below.

1.6.2 SPI-2 T3SS translocated effectors

The functions of the SPI-2 T3SS effectors are less well understood than those of the SPI-1 effectors, but collectively SPI-2 effectors broadly enable the intracellular replication of *Salmonella* through manipulation of host trafficking pathways, autophagy, inflammatory signaling and cell death, while also mediating maturation and expansion of the SCV (50, 64, 105, 106, 156). Generally, SPI-2 effectors are less well conserved across serovars (105), perhaps suggesting distinct roles in certain host species. At least 25 effectors have been identified as substrates of the SPI-2 T3SS (Table 1.1), though most of these are located outside the SPI-2 genomic island itself (200). Further characterisation of the SPI-2 T3SS effectors, including their host targets, biochemical activity, and contributions to pathogenesis is required to more fully understand the molecular and cellular activities that enable intracellular survival and replication of *Salmonella* spp.

1.6.2.1 SCV maturation, migration, and tubular network formation

Following the loss of early endosomal markers, the SCV acquires a number of late endosomal markers including LAMP1, Rab7, cholesterol, and vacuolar ATPase (191, 201-204). As the SCV matures, the luminal environment becomes acidified and enriched for antimicrobial peptides, and these environmental cues are sensed by various two-component systems as described above. These systems subsequently induce expression of the functional

SPI-2 T3SS which penetrates the SCV membrane to form a protein channel that is continuous with the host cell cytoplasm (150, 205, 206).

Many effectors of the SPI-2 T3SS play roles in positioning and expanding the SCV. SifA plays a critical role in SCV stability and connects the SCV to the host microtubular network by binding to the host protein SKIP (207). PipB2, SseF, and SseG are also involved in linking the SCV to motor proteins (208, 209), which may provide the mechanism by which the SCV migrates towards the host nucleus. SseF and SseG act as a complex to maintain the position of the SCV near the nucleus and microtubule-organising centre (MTOC) (209, 210), and along with SifA may be involved in the acquisition of host metabolites by redirection of exocytic vesicles (211). The SCV is stabilised by the formation of an actin meshwork, a process which appears to be mediated by a complex interaction between SipA, SteA, SteC, SseI, and SspH2, and inhibited by SpvB (212-214). Meanwhile, SseJ functions as a glycerophospholipid-cholesterol acyltransferase to modify the cholesterol and phospholipid content of the SCV membrane (215). Replication of the bacteria within the perinuclear SCV is accompanied by the formation of *Salmonella*-induced filaments (SIFs), long protrusions that extend along the host microtubules and are expanded by fusion with host lysosomal proteins. The formation and extension of SIFs is mediated by the effectors SifA, SopD2, PipB2, SseF, and SseG (70, 216-218), while this process is antagonised by SpvB and SseJ (210, 219). The SIF network accesses host endosomal cargo, and the lumen of the SIF network is continuous with the lumen of the SCV, so the formation of the SIF network appears to enable vacuolar *Salmonella* to access nutrients to support intracellular replication (71). The large number of SPI-2 effectors involved in the development and maintenance of the SCV-SIF network demonstrates the importance of this activity to permitting efficient intracellular replication, and deletion mutants of *sifA*, *sseJ*, and *pipB2* are attenuated in mouse models of systemic infection (208, 216, 220).

1.6.2.2 Manipulation of immune signaling

Many effectors of the SPI-2 T3SS are implicated in inhibition of innate immune signaling. PipA, GogA, and GtgA are zinc metalloproteases that cleave the NF-κB transcription factors p65, RelB, and cRel within a conserved Rel-homology domain and are thus anti-inflammatory *in vivo* (221, 222). SseL is a deubiquitinase that inhibits the degradation of IκBα and thus supresses NF-κB signaling (223). SpvD interacts with the nuclear transporter Exportin-2 to indirectly prevent nuclear import of p65 (224), but while SpvD is predicted to be cysteine protease it does not appear to cleave Exportin-2 (225), and so the mechanism by which SpvD inhibits translocation of p65 requires further investigation. SarA is a recently discovered effector that interacts with STAT3 to induce production of the anti-inflammatory cytokine IL-10, and *sarA* mutants are less virulent in both intraperitoneal and competitive chronic oral infection models (226). GogB inhibits IκBα degradation through interactions with FBXO22 and Skp1 and thus prevents NF-κB activation (227). SspH2 is an E3 ubiquitin ligase that interacts with Nod1 and SGT1 to enhance IL-8 secretion, although the mechanism is not clear. (228). SlrP appears to inhibit IL-1β secretion by preventing activation of caspase 1, though the mechanism for this is also not well defined. Further, SlrP reportedly functions as an anti-virulence mechanism to promote host survival and subsequent bacterial transmission (229).

A more recent area of research describes effector-mediated interference of host adaptive immunity. One study identified a number of SPI-2 effectors that inhibit migration of infected dendritic cells towards CCL19, including PipB2, SifA, SlrP, SpiC, SseF, SseI, and SspH2 (230). Given the diverse functions of these effectors, it is likely that this phenotype arises through a range of mechanisms. SseI interacts with the cell migration regulator IQGAP1 and inhibits migration of infected primary macrophages and dendritic cells *in vitro*,

and also suppresses migration of dendritic cells to the spleen *in vivo* (231). Another study identified a range of effectors that contribute to the inhibition of antigen presentation of dendritic cells, including PipB2, SifA, SlrP, SopD2, and SspH2 (232), though this study utilised deletion mutants of these effectors and so further work is needed to confirm these findings and identify a mechanism. Separately, SteD is reported to manipulate the E3 ligase MARCH to ubiquitylate and degrade mature MHCII, resulting in decreased T-cell activation *in vivo* (233, 234).

1.6.3 Uncharacterised and poorly understood effectors

Considerable work remains to fully characterise the substrates of the SPI-2 T3SS. Many effectors are only partially characterised, some have disputed function or host targets, and others have no described role in pathogenesis. A proteomics-based screen for novel effectors revealed a number of novel SPI-2 T3SS effectors, including SteE and CigR, though these effectors remain otherwise undescribed (235). A transposon mutagenesis screen also revealed a number of undescribed effectors including SteB (154), which remains undescribed. SpiC was originally implicated in avoiding phagolysosome fusion (236) and reportedly interacts with the host protein Hook3 (237), though later studies have failed to show translocation of SpiC into the cytosol (238) and so SpiC remains a disputed effector. SrgE and SrfJ have been shown to be translocated by the SPI-2 T3SS but have no described function (239, 240). SifB shows some sequence similarity to SifA and appears to localise to the SCV-SIF network, but a *sifB* mutant is not impaired for intracellular replication, in contrast to *sifA* mutants (220). PipB is highly similar to PipB2 and also localises to the SCV-SIF network, but little is known regarding its function (111, 241). SseK1 and SseK2 were identified based on homology to NleB1 (242), an effector of enteropathogenic *E. coli*, and along with SseK3 represent putative glycosyltransferases that may target host signaling

proteins (243). Ultimately, further characterisation of these effectors and discovery of other undescribed effectors will lead to a more complete understanding of how *Salmonella* manipulates host cells to promote replication and transmission.

1.7 The SseK effector family

SseK1, SseK2, and SseK3 comprise a family of highly similar effectors that are translocated by the SPI-2 system during infection (242, 243). The SseK family show high sequence similarity to NleB1, an effector protein from enteropathogenic *E. coli* (EPEC). NleB1 functions as an arginine glycosyltransferase, and catalyses the addition of *N*-acetylglucosamine (GlcNAc) to arginine residues of the mammalian signaling adaptors FADD and TRADD (244, 245). This glycosylation event inhibits NF-κB signaling and prevents host cell death via extrinsic apoptosis, enabling EPEC to persist on the surface of infected enterocytes.

SseK1 and SseK2 were originally identified as homologues of NleB from *Citrobacter rodentium*, and were subsequently shown to be translocated in a SPI-2 dependent manner using the adenylate cyclase reporter system (242). Further, SseK1 was shown to be translocated in higher levels and at earlier timepoints than SseK2, which may suggest these effectors have different functions during infection. In subcellular localisation experiments, SseK1 was shown to localise to the cytoplasm of the host cell by cellular fractionation and by immunofluorescence microscopy (242). Neither SseK1 nor SseK2 appeared to contribute to the formation of the SCV-SIF network, while *sseK1, sseK2 and sseK1sseK2* mutants were not attenuated following intraperitoneal injection in BALB/c mice (242).

A later study identified SseK3 by comparing the genomes of the pathogenic *S.* Typhimurium SL1344 and the less virulent strain *S.* Typhimurium LT2 (243). Subsequent experiments demonstrated expression and translocation of SseK3 into mouse bone marrow-

derived macrophages and that *sseK3* expression was regulated by the SsrAB operon, although the authors were unable to conclusively demonstrate that translocation was SPI-2 dependent. Further, no phenotype was observed for intracellular replication of a *sseK1sseK2sseK3* triple mutant strain during macrophage infection, while a competitive index experiment in mice showed attenuation of the triple mutant relative to wild-type. However, this phenotype was also observed for an *sseK1sseK2* double mutant suggesting this effect was not due to SseK3 (243).

Few other studies have advanced the understanding of the host substrates of the SseK family or the contribution to virulence. One approach utilised quantitative PCR-determined competitive indices to assess persistence of single deletion mutants following intraperitoneal injection of 129SvJ mice, and found neither SseK1, SseK2 nor SseK3 contributed to persistence over a 14-day period (246). It should be noted that this study tested single deletion mutants, and did not consider complementarity or redundancy between effectors. In contrast to these results, another study carried a competitive index infection to 28 days and showed an attenuation of an *sseK2* mutant relative to wild-type (247). Separately, *in vitro* approaches showed an *sseK1sseK2sseK3* triple mutant replicated poorly in RAW264.7 macrophages relative to wild-type, but there was no observed replication defect in HeLa cells or CaCo2 epithelial cells (248). This same study assessed bacterial loads in systemic organs following oral infection of C57BL/6 mice and observed no reduction in bacterial counts for *sseK1* or *sseK2* single mutants, nor for an *sseK1sseK2sseK3* triple mutant. The conflicting results presented across these studies likely arises from differences in methodology, route of infection, genetic background of the various mouse models, and resident microbiotia, and so further work is needed to elucidate the contribution of the SseK family to *Salmonella* virulence.

Given the strong sequence similarity to NleB1, it is likely the SseK effectors have similar biochemical activity and host substrates. Indeed, some reports suggest SseK1 functions as a glycosyltransferase and targets the host protein TRADD, an adaptor protein involved in inflammatory and apoptotic signaling pathways (245). Further, SseK1 appears to inhibit activation of NF-κB following stimulation with TNF, and the activity of SseK1 is dependent on a conserved DxD catalytic motif (245). These *in vitro* approaches provide a promising avenue for interrogating the activity of the SseK effectors, given that NleB1 is relatively well described with regard to biochemical activity and contributions to virulence during EPEC infection.

1.8 Enteropathogenic *E. coli* and NleB1

Enteropathogenic *E. coli* achieves colonisation of the gut via T3SS-dependent translocation of an array of effector proteins. These effectors contribute to the intimate attachment of the bacteria to host enterocytes, localised effacement of microvilli on the apical surface, and manipulation of the actin cytoskeleton, resulting in the formation of a raised pedestal-like structure beneath the adherent bacteria (249, 250). While EPEC remains an extracellular pathogen, the strong sequence similarity between NleB1 of EPEC and the SseK family of *Salmonella* may suggest a conserved activity for these proteins.

NleB1 has now been well characterised as an arginine glycosyltransferase that targets the host Fas-associated death domain protein (FADD) by the addition of a single *N*-acetylglucosamine (GlcNAc) to Arg117 in the death domain of FADD (244, 245). FADD functions as a signaling adaptor in the extrinsic apoptotic pathway (251), and this glycosylation event prevents assembly of the death inducing signaling complex (DISC) and thus prevents caspase 8 mediated cell death, enabling the extracellular EPEC to persist on the apical surface of infected enterocytes. NleB1 additionally catalyses similar glycosylation of

other death-domain proteins, including TRADD and RIPK1 (244, 245), and when overexpressed can function as an inhibitor of NF-κB activation induced by the cytokine TNF (252-254). Thus, the inhibition of NF-κB signaling by NleB1 is well described, and as some evidence suggests SseK1 has a similar effect (245), it is probable that the host targets of SseK1 are involved in these signaling pathways.

The conservation of particular amino acid regions between NleB1 and the SseK family support the hypothesis that the biochemical activity of these effectors is conserved, if not the precise host substrates. All three SseK family members and NleB1 share a conserved Rossman fold and a signature DxD catalytic motif, which is required for glycosyltransferase activity (255, 256). Additionally, a single glutamate residue in NleB1 (E253) is required for the inhibition of NF-κB signaling in response to TNF (245). This glutamate is conserved in all SseK family members, and is likely important for the catalytic activity of these glycosyltransfersases. Collectively, biochemical and structural information on the activity of NleB1 provides opportunities to explore the function of the SseK effectors.

1.9 Innate immune signaling

Given that the described substrates of NleB1 contain a conserved death domain that is critical for induction of signaling pathways, and that previous reports suggest SseK1 targets TRADD, it is likely that the host targets of the SseK effectors are death domain-containing proteins. These include receptors and adaptors in the Fas, TNF, and TRAIL signaling pathways that are induced by extracellular ligands and initiate complex signaling cascades leading to inflammatory signaling or cell death through a variety of mechanisms.

Binding of extracellular TNF to the membrane-associated receptor TNFR1 potentiates a signaling cascade that can induce either inflammatory cytokine production or programmed cell death. The adaptor protein TRADD is recruited to the cytoplasmic death domain of

TNFR1 and participates in the formation of complex I, a signaling platform that includes other adaptor proteins such RIPK1, TRAF2, and the E3 ligases cIAP1 and cIAP2 (257, 258). The signaling cascade induced by complex I leads to the induction of the canonical NF-κB pathway, which results in the secretion of pro-inflammatory cytokines. TNF stimulation can also potentiate the formation of complex II, which includes TRADD and the related adaptor protein FADD, as well as RIPK1, RIPK3, and MLKL (259). Signaling via complex II can induce programmed cell death via apoptosis or necroptosis (260). In both cascades, the death domain regions of TRADD and FADD are critical in mediating the protein-protein interactions that underpin complex formation (261).

In a manner similar to TNF signaling, the extracellular ligand TRAIL recognises a cognate membrane-associated receptor protein. However, TRAIL binds to four different receptors, termed TRAIL-R1 (262), TRAIL-R2 (263), TRAIL-R3 (264), and TRAIL-R4 (265). Only TRAIL-R1 and TRAIL-R2 are capable of potentiating immune signaling, as TRAIL-R3 does not have an intracellular domain and TRAIL-R4 contains a truncated death domain. Interestingly, mice possess only one TRAIL-R, which appears to be functionally analogous to the human TRAIL-R1 and TRAIL-R2 (266). Similar to TNF signaling, TRAIL stimulation leads to the formation of a signaling complex that comprises FADD, TRAF2, RIPK1 and caspase 8 (267, 268). This complex can induce a range of signaling outcomes ranging from the promotion of cell survival via ubiquitination of caspase-8, pro-inflammatory cytokine production, or apoptotic cell death via caspase 8 and caspase 3 (266, 269). Alternatively, TRAIL stimulation can induce the formation of a second complex that is implicated in the induction of programmed cell death via necroptosis, but under certain conditions can also stimulate apoptosis or cytokine production (270).

The diversity of outcomes that are driven by death receptor-mediated innate immune signaling pathways provide a rapid and potent means for cells to appropriately respond to

bacterial infection, but this simultaneously exerts a significant evolutionary pressure for pathogens to develop mechanisms to manipulate these pathways for their benefit. In particular, homotypic death-domain interactions between receptor proteins and adaptor proteins are critical for complex formation, and given that at least one pathogen has evolved a means for antagonising these interactions (244, 245), it is likely that other pathogens have acquired similar mechanisms.

1.10 Aims

Given the importance of these signaling adaptors in mediating inflammatory responses and cell death, antagonising death domain-containing proteins represents an attractive target for bacterial effector proteins. Based on the well-described activities of the EPEC homologue NleB1 and the strong sequence similarity of the SseK family, we hypothesised that the SseK effectors are arginine glycosyltransferases that target a subset of death domain-containing proteins during *Salmonella* infection. The primary aim of this thesis was to identify the host proteins that are glycosylated by the SseK effectors during *Salmonella* infection.

The specific aims of this thesis were:

1) To identify the host binding partners of SseK1, SseK2, and SseK3 via *in vitro* screening assays.
2) To characterise the glycosyltransferase activity of the SseK effectors and identify target amino acids of host substrates.
3) To determine the contribution of these glycosylation events to virulence *in vitro* and *in vivo.*

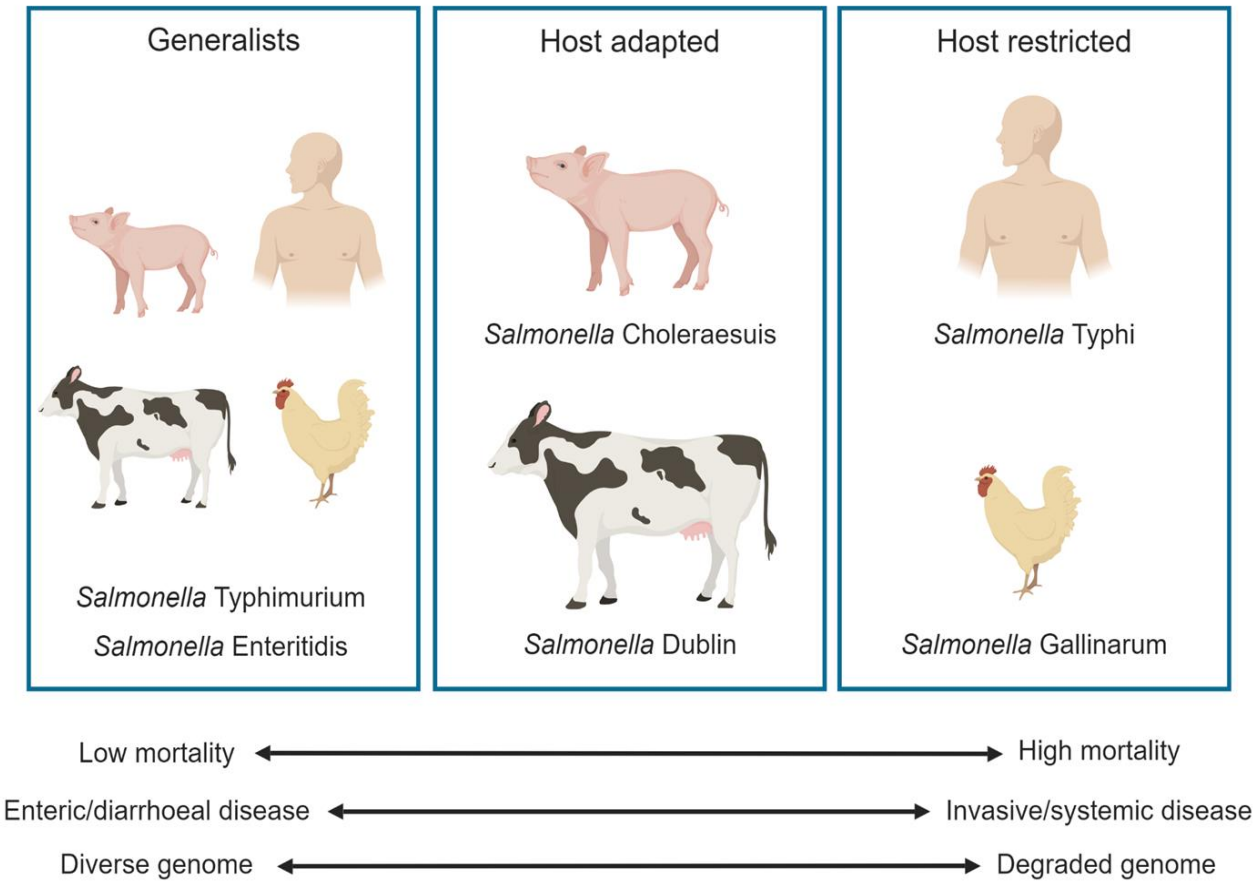

Figure 1.1 Host specificity and genotypic adaptation in Salmonella

Some serovars of *Salmonella* remain capable of infecting a broad range of hosts, while others adapt to cause disease in particular hosts, and others still become specifically adapted to certain hosts and lose the ability to infect other hosts. This adaptation is accompanied by genomic degradation in which genes that are no longer required in a particular host niche become pseudogenes or lost completely. Generally, host restricted strains are associated with systemic disease and high mortality, while generalist strains are associated with a self-limiting diarrhoeal disease and low mortality. Adapted from (79).

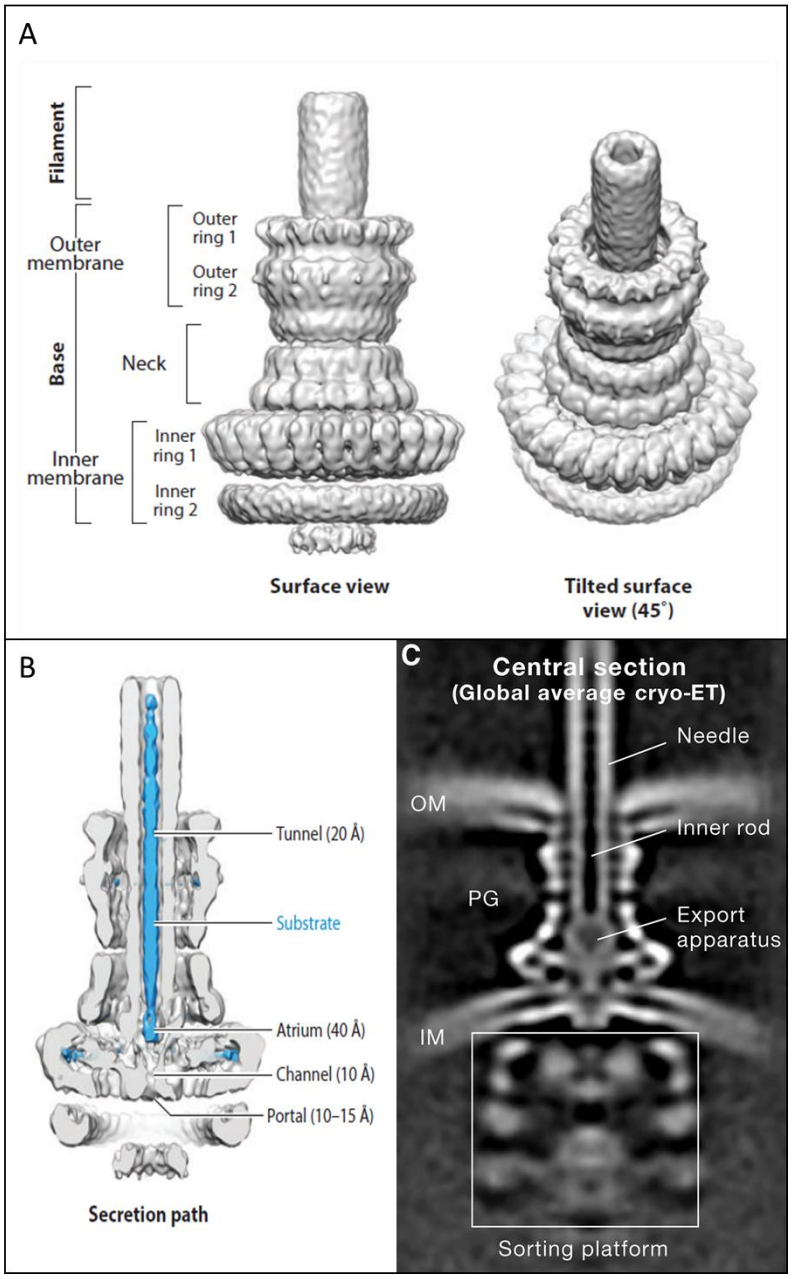

Figure 1.2 Structure of the Salmonella type three secretion system

A) 3-D reconstruction of cryo-electron microscopy observations of the *S.* Typhimurium needle complex. Various substructures are noted along with their positioning in the bacterial cell wall. B) Half-sectioned view of the T3SS needle complex highlighting a substrate within the central tunnel. C) Cryo-electron microscopy observation of the *S.* Typhimurium T3SS injectisome. Various substructures are noted along with their positioning in the bacterial cell well. A) and B) adapted from (114), C) adapted from (120).

SPI-1 T3SS			
Effector	**Host targets**	**Biochemical activity**	**Function**
AvrA	MAP kinase kinases	Acetyltransferase	Inhibits NF-kB signalling, inhibits IL-8 production, stabilises tight junctions
SipA	F-actin		Inhibits actin depolymerisation. Disrupts tight junctions. Promotes secretion of chemoattractant hepoxillin A3
SipB	Caspase-1 inflammasome		SPI-1 T3SS translocase component. Induces secretion of IL-1β and IL-18
SipC	Actin		SPI-1 T3SS translocase component. Induces nucleation of actin, bundles actin filaments
SipD			SPI-1 T3SS translocase component.
SopA		E3 ubiquitin ligase	Induces neutrophil transmigration
SopB	SGEF, RhoG	Phosphoinositide phosphatase	Actin rearrangement. Promotes secretion of cellular chloride ions. Disrupts tight junctions.
SopD			Promotes membrane fission, macropinosome formation
SopE	Cdc42, Rac-1	GEF mimic	Mimics GEFs to activate Cdc42 and Rac-1, leading to membrane ruffling and engulfment. Induces IL-8 secretion.
SopE2	Cdc42, Rac-1	GEF mimic	Mimics GEFs to activate Cdc42 and Rac-1, leading to membrane ruffling and engulfment. Induces IL-8 secretion.
SptP	Cdc42, Rac-1	GTPase activation	Reverses cytoskeletal changes induced by SopE, SopE2
SPI-1 and SPI-2 T3SS			
GtgA	p65, RelB, cRel	Zing metalloprotease	Inhibits NF-κB inflammatory signalling
SlrP		E3 ubiquitin ligase	Inhibits IL-1β through regulating inflammasome activation

SspH1	PKN1	E3 ubiquitin ligase	Inhibits NF-κB activation and subsequent IL-8 secretion
SteA	PI(4)P		Contributes to SCV-actin interaction, SCV-SIF network
SteB			
SPI-2 T3SS			
CigR			
GogA	p65, RelB, cRel	Zing metalloprotease	Inhibits NF-κB inflammatory signalling
GogB	FBXO22, Skp1		Inhibits IκB degradation, prevents NF-κB activation
GtgE	Rab29, Rab32, Rab38	Cysteine protease	Cleaves host Rabs to promote intracellular replication
PipA	p65, RelB, cRel	Zing metalloprotease	Inhibits NF-κB inflammatory signalling
PipB			
PipB2	Kinesin-1		Contributes to SCV-motor protein interactions
SifA	SKIP		Promotes SCV stability. Promotes SCV-SIF network formation. Promotes acquisition of metabolites. Relocation of SCV to perinuclear region.
SifB			
SopD2	Rab7, Rab32		Contributes to SCV-SIF network
SpiC	Hook3		Avoidance of phagolysosome fusion
SpvB	Actin	ADP-ribosyl transferase	Antagonises SCV-SIF network formation/stability

SpvC		Phosphothreonine lyase	Inhibits Jnk, Erk, and p38 MAP kinases
SpvD	Exportin-2	Cysteine protease	Inhibits p65 nuclear translocation
SrfJ			
SrgE			
SseF			Formation of SCV-SIF network. Linking of SCV to motor proteins. Migration of SCV to perinuclear region.
SseG			Formation of SCV-SIF network. Linking of SCV to motor proteins. Migration of SCV to perinuclear region.
SseI	IQGAP1	Cysteine protease	Inhibits migration of dendritic cells and primary macrophages
SseJ		Glycerophospholipid-cholesterol acyltransferase	Modifies the cholesterol and phospholipid content of the SCV membrane
SseK1		Glycosyltransferase	Modifies TRADD, inhibits NF-κB signalling
SseK2			
SseK3			
SseL	IκBα	Deubiquitinase	Supresses NF-κB signalling
SspH2	Nod1, SGT1	E3 ubiquitin ligase	Enhances IL-8 secretion
SteC		Kinase	Contributes to SCV-actin interaction. Formation of SCV-SIF network.
SteD	MARCH		Indirectly degrades mature MHCII, resulting in decreased T-cell activation
SteE	STAT3		Induces production of the anti-inflammatory cytokine IL-10

Table 1.1 Effector proteins of the Salmonella SPI-1 and SPI-2 T3SS

More than 40 substrates of the SPI-1 and SPI-2 T3SSs have been observed across the various serovars of *Salmonella*. This table represents a summary of the current understanding of these effector proteins, with respect to their cognate secretion system, known host targets, biochemical activity, and function.

Chapter Two

Materials and methods

CHAPTER 2: Materials and methods

2.0 Figures

Certain figures in this thesis were created using BioRender.

2.1 Chemicals and reagents

All chemicals and reagents used in this study were of analytical or laboratory grade. Chemicals and reagents were purchased from Sigma-Aldrich (Missouri, USA), Merck (Hesse, Germany), or Chem Supply (South Australia, Australia), unless otherwise stated. Antibiotics were obtained from Astral Scientific (New South Wales, Australia), Amresco (Ohio, USA), or Sigma-Aldrich (Missouri, USA). Tissue culture media components were obtained from Thermo Fisher Scientific (Massachusetts, USA).

2.2 Strains and plasmids

The bacterial and yeast strains used in this study are listed in Table 2.1, and plasmids are listed in Table 2.2. All *E. coli* and *Salmonella* strains were grown in lysogeny broth (LB) (1% (w/v) tryptone, 0.5% (w/v) yeast extract, 171 mM NaCl, pH 7.2) at 37 °C in the presence of ampicillin (100 μg/ml), kanamycin (100 μg/ml), or streptomycin (50 μg/ml), as required.

2.3 Oligonucleotides

Synthetic oligonucleotides used for polymerase chain reactions were ordered from Sigma-Aldrich (New South Wales, Australia). Oligonucleotides used in this study are listed in Table 2.3.

2.4 DNA extraction, amplification, and manipulation

2.4.1 Plasmid DNA extraction

Plasmid DNA was extracted from overnight cultures using the QIAprep® Spin Miniprep kit or the QIAGEN Plasmid Midi Kit (QIAGEN, California, USA), according to the manufacturer's instructions.

2.4.2 cDNA synthesis

cDNA was generated from RNA extracted from HeLa cells by reverse transcription using the QuantiTect® Reverse Transcription kit (QIAGEN), according to the manufacturer's instructions.

2.4.3 Polymerase chain reaction (PCR)

PCR amplifications were performed using AmpliTaq Gold® DNA polymerase (Life Technologies, Victoria, Australia). Reactions were prepared to a total volume of 50 µl and comprised 0.1 U/µl AmpliTaq Gold® DNA polymerase, 0.7 mM of each dNTP, 0.2 µM of each primer, one tenth reaction volume of 10x PCR buffer, 2 mM $MgCl_2$, and 100 ng of template DNA. PCR amplifications were performed in a GS482 G-STORM thermal cycler (G-STORM, Somerset, UK). PCR conditions varied depending on primer composition and size of amplicons. Generally, PCR conditions involved a hot start of 95 °C for 5 minutes, followed by 30 cycles of 95 °C for 1 minute, 48 to 66 °C for 2 minutes, and 68 to 72 °C for 1 minute, with a final extension of 70 °C for 5 minutes. Reactions were held at 4 to 10 °C indefinitely, when necessary.

2.4.4 Colony PCR

Colony PCR amplifications were performed using GoTaq® DNA polymerase (Life Technologies). Single colonies were picked from lysogeny broth agar plates with sterile pipette tips and used as DNA templates for colony PCR amplifications. Reactions were prepared to a total volume of 20 µl and comprised GoTaq® Green Master Mix at 1x final concentration and 0.1 µM of each primer. PCR conditions involved a hot start of 95 °C for 5 minutes, followed by 30 to 35 cycles of 95 °C for 30 seconds, 52 to 55 °C for 30 seconds, and 72 °C for 30 seconds to 3 minutes, with a final extension of 72 °C for 5 minutes. Reactions were held at 4 to 10 °C indefinitely, when necessary.

2.4.5 Electrophoresis, resolution, and purification of DNA

DNA products were mixed with 6 x gel loading dye (NEB) and loaded to 1% - 2% (w/v) agarose gels stained with 1 x SYBR® Safe DNA Gel Stain (Invitrogen, California, USA).

Electrophoresis was performed in TAE buffer (40 mM Tris, 0.114 % (v/v) glacial acetic acid, 1 mM EDTA (pH 8.3)). Approximate size of DNA products was estimated by comparison to 100 bp or 1 kb DNA ladders (NEB). DNA products were visualised using a UV transilluminator (Syngene, Cambridge, UK), and digital images of DNA products were acquired using a G:BOX HR gel documentation and analysis system (Syngene, Cambridge, UK). DNA products were excised under UV illumination and purified using the Wizard SV Gel and PCR Clean-Up System (Promega, Wisconsin, USA).

2.4.6 Restriction enzyme digestion

Restriction enzyme digestions were performed using enzymes and buffers from NEB (Maryland, USA) and Roche (Basel, Switzerland), according to the manufacturer's

instructions. Reactions were prepared to a total volume of 30 µl and comprised 1 to 2 µg DNA, 5 to 10 units of restriction enzyme, and one tenth reaction volume of 10 x restriction buffer. Reactions were made to the total volume with dH_2O. Reactions were incubated at 37 °C for 3 hours.

2.4.7 DNA ligation

DNA ligation reactions were prepared at an insert:vector molar ratio of 5:1. Reactions were prepared to a total volume of 20 µl and comprised 1 µl of T4 DNA ligase (NEB), one tenth reaction volume of 10 x reaction buffer (NEB), and the remaining reaction volume comprised insert DNA, vector DNA, and dH_2O as necessary. Reactions were incubated either at room temperature for 30 minutes, or at 4 °C overnight.

2.4.8 DNA sequencing and analysis

DNA sequencing was performed using the BigDye™ Terminator v3.1 Cycle Sequencing Kit (Thermo Fisher Scientific), according to the manufacturer's instructions. Sequencing PCR conditions involved a hot start of 95 °C for 1 to 2 minutes, followed by 25 to 30 cycles of 95 °C for 10 to 30 seconds, 50 °C for 5 to 10 seconds, and 60 °C for 4 minutes. Reactions were held at 4 to 10 °C indefinitely, when necessary. Capillary electrophoresis was performed by the Australian Genome Research Facility (Victoria, Australia). Analysis of DNA sequences was performed using Sequencher® version 5.0.1 sequence analysis software (Gene Codes Corporation, Ann Arbor, Michigan, USA).

2.4.9 Site-directed mutagenesis

Site-directed mutagenesis of plasmid constructs was performed using the QuikChange II Site-Directed Mutagenesis kit (Stratagene, California, USA), according to the manufacturer's instructions. Mutagenesis PCR conditions involved a hot start of 95 °C for 30 seconds, followed by 18 cycles of 95 °C for 30 seconds, 55 °C for 1 minute, and 68 °C for 1 to 3 minutes, with a final extension of 72 °C for 7 minutes. Reactions were held at 4 to 10 °C indefinitely, when necessary. Completed reactions were digested with *Dpn*I at 37 °C overnight.

2.5 Bacterial transformation

2.5.1 Preparation of chemically competent *E. coli* cells

Bacterial strains were grown in 10 ml LB broth overnight at 37 °C with shaking at 180 rpm, with the required antibiotic added when necessary. Overnight cultures were subinoculated 1:100 in 100 ml SOB media (2% (w/v) tryptone, 0.5% (w/v) yeast extract, 10 mM NaCl, 2.5 mM KCl, 10 mM $MgCl_2$, 10 mM $MgSO_4$) and grown at 16 °C with shaking at 200 rpm to an OD_{600} of 0.4 to 0.8. The bacterial cells were then harvested by centrifugation at 2500 rpm for 15 minutes at 4 °C, resuspended in 0.4 volume ice cold transformation buffer (10 mM PIPES, 15 mM $CaCl_2$, 55 mM $MnCl_2$, 250 mM KCl, pH 6.7) and incubated on ice for 10 minutes. The bacterial cells were pelleted again and resuspended in 0.04 volume of ice-cold transformation buffer. DMSO (Sigma) was added to a final concentration of 7.5 % (v/v) and the cells were incubated on ice for 10 minutes. Competent cells were then frozen on dry ice and stored at -80 °C in 50 µl aliquots until required.

2.5.2 Chemical transformation

Chemical transformation was performed by adding 100 to 200 ng DNA to 50 µl of chemically competent bacteria. Reactions were incubated on ice for 45 to 60 minutes, then heat shocked at 42 °C for 90 seconds, and incubated on ice for 2 minutes. Reactions were then added to 1 ml of SOC media (2% (w/v) tryptone, 0.5% (w/v) yeast extract, 10 mM NaCl, 2.5 mM KCl, 10 mM $MgCl_2$, 10 mM $MgSO_4$ and 20 mM glucose), and incubated for 75 minutes at 37 °C with shaking at 180 rpm. Volumes of the reaction were then plated to selective media and incubated at 37 °C overnight to select for transformants.

2.5.3 Preparation of electrocompetent *Salmonella* cells

Bacterial strains were cultured in 10 ml LB broth supplemented with antibiotics when required overnight at 37°C with shaking at 180 rpm. Overnight cultures were subinoculated 1:100 in 10 ml LB and grown at 37 °C with shaking at 180 rpm to an OD_{600} of 0.8. Bacteria were pelleted at 4000 rpm for 10 minutes at 4 °C, and resuspended in 10 ml of ice-cold distilled water. Bacteria were pelleted as previously, and resuspended in 5 ml of ice-cold distilled water. Bacteria were pelleted as previously, and resuspended in 2.5 ml ice-cold distilled water containing 10% (v/v) glycerol. Bacteria were pelleted as previously, and resuspended in 1 ml ice-cold distilled water containing 10% glycerol. Bacteria were pelleted at 4000 rpm for 2 minutes at 4 °C, and resuspended in 500 µl of distilled water containing 10% glycerol. Bacteria were pelleted as previously, and resuspended in 150 µl of distilled water containing 10% glycerol, then used for electroporation immediately.

2.5.4 Electroporation

Electroporation was performed by adding approximately 200 ng of DNA to 50 µl of electrocompetent bacteria. Reactions were transferred to pre-chilled 0.1 cm gap

electroporation cuvettes (Cell Projects, Kent, UK) and electroporated using a Bio-Rad Micropulser electroporator, with settings of 1.8 V, 25 μF capacitance, and 200 Ω resistance for 4 to 6 milliseconds. Reactions were then transferred to flasks containing 1 ml SOC media. Flasks were incubated for 90 minutes at 37 °C with shaking at 180 rpm. Volumes of the reaction were then plated to selective media and incubated at 37 °C overnight to select for transformants.

2.6 Construction of expression vectors

2.6.1 Construction of vectors to express HA-tagged SseK1, SseK2, and SseK3 catalytic mutants

Site-directed mutagenesis was performed according to the protocol described in section 2.4.9. pTrc99A-SseK1$_{DxD(229-231)AAA}$, pTrc99A-SseK2$_{DxD(239-241)AAA}$, and pTrc99A-SseK3$_{DxD(226-228)AAA}$ were generated using pTrc99A-SseK1, pTrc99A-SseK2, or pTrc99A-SseK3 as template DNA and amplified by PCR using the primer pairs SseK1$_{DxD-F/R}$, SseK2$_{DxD-F/R}$, or SseK3$_{DxD-F/R}$, respectively. pTrc99A-SseK1$_{E255A}$, pTrc99A-SseK2$_{E271A}$, and pTrc99A-SseK3$_{E258A}$ were generated using pTrc99A-SseK1, pTrc99A-SseK2, or pTrc99A-SseK3 as template DNA and amplified by PCR using the primer pairs SseK1$_{E255A-F/R}$, SseK2$_{E271A-F/R}$, or SseK3$_{E258A-F/R}$, respectively. Plasmids were sequenced using the primer pair pTrc99A$_{F/R}$.

2.6.2 Construction of vectors to express GFP-tagged SseK1 and SseK3 catalytic mutants

Site-directed mutagenesis was performed according to the protocol described in section 2.4.9. pEGFP-C2-SseK1$_{E255A}$ and pEGFP-C2-SseK3$_{E258A}$ were generated using

pEGFP-C2-SseK1 or pEGFP-C2-SseK3 as template DNA and amplified by PCR using the primer pairs $SseK1_{E255A-F/R}$ or $SseK3_{E258A-F/R}$, respectively. Plasmids were sequenced using the primer pair $pEGFP\text{-}C2_{F/R.}$

2.6.3 Construction of vectors to express GAL4 binding domain fused-SseK1 and SseK2 catalytic mutants

Site-directed mutagenesis was performed according to the protocol described in section 2.4.9. pGBKT7-BD-$SseK1_{DxD(229-231)AAA}$ and pGBKT7-BD-$SseK2_{DxD(239-241)AAA}$ were generated using pGBKT7-BD-SseK1 or pGBKT7-BD-SseK2 as template DNA and amplified by PCR using the primer pairs $SseK1_{DXD-F/R}$ or $SseK2_{DXD-F/R}$, respectively. pGBKT7-BD-$SseK1_{E255A}$ and pGBKT7-BD-$SseK2_{E271A}$ were generated using the primer pairs $SseK1_{E255A-F/R}$ or $SseK2_{E271A-F/R}$, respectively. Plasmids were sequenced using the primer pair $pGBKT7\text{-}BD_{F/R.}$

2.6.4 Construction of vectors to express human GSTP1

pFLAG-GSTP1 was constructed by amplifying human *GSTP1* from HeLa cDNA using AmpliTaq Gold® DNA polymerase and the primer pair $GSTP1\text{-}pFLAG_{F/R}$. The PCR product was purified and digested with *Xba*I and *Bam*HI, then ligated into p3xFLAG-Myc-CMV-24. Ligation reactions were used to transform chemically competent XL1-Blue cells, and transformants were selected by plating to LB agar containing ampicillin. Transformants were verified by colony PCR using GoTaq® DNA polymerase and the primer pair $pFLAG_{F/R}$. Plasmids were extracted from transformants and sequenced using the primer pair $pFLAG_{F/R.}$

pET28a-GSTP1 was constructed by amplifying human *GSTP1* from HeLa cDNA using AmpliTaq Gold® DNA polymerase and the primer pair $GSTP1\text{-}pET28a_{F/R.}$ The PCR

product was purified and digested with *Eco*RI and *Hin*DIII, then ligated into pET28a. Ligation reactions were used to transform chemically competent XL1-Blue cells, and transformants were selected by plating to LB agar containing ampicillin. Transformants were verified by colony PCR using GoTaq® DNA polymerase and the primer pair $pET28a_{F/R}$. Plasmids were extracted from transformants and sequenced using the primer pair $pET28a_{F/R}$.

pGADT7-AD-GSTP1 was constructed by amplifying human *GSTP1* from HeLa cDNA using AmpliTaq Gold® DNA polymerase and the primer pair $GSTP1\text{-}pGADT7_{F/R.}$ The PCR product was purified and digested with *Eco*RI and *Bam*HI, then ligated into pGADT7-AD. Ligation reactions were used to transform chemically competent XL1-Blue cells, and transformants were selected by plating to LB agar containing ampicillin. Transformants were verified by colony PCR using GoTaq® DNA polymerase and the primer pair $pGADT7\text{-}AD_{F/R}$. Plasmids were extracted from transformants and sequenced using the primer pair $pGADT7\text{-}AD_{F/R}$.

2.6.5 Construction of vectors to express human PCMT1

pFLAG-PCMT1 was constructed by amplifying human *PCMT1* from HeLa cDNA using AmpliTaq Gold® DNA polymerase and the primer pair $PCMT1\text{-}pFLAG_{F/R.}$ The PCR product was purified and digested with *Xba*I and *Bam*HI, then ligated into p3xFLAG-Myc-CMV-24. Ligation reactions were used to transform chemically competent XL1-Blue cells, and transformants were selected by plating to LB agar containing ampicillin. Transformants were verified by colony PCR using GoTaq® DNA polymerase and the primer pair $pFLAG_{F/R}$. Plasmids were extracted from transformants and sequenced using the primer pair $pFLAG_{F/R.}$

pGADT7-AD-PCMT1 was constructed by amplifying human *PCMT1* from HeLa cDNA using AmpliTaq Gold® DNA polymerase and the primer pair $PCMT1\text{-}pGADT7_{F/R.}$

The PCR product was purified and digested with *Eco*RI and *Bam*HI, then ligated into pGADT7-AD. Ligation reactions were used to transform chemically competent XL1-Blue cells, and transformants were selected by plating to LB agar containing ampicillin. Transformants were verified by colony PCR using GoTaq® DNA polymerase and the primer pair $pGADT7_{F/R}$. Plasmids were extracted from transformants and sequenced using the primer pair $pGADT7_{F/R.}$

2.6.6 Construction of vectors to express human TRADD mutants

Site-directed mutagenesis was performed according to the protocol described in section 2.4.9. pFlag-$hTRADD_{R245A}$ was generated using pFlag-hTRADD as template DNA and amplified by PCR using the primer pair $hTRADD_{R245A\text{-}F/R}$. pFlag-$hTRADD_{R235A/R245A}$ was generated using pFlag-$hTRADD_{R235A}$ as template DNA and amplified by PCR using the primer pair $hTRADD_{R245A\text{-}F/R}$. Plasmids were sequenced using the primer pair p3xFlag-Myc-$CMV\text{-}24_{F/R.}$

2.6.7 Construction of vectors to express human $TRAILR2_{DD}$

pFLAG-$hTRAILR2_{DD}$ was constructed by amplifying human *TNFRSF10B* from pGADT7-DD- $hTRAILR2_{DD}$ using AmpliTaq Gold® DNA polymerase and the primer pair $hTRAILR2_{DD\text{-}F}$ / $hTRAILR2_{DD\text{-}R}$. The PCR product was purified and digested with *Eco*RI and *Bam*HI, then ligated into p3xFLAG-Myc-CMV-24. Ligation reactions were used to transform chemically competent XL1-Blue cells, and transformants were selected by plating to LB agar containing ampicillin. Transformants were verified by colony PCR using GoTaq® DNA polymerase and the primer pair $pFLAG_F$ / $pFLAG_R$. Plasmids were extracted from transformants and sequenced using the primer pair $pFLAG_F$ / $pFLAG_{R.}$

2.7 Mammalian cell culture

2.7.1 Mammalian cells, media, and maintenance

HEK293T cells (human embryonic kidney 293 cells expressing the SV40 large T-antigen), HeLa cells (human cervical cancer cells), and RAW264.7 cells (murine leukemic monocyte-macrophage cells) were maintained in DMEM, low glucose with GlutaMAX™ supplement and pyruvate (DMEM (1X) + GlutaMAX(TM)-I) (Gibco, Life Technologies, NY, USA). Tissue culture media was further supplemented with 10% (v/v) heat-inactivated foetal bovine serum (FBS) (Thermo Fisher Scientific). Cells were maintained in a 37 °C, 5% CO_2 incubator, and passaged to a maximum of 35 times. HEK293T and HeLa cells were split when cells reached 80 to 90% confluency with 1 ml 0.05% Trypsin-EDTA (1X) (Gibco, LifeTechnologies) per 75 cm^2 of tissue culture, then resuspended with 10 volumes of DMEM supplemented with FBS. RAW264.7 cells were physically detached with a cell scraper and further diluted in fresh DMEM supplemented with FBS.

2.7.2 Transfection of mammalian cells

HEK293T and HeLa cells were transfected using FuGENE®6 transfection reagent (Promega), according to the manufacturer's instructions. Cells were transfected one day after seeding to achieve 80 to 90% confluency. Transfection reagent was mixed with the reduced serum medium Opti-MEM®I (1X) + GlutaMAX(TM)-I (Gibco, Life Technologies), and incubated at room temperature for 5 minutes. Plasmid DNA was added at a transfection reagent:DNA ratio of 3:1, and incubated at room temperature for 25 minutes. The reaction was added to previously seeded cells and incubated at 37 °C, 5% CO_2 for 16 to 24 hours.

2.8 Yeast two-hybrid experiments

2.8.1 Yeast culture conditions

S. cerevisiae strains were plated to YDPA (2% (w/v) peptone, 1% (w/v) yeast extract, 2% agar, 2% (v/v) glucose, supplemented with 24 μg/ml adenine and 15 μg/ml kanamycin) or YMM plates (0.6% (w/v) Difco yeast nitrogen base without amino acids (BD Bioscience), 2.2% (w/v) agar, 2% (v/v) glucose), as necessary.

2.8.2 Yeast transformation

Yeast strain *S. cerevisiae* Y2H Gold (Clontech, California, USA) was transformed or cotransformed with plasmid DNA using the established lithium acetate method (Gietz *et al.*, 1995). Transformants were plated to selective media as required to select for successful single or double transformation. When validating interactions between two proteins, transformants were subsequently plated to highly selective media. Briefly, *S. cerevisiae* Y2H Gold was streaked to YPDA and incubated at 30 °C for 3 days. Healthy colonies were used to inoculate 10 ml YPDA broth at a starting OD_{600} of 0.2, and incubated at 30 °C with shaking at 200 rpm to an OD_{600} of 0.6-0.8. The yeast culture was centrifuged at 4000 rpm for 7 minutes, and the pellet was resuspended in sterile distilled water, and centrifuged again. The yeast culture was then resuspended in 100 mM lithium acetate, vortexed thoroughly, and centrifuged again. The lithium acetate supernatant was removed, and yeast were resuspended in 400 mM lithium acetate, vortexed thoroughly, and centrifuged again. The lithium acetate supernatant was removed, and yeast were resuspended in polyethylene glycol (PEG 3350, Sigma-Aldrich), 1 M lithium acetate, salmon sperm ssDNA at a final concentration of 2 mg/ml, and plasmid DNA as appropriate. This reaction was incubated at 30 °C for 30 minutes, then subjected to heat shock at 42 °C for 20 minutes. The reaction was briefly centrifuged, and the supernatant removed. The yeast pellet was resuspended in distilled water

and plated to both SD/Trp-Leu and SD/Trp-Leu-Ade-His selective media, then incubated at 30 °C for 3 days.

2.8.3 Preparation of protein extracts from yeast

To confirm successful expression of constructs required for yeast two-hybrid screening, transformed yeast were grown in selective media overnight at 30 °C with shaking at 200 rpm. Cultures were standardised to an OD_{600} of 2.5, then centrifuged at 4000 rpm. Yeast were resuspended in water and 0.2 M NaOH, then incubated for 5 minutes at room temperature. Yeast were centrifuged briefly, the supernatant was removed, and the pellet was resuspended in 4x lithium dodecyl sulfate (LDS) sample buffer (Life Technologies) and dithiothreitol (DTT, Science Supply Australia, Victoria, Australia) to a final concentration of 50 mM, then boiled at 90 °C for 10 minutes. Samples were electrophoresed and analysed by protein staining and immunoblotting.

2.8.4 Yeast two-hybrid HeLa library screen

To identify the mammalian substrates of SseK1 and SseK2, strains of *S. cerevisiae* Y2H Gold transformed to express these proteins as fusion constructs were mated with a normalised pretransformed HeLa cDNA yeast library (Clontech), according to the manufacturer's instructions. Mated yeast were plated to double-dropout (SD-Trp-Leu) or quadruple-dropout (SD-Trp-Leu-Ade-His) media to select for diploid yeast that express interacting bait and prey proteins. Plates were incubated at 30 °C and monitored for up to 20 days. Colonies appearing on selective media were passaged onto quadruple-dropout media to confirm the protein-protein interaction. These colonies were selected for plasmid extraction using a Zymoprep™ Yeast Plasmid Miniprep I kit (Zymo Research Corp., CA, USA). Recovered prey plasmids were transformed into XL1-Blue *E. coli*, plated to selective media,

then extracted as in section 2.4.1 of this thesis ahead of sequencing to confirm the identity of the prey cDNA.

Protein-protein interactions were further validated by cotransforming the recovered prey plasmid and the original bait plasmid into *S. cerevisiae* Y2H Gold, then plating to selective media. Digital images of these media were acquired under white light using an MFChemiBis imaging station (DNR Bio-Imaging Systems, Israel).

2.9 *Salmonella* infection of mammalian cell lines

2.9.1 *Salmonella* infection of HeLa cells

HeLa cells were seeded to 24 well plates at a concentration of 2 x 10^5 cells per well one day before infection. 10 ml LB broths containing appropriate antibiotic were inoculated with *Salmonella* strains and incubated at 37 °C overnight with shaking at 180 rpm. On the day of infection, overnight cultures were subinoculated 1:100 in fresh 10 ml LB broth, and incubated at 37 °C with shaking at 180 rpm for 3 hours. The OD_{600} readings of the subculture were read and used to estimate bacterial counts. Cells were then infected at a multiplicity of infection (MOI) of 50. 24 well plates were centrifuged at 1500 rpm for 5 minutes at room temperature to promote and synchronise infection. Infected cells were incubated at 37 °C, 5% CO_2 for 30 minutes. Culture media was replaced with media containing 100 μg/ml gentamycin (Pharmacia, Washington, USA), and cells were incubated at 37 °C, 5% CO_2 for a further 1 hour. Culture media was replaced with media containing 10 μg/ml gentamycin, and where necessary, 1 mM IPTG, and cells were incubated at 37 °C, 5% CO_2 to the required time, post infection.

2.9.2 *Salmonella* infection of RAW264.7 cells

RAW264.7 cells were seeded to 24 well plates at a concentration of 3 x 10^5 cells per well one day before infection. 10 ml LB broths containing appropriate antibiotic were inoculated with *Salmonella* strains and incubated at 37 °C overnight with shaking at 180 rpm. On the day of infection, the OD_{600} readings of the overnight culture were read and used to estimate bacterial counts. Cells were then infected at a multiplicity of infection (MOI) of 10, following the protocol described in section 2.9.1 of this thesis.

2.10 Immunofluorescence microscopy

At required timepoints post-transfection or –infection, cells were fixed in 4% (w/v) paraformaldehyde (Sigma) in PBS for 12 minutes on ice. Cells were washed 3 times with PBS, then incubated in 50 mM NH_4Cl at room temperature for 20 minutes. Cells were washed twice with PBS, then incubated in 0.2% (v/v) Triton X-100 in PBS at room temperature for 3 minutes. Cells were washed three times with PBS, then blocked in 3% (w/v) BSA in PBS at room temperature for 30 minutes. Cells were then incubated in the appropriate primary antibody for 1 hour at room temperature. Cells were washed three times with PBS, then incubated in the appropriate Alexa-Fluor conjugated secondary antibody for 30 minutes at room temperature. Cells were subsequently stained with Hoechst solution diluted in PBS for 10 minutes at room temperature. Coverslips were mounted onto microscope slides using Prolong Gold mounting agent (Life Technologies). Cells were visualised and digital images acquired using a Zeiss confocal laser scanning microscope with a 100x/EC Epiplan-Apochromat oil immersion objective.

2.11 Immunoprecipitation

2.11.1 Immunoprecipitation by haemagglutinin tag

At required time points post-infection, cells were washed twice with cold PBS, then lysed in cold 1 x KalB lysis buffer (50 mM Tris-HCl pH 7.4, 150 mM NaCl, 1 mM EDTA, 1% (vol/vol) Triton X-100) supplemented with 2 mM Na_3VO_4, 10 mM NaF, 1 mM PMSF, and 1 x EDTA-free Complete protease inhibitor cocktail (Roche). Cell lysate was incubated for at least 30 minutes on ice, then cell debris was pelleted at 13000 rpm at 4 °C for 12 minutes.

A 60 µl sample of the soluble fraction was taken as an input sample, mixed with 20 µl LDS and DTT, and heated to 70 °C for 10 minutes. Haemagglutinin-tagged protein was affinity purified using 50 µl of anti-HA tag mAB magnetic beads (MBL International Corporation). Beads were first washed twice with lysis buffer, then mixed with the remaining soluble protein fraction and incubated rotating at 4 °C overnight. Following this, beads were washed three times with KalB lysis buffer. Bound haemagglutinin-tagged protein was eluted by incubating beads in 60 µl of 100 µg/ml HA peptide (Sigma-Aldrich), rotating at 4 °C for 30 minutes. Eluate was mixed with 4 x LDS and DTT, and heated to 70 °C for 10 minutes. Input and eluate samples were electrophoresed, then visualised either by protein stain or immunoblot.

2.11.2 Immunoprecipitation by GFP-Trap®

At required time points post-transfection, cells were lysed and the insoluble fraction removed as described in section 2.11.1. Immunoprecipitation of GFP fusion proteins was performed using a GFP-Trap®-M kit (Chromotek, Germany), according to the manufacturer's instructions. Bound protein was eluted by boiling in LDS and DTT at 80 to 90 °C for 10

minutes. Input and eluate samples were electrophoresed, then visualised either by protein stain or immunoblot.

2.11.3 Immunoprecipitation by Anti-FLAG® M2 Magnetic Beads

At required time points post-transfection, cells were lysed and the insoluble fraction removed as described in section 2.11.1. Immunoprecipitation of FLAG-tagged proteins was performed using Anti-FLAG® M2 Magnetic Beads (Sigma-Aldrich), according to the manufacturer's instructions. Bound protein was eluted by incubating beads in 60 µl of 150 µg/ml Flag peptide (Sigma-Aldrich), rotating at 4 °C for 30 minutes. Eluate was mixed with LDS and DTT, and boiled at 80 to 90 °C for 10 minutes. Input and eluate samples were electrophoresed, then visualised either by protein stain or immunoblot.

2.12 Protein electrophoresis and visualisation

2.12.1 Bolt® protein gel electrophoresis

Cells were lysed in cold 1 x KalB lysis buffer (50 mM Tris-HCl pH 7.4, 150 mM NaCl, 1 mM EDTA, 1% (vol/vol) Triton X-100) supplemented with 2 mM Na_3VO_4, 10 mM NaF, 1 mM PMSF, and 1 x EDTA-free Complete protease inhibitor cocktail (Roche). Cell lysate was incubated for at least 30 minutes on ice, then cell debris was pelleted at 13000 rpm at 4 °C for 12 minutes. The soluble protein fraction was mixed with 4 x Bolt® LDS sample buffer (Life Technologies) and DTT (Astral Scientific) to a final concentration of 50 mM. Proteins were boiled at 80 to 90 °C for 10 minutes, then loaded to Bolt® 4-12% Bis-Tris Plus gels (Life Technologies) alongside SeeBlue® pre-stained protein ladder (Life Technologies). Proteins were separated by electrophoresis using an XCell SureLock™ Mini-Cell system (Life Technologies) with 1 x Bolt® MES SDS or 1 x Bolt® MOPS SDS running buffer (Life Technologies), according to the manufacturer's instructions.

2.12.2 Protein visualisation using gel stains

Following electrophoresis, gels were stained with either Coomassie Blue stain (0.025% (w/v) Coomassie Brilliant blue, 40% (v/v) methanol, 10% (v/v) glacial acetic acid), or colloidal Coomassie Blue stain (0.025% (w/v) Coomassie Brilliant Blue G-250, 5% (w/v) aluminium sulphate, 10% (v/v) ethanol, 2% (v/v) orthophosphoric acid). Gels were stained overnight or as required, with shaking at 60 rpm. Gels were then destained with Coomassie destain solution (10% (v/v) ethanol, 2% (v/v) orthophosphoric acid) for 1 hour or as required, with shaking at 60 rpm. Gels were finally rinsed in dH_2O, and imaged under whitelight using an MFChemiBis imaging station.

Where required, prior to staining with Coomassie, gels were stained with SYPRO® Ruby protein gel stain (Sigma-Aldrich) according to the manufacturer's instructions, and imaged under UV illumination. Briefly, following electrophoresis gels were incubated in SYPRO® Ruby fixative buffer (50% (v/v) methanol, 7% (v/v) acetic acid) at room temperature for 1 hour with shaking at 60 rpm. Gels were then incubated in SYPRO® Ruby stain at 4 °C overnight with shaking at 60 rpm. Next, gels were incubated in SYPRO® Ruby wash buffer (10% (v/v) methanol, 7% (v/v) acetic acid) at room temperature for 30 minutes with shaking at 60 rpm. Gels were rinsed with dH_2O and imaged under UV illumination using an MFChemiBis imaging station.

2.12.3 Immunoblotting

Following electrophoresis, proteins were transferred onto nitrocellulose membranes using the iBlot2® gel transfer device (Life Technologies) and iBlot2® nitrocellulose transfer stacks (Life Technologies), according to the manufacturer's instructions. Membranes were blocked in 5% (w/v) skim milk in TBS (20 mM Tris, 50 mM NaCl, pH 8.0) with 0.1% (v/v)

Tween 20 at room temperature for at least 1 hour with shaking at 60 rpm. Membranes were rinsed and washed in TBS Tween, then probed with one of the following primary antibodies as required at 4 °C overnight with shaking at 60 rpm: mouse monoclonal anti-Golgin-97 (Invitrogen), mouse monoclonal anti-His (Bio-Rad), rabbit polyclonal anti-GST (Cell Signaling), mouse monoclonal anti-*O*-GlcNAc (Cell Signaling), rabbit monoclonal anti-ArgGlcNAc (Abcam), rabbit polyclonal anti-VDAC (Millipore), mouse monoclonal anti-GAPDH (Cell Signaling), mouse monoclonal anti-caspase 8 (Cell Signaling), rabbit monoclonal anti-caspase 3 (Cell Signaling), rabbit monoclonal anti-TNFR1 (Cell Signaling), rabbit monoclonal anti-RIPK1 (Cell Signaling), rabbit polyclonal anti-TRAF2 (Cell Signaling), mouse monoclonal anti-cIAP1 (R&D systems), mouse monoclonal anti-HA (BioLegend), mouse monoclonal anti-GFP (Roche), mouse monoclonal anti-Flag M2-HRP (Sigma), mouse monoclonal anti-TRADD (BD Transduction Lab) or mouse monoclonal anti-β-actin (Sigma). Membranes were again rinsed and washed in TBS Tween, then probed with secondary antibodies as required at room temperature for one hour with shaking at 60 rpm. Membranes were rinsed and washed in TBS Tween at room temperature for at least 45 minutes with shaking at 60 rpm. Antibody binding was detected using chemiluminescent substrates for horseradish peroxidase (HRP) (ECL western blotting reagents (GE Healthcare) or ECL Prime western blotting reagent (Amersham, USA), according to the manufacturer's instructions, and visualised using an MFChemiBis imaging station.

For membranes required to be developed twice using two sets of primary antibodies, Restore™ PLUS Western Blot stripping buffer (Thermo Fisher Scientific) was applied on the blots with shaking at 60 rpm for 10 min following first time development. The stripped membranes were rinsed and washed in TBS Tween before being blocked in 5% (w/v) skim milk in TBS Tween with shaking at 60 rpm for 60 min at room temperature. Blocked

membranes were rinsed and washed in TBS Tween, and then probed with the additional primary antibody.

2.13 *In vitro* assays using recombinant proteins

2.13.1 Recombinant protein production

His-tagged and GST-tagged fusion proteins were purified from bacterial cultures using Novagen His-Bind® purification kit or Novagen GST-Bind™ purification kit, respectively, according to the manufacturer's instructions. Briefly, plasmids encoding either 6 x His-tagged or GST-tagged fusion proteins were transformed into BL21 C43 (DE3) *E. coli*. Overnight cultures grown in LB with appropriate antibiotics were used to inoculate a 200 mL LB subculture (1:100) which was grown for 3 hours at 37 °C with shaking at 180 rpm to an optical density of 0.6. Subcultures were induced with 1 mM isopropyl-β-D-thiogalactopyranoside (IPTG; AppliChem, Darmstadt, Germany), and grown for a further 3 hours. Cultures were then centrifuged at 10000 rpm at 4 °C for 15 minutes, then resuspended in the appropriate resuspension buffer. Resuspended bacteria were lysed using an EmulsiFlex-C3 High Pressure Homogenizer (Avestin), according to the manufacturer's instructions. Lysates were centrifuged at 13000 rpm at room temperature for 30 minutes, and proteins were purified from the soluble fraction by either nickel- or glutathione-affinity chromatography, according to the manufacturer's instructions.

2.13.2 *In vitro* glycosylation assay

Protein concentrations were determined using a bicinchoninic acid (BCA) kit (Thermo Fisher Scientific). Recombinant proteins (approximately 1 µg) were incubated alone, together, and in the presence of 1 mM UDP-GlcNAc (Sigma-Aldrich). Reactions were made to a total volume of 80 µl in TBS (50 mM Tris, 150 mM NaCl, pH 7.6) supplemented

with 10 mM $MgCl_2$ and 10 mM $MnCl_2$. Reactions were incubated at 37 °C for 4 hours. To detect *in vitro* glycosylation, reactions were either electrophoresed and probed by Western blot, or processed for mass spectrometry analysis as below.

2.14 Mass spectrometry experiments

2.14.1 Digestion of gel-separated proteins

Affinity purified proteins were separated using SDS-PAGE, fixed and visualized with Coomassie G-250 according to protocol of Kang *et al.* (2002). Bands of interest were excised and destained in a 50:50 solution of 50 mM NH_4HCO_3 / 100% ethanol for 20 minutes at room temperature with shaking at 750 rpm. Destained samples were then washed with 100% ethanol, vacuum-dried for 20 minutes and rehydrated in 50 mM NH_4HCO_3 plus 10 mM DTT. Reduction was carried out for 60 minutes at 56 °C with shaking. The reducing buffer was then removed and the gel bands washed twice in 100% ethanol for 10 minutes to remove residual DTT. Reduced ethanol washed samples were sequentially alkylated with 55 mM Iodoacetamide in 50 mM NH_4HCO_3 in the dark for 45 minutes at room temperature. Alkylated samples were then washed with two rounds of 100% ethanol and vacuum-dried. Alkylated samples were then rehydrated with 12 ng/µl trypsin (Promega) in 40 mM NH_4HCO_3 at 4 °C for 1 hour. Excess trypsin was removed, gel pieces were covered in 40 mM NH_4HCO_3 and incubated overnight at 37 °C. Peptides were concentrated and desalted using C18 stage tips (Ishihama *et al.*, 2006, Rappsilber *et al.*, 2007) before analysis by LC-MS.

2.14.2 Identification of ArgGlcNAc affinity enriched proteins using reversed phase LC-MS

Purified peptides prepared were re-suspend in Buffer A* (0.1% trifluoroacetic acid, 2% acetonitrile, MeCN) and separated using an in house packaged 25 cm, 75 µm inner diameter, 360 µm outer diameter, 1.7 µm 130 Å CSH C18 (Waters, Manchester, UK) reverse phase analytical column with an integrated HF etched nESI tip. Samples were loaded directly onto the column using a ACQUITY UPLC M-Class System (Waters) at 600 nL/minute for 20 minutes with Buffer A (0.1% formic acid) and eluted at 300 nL/minute using a gradient altering the concentration of Buffer B (99.9% ACN, 0.1% FA) from 0% to 32% B over 90 minutes, then from 32% to 40% B in the next 10 minutes, then increased to 80% B over an 8 minute period, held at 100% B for 2 minutes, and then dropped to 0% B for another 20 minutes. RP separated peptides were infused into a Q-Exactive (Thermo Fisher Scientific) mass spectrometer and data acquired using data dependent acquisition. One full precursor scan (resolution 70,000; 350-2,000 m/z, AGC target of 3×10^6) followed by 10 data-dependent HCD MS-MS events (resolution 17.5 k AGC target of 1×10^5 with a maximum injection time of 200 ms, NCE 28 with 20% stepping) were allowed with 35 s dynamic exclusion enabled.

2.14.3 Isolation of proteins for Arg-glycosylation peptide-affinity purification

Infected cells were washed three times in ice-cold PBS and lysed by scraping with ice-cold guanidinium chloride lysis buffer (6 M GdmCl, 100 mM Tris pH 8.5, 10 mM TCEP, 40 mM 2-Chloroacetamide) on a bed of ice according to the protocol of Humphrey *et al.* (2015). Lysates were collected and boiled at 95 ˚C for 10 minutes with shaking at 2000 rpm to shear DNA and inactivate protease activity. Lysates were then cooled for 10 minutes on ice then boiled again at 95 ˚C for 10 minutes with shaking at 2000 rpm. Lysates were cooled and

protein concentration determined using a BCA assay. 2 mg of protein from each sample was acetone precipitated by mixing 4 volumes of ice-cold acetone with one volume of sample. Samples were precipitated overnight at -20 ˚C and then spun down at 4000 G for 10 minutes at 4 ˚C. The precipitated protein pellets were resuspended with 80% ice-cold acetone and precipitated for an additional 4 hours at -20 ˚C. Samples were spun down at 17000 G for 10 minutes at 4 ˚C to collect precipitated protein, the supernatant was discarded and excess acetone driven off at 65 ˚C for 5 minutes.

2.14.4 Digestion of complex protein lysates

Dried protein pellets were resuspended in 6 M urea, 2 M thiourea, 40 mM NH_4HCO_3 and reduced / alkylated prior to digestion with Lys-C (1/200 w/w) then trypsin (1/50 w/w) overnight as previously described (Scott *et al.*, 2011). Digested samples were acidified to a final concentration of 0.5% formic acid and desalted with 50 mg tC18 SEP-PAK (Waters corporation, Milford, USA) according to the manufacturer's instructions. Briefly, tC18 SEP-PAKs were conditioned with buffer B (80% ACN, 0.1% formic acid), washed with 10 volumes of Buffer A* (0.1% TFA, 2% ACN), sample loaded, column washed with 10 volumes of Buffer A* and bound peptides eluted with buffer B then dried.

2.14.5 Arg-glycosylation affinity purification

Peptide affinity purification was accomplished according to the protocol of Udeshi *et al.* (2013), modified to allow for Arg-GlcNAc enrichment. Briefly, aliquots of 100 µl of Protein A/G plus Agarose beads (Santa Cruz, Santa Cruz CA) were washed three times with 1 ml of immunoprecipitation buffer (IAP, 10 mM Na_3PO_4, 50 mm NaCl, 50 mM MOPS, pH 7.2) and tumbled overnight with 10 µg of anti-Arg-GlcNAc antibody (ab195033, Abcam) at 4 ˚C. Coupled anti-Arg-GlcNAc beads were then washed three times with 1 ml of 100 mM

sodium borate (pH 9) to remove non-bound proteins and cross-linked for 30 minutes rotating using 20 mM Dimethyl Pimelimidate (Thermo Fisher Scientific) in 100 mM HEPES, pH 8.0. Cross-linking was quenched by washing beads with 200 mM ethanolamine, pH 8.0, three times then rotating the beads in an additional 1 ml 200 mM ethanolamine, pH 8.0 for 2 hours at 4 ˚C. Beads were washed three times with IAP buffer and used immediately.

Purified peptides were resuspended in 1 ml IAP buffer and the pH checked to ensure compatibility with affinity conditions. Peptide lysates were then added to the prepared cross-linked anti-Arg-GlcNAc antibody beads and rotated for 3 hours at 4 ℃. Upon completion antibody beads were spun down at 3000 G for 2 minutes at 4 ℃ and the unbound peptide lysates collected. Antibody beads were then washed six times with 1 ml of ice-cold IAP buffer and Arg-GlcNAc peptides eluted using two rounds of acid elution. For each elution round, 100 µl of 0.2% TFA was added and antibody beads allowed to stand at room temperature with gentle shaking every minute for 10 minutes. Peptide supernatants were collected and desalted using C18 stage tips (Ishihama *et al.*, 2006, Rappsilber *et al.*, 2007) before analysis by LC-MS.

2.14.6 Identification of Arg-GlcNAc affinity enriched peptides and FLAG-tagged proteins using reversed phase LC-MS

Purified peptides prepared were re-suspend in Buffer A* and separated using a two-column chromatography set up composed of a PepMap100 C18 20 mm x 75 µm trap and a PepMap C18 500 mm x 75 µm analytical column (Thermo Fisher Scientific). Samples were concentrated onto the trap column at 5 µL/min for 5 minutes and infused into an Orbitrap Fusion™ Lumos™ Tribrid™ Mass Spectrometer (Thermo Fisher Scientific) at 300 nl/minute via the analytical column using an Dionex Ultimate 3000 UPLC (Thermo Fisher Scientific). 125 minute gradients were run altering the buffer composition from 1% buffer B to 28% B

over 90 minutes, then from 28% B to 40% B over 10 minutes, then from 40% B to 100% B over 2 minutes, the composition was held at 100% B for 3 minutes, and then dropped to 3% B over 5 minutes and held at 3% B for another 15 minutes. The Lumos™ Mass Spectrometer was operated in a data-dependent mode automatically switching between the acquisition of a single Orbitrap MS scan (120,000 resolution) every 3 seconds and Orbitrap EThcD for each selected precursor (maximum fill time 100 ms, AGC 5*104 with a resolution of 30000 for Orbitrap MS-MS scans). For parallel reaction monitoring (PRM) experiments the known tryptic Arg-modified sites of TRADD (Li *et al.*, 2013) and FADD (Pearson *et al.*, 2013) (Uniprot accession: B2RRZ7 and Q3U0V2 respectively) were monitored using the predicted m/z for the +2 and +3 charge states. Data-independent acquisition was performed by switching between the acquisition of a single Orbitrap MS scan (120000 resolution, m/z 300-1500) every 3 seconds and Orbitrap EThcD for each PRM precursor (maximum fill time 100 ms, AGC $5*10^4$ with a resolution of 60000 for Orbitrap MS-MS scans).

2.14.7 Mass spectrometry data analysis

Identification of proteins and Arg-glycosylated peptides was accomplished using MaxQuant (v1.5.3.1) (Cox and Mann, 2008). Searches were performed against the Mouse (Uniprot proteome id UP000000589 - Mus musculus, downloaded 18-05-2016, 50306 entries), *Salmonella* Typhimurium SL1344 (Uniprot proteome id UP000008962- *Salmonella* Typhimurium SL1344, downloaded 18-05-2016, 4,657 entries) or human (Uniprot proteome id UP000005640- *Homo sapiens*, downloaded 24/10/2013, 84,843 entries) proteomes depending on the samples with carbamidomethylation of cysteine set as a fixed modification. Searches were performed with trypsin cleavage specificity allowing 2 miscleavage events and the variable modifications of oxidation of methionine, N-Acetylhexosamine addition to arginine (Arg-GlcNAc) and acetylation of protein N-termini. The precursor mass tolerance

was set to 20 parts-per-million (ppm) for the first search and 10 ppm for the main search, with a maximum false discovery rate (FDR) of 1.0% set for protein and peptide identifications. To enhance the identification of peptides between samples the Match Between Runs option was enabled with a precursor match window set to 2 minutes and an alignment window of 10 minutes. For label-free quantitation, the MaxLFQ option within Maxquant (Cox *et al.*, 2014) was enabled in addition to the re-quantification module. The resulting protein group output was processed within the Perseus (v1.4.0.6) (Tyanova *et al.*, 2016) analysis environment to remove reverse matches and common protein contaminates prior. For LFQ comparisons missing values were imputed using Perseus and Pearson correlations visualized using Matlab R2015a (http://www.mathworks.com).

2.15 Mouse infection studies.

All experiments involving mice were approved by the Animal Ethics Committee at The University of Melbourne, under project number 1613898. All experiments were conducted in accordance with the Australian Code of Practice for the Care and Use of Animals for Scientific Purposes, 8th edition, 2013. C57BL/6 and *Trail-R*$^{-/-}$ mice were obtained from John Silke at the Walter and Elisa Hall Institute, Melbourne, Australia, and were acclimatised at the Peter Doherty Institute for Infection and Immunity for 1 week prior to infection. For intravenous infection, *S.* Typhimurium strain BRD509 (271, 272) was sub-cultured from a fresh broth culture, grown shaking at 180 rpm until the mid-logarithmic phase, and frozen down with 10% glycerol at -80°C until use. Mice were intravenously injected via the tail vein with 2×10^5 CFU in 200 µl sterile PBS. At designated time points, mice were euthanised by CO_2 asphyxiation and spleen and liver were resected for enumeration of bacterial load and quantification of cytokine levels. Serum was also collected for cytokine analysis.

2.16 Cytokine analysis

The BD™ Cytometric Bead Array (CBA) Mouse Inflammation Kit (BD Biosciences) was used to quantify cytokines in tissue homogenates and serum as per manufacturer's instructions. Prepared CBA assay samples were analysed for the presence of six mouse cytokine markers of inflammation (IL-6, IL-10, MCP-1, IFNγ, TNF and IL-12p70) using a BD™ FACS Canto II. The detection limit (dotted line) for cytokine concentration was determined as the lowest data point on the standard curve that had >80% actual recovery compared to expected concentration.

Table 2.1 Strains used in this study

Table 2.1.1 *E. coli* strains

Strain	Relevant characteristics	Reference
XL1-Blue	*E. coli recA1 endA1 gyrA96 thi-1 hsdR17 supE44 relA1 lac[F'proAB lacIqZΔM15 Tn10 (Tet^r)]*	Stratagene
DH5α	laboratory strain K-12 *endA1 hsdR17* (r_k^- m_k^+) *supE44 thi-1 recA1 gyrA* (Nal^R) *relA* Δ(*lacIZYA-argF*) U169 deo*R* (Φ80*d*lacΔ[*lacZ*]M15)	(273)
BL21 C43 (DE3)	*E. coli used for expression of proteins for affinity purification*	Novagen

Table 2.1.2 *Salmonella* strains

Strain	Relevant characteristics	Reference
SL1344	Wild type *S. enterica* serovar Typhimurium strain SL1344	Nathaniel Brown
Δ*sseK1/2/3*	SL1344 Δ*sseK1*Δ*sseK2*Δ*sseK3*	(243)
Δ*sseK2/3*	SL1344 Δ*sseK2*Δ*sseK3*	(243)
Δ*sseK1/3*	SL1344 Δ*sseK1*Δ*sseK3*	(243)
Δ*sseK1/2*	SL1344 Δ*sseK1*Δ*sseK2*	(242)
Δ*sseK1*	SL1344 Δ*sseK1*	(242)
Δ*sseK2*	SL1344 Δ*sseK2*	(242)
Δ*sseK3*	SL1344 Δ*sseK3*	(243)
Δ*ssaR*	SL1344 Δ*ssaR*	Nathaniel Brown
BRD509	SL1344 Δ*aroA* Δ*aroD*	(274, 275)

Table 2.1.3 *S. cerevisiae* strains

Strain	Relevant characteristics	Reference
S. cerevisiae Y2H gold	*MATa, trp1-901, leu2-3, 112, ura3-52, his3-200, gal4Δ, gal80Δ, LYS2 : : GAL1$_{UAS}$–Gal1$_{TATA}$–His3, GAL2$_{UAS}$–Gal2$_{TATA}$–Ade2 URA3 : : MEL1$_{UAS}$–Mel1$_{TATA}$ AUR1-C MEL1*	Clontech
S. cerevisiae AH 109	*MATa, trp1-901, leu2-3, 112, ura3-52, his3-200, gal4*Δ, *gal80*Δ, *LYS2::GAL1$_{UAS}$-GAL1$_{TATA}$-HIS3, GAL2$_{UAS}$GAL2$_{TATA}$-ADE2, URA3::MEL1$_{UAS}$-MEL1$_{TATA}$-lacZ*	Clontech

Table 2.2 Plasmids used in this study

Plasmid	Relevant characteristics	Reference
pTrc99A	Cloning vector for expression of proteins from P*trc*	Pharmacia Biotech
pTrc99A-SseK1	*sseK1* from *S.* Typhimurium SL1344 in pTrc99A, Amp^R	Tania Wong
pTrc99A-SseK1$_{DxD(229-231)AAA}$	*sseK1* from *S.* Typhimurium SL1344 in pTrc99A, with DxD(229-231) putative catalytic motif mutated to AAA, Amp^R	This study
pTrc99A-SseK1$_{E255A}$	*sseK1* from *S.* Typhimurium SL1344 in pTrc99A, with Glu255 catalytic site mutated to Ala, Amp^R	This study
pTrc99A-SseK2	*sseK2* from *S.* Typhimurium SL1344 in pTrc99A, Amp^R	Tania Wong
pTrc99A-SseK2$_{DxD(239-241)AAA}$	*sseK2* from *S.* Typhimurium SL1344 in pTrc99A with DxD(239-241) putative catalytic motif mutated to AAA, Amp^R	This study
pTrc99A-SseK2$_{E271A}$	*sseK2* from *S.* Typhimurium SL1344 in pTrc99A, with Glu271 catalytic site mutated to Ala, Amp^R	This study
pTrc99A-SseK3	*sseK3* from *S.* Typhimurium SL1344 in pTrc99A, Amp^R	Tania Wong
pTrc99A-SseK3$_{DxD(226-228)AAA}$	*sseK3* from *S.* Typhimurium SL1344 in pTrc99A with DxD(226-228) putative catalytic motif mutated to AAA, Amp^R	This study
pTrc99A-SseK3$_{E258A}$	*sseK3* from *S.* Typhimurium SL1344 in pTrc99A, with Glu258 catalytic site mutated to Ala, Amp^R	This study
pEGFP-C2	N-terminal Green fluorescent protein (GFP) expression vector	Clontech
pEGFP-C2-NleB1	*nleB1* from EPEC E2348/69 in pEGFP-C2, Kan^R	(244)

pEGFP-C2-SseK1	*sseK1* from *S.* Typhimurium SL1344 in pEGFPC2, Kan^R	Michelle Kelly
pEGFP-C2-$SseK1_{DxD(229-231)AAA}$	*sseK1* from *S.* Typhimurium SL1344 in pEGFPC2 with DxD(229-231) putative catalytic motif mutated to AAA, Kan^R	Tania Wong
pEGFP-C2-$SseK1_{E255A}$	*sseK1* from *S.* Typhimurium SL1344 in pEGFP-C2, with Glu255 catalytic site mutated to Ala, Kan^R	This study
pEGFP-C2-SseK2	*sseK2* from *S.* Typhimurium SL1344 in pEGFPC2, Kan^R	Tania Wong
pEGFP-C2-$SseK2_{DxD(239-241)AAA}$	*sseK2* from *S.* Typhimurium SL1344 in pEGFPC2 with DxD(239-241) putative catalytic motif mutated to AAA, Kan^R	Tania Wong
pEGFP-C2-SseK3	*sseK3* from *S.* Typhimurium SL1344 in pEGFPC2, Kan^R	Tania Wong
pEGFP-C2-$SseK3_{DxD(226-228)AAA}$	*sseK3* from *S.* Typhimurium SL1344 in pEGFPC2 with DxD(226-228) putative catalytic motif mutated to AAA, Kan^R	Tania Wong
pEGFP-C2-$SseK3_{E258A}$	*sseK3* from *S.* Typhimurium SL1344 in pEGFPC2, with Glu258 catalytic site mutated to Ala, Kan^R	This study
p3xFLAG-*Myc*-CMV-24	Dual tagged N-terminal Met-3xFLAG and C-terminal *c-myc* expression vector	Sigma-Aldrich
pFLAG-FADD	Full length FADD in p3xFLAG-Myc-CMV-24, Amp^R	Ashley Mansell
pFLAG-$FADD_{R117K}$	Mouse *FADD* carrying the mutation R117K in p3xFLAG-*Myc*-CMV-24, Amp^R	Cristina Giogha
pFLAG-TRADD	Human TRADD in p3xFLAG-*Myc*-CMV, Amp^R	Ashley Mansell
pFLAG-$TRADD_{R235A}$	Human TRADD with Arg235 mutated to Ala, in p3xFLAG-*Myc*-CMV, Amp^R	Cristina Giogha
pFLAG-$TRADD_{R245A}$	Human TRADD with Arg245 mutated to Ala, in p3xFLAG-*Myc*-CMV, Amp^R	This study

pFLAG-TRADD$_{R235A,R245A}$	Human TRADD with Arg235 and Arg245 mutated to Ala, in p3xFLAG-*Myc*-CMV, Amp^R	This study
pFLAG-GSTP1	Human GSTP1 in p3xFLAG-*Myc*-CMV, Amp^R	This study
pFLAG-PCMT1	Human PCMT1 in p3xFLAG-*Myc*-CMV, Amp^R	This study
pFLAG-hTRAILR2$_{DD}$	Human TRAILR2 death domain in p3xFLAG-*Myc*-CMV, Amp^R	This study
pFLAG-hTNFR1$_{DD}$	Human TNFR1 death domain in p3xFLAG-*Myc*-CMV, Amp^R	Cristina Giogha
pET28a	Bacterial expression vector with T7lac promoter including N-terminal 6 x Histidine tag	Novagen
pET28a-FADD	Full length FADD in pET28a, Kan^R	(244)
pET28a-GSTP1	Human GSTP1 in pET28a, Kan^R	This study
pET28a-hTRAILR2$_{DD}$	Human TRAILR2 death domain in pET28a, Kan^R	Cristina Giogha
pGEX-4T-1	N-terminal glutathione S-transferase (GST) cloning/expression vector	GE Healthcare
pGEX-NleB1	*nleB1* from EPEC E2348/69 in pGEX-4T-1, Amp^R	(244)
pGEX-SseK1	*sseK1* from *S.* Typhimurium SL1344 in pGEX-4T-1, Amp^R	Michelle Kelly
pGEX-SseK3	*sseK3* from *S.* Typhimurium SL1344 in pGEX-4T-1, Amp^R	Tania Wong
pGADT7-AD	High copy number yeast expression vector carrying a GAL4 activation domain, Amp^R (bacterial selection), Leu (selectable marker in yeast)	Clontech
pGADT7-AD-FADD	Human FADD in pGADT7-AD, Amp^R, Leu	Tania Wong
pGADT7-AD-FADD$_{DD}$	Death domain of FADD in pGADT7-AD, Amp^R, Leu	Tania Wong

pGADT7-AD-GSTP1	Human GSTP1 in in pGADT7-AD, Amp^R, Leu	This study
pGADT7-AD-PCMT1	Human PCMT1 in in pGADT7-AD, Amp^R, Leu	This study
pGADT7-AD-$TNFR1_{DD}$	Death domain of TNFR1 in pGADT7-AD, Amp^R, Leu	Tania Wong
pGADT7-AD-$hTRAILR2_{DD}$	Death domain of DR5 in pGADT7-AD, Amp^R, Leu	Tania Wong
pGBKT7-BD	High copy number yeast expression vector carrying a GAL4 DNA binding domain, Kan^R (bacterial selection), Trp (selectable marker in yeast)	Clontech
pGBKT7-BD-NleB1	*nleB1* from EPEC E2348/69 in pGBKT7, Kan^R, Trp	Tania Wong
pGBKT7-BD-SseK1	*sseK1* from *S.* Typhimurium SL1344 in pGBKT7, Kan^R, Trp	Tania Wong
pGBKT7-BD-SseK1 DxD(229-231)AAA	*sseK1* from *S.* Typhimurium SL1344 in pGBKT7, with DxD(229-231) putative catalytic motif mutated to AAA, Kan^R, Trp	This study
pGBKT7-BD-$SseK1_{E255A}$	*sseK1* from *S.* Typhimurium SL1344 in pGBKT7, with Glu255 catalytic site mutated to Ala, Kan^R, Trp	This study
pGBKT7-BD-SseK2	*sseK2* from *S.* Typhimurium SL1344 in pGBKT7, Kan^R, Trp	Tania Wong
pGBKT7-BD-SseK2 DxD(239-241)AAA	*sseK2* from *S.* Typhimurium SL1344 in pGBKT7 with DxD(239-241) putative catalytic motif mutated to AAA, Kan^R, Trp	This study
pGBKT7-BD-$SseK2_{E271A}$	*sseK2* from *S.* Typhimurium SL1344 in pGBKT7, with Glu271 catalytic site mutated to Ala, Kan^R, Trp	This study
pGBKT7-BD-SseK3	*sseK3* from *S.* Typhimurium SL1344 in pGBKT7, Kan^R, Trp	Tania Wong

Table 2.3 Primers used in this study

Primer	Primer sequence 5'-3'
$pTrc99A_F$	CGGTTCTGGCAAATATTC
$pTrc99A_R$	GCAGTTCCCTACTCTCGC
$p3xFlag\text{-}Myc\text{-}CMV\text{-}24_F$	AATGTCGTAATAACCCCGCCCCGTTGACGC
$p3xFlag\text{-}Myc\text{-}CMV\text{-}24_R$	TATTAGGACAAGGCTGGTGGGCAC
$pEGFP\text{-}C2_F$	AACACCCCCATCGGCG
$pEGFP\text{-}C2_R$	GTAACCATTATAAGCTGC
$pGBKT7\text{-}BD_F$	AATACGACTCACTATAGG
$pGBKT7\text{-}BD_R$	CGTTTTAAAACCTAAGAGTC
$pGADT7\text{-}AD_F$	AATACGACTCACTATAGG
$pGADT7\text{-}AD_R$	GGTGCACGATGCACAG
$pGEX\text{-}4T\text{-}1_F$	CGTATTGAAGCTATCCCACAA
$pGEX\text{-}4T\text{-}1_R$	GGGAGCTGCATGTGTCAGAG
$pET28a_F$	AATACGACTCACTATAGG
$pET28a_R$	GCTAGTTATTGCTCAGCGG
$SseK1_F$	CGGAATTCATGGAGCATTTAATTGTTATGATCCC
$SseK1_R$	CGGGATCCCTACGCATAATCCGGCACATCATACGGATA CGCATAATCCGGCACATCATACGGATACTGCACATGCC TCGCCC
$SseK2_F$	CGGAATTCATGGCACGTTTTAATGCCG
$SseK2_R$	CGGGATCCTTACGCATAATCCGGCACATCATACGGATA CGCATAATCCGGCACATCATACGGATACCTCCAAGAAC TGGCAG
$SseK3_F$	CGGAATTCATGTTTTCTCGAGTCAGAGG
$SseK3_R$	CGGGATCCTTACGCATAATCCGGCACATCATACGGATA CGCATAATCCGGCACATCATACGGATATCTCCAGGAGC TGATAGTC
$GST\text{-}SseK3_F$	CGCGAATTCATGTTTTCTCGAGTCAGAGGTTTTC
$GST\text{-}SseK3_R$	CGCGTCGACTTATCTCCAGGAGCTGATAGTCAAACTGC
$FADD_F$	CGCGAATTCATGCTGTGTGCAGCATTTAACGTCATATG
$FADD_R$	CGCGGATCCTTACTGCTGAACCTCTTGTACCAGG

$hTNFR1_{DD-F}$	CGCCATATGATGACGCTGTACGCCGTGGTGG
$hTNFR1_{DD-R}$	CGCGGATCCTCACTCGATGTCCTCCAGGCAGC
$hTRAILR2_{DD-F}$	CGCGAATTCATGGATCCCACTGAGACTCTGAGAC
$hTRAILR2_{DD-R}$	CGCGGATCCTTAGAACTTTCCAGAGCTCAACAAGTG
$SseK1_{DXD-F}$	GGTGTATATATCTTGCTGCTGCTATGATTATCACGGAAAAACTGG
$SseK1_{DXD-R}$	CCAGTTTTTCCGTGATAATCATAGCAGCAGCAAGATATATACACC
$SseK2_{DXD-F}$	GTGGGTGCATATATCTTGCTGCAGCTATGTTACTTACTGATAAAC
$SseK2_{DXD-R}$	GTTTATCAGTAAGTAACATAGCTGCAGCAAGATATATGCACCCAC
$SseK3_{DXD-F}$	CTGGAGGTGGCTGCATATATCTTGCTGCTGCTATGTTACTTACAG
$SseK3_{DXD-R}$	CTGTAAGTAACATAGCAGCAGCAAGATATATGCAGCCACCTCCAG
$SseK1_{E255A-F}$	CGTGCTTCTATGGCAAACGGGATAATAGCT
$SseK1_{E255A-R}$	AGCTATTATCCCGTTTGCCATAGAAGCACG
$SseK2_{E271A-F}$	TGTTAGCCTTGCAAATGGGATTATTGCTGT
$SseK2_{E271A-R}$	ACAGCAATAATCCCATTTGCAAGGCTAACA
$SseK3_{E258A-F}$	GCATGAGTCTTGCAAATGGGATTATCGCCG
$SseK3_{E258A-R}$	CGGCGATAATCCCATTTGCAAGACTCATGC
$hTRADD_{R235A-F}$	CGCAAGGTGGGGGCCTCACTGCAGCGAG
$hTRADD_{R235A-R}$	CTCGCTGCAGTGAGGCCCCCACCTTGCG
$hTRADD_{R245A-F}$	CGCCGGGTCCGCCAGCGCCCGG
$hTRADD_{R245A-R}$	CCGGGCGCTGGCGGACCCGGCG
$GFPS1_{F}$	AAAGAATTCATGGAGCATTTAATTGTTATG
$GFPS1_{R}$	AAAGGATCCCTACTGCACATGCCTCG
$hTRAILR2_{DD-F2}$	CGCGAATTCATGGATCCCACTGAGACTCTGAGAC
$hTRAILR2_{DD-R2}$	CCAAGCTTTTAGAACTTTCCAGAGCTCAACAAGTGG
$GSTP1\text{-}pGADT7_{F}$	CCCGAATTCATGCCGCCCTACACCGTGGTC
$GSTP1\text{-}pGADT7_{R}$	CCCGGATCCTCACTGTTTCCCGTTGCCATT

GSTP1-pFLAG$_F$	CCCTCTAGAATGCCGCCCTACACCGTGGTC
GSTP1-pFLAG$_R$	CCCGGATCCTCACTGTTTCCCGTTGCCATT
GSTP1-pET28a$_F$	CCCGAATTCATGCCGCCCTACACCGTGGTC
GSTP1-pET28a$_R$	CCCAAGCTTTCACTGTTTCCCGTTGCCATT
PCMT1-pGADT7$_F$	CCCGAATTCATGGCCTGGAAATCCGGCGGC
PCMT1-pGADT7$_R$	CCCGGATCCTCACTTCCACCTGGACCACTG
PCMT1-pFLAG$_F$	CCCTCTAGAATGGCCTGGAAATCCGGCGGC
PCMT1-pFLAG$_R$	CCCGGATCCTCACTTCCACCTGGACCACTG

Chapter Three

Characterising the subcellular activity and host binding partners of the SseK effectors

CHAPTER 3. Characterising the subcellular activity and host binding partners of the SseK effectors.

3.1. Introduction

Many intracellular pathogens rely on type three secretion systems (T3SS) to deliver cohorts of bacterial effector proteins into host cells during infection. Pathogenic serovars of *Salmonella* deploy two distinct T3SS to achieve different outcomes in the host, firstly employing the SPI-1 encoded T3SS to mediate invasion into non-phagocytic cells and induction of a potent and localised immune response (50, 64, 156), and secondly utilising the SPI-2 encoded T3SS to promote intracellular survival through maturation of the *Salmonella*-containing vacuole (SCV) and interference with innate and adaptive immune responses (105, 106). The importance of these T3SSs is well described but the contribution of individual effectors has been more difficult to elucidate, partially due to redundant or overlapping function of these effector proteins. Characterising the contribution of effectors to virulence represents a significant challenge, and exploring how effectors manipulate host cells promises a deeper understanding of host-pathogen interactions and provides opportunities for the development of novel anti-virulence therapeutics.

SseK1, SseK2, and SseK3 represent a family of highly-related effectors that appear to be sporadically distributed throughout the sequenced *Salmonella* serovars (105, 276). These effectors are strong homologues of the effector NleB1 from enteropathogenic *E. coli*, which functions as a glycosyltransferase to mediate the transfer of a single moiety of *N*-acetylglucosamine to a conserved arginine residue within the death domain of the host signaling adaptors FADD and TRADD (244, 245). Several key domains and motifs that are required for the function of NleB1 are conserved between the SseK effectors (245), leading to speculation that these effectors are also glycosyltransferases and indeed may catalyse a

similar modification of host death-domain proteins. During EPEC infection, NleB1-mediated glycosylation of TRADD and FADD inhibits NF-κB signaling and impairs host cell death via apoptosis, promoting survival of the infected cell (244, 245). However, it has not convincingly been established that the primary role of the SseK effectors is to glycosylate death domain proteins during *Salmonella* infection.

Since the first report in 2004 (242), there have been only incremental advances in the field to suggest the true role of the SseK effectors in *Salmonella* infection. Many of these reports have focused on demonstrating the translocation of these effectors into host cells and characterising the contribution to virulence in systemic models of infection (242, 243, 248). Much of the existing data in the literature is contradictory, and these conflicts may arise from differences in methodology. Few reports have offered insight as to the host substrates of these effectors – one study demonstrates SseK1-mediated glycosylation of the host signaling adaptor TRADD through the use of recombinant proteins in *in vitro* glycosylation assays (245), while a later study showed SseK1 did not interact with the death domain of TRADD via yeast-two hybrid assays (276). *In vivo*, one early report demonstrated no attenuation for Δ*sseK1*, Δ*sseK2* and Δ*sseK1*Δ*sseK2* mutants in BALB/c mice infected intraperitoneally (242), while another report described a competitive index experiment in which an Δ*sseK1sseK2* mutant was outcompeted by wild-type in 129/SvImJ mice (243), and a later experiment showed no reduction in bacterial loads for an Δ*sseK1sseK2sseK3* mutant recovered from organs of C57BL/6 mice (248).

Thus, the host substrates of the SseK effectors are disputed and their contribution to virulence remains poorly characterised. The aim of this chapter was to screen for unreported host substrates of the SseK effectors and to confirm these protein-protein interactions *in vitro*, while also validating previously reported findings. Here, we confirmed the sub-cellular localisation of the SseK effectors during infection and performed several screens to identify

novel host substrates. We identified a range of host proteins that bound to SseK1 during infection, among them the glutathione transferase GSTP1 and the methyltransferase PCTM1, suggesting the viability of these screening approaches for the study of effectors from *Salmonella* and other pathogens.

3.2. Results

3.2.1. Catalytic inactivation of the SseK effectors does not affect sub-cellular localisation

The sub-cellular localisation of effector proteins following translocation into the host cell is often suggestive of their function, and observing this localisation represents an early step in the characterisation of effectors. Initial data showed SseK1 to be localised to the cytoplasm of the host cell (242), while later work confirmed this finding and further showed that SseK2 and SseK3 localised to the host Golgi (276). To confirm and extend these findings, we generated catalytically inactivated N-terminal GFP-tagged $SseK1_{DxD(229\text{-}231)AAA}$, $SseK2_{DxD(239\text{-}241)AAA}$, and $SseK3_{DxD(226\text{-}228)AAA}$ via site-directed mutagenesis and transfected HeLa cells with these plasmids. Using immunofluorescence microscopy we observed a localisation phenotype consistent with previous reports, as SseK1 was shown to be localised throughout the host cell, while SseK2 and SseK3 co-localised with the trans-Golgi marker Golgin-97 (Fig 3.1). The catalytically inactivated mutants had a similar localisation phenotype to the respective native effectors, suggesting the localisation of these effectors is not a function of their catalytic activity (Fig 3.1).

3.2.2. Sub-cellular localisation of the SseK effectors during *S.* Typhimurium infection

Previous reports describing the sub-cellular localisation of the SseK effectors were performed via transfection of plasmids into mammalian cells (242, 276). Thus, these experiments have not been performed in the context of infection, and these observations may not represent the true localisation during bacterial infection. To validate these findings during *Salmonella* infection, we constructed plasmids encoding C-terminal HA-tagged versions of SseK1, SseK2, and SseK3, and then complemented an Δ*sseK1sseK2sseK3* mutant with each of these plasmids.

HeLa cells were infected with each of these strains, and after 18 hours of infection cells were imaged by immunofluorescence microscopy. Consistent with transfection experiments, SseK1 was shown to be localised throughout the infected host cell, while SseK2 and SseK3 co-localised to the host trans-Golgi marker Golgin-97 (Fig 3.2). These data confirm the localisation of these effectors after translocation into the host cell, and together may suggest SseK1 has a different range of host targets to SseK2 and SseK3.

3.2.3. Identification of binding partners of SseK1 via yeast two-hybrid screening.

Identifying the host targets of the SseK effectors remains a priority, and previous attempts to identify targets suggested SseK1 binds the host signaling adaptor TRADD (245). Another study utilised yeast two-hybrid assays to detect interactions between SseK1 and a range of death domain-containing proteins, and in this system SseK1 did not stably bind to the death domains of FADD, TRADD, RIPK1, MyD88, Fas, TNFR1, TRAILR2, IRAK1, or IRAK4 (276). These studies have produced conflicting data and so there is no consensus as to whether TRADD is the preferred substrate of SseK1, and there may remain other undescribed host substrates. While the host targets may indeed be death domain-containing proteins, the

true range of putative substrates is best explored through non-biased screening of protein-protein interactions. Here, we utilised a highly selective yeast two-hybrid system to screen for novel protein-protein interactions. We constructed the plasmids pGBKT7-BD-SseK1$_{DxD(229-231)AAA}$ and pGBKT7-BD-SseK1$_{E255A}$ encoding for a GAL4 binding domain fused to the putative catalytic mutants of SseK1, in order to avoid overcome the transient nature of enzyme-substrate interactions. Next, *S. cerevisiae* strain Y2HGold was transformed with each of these plasmids, and the resulting transformants were plated to media to select for transformation, to ensure expression of the constructs was not toxic to the transformed yeast, and to ensure no auto-activation of selective phenotypes in the absence of the activation domain.

To identify binding partners of SseK1, the transformed strains were mated with a normalised yeast two-hybrid HeLa cDNA library, and plated first to moderately-selective DDO (SD-Trp-Leu) plates. Colonies were subsequently picked and replated to highly-selective QDO (SD-Trp-Leu-Ade-His) plates. Plasmids were extracted from QDO-tolerant colonies and sequenced to identify the HeLa cDNA encoding the potential binding partner of SseK1. In these screens, eight putative binding partners were identified for SseK1$_{DxD(229-231)AAA}$ (Table 3.1), while two binding partners were identified for SseK1$_{E255A}$ (Table 3.2). In both screens, COP9 signalosome complex subunit 5 was identified as a putative binding partner, however this protein is commonly identified in yeast two-hybrid screening as a false positive (277) and is unlikely to represent a true substrate. Other identified candidates included the mitochondrial ribosomal proteins L48 and L10; as well as Snapin which participates in a complex involved in lysosome-related organelle biogenesis and vesicular trafficking; and zinc finger protein 251 which has an unknown function. The possible implications of these findings are discussed below.

This yeast two-hybrid screen was repeated using constructs expressing pGBKT7-BD-SseK2$_{DxD(239-241)AAA}$ and pGBKT7-BD-SseK2$_{E271A}$, however in this screen mated yeast were plated directly to highly selective QDO plates in an effort to reduce the incidence of false positive hits that were detected in the previous screens. Using this approach, no QDO-tolerant colonies were detected. Lastly, pGBKT7-BD-SseK3$_{DxD(226-228)AAA}$ and pGBKT7-BD-SseK3$_{E258A}$ were constructed but preliminary expression checks failed to detect appropriate expression of the SseK3 fusion proteins, and so these constructs were deemed unsuitable for yeast two-hybrid screening. Overall, yeast two-hybrid screening did not appear to be an effective and reliable means for identifying the binding partners of the SseK effectors, perhaps due to the transient nature of glycosyltransferase-substrate interactions.

3.2.4. Identification of binding partners of SseK1 via immunoprecipitation and mass spectrometry.

Next, we sought to screen for novel protein-protein interactions in the context of infection by using a highly sensitive mass spectrometry approach. Here, we infected HeLa cells with *S.* Typhimurium Δ*sseK1sseK2sseK3* and Δ*sseK1sseK2sseK3* complemented with pTrc99A-SseK1, which overexpresses an SseK1-HA fusion protein and thus increases the chances of enriching SseK1 and bound host proteins. Cells were lysed after 18 hours of infection and SseK1-HA was enriched from the whole cell lysate by anti-HA immunoprecipitation. The immunoprecipitate was subsequently processed by the filter aided sample preparation (FASP) method, a technique that involves the in-filter generation of tryptic peptides from liquid volumes, and these peptides were analysed via liquid chromatography mass spectrometry (LC/MS).

We observed successful enrichment of SseK1-HA in lysates infected with the complemented strain but not in the Δ*sseK1sseK2sseK3* mutant (Fig 3.3A), as expected.

However, no other proteins were detected above a selective threshold of peptide fold-enrichment and statistical significance, indicating no host proteins were bound stably to SseK1-HA. Separately, this experiment was repeated to compare cells infected with Δ*sseK1sseK2sseK3* and Δ*sseK1sseK2sseK3* complemented with pTrc99A-SseK1$_{DxD(229-231)AAA}$ (Fig 3.3B). Again we observed successful enrichment of SseK1$_{DxD(229-231)AAA}$-HA but no other proteins were significantly enriched. Interestingly we observed significantly reduced enrichment of SseK1$_{DxD(229-231)AAA}$ (Fig 3.3B) compared to observed levels of SseK1-HA (Fig 3.3A), possibly suggesting this mutation has an impact on expression levels or protein stability. Overall these results demonstrate the viability of this experimental approach for enriching tagged effectors from infected cell lysate, but in this instance did not identify new host substrates.

3.2.5. Identification of proteins cross-linked to SseK1 via immunoprecipitation and mass spectrometry.

SseK1 is predicted to function as a glycosyltransferase based on homology to the well-characterised effector NleB1 from EPEC (245). Glycosyltransferases typically interact with their substrates transiently, and so approaches that rely on binding affinity may be confounded by the transient nature of the interaction between SseK1 and its unknown substrates.

To improve on the immunoprecipitation experiments described above, we repeated these experiments with the addition of chemically cross-linking protein interactions by treatment with formaldehyde immediately prior to cell lysis. In addition, we used an SseK1$_{E255A}$ mutant which is rendered catalytically inactive to explore if this mutation increased the binding affinity between SseK1 and its bound substrate. Analysis of tryptic peptides generated from these experiments showed successful enrichment of SseK1$_{E255A}$-HA

(Fig 3.4), recapitulating the technical success of this approach. Further, we identified two host proteins that were significantly enriched above a high stringency threshold of significance. We detected two isoforms of the host glutathione transferase GSTP1 and the methyltransferase PCMT1 (Fig 3.4). Thus, these proteins represent novel putative substrates of SseK1 during *S.* Typhimurium infection.

3.2.6. Validation of the interaction between SseK1 and the putative substrates GSTP1 and PCTM1

Identification of novel substrates of bacterial effectors in screening experiments requires further validation to confirm the interaction. Here, we attempted to confirm and characterise the interaction between SseK1 and both GSTP1 and PCMT1 through an array of *in vitro* approaches. First, we examined protein binding via yeast two-hybrid assays. Auxotrophic *S. cerevisiae* Y2H gold was co-transformed with vectors pGBKT7-SseK1 and either pGADT7-GSTP1 or pGADT7-PCTM1, then plated to media to select for co-transformation (DDO) and to select for protein-protein interaction (QDO). We observed growth for yeast expressing the positive control proteins NleB1 and FADD which are known to interact (244) but not for yeast expressing SseK1 and either GSTP1 (Fig 3.5A) and PCMT1 (Fig 3.5B). Next, we co-transfected HEK293T cells with vectors expressing GFP-SseK1 or GFP-SseK1$_{E255A}$ and either Flag-GSTP1 (Fig 3.5C) or Flag-PCMT1 (Fig 3.5D). The Flag-fusion proteins were enriched from cell lysate by anti-Flag immunoprecipitation and both inputs and immunoprecipitates were probed with antibodies to demonstrate enrichment and co-pulldown of the GFP-tagged effectors. These results showed successful enrichment of the Flag-fusion proteins but no compelling evidence of co-enriched GFP-effectors amongst background signal evident on the immunoblots (Fig 3.5C, 3.5D). However given these approaches rely on stable binding between SseK1 and its substrates, it is possible

that the interaction is not stable enough to observe in these experiments. Thus, we lastly purified recombinant GST-SseK1 and His-GSTP1 and performed an *in vitro* glycosylation assay. Recombinant proteins were incubated in the presence of UDP-GlcNAc which acts the sugar donor for NleB1-mediated glycosylation of FADD (244). Immunoblots were probed with an anti-*O*-GlcNAc antibody, and while we observed NleB1-mediated glycosylation of the positive control FADD we did not observe glycosylation of GSTP1 in the presence of SseK1.

Collectively, while we observed binding between overexpressed SseK1 and the endogenous host proteins GSTP1 and PCMT1 in the context of *S.* Typhimurium infection, these findings were not convincingly supported by *in vitro* validation experiments. This data may suggest the interaction between SseK1 and these substrates requires factors that are present in the context of infection. Further work is needed to fully validate these interactions and to explore the consequence of these events during infection.

3.3. Discussion

Characterising the function and activity of effector proteins provides insight into the specific mechanisms by which pathogens are able to subvert host cells during infection. Pathogenic serovars of *Salmonella* are heavily dependent on both the SPI-1 and SPI-2 encoded T3SS to achieve infection, given that mutants deficient for these T3SS are strongly attenuated in murine models of infection (98, 99, 101). More than 40 effectors have been identified across serovars of pathogenic *Salmonella*, and many of these remain only partially characterised or have no known function (64, 105). The SseK family of effectors remain poorly understood, and while there are several conflicting reports describing the role these proteins play during infection *in vivo* (242, 243, 248), there are relatively few reports describing the biochemical function and host targets of these effectors (245, 276). Given

these effectors are strong homologues of the glycosyltransferase NleB1 from enteropathogenic *E. coli* (276), it is possible these effectors have a similar function and may glycosylate host proteins during *Salmonella* infection. However, these effectors show a high degree of similarity and may have overlapping or redundant functions. Identifying the host proteins that interact with each of the three SseK effectors represents a critical step in elucidating the function of these effectors and reconciling the conflicts that have arisen in previous reports. In this chapter, we sought to identify novel host substrates for the SseK effectors through a variety of non-biased screens, while also validating key findings from previous studies.

We demonstrated the sub-cellular localisation of the SseK effectors following transfection into host cells and established that catalytic activity of these effectors was not required for localisation (Fig 3.1). GFP-SseK1 was localised throughout the host cell while GFP-SseK2 and GFP-SseK3 co-localised with the host Golgi markers Golgin-97 and GM-130, which suggests SseK1 may play a different role than SseK2 and SseK3. These phenotypes were further demonstrated in the context of infection (Fig 3.2), demonstrating that the localisation observed in transfection experiments is consistent with that of bacterially-translocated SseK effectors. These phenotypes are in contrast to many of the SPI-2 T3SS effectors which predominantly localise to the SCV-SIF network (64). SseF and SseG are critical for tethering the SCV to the Golgi, while SteA was initially reported to localise to the Golgi (154), but in later studies was shown to be localised to the SCV-SIF network and the host plasma membrane (278). The type IV effector BspC from *Brucella* shows a similar Golgi localisation phenotype (279) but the functional significance remains unknown. The colocalisation of SseK2 and SseK3 with the Golgi may suggest these effectors play a role in manipulating the function of the Golgi, though this remains to be explored.

During the course of this study, another report was published that similarly demonstrated co-localisation of GFP-SseK3 with the trans-Golgi marker p230 (280) and that this localisation was conserved in the catalytically inactivated GFP-SseK3$_{DxD(226-228)AAA}$, thus validating the findings reported here. This study also described an interaction between SseK3 and the E3 ubiquitin ligase TRIM32, though TRIM32 was further shown to be not glycosylated by SseK3 *in vitro*, and so this interaction requires further validation. Intriguingly this paper also reported SseK3-mediated inhibition of NF-κB activation following TNF stimulation at levels comparable to that of NleB1, suggesting a possible conservation of function between SseK3 and NleB1.

In this study we performed a number of screens to identify unreported substrates of the SseK effectors. Yeast two-hybrid screening has long been used to identify novel interactions between bacterial effectors and their host substrates (182, 281, 282). Indeed, the interaction between the EPEC homologue NleB1 and its substrates TRADD and FADD were first reported by yeast two-hybrid screening (244, 245), and so it is possible that the substrates of the SseK effectors can be discovered through this approach. A previous study utilised yeast-two hybrid assays to determine SseK1 does not stably bind to a range of mammalian death-domain proteins (276), but screening a cDNA library provides the opportunity to discover novel interactions with unexpected substrates. Through this approach we discovered eight putative binding partners for SseK1$_{DxD(229-231)AAA}$ (Table 3.1) and two binding partners for SseK1$_{E255A}$ (Table 3.2). The only protein conserved between both screens was COP9 signalosome complex subunit 5, but this has been previously shown to directly interact with the DNA-binding domain of GAL4 and thus represents a false positive that commonly arises in yeast two-hybrid screens (277). A further three recovered clones carried cDNA encoding Snapin, an adaptor protein that associates with the SNARE complex and plays roles in vesicular docking and fusion (283). Snapin also participates in the BLOC-1

complex which is involved in biogenesis of organelles of the endosomal-lysosomal system (284). More recent work has implicated Snapin in lysosome acidification and autophagosome maturation (285). Bacterial interference with Snapin has not been reported, but this interaction may provide new insight into the interplay between intracellular *Salmonella* and the endosomal-lysosomal system, and thus warrants further investigation. Other candidate substrates identified in this screen, including adenylosuccinate synthetase and the mitochondrial ribosomal proteins L10 and L48, were only isolated once in this screen, and so these may not represent genuine substrates of SseK1. Overall, yeast two-hybrid screening identified several putative host substrates of SseK1, which may warrant further investigation in future.

Screening for protein-protein interactions during infection provides better opportunities to identify novel substrates of bacterial effectors. Here we utilised immunoprecipitation to enrich for overexpressed SseK1-HA and any bound substrates, which were identified by LC/MS analysis of tryptic peptides generated from the HA-enriched fraction. In this experiment we successfully enriched the bait proteins SseK1-HA (Fig 3.3A) and SseK1$_{DxD(229\text{-}231)AAA}$-HA (Fig 3.3B), suggesting this approach is a viable means of enriching for bacterial effectors from host cell lysates. No host proteins were co-enriched above a stringent threshold of significance, which may suggest the interaction between SseK1 and its host substrates is transient, or the host targets are not present in the tested cell line, or that this effector acts on a non-protein target. To advance this inquiry, we chemically treated infected cells with formaldehyde to cross-link protein interactions, which hypothetically may increase the chance of detecting proteins that interact transiently with SseK1. In this experiment we detected two isoforms of the host gluthathione transferase GSTP1 and also the methyltransferase PCMT1 (Fig 3.4). These results suggest formaldehyde-mediated crosslinking of protein interactions can increase the chances of detecting bound substrates

during immunoprecipitation, and demonstrate the viability of this strategy for the characterisation of bacterial effectors.

GSTP1 plays diverse roles in cellular detoxification, anti-oxidation, and anti-inflammation during mammalian cell homeostasis (286-288). The primary biochemical function of GSTP1 and other GST enzymes is to conjugate glutathione to electrophilic sites of a range of exogenous substrates (286, 287). There is considerable interest in the function of GST enzymes as targets for the development of cancer therapeutics and markers of cancer drug resistance (289-291), though there appear to be no reports of bacterial inhibition of GSTP1 during infection. Some reports have demonstrated an anti-apoptotic role for GSTP1 through binding to JNK1 and preventing phosphorylation and activation of c-Jun (292), while other reports show binding between GSTP1 and TRAF2, which prevents the activation of ASK1 and inhibits apoptosis (293). Given the roles GSTP1 plays in indirectly inhibiting apoptosis, SseK1-mediated glycosylation of GSTP1 might represent a mechanism for promoting apoptotic cell death, though this remains to be established experimentally. The GSTP1-b isoform detected in this experiment bears the commonly reported Ile-105-Val mutation, and this isoform reportedly has a decreased enzymatic activity and is less efficient at detoxification (287). GSTP1 reportedly localises to both the nucleus and the cytoplasm of the host cell (287), which is consistent with the localisation of SseK1 reported here (Fig 3.1, Fig 3.2) and elsewhere (276). However, *in vitro* data presented here does not support protein binding (Fig 3.5A, Fig 3.5C) or SseK1-mediated O-glycosylation (Fig 3.5E), and so the interaction between SseK1 and GSTP1 remains to be explored. It is possible that the SseK1-GSTP1 interactions requires factors that are present during infection, or that the interaction is transient such that it is detectable following cross-linking but not during these *in vitro* validation studies. Further, the inability to detect glycosylation of GSTP1 in the presence of recombinant SseK1 and UDP-GlcNAc may indicate another sugar donor is required for

glycosylation, or that the modification is not detected by an antibody raised against O-glycosylation. Alternatively, it is possible that the observed interaction between SseK1 and GSTP1 represents a host-mediated response to effector intoxication, given GSTP1 itself acts enzymatically to promote the excretion or compartmentalisation of a range of substrates (288, 291). Ultimately GSTP1 may represent a genuine substrate of SseK1 but further work remains to confirm these findings.

PCMT1 is an isoaspartyl carboxyl O-methyltransferase (PIMT) that contributes to protein repair of L-isoaspartyl and D-aspartyl residues through its methyl esterification activity (294, 295). PCMT1 is not described in the context of bacterial infection, and it is debatable whether antagonising protein repair of specific residues would significantly contribute to virulence of an intracellular pathogen. Validation experiments performed here were not supportive of protein binding (Fig 3.5B, Fig 3.5D), and so the interaction between SseK1 and PCMT1 requires further investigation to confirm this interaction is genuine.

Collectively, these data confirm and extend findings reporting the subcellular localisation phenotypes of the SseK effectors, which may suggest SseK1 plays a distinct role to SseK2 and SseK3. We describe a mass spectrometry-based approach to enriching bacterial effectors from host cell lysates, and demonstrate that chemically cross-linking protein interactions can improve the detection of transiently bound substrates. GSTP1 and PCMT1 were identified as putative substrates of SseK1, though further work remains to validate these interactions and demonstrate a contribution to virulence. These data provide fundamental insights into the subcellular activity of the SseK family but suggests approaches that rely on binding affinity between proteins may be confounded by the enzymatic nature of these effectors, and that the function of these effectors may be better explored by characterising their biochemical activity.

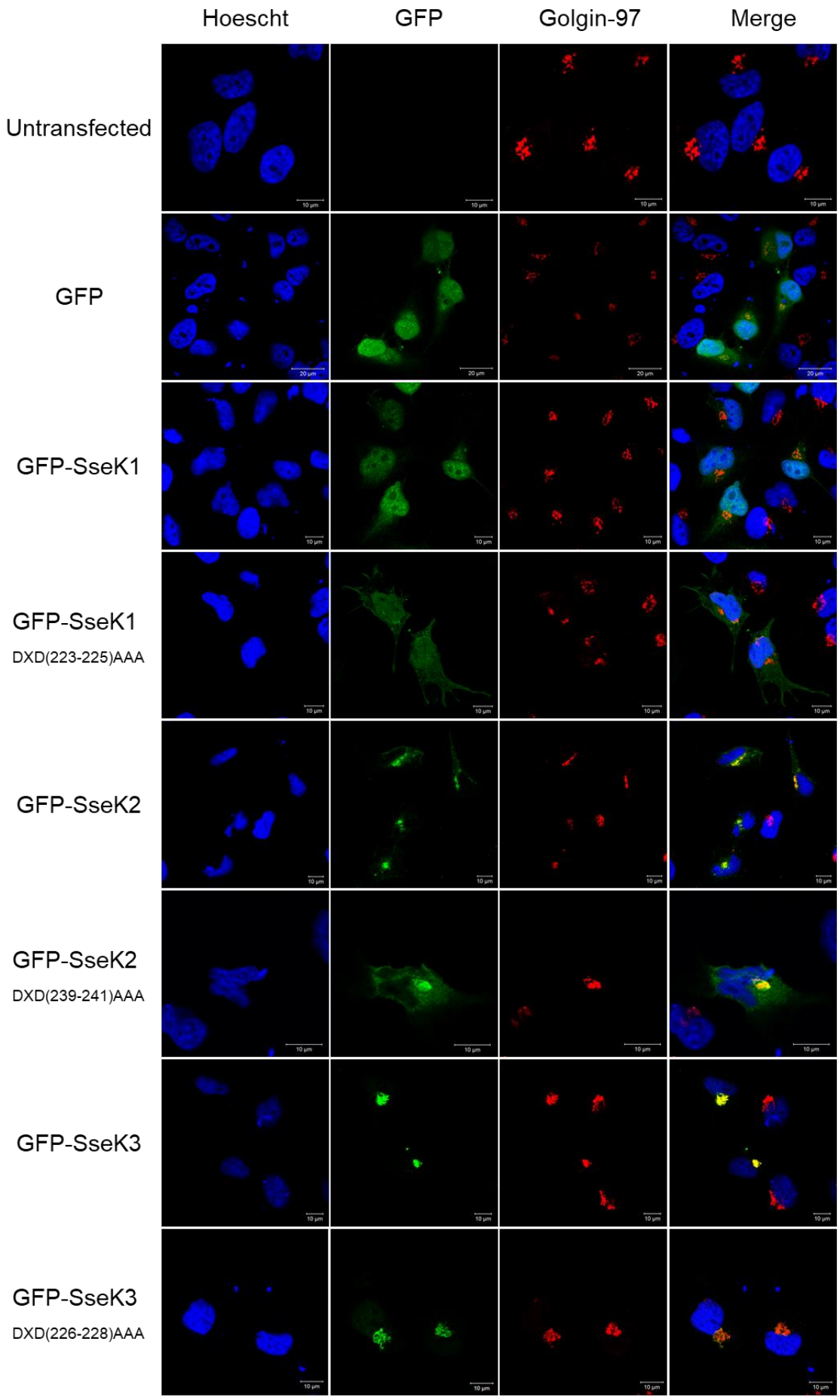
Hoescht
GFP
Golgin-97
Merge
Untransfected
GFP
GFP-SseK1
GFP-SseK1
DXD(223-225)AAA
GFP-SseK2
GFP-SseK2
DXD(239-241)AAA
GFP-SseK3
GFP-SseK3
DXD(226-228)AAA

Figure 3.1 Subcellular localisation of ectopically expressed GFP-SseK effectors

Representative immunofluorescence fields of HeLa cells ectopically expressing GFP-SseK effectors or catalytic mutants, as indicated. Cells were fixed and permeabilized at 18 hours post transfection. The *trans*-Golgi network was visualised using anti-Golgin-97 antibody (red). Cell nuclei were visualised with Hoechst stain (blue). Representative image of at least three independent experiments.

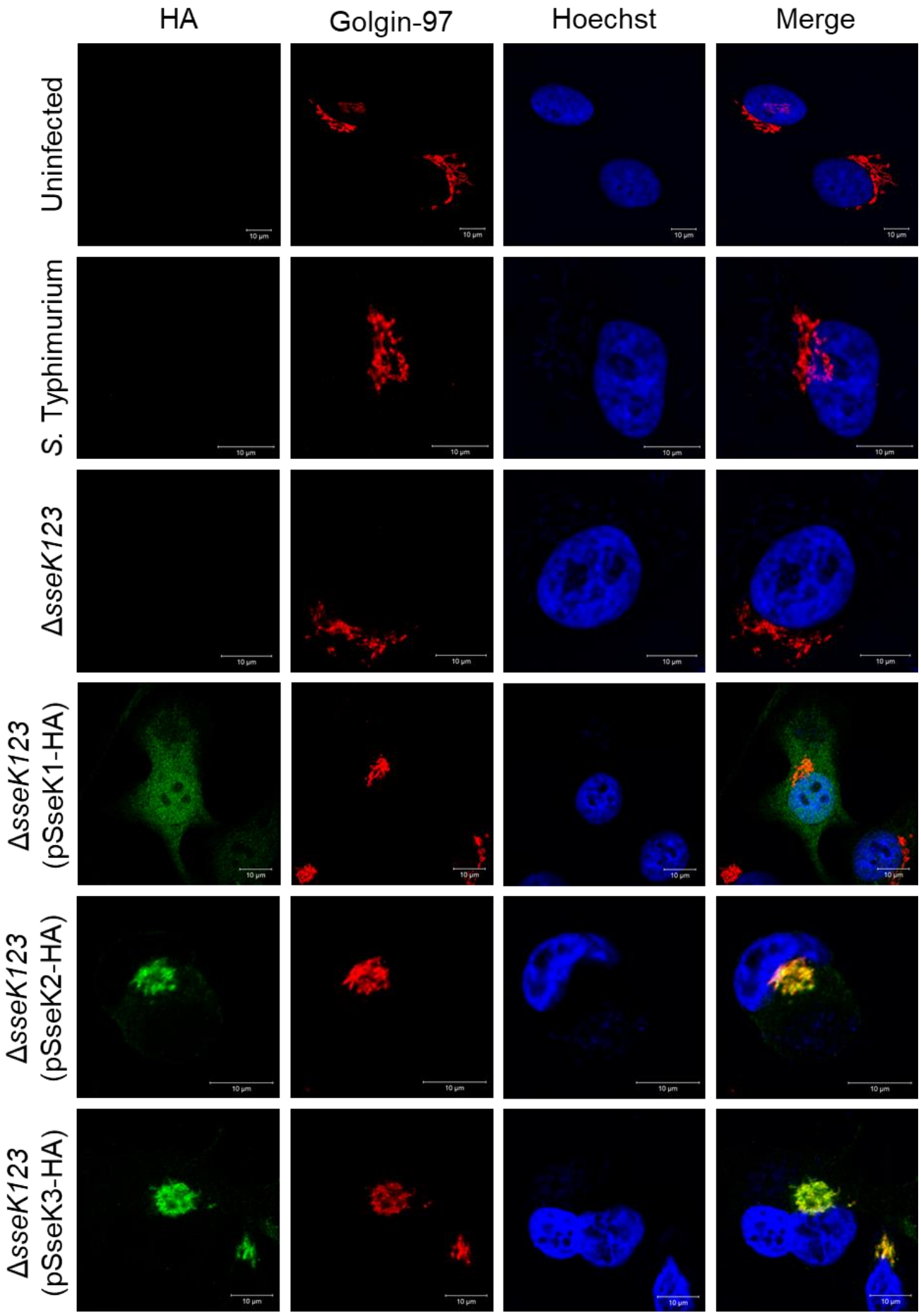
HA
Golgin-97
Hoechst
Merge
Uninfected
S. Typhimurium
ΔsseK123
ΔsseK123 (pSseK1-HA)
ΔsseK123 (pSseK2-HA)
ΔsseK123 (pSseK3-HA)
10 µm

Figure 3.2. Subcellular localisation of SseK-HA effectors during *S.* Typhimurium infection.

Representative immunofluorescence fields of HeLa cells infected with *S.* Typhimurium expressing SseK-HA fusion proteins. Cells were fixed and permeabilized 18 hours post infection. SseK-HA effectors were visualised using anti-HA antibody (green). The *trans*-Golgi network was visualised using anti-Golgin-97 antibody (red). Cell nuclei were visualised with Hoechst stain (blue). Representative image of at least three independent experiments.

Protein	GenBank accession number	Amino acids	Function	Localisation	Number of times recovered in Y2H screen
COP9 signalosome complex subunit 5	NP_006828.2	334	Forms part of COP9 complex, involved in diverse cellular and developmental processes	Cytoplasm, nucleus	6
SNARE-associated protein Snapin	NP_036569.1	136	Vesicle trafficking	Membrane, cytoplasm	3
Adenylosuccinate synthetase	CAA47123.1	457	Purine nucleotide biosynthesis	Cytoplasm	1
Mitochondrial ribosomal protein L48	EAW74913.1	261	Mitochondrial protein synthesis	Mitochondria	1
Mitochondrial ribosomal protein L10	NP_660298.2	261	Mitochondrial protein synthesis	Mitochondria	1

Heterogeneous nuclear ribonucleoprotein L-like isoform 1	AAH17480.1	542	Regulator of alternative splicing	Nucleus, ribosome	1
Spermatogenesis associated protein 5-like protein 1	AAH00981.1	753	Unknown	Cytoplasm	1
Structural maintenance of chromosomes protein 1A (SMC1A)	CAI42646.1	1233	Chromosome cohesion during cell cycle and DNA repair	Cytoplasm, nucleus	1

Table 3.1. Potential binding partners of SseK1$_{DXD(223-225)AAA}$ observed in yeast two-hybrid screen.

The yeast strain *S. cerevisiae* Y2H Gold was transformed with pGBKT7-SseK1$_{DXD(223-225)AAA}$ and mated with the yeast strain *S. cerevisiae* Y187 transformed with a HeLa cDNA library. Mated yeast were plated to selective DDO (SD-Trp-Leu) and QDO (SD-Trp-Leu-Ade-His) media to select for diploid cells expressing the reporter genes. Yeast colonies were subsequently patched to DDO and QDO media to confirm protein interaction. Plasmids were extracted from colonies patched to QDO media, and sequenced to identify the HeLa cDNA encoding for the putative binding partner.

Protein	GenBank accession number	Amino acids	Function	Localisation	Number of times recovered in Y2H screen
COP9 signalosome complex subunit 5	NP_006828.2	334	Forms part of COP9 complex, involved in diverse cellular and developmental processes	Cytoplasm, nucleus	2
Zinc finger protein 251	NP_612376.1	671	Unknown, possible role in transcriptional regulation	Nucleus	2

Table 3.2. Potential binding partners of SseK1$_{E253A}$ observed in yeast two-hybrid screen.

The yeast strain *S. cerevisiae* Y2H Gold was transformed with pGBKT7-SseK1$_{E253A}$ and mated with the yeast strain *S. cerevisiae* Y187 transformed with a HeLa cDNA library. Mated yeast were plated to selective DDO (SD-Trp-Leu) and QDO (SD-Trp-Leu-Ade-His) media to select for diploid cells expressing the reporter genes. Yeast colonies were subsequently patched to DDO and QDO media to confirm protein interaction. Plasmids were extracted from colonies patched to QDO media, and sequenced to identify the HeLa cDNA encoding for the putative binding partner.

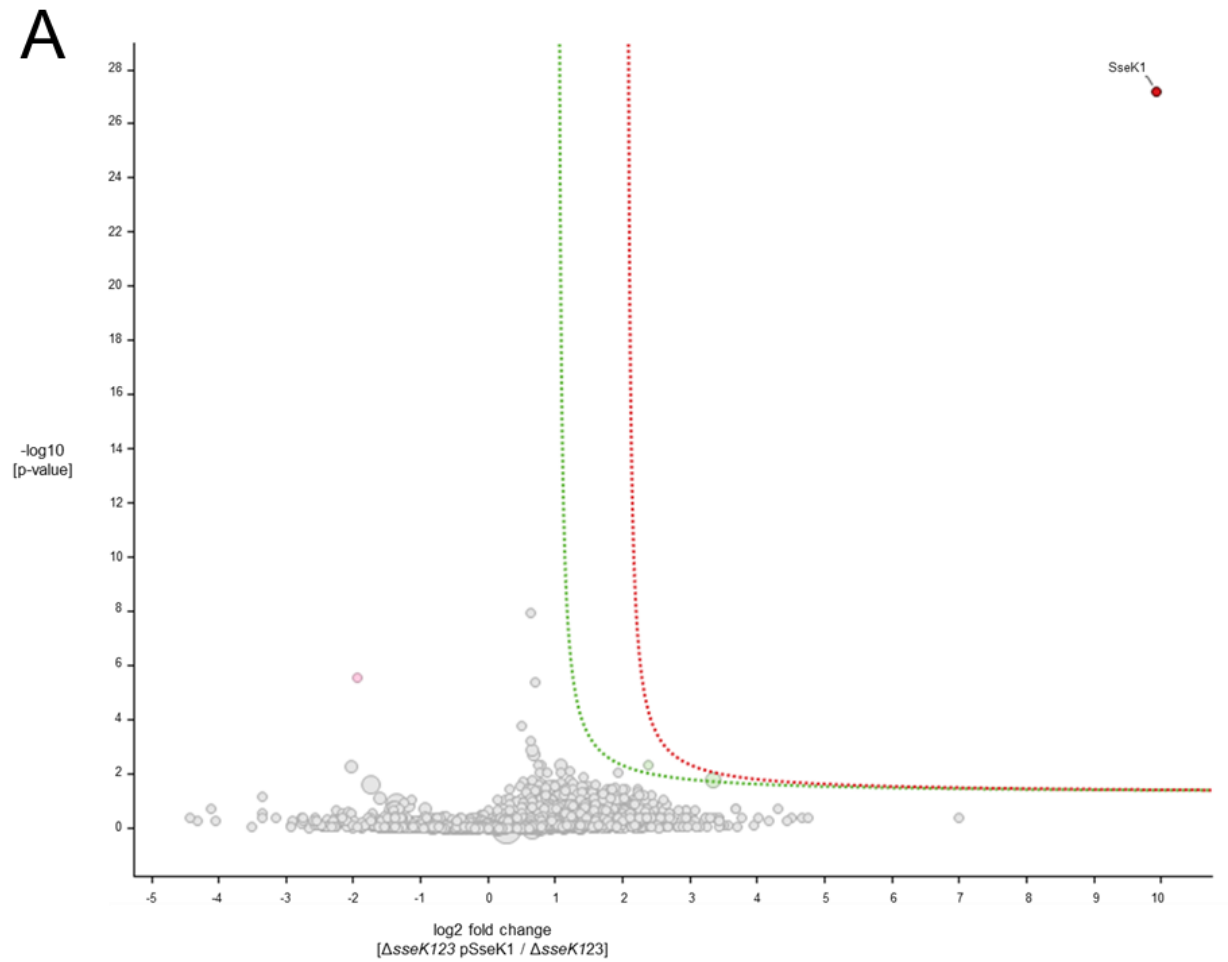
A
SseK1
-log10
[p-value]
log2 fold change
[ΔsseK123 pSseK1 / ΔsseK123]

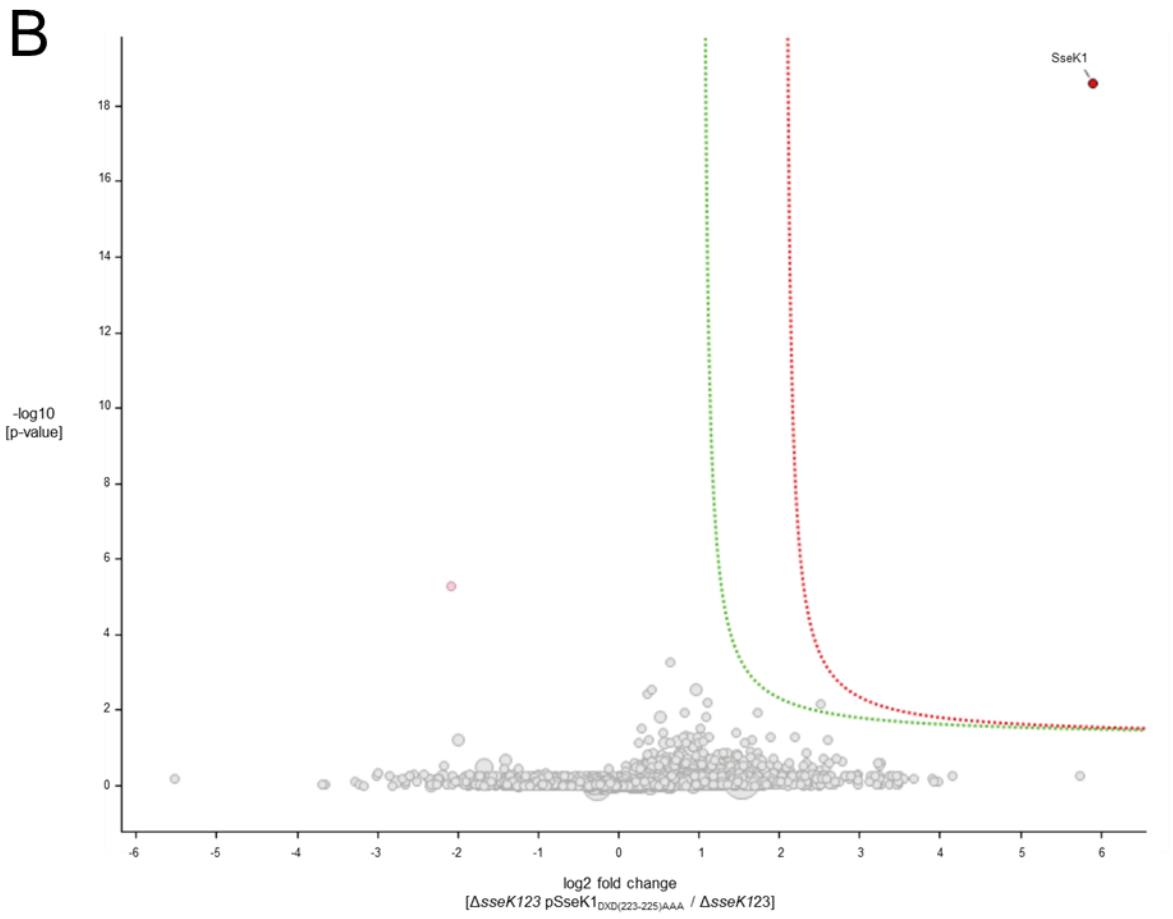
B
SseK1
-log10
[p-value]
log2 fold change
[ΔsseK123 pSseK1DXD(223-225)AAA / ΔsseK123]

Figure 3.3. Enrichment of host substrates bound to SseK1 during *S.* Typhimurium infection.

LC-MS quantification of tryptic peptides of anti-HA immunoprecipitate enriched from HeLa cells infected with *S.* Typhimurium. Cells were lysed after 18 hours infection and tryptic peptides were generated by filter aided sample preparation. Enriched peptides are presented as a volcano plot depicting mean log2 ion intensity peptide ratios of Δ*sseK1sseK2sseK3* pTrc99A versus (A) Δ*sseK1sseK2sseK3* pTrc99A-SseK1 or (B) Δ*sseK1sseK2sseK3* pTrc99A-SseK1$_{DXD(223\text{-}225)AAA}$, plotted against logarithmic *t* test *p* values from biological triplicate experiments. Dotted lines represent thresholds of fold change enrichment.

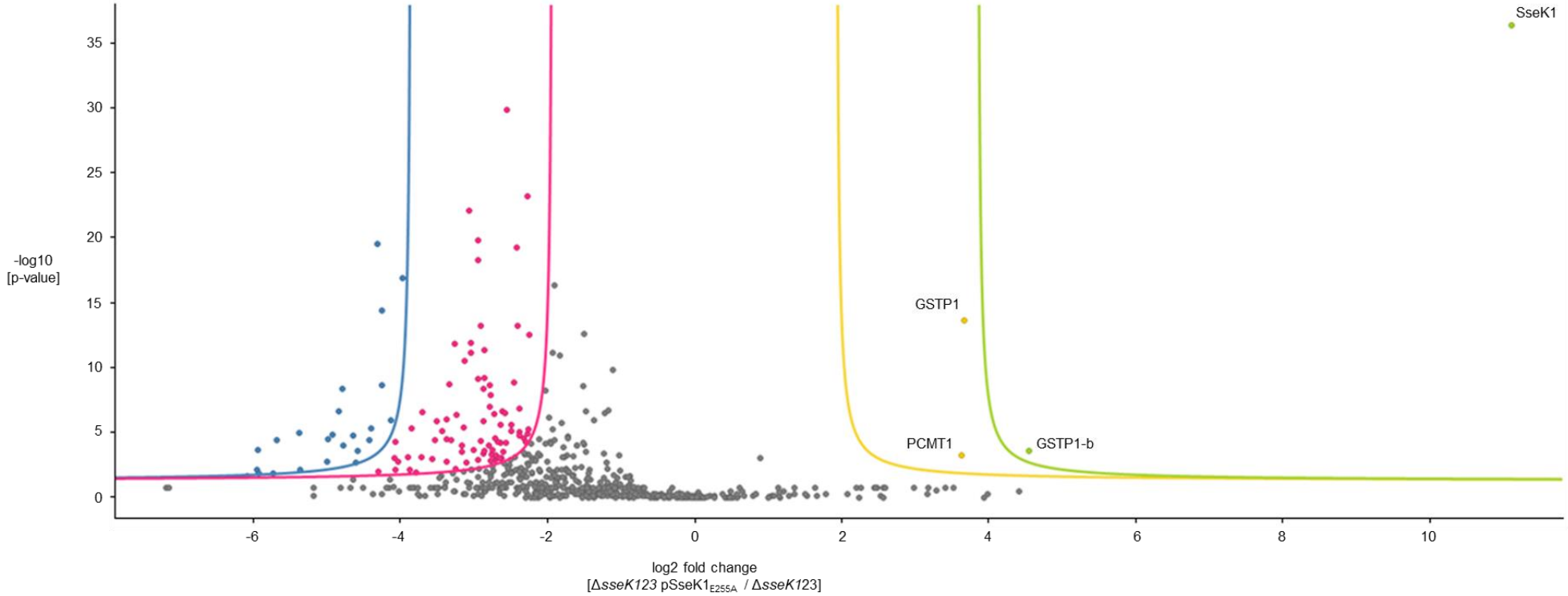

Figure 3.4. Enrichment of host substrates cross-linked to SseK1$_{E253A}$ during *S.* Typhimurium infection.

LC-MS quantification of tryptic peptides from anti-HA immunoprecipitate enriched from HeLa cells infected with *S.* Typhimurium. Cells were lysed after 18 hours infection, protein-protein interactions were cross-linked using 1% formaldehyde, and tryptic peptides were generated by filter aided sample preparation. Enriched peptides are presented as a volcano plot depicting mean log2 ion intensity peptide ratios of Δ*sseK1sseK2sseK3* pTrc99A-SseK1$_{E253A}$ versus Δ*sseK1sseK2sseK3* pTrc99A, plotted against logarithmic *t* test *p* values from biological triplicate experiments. Dotted lines represent thresholds of fold change enrichment.

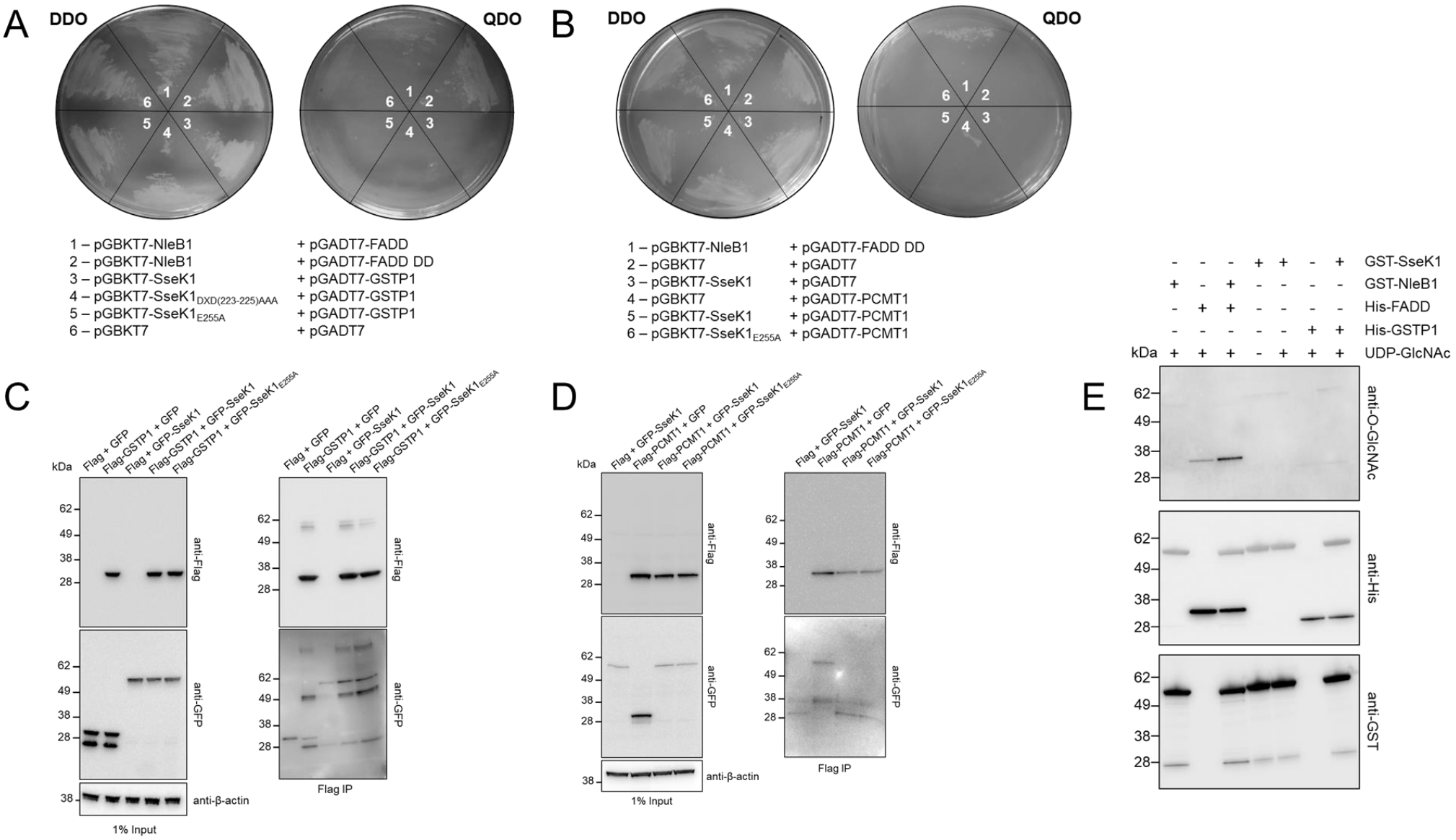
A
DDO
QDO
1 – pGBKT7-NleB1
2 – pGBKT7-NleB1
3 – pGBKT7-SseK1
4 – pGBKT7-SseK1DXD(223-225)AAA
5 – pGBKT7-SseK1E255A
6 – pGBKT7
+ pGADT7-FADD
+ pGADT7-FADD DD
+ pGADT7-GSTP1
+ pGADT7-GSTP1
+ pGADT7-GSTP1
+ pGADT7
B
DDO
QDO
1 – pGBKT7-NleB1
2 – pGBKT7
3 – pGBKT7-SseK1
4 – pGBKT7
5 – pGBKT7-SseK1
6 – pGBKT7-SseK1E255A
+ pGADT7-FADD DD
+ pGADT7
+ pGADT7
+ pGADT7-PCMT1
+ pGADT7-PCMT1
+ pGADT7-PCMT1
C
kDa
Flag + GFP
Flag-GSTP1 + GFP
Flag + GFP-SseK1
Flag-GSTP1 + GFP-SseK1
Flag-GSTP1 + GFP-SseK1E255A
anti-Flag
anti-GFP
anti-β-actin
1% Input
Flag IP
D
kDa
Flag + GFP-SseK1
Flag-PCMT1 + GFP
Flag-PCMT1 + GFP-SseK1
Flag-PCMT1 + GFP-SseK1E255A
anti-Flag
anti-GFP
anti-β-actin
1% Input
Flag IP
E
GST-SseK1
GST-NleB1
His-FADD
His-GSTP1
UDP-GlcNAc
kDa
anti-O-GlcNAc
anti-His
anti-GST

Figure 3.5. Validation of putative host substrates of SseK1.

(A) *S. cerevisiae* Y2H Gold co-transformed with pGBKT7-SseK1 and pGADT7-GSTP1 and plated to selective media to observe correct transformation (left) and validate protein-protein interactions (right). (B) *S. cerevisiae* Y2H Gold co-transformed with pGBKT7-SseK1 and pGADT7-PCMT1 and plated to selective media to observe correct transformation (left) and validate protein-protein interactions (right). (C) Immunoblot of inputs and immunoprecipitates (IP) of anti-FLAG immunoprecipitations performed on lysates of HEK293T cells co-transfected with pFLAG-GSTP1 and pEGFP-SseK1 or pEGFP-SseK1$_{E255A}$. (D) Immunoblot of inputs and immunoprecipitates (IP) of anti-FLAG immunoprecipitations performed on lysates of HEK293T cells co-transfected with pFLAG-PCMT1 and pEGFP-SseK1 or pEGFP-SseK1$_{E255A}$. (E) Immunoblot of recombinant GST-SseK1 and His-GSTP1 following co-incubation at 37°C for 5 hours. Proteins were detected with anti-O-GlcNAc, anti-His, anti-GST, and anti-β-actin antibodies as indicated. Representative immunoblot of at least three independent experiments. DDO: double drop-out media, QDO: quadruple drop-out media

Chapter Four

Characterising the arginine glycosyltransferase activity of the SseK effectors

CHAPTER 4. Characterising the arginine glycosyltransferase activity of the SseK effectors.

4.1. Introduction

SseK1, SseK2, and SseK3 are predicted to be glycosyltransferases based on strong homology to the arginine glycosyltransferase NleB1 from enteropathogenic *E. coli* (EPEC). Several conserved regions reported to be required for the glycosyltransferase activity of NleB1 are conserved in the SseK effectors, and these regions are also required for the NleB1-dependent inhibition of NF-κB signaling and apoptosis during EPEC infection (244, 245, 276, 296). NleB1 functions as an arginine glycosyltransferase and catalyses the addition of *N*-acetylglucosamine (GlcNAc) to specific arginine residues of the mammalian signaling adaptors FADD and TRADD, a modification termed Arg-GlcNAcylation (244, 245). The interaction between NleB1 and both FADD and TRADD was originally observed in yeast two-hybrid screening (244, 245), and so it was hypothesised that the substrates of the homologous effector SseK1 could be similarly discovered through yeast-two hybrid screening or through other assays that rely on protein-protein interactions.

However, these approaches have produced conflicting or inconsistent evidence regarding the host targets of the SseK effectors. One study utilised yeast two-hybrid assays to demonstrate SseK1 does not bind to a range of mammalian death-domain proteins including TRADD (276), despite an earlier report demonstrating glycosylation of recombinant TRADD in an *in vitro* glycosylation assay (245). Another study showed binding of SseK3 to TRIM32 by co-immunoprecipitation but also showed SseK3 did not glycosylate TRIM32, nor did SseK3 influence the ubiquitylation of TRIM32 (280). In the previous chapter, we used immunoprecipitation and quantitative mass spectrometry to show binding of SseK1 to the host proteins GSTP1 and PCTM1 (section 3.2.5), but these interactions were not

convincingly validated (section 3.2.6). Given that studies relying on protein-protein interactions have not convincingly identified the substrates of the SseK effectors, and that glycosyltransferases transiently interact with their substrates, utilising the glycosyltransferase activity of these effectors may prove a more successful approach.

Glycosyltransferases represent a superfamily of enzymes that catalyse the transfer of saccharide groups from a donor nucleoside diphosphate sugar to a glycosyl acceptor molecule (297). Glycosyltransferases can be further organised into families based on their affinity for a specific sugar donor, for example the glucosyltransferases and galactosyltransferases that catalyse the transfer of glucose and galactose respectively (298). Glycosyltransferases interact with a range of donor nucleotide sugars, including UDP-glucose, UDP-galactose, and UDP-GlcNAc, and mediate glycosyl transfer to a receptor molecule. Further characterisation of a glycosyltransferase is determined by the site of glycosylation, with *N*-glycosylating enzymes targeting sugar moieties to nitrogen atoms of asparagine residues and *O*-glycosylating enzymes targeting oxygen atoms most commonly of serine or threonine residues (297, 298). Thus, the reports describing NleB1-mediated *N*-GlcNAcylation of arginine residues represented novel glycobiology that is not otherwise reported in either bacterial or mammalian metabolism (244, 245).

A recent report described the development of an antibody raised against a synthetically produced glycopeptide bearing an arginine *N*-GlcNAcyl group (299). This antibody was shown to specifically recognise Arg-GlcNAcylation of FADD catalysed by active NleB1, but did not recognise *O*-GlcNAcyl groups transferred by the mammalian *O*-GlcNActransferase OGT nor the *Clostridium novyi* α-toxin GlcNActransferase. Further, the authors successfully detected NleB1-dependent Arg-GlcNAcylation of FADD, TRADD, and RIPK1 following ectopic expression in mammalian cells, demonstrating the viability of this antibody in detecting a range of previously described substrates (299). Recently, this Arg-

GlcNAc antibody became commercially available, and may represent a useful means of identifying other enzymes that catalyse this rare glycosylation event.

Based on strong homology to the well-characterised effector NleB1 which catalyses the addition of *N*-acetylglucosamine to arginine residues (Arg-GlcNAc), we hypothesised that the SseK effectors also functioned as Arg-GlcNAc glycosyltransferases. The aim of this chapter was to determine the potential of the SseK effectors to catalyse arginine glycosylation of host proteins. Here, we used an anti-Arg-GlcNAc antibody in immunoblotting and immunofluorescence microscopy to establish that SseK1 and SseK3 are indeed Arg-GlcNAc glycosyltransferases. Further, we developed a method utilising immunoprecipitation and mass spectrometry to enrich arginine glycosylated proteins from infected cell lysates and thus identified novel host targets of SseK1. We demonstrated SseK1 does glycosylate the host signaling adaptor TRADD during *Salmonella* infection, but that an unexpected array of other host and bacterial proteins were also glycosylated.

4.2. Results

4.2.1. SseK1 and SseK3 catalyse arginine glycosylation of host proteins.

Previous reports have demonstrated the EPEC effector NleB1 catalyses arginine glycosylation of host proteins (244, 245), and an antibody raised against glycosylated arginine is commercially available (299). We hypothesised the SseK effectors may also catalyse arginine glycosylation based on sequence homology to NleB1. Here, we infected RAW264.7 cells with a *Salmonella* Typhimurium SL1344 *ΔsseK1sseK2sseK3* deletion mutant complemented with HA-tagged versions of either native SseK1, SseK2 or SseK3, catalytic triad mutants, or mutants lacking the conserved glutamic acid ($SseK1_{E255A}$, $SseK2_{E271A}$, and $SseK3_{E258A}$). Cell lysates were assessed by immunoblot using an antibody specific for arginine glycosylation (Fig. 4.1A and 4.1B). Native SseK1 and SseK3, but not

SseK2, catalysed Arg-GlcNAcylation, while all catalytic triad mutants and glutamic acid mutants showed no activity. Notably, overexpression of both SseK1 and SseK3 increased levels of arginine glycosylation relative to wild-type SL1344, suggesting that overexpression may cause non-authentic Arg-GlcNAcylation of host substrates. No bands corresponding to arginine glycosylated protein were detected in the *ΔsseK1sseK2sseK3* mutant, suggesting no other effectors present in *S.* Typhimurium SL1344 can mediate this glycosylation event. Collectively these data establish that SseK1 and SseK3 mediate arginine glycosylation of host proteins during *S.* Typhimurium infection.

4.2.2. Arginine glycosylated host substrates co-localise with SseK1 and SseK3 during *Salmonella* infection.

Next, we visualised the localisation of arginine glycosylated protein within host cells during infection. We again utilised an Δ*sseK1sseK2sseK3* mutant strain complemented with plasmids expressing C-terminal HA-tagged SseK effectors or catalytically inactivated effectors. RAW264.7 cells were infected for 20 hours with each of these strains, before being fixed and prepared for immunofluorescence microscopy. As previously, we observed a broadly localised cytoplasmic signal for SseK1, while SseK2 and SseK3 showed a more localised pattern consistent with the Golgi localisation observed previously (Fig 3.1, Fig 3.2). Here, we observed signal corresponding to arginine glycosylation distributed throughout the infected host cell only in cells infected with bacteria expressing active SseK1 (Fig 4.2). This glycosylation signal co-localised with the signal for SseK1. In contrast, in the presence of active SseK3, arginine glycosylation showed a more punctate localisation and was similarly co-localised with SseK3 (Fig 4.2), consistent with the Golgi localisation reported above. Cells infected with bacteria expressing the catalytically inactivated SseK1$_{E255A}$ or SseK3$_{E258A}$ showed no evidence of arginine glycosylation (Fig 4.2), further supporting the hypothesis that

this conserved glutamate is required for glycosyltransferase activity. Similarly, no arginine glycosylation signal was detected in the presence of SseK2 or SseK2$_{E271A}$ (Fig 4.2), further suggesting that this effector does not catalyse this particular glycosylation event. The absence of glycosylation observed in the Δ*sseK1sseK2sseK3* mutant indicates no other effectors of *S.* Typhimurium SL1344 can mediate arginine glycosylation, while the weaker signal for the wild type strain further suggests the impact of overexpression on the function of these effectors.

4.2.3. Identifying host substrates of SseK1 by enrichment of arginine-glycosylated protein from infected cell lysate.

The host targets of SseK1 remain poorly characterised, and identifying these substrates will lead to a deeper understanding of the role of this effector during infection. In the previous chapter we utilised immunoprecipitation and mass spectrometry to identify novel binding partners of SseK1 (section 3.2.5), though these interactions were not conclusively validated. Here, we advanced these approaches by conjugating anti-ArgGlcNAc antibody to protein A/G beads to perform an immunoprecipitation to enrich specifically for arginine glycosylated proteins from infected cell lysates. RAW264.7 cells were infected with a Δ*sseK1sseK2sseK3* mutant complemented with either SseK1-HA or the catalytically inactivated SseK1$_{E255A}$-HA. Cells were lysed after 20 hours of infection and cell lysates were incubated with pre-prepared anti-ArgGlcNAc beads overnight, then boiled to elute bound antibody and protein. Eluted proteins were resolved by gel electrophoresis then subjected to in-gel tryptic digestion, and tryptic peptides were subsequently analysed by liquid chromatography mass spectrometry (LC/MS).

We detected successful enrichment of peptides bearing arginine glycosylation from cells containing native SseK1, and no glycosylated peptides for cells containing the

catalytically inactivated SseK1$_{E255A}$ (Fig 4.3A). Fifteen unique substrates were enriched in this experiment, and the specific glycosylated arginine was identified for all detected substrates. Notably, we detected the host signaling adaptor TRADD, which has been previously suggested to be a substrate of SseK1 (244, 245). Further, we identified the specific site of modification as Arg243 (Fig 4.3B), which represents a novel site of glycosylation. Other highly enriched host substrates included Prohibitin-2 (PHB2), Tropomyosin alpha-3 chain (TPM3), 14-3-3 protein epsilon (YWHAE), and Docking protein 2 (DOK2). Strikingly, we also detected arginine glycosylation of several *Salmonella* proteins, including the two-component response regulators OmpR and ArcA. This finding suggests that under these experimental conditions *S.* Typhimurium utilises SseK1 to glycosylate arginine residues of bacterial proteins as well as host substrates during infection.

4.2.4. Identifying host substrates of SseK1 by enrichment of arginine-glycosylated peptide from infected cell lysate.

To confirm and extend these findings, we modified the above ArgGlcNAc immunoprecipitation approach by generating tryptic peptides from whole cell lysate prior to enrichment with ArgGlcNAc beads. This approach differs in that soluble arginine glycosylated peptides are available for interactions with anti-ArgGlcNAc beads, rather than enriching entire proteins as above. Hypothetically, this approach improves the chances of detecting substrates bearing glycosylated arginine residues, as sites that may be obscured by folded or partially-folded proteins become more accessible. Using peptides derived from host cells infected with *S.* Typhimurium *ΔsseK1sseK2sseK3* over-expressing either SseK1 or inactive SseK1$_{E255A}$, label-free MS based quantification revealed a significantly broader range of substrates that were only modified in the presence of active SseK1 (Fig 4.4A). Among the diversity of substrates we again identified TRADD bearing glycosylation at

Arg243 (Fig 4.4B), consistent with the previous experiment (Fig 4.3). We also observed an unexpectedly expanded array of bacterial proteins bearing arginine glycosylation, again including two-component response regulators OmpR and ArcA, as well as the ribosome-associated proteins RpsA and RbfA, and transcription-associated proteins RpoD and NusA (Fig 4.4A). These data demonstrate a previously unanticipated range of substrates for SseK1 during infection, with new implications for effector-mediated self-glycosylation of bacterial protein.

4.2.5. Detection of endogenous-level arginine glycosylation suggests TRADD is the preferred substrate of SseK1.

Thus far, we have developed and validated a novel method for enriching arginine glycosylated proteins from infected cell lysates (Fig 4.3, Fig 4.4). However we have also shown that overexpression of SseK1 and SseK3 appeared to increase arginine glycosylation activity relative to wild type levels of expression (Fig 4.1, Fig 4.2). Here, we explored the activity of endogenous levels of SseK1 during *S.* Typhimurium infection. RAW264.7 cells were infected with either a Δ*sseK2sseK3* double deletion mutant or the Δ*sseK1sseK2sseK3* triple deletion mutant, thus allowing for interrogation of endogenous SseK1. We initially performed the peptide enrichment approach utilised in section 4.2.4, but LC/MS analysis of tryptic peptides generated here failed to detect any arginine glycosylation of either host or bacterial proteins, perhaps suggesting the endogenous level of substrate modification is below the level of detection for this approach.

To improve detection of glycosylated substrates, we applied parallel reaction monitoring, a targeted high-resolution MS approach (300), to specifically observe the Arg-GlcNAcylated species of murine TRADD (mTRADD) and the related signaling adaptor FADD. Using this approach, we observed arginine glycosylation of mTRADD in the

presence of SseK1 (Fig 4.5A). We identified Arg233 as the site of modification (Fig 4.5B) which is distinct from the Arg243 modification we reported in sections 4.2.3 and 4.2.4. However, Arg233 is the equivalent of the previously reported Arg235 of human TRADD (hTRADD) which is glycosylated by NleB1 from EPEC *in vitro* (245). Here, we detected no evidence to support arginine glycosylation of FADD, despite the fact that mFADD was readily detectable within the input control samples. This suggested TRADD was the preferred substrate when SseK1 was translocated at native levels during infection.

4.2.6. SseK1 glycosylates death domain-containing proteins *in vitro*.

Our data suggests mTRADD is a preferred host substrate of SseK1 during infection of RAW264.7 cells. Previous reports have suggested recombinant SseK1 can mediate glycosylation of recombinant TRADD *in vitro* (245), while other data suggests SseK1 does not bind to the death domain of TRADD in yeast two-hybrid assays (276). To confirm and characterise the interaction between SseK1 and human TRADD, we transfected HEK293T cells with plasmids encoding variants of GFP-SseK1 and Flag-TRADD, then performed immunoblots on cell lysates with anti-ArgGlcNAc antibody. We observed arginine glycosylation of Flag-TRADD in the presence of SseK1 and the positive control NleB1, but not in the presence of the inactivated SseK1$_{E255A}$ (Fig 4.6A). NleB1 reportedly modifies TRADD at Arg235 (245), and previously we observed glycosylation of the equivalent Arg233 in mTRADD (Fig 4.2.5). Here we transfected HEK29T cells with a plasmid encoding for Flag-TRADD$_{R235A}$ and again probed for arginine glycosylation. While we observed significantly reduced glycosylation in the presence of NleB1, we detected no apparent reduction in the intensity of arginine glycosylation for cells expressing SseK1 (Fig 4.2.5), suggesting other arginine residues are glycosylated by SseK1 under these experimental conditions. Separately, we repeated this experiment to explore SseK1-mediated glycosylation

of the related signaling adaptor FADD. We observed arginine glycosylation of FADD in the presence of both NleB1 and SseK1 (Fig 4.6B), suggesting SseK1 can also target FADD *in vitro*. NleB1 is known to modify FADD at Arg117 (244) and while we observed a total loss of signal corresponding to arginine glycosylation in cells co-expressing NleB1 and $FADD_{R117K}$, we observed a significant but not complete reduction in signal for cells expressing SseK1 and $FADD_{R117K}$, indicating this arginine is likely the primary site of modification *in vitro* (Fig 4.6 B). Collectively these data confirm the interaction between SseK1 and TRADD, but do not resolve the identity of the preferred site of modification.

4.2.7. Overexpression of SseK1 alters the sites of glycosylation within the death domain of TRADD.

Thus far we have demonstrated that overexpressed SseK1 glycosylates mTRADD at Arg243 during infection of murine RAW264.7 cells (section 4.2.3, section 4.2.4), while endogenous levels of SseK1 seem to catalyse glycosylation of Arg233 under the same infection conditions (section 4.2.5). Separately, we observed SseK1-mediated glycosylation of human TRADD during transfection of mammalian cells, but there was no reduction in glycosylation of the $hTRADD_{R235A}$ mutant (section 4.2.6). Arg235 of hTRADD is equivalent to Arg233 of mTRADD, while Arg245 of hTRADD is the equivalent of Arg243 of mTRADD. Here we aimed to resolve the discrepancies observed thus far and identify the preferred sites of arginine glycosylation in hTRADD.

We used site-directed mutagenesis to generate the single mutants TRADD Arg235Ala and Arg245Ala, as well as a double mutant in which both arginine residues were mutated to alanine. Plasmids encoding Flag-tagged fusions of these mutants were co-transfected into HEK293T cells along with GFP-SseK1, and immunoblotted to detect arginine glycosylation. Both Flag-$hTRADD_{R235A}$ and Flag-$hTRADD_{R245A}$ were Arg-GlcNAcylated at levels

comparable to native Flag-hTRADD, while modification of the double mutant Flag-hTRADD$_{R235A/R245A}$ was significantly reduced (Fig 4.7A). While this result suggests both Arg235 and Arg245 can act as redundant sites of glycosylation, we detected a faint band at the corresponding size for the TRADD$_{R235A/R245A}$ double mutant, suggesting there may be other less preferred sites of glycosylation. To identify further possible sites of modification, Flag-hTRADD was enriched from cells co-transfected with pEGFP-SseK1 by anti-Flag immunoprecipitation, subjected to tryptic digestion and analysed by LC-MS. Under these conditions, we detected several further sites of modification at Arg239, Arg278, and Arg224 (Fig 4.7B), demonstrating that SseK1 is capable of glycosylating other arginine residues within TRADD during following ectopic expression in mammalian cells. Collectively these data suggest SseK1 preferentially targets both Arg235 and Arg245 of human TRADD while other sites can be glycosylated to a lesser degree.

4.2.8. The catalytic activity of SseK1 does not impact caspase 8 cleavage or IL-8 secretion.

Arginine glycosylation of TRADD by the EPEC effector NleB1 is required for bacterial inhibition of NF-κB signaling and prevention of apoptotic cell death (244, 245). We have observed the related effector SseK1 catalyses arginine glycosylation of TRADD during *S.* Typhimurium infection. Previous reports utilising an NF-κB dependent luciferase reporter assay demonstrated both SseK1 and SseK3 inhibit NF-κB activation following TNF stimulation in HeLa cells (276). Here we undertook preliminary investigations into the impact of SseK1 glycosyltransferase activity on host cell signaling events. Firstly we examined the cleavage of caspase 8 during *S.* Typhimurium infection. RAW264.7 cells were infected with selected *S.* Typhimurium mutant strains, followed by induction of the TNF-dependent apoptotic signaling pathway by co-stimulation with TNF and birinapant, a second

mitochondrial-derived activator of caspases (SMAC) mimetic compound (301, 302). Cell lysates were collected after 5.5 hours of stimulation and immunoblots were performed to detect cleavage of caspase 8. We observed a band at approximately 14kDa in all stimulated conditions, corresponding to the p18 subunit of cleaved caspase 8 (Fig 4.8A). There was no apparent inhibition of caspase 8 cleavage in cells infected with either wild type SL1344, the Δ*sseK1sseK2sseK3* triple mutant, or the Δ*sseK1sseK2sseK3* mutant complemented with active SseK1. These data suggest SseK1 does not inhibit caspase 8 cleavage following TNF treatment under these experimental conditions.

Next, we quantified production of the pro-inflammatory chemokine interleukin-8 (IL-8) during *S.* Typhimurium infection. RAW264.7 cells were infected with a panel of *S.* Typhimurium SL1344 mutants then stimulated with TNF for 5.5 hours to induce expression and secretion of IL-8. Cell supernatant was collected and IL-8 levels were quantified via ELISA. In all stimulated conditions we observed significant increases in IL-8 production as expected, however there was no significant differences in the levels of IL-8 between uninfected cells or cells infected with either wild type SL1344, a SPI-2 translocation-deficient Δ*ssaR* mutant, the Δ*sseK1sseK2sseK3* mutant, nor the Δ*sseK1sseK2sseK3* mutant complemented with either SseK1 or $SseK1_{DxD(223\text{-}225)AAA}$ (Fig 4.8B). These data suggest neither SseK1 nor the SseK effectors collectively function to inhibit IL-8 secretion during infection of RAW264.7 cells. Overall, further work is required to more fully explore the phenotypic consequences of SseK1-mediated glycosylation of TRADD during infection, and to elucidate how this activity contributes to virulence.

4.3. Discussion

Several bacterial pathogens utilise glycosyltransferases to promote virulence. Different species of *Clostridium* employ various glycosyltransferases during infection,

including the *C. novyi* GlcNActransferase α-toxin, the *C. difficile* glucosyltransferase toxins A and B, and the *C. sordellii* glucosyltransferase lethal toxin (303-305). Pathogenic strains of *Legionella pneumophila* also utilise glycosyltransferase effectors during infection. The related effectors Lgt1, Lgt2, and Lgt3 function as glucosyltransferases to inactivate elongation factor 1A (306), while SetA is also a glucosyltransferase which reportedly targets the small GTPase Rab1 to inhibit secretory pathways (307). Thus while glycosyltransferase effectors are described in multiple bacterial pathogens, NleB1 from EPEC remains the only described example of a glycosyltransferase that is capable of catalysing Arg-GlcNAcylation (244, 245). An antibody that specifically recognises GlcNAcylated arginine species recently became commercially available, and this antibody can detect NleB1-mediated glycosylation of various death domain proteins during ectopic expression (299). Given the SseK effectors are strong homologues of NleB1, we hypothesised these effectors may also catalyse Arg-GlcNAcylation and, if so, the uniquely glycosylated substrates could be detected using an anti-Arg-GlcNAc antibody. In this chapter, we aimed to establish if the SseK effectors catalyse arginine glycosylation and to identify all potential glycosylated host substrates using the highly-specific anti-Arg-GlcNAc antibody.

In this study, we demonstrated that SseK1 and SseK3 are capable of catalysing arginine glycosylation during *S.* Typhimurium infection. Immunoblotting the lysates of RAW264.7 cells infected with wild type SL1344 revealed one clear band between 28kDa and 38kDa and a second fainter band at 28kDa, while no bands were detectable in the Δ*sseK1sseK2sseK3* mutant (Fig 4.1A) These data suggest endogenous levels of the SseK effectors collectively result in arginine glycosylation of at least two substrates, and that no other effectors from *S.* Typhimurium SL1344 are capable of catalysing this reaction. Overexpression of SseK1 and SseK3 by complementation restored arginine glycosylation and appeared to broaden the possible range of glycosylated substrates (Fig 4.1A, Fig 4.1B),

suggesting overexpression of these effectors impacts not only the level of activity of these effectors but also promotes the glycosylation of other substrates. For both SseK1 and SseK3, mutating the conserved DxD catalytic triad or a conserved glutamate to alanine residues abrogated catalytic activity (Fig 4.1A, Fig 4.1B). No signal corresponding to arginine glycosylation was detected in the presence of SseK2, suggesting this effector does not catalyse Arg-GlcNAcylation. SseK2 and SseK3 are highly similar at the amino acid level and have the same subcellular localisation pattern, and so the differential glycosylation presented here was unexpected. It is possible that SseK2 utilises another sugar donor molecule or otherwise catalyses a different glycosidic linkage that is not specifically recognised by an anti-ArgGlcNAc antibody. Future work is needed to characterise the biochemistry mediated by SseK2.

We next visualised arginine glycosylation by immunofluorescence microscopy and observed differences between the activity of SseK1 and SseK3. Arginine glycosylated protein was localised throughout the nucleus and cytoplasm in the presence of SseK1, while more punctate and restricted to the perinuclear region in the presence of SseK3 (Fig 4.2). In both cases, arginine glycosylated protein was co-localised with the respective effector protein, suggesting proteins that are glycosylated by SseK3 are localised to the Golgi. We also visualised endogenous level of arginine glycosylation catalysed by wild type *S.* Typhimurium SL1344, and here we observed small punctate structures again in the perinuclear region (Fig 4.2). It is possible this represents endogenous SseK3-mediated glycosylation of the host Golgi. Overall, these data further distinguish the SseK effectors from one another at a phenotypic level, despite the high level of similarity between these effectors at an amino acid level. Based on the differential localisation phenotypes of SseK1 and SseK3 and the differences observed for their glycosylated substrates, it is likely these effectors target different host proteins and play different roles in infection.

Having established that SseK1 functions as an arginine glycosyltransferase, we developed and applied a method to identify the glycosylated host substrates by combining Arg-GlcNAc specific immunoprecipitation and quantitative mass spectrometry. We demonstrated the viability of this approach in enriching both whole proteins (Fig 4.3) and tryptic peptides (Fig 4.4) that bore glycosylated arginine residues and successfully identified a broad range of glycosylated substrates. In both experiments, we detected glycosylation of the signaling adaptor mTRADD and identified the site of modification as Arg243. While a previous report showed recombinant SseK1 modifies hTRADD *in vitro*, we observed here this interaction occurring in the context of *S.* Typhimurium infection. Further, the site of modification previously reported was Arg235 of hTRADD, while we observed Arg243 of mTRADD, and thus this represents a novel site of modification. These data suggest SseK1 and NleB1 may both target TRADD during infection, and given NleB1-mediated glysocylation of TRADD inhibits NF-κB signaling and apoptosis, this might suggest a role for SseK1 in inhibiting inflammatory or cell death pathways, though further work remains to explore this hypothesis.

We detected also a number of other glycosylated host proteins that were significantly enriched in the presence of active SseK1. Prohibitin-2 (PHB2) is a membrane protein with functions that differ based on its subcellular localisation, and is implicated in functions as diverse as transcription activation, cell cycle regulation, mitochondrial biogenesis but also plays roles in apoptotic signaling (308). Thus SseK1-mediated inhibition of prohibitin-2 might represent a means for *S.* Typhimurium to inhibit apoptosis though this has not yet been demonstrated. Interestingly, the Vi toxin of *S.* Typhi reportedly targets both prohibitin-1 and -2 to suppress innate immunity and prevent T-cell activation (309, 310). Thus, SseK1-mediated glycosylation of prohibitin-2 may represent a new means for non-typhoidal *Salmonella* to similarly interfere with host immunity. Other proteins glycosylated by SseK1

included: tropomyosin alpha-3 chain (TPM3) which is involved in stabilising the actin cytoskeleton (311); the epsilon isoform of 14-3-3 protein (YWHAE) which is part of a protein family that is implicated in a diverse range of cellular processes including signal transduction, apoptosis, DNA repair, and cell cycle regulation (312); and docking protein 2 (DOK2) which reportedly acts as a scaffold to mediate the assembly of a range of immune signaling complexes. (308).

Effectors typically target host proteins during infection, yet here we unexpectedly discovered a diversity of bacterial proteins that were glycosylated in the presence of SseK1 during infection (Fig 3.3, Fig 3.4). In both experiments, we detected glycosylation of the two-component response regulators OmpR and ArcA, which along with a range of other similar two-component systems co-ordinates bacterial sensing of the environment and a concomitant regulatory shift in gene expression, enabling a bacterium to express the appropriate transcriptional profile (140, 141). Arginine glycosylation is typically understood to be deleterious to protein function, at least in the reports describing FADD and TRADD modification during EPEC infection (244, 245), and so it was unexpected to discover glycosylation of critical components of the sensing/regulatory systems that contribute to *Salmonella* virulence. Indeed, the EnvZ-OmpR two-component system contributes to regulation of the SsrA-SsrB two-component system, which in turn controls expression of the SPI-2 T3SS and subsequent translocation of effectors (149-151). Separately, the ArcA-ArcB system reportedly controls a transcriptional response to reactive oxygen species (ROS) resistance (313). The consequences of these modifications on two-component signaling remain to be explored, but may suggest new mechanisms by which *Salmonella* self-regulates two-component signaling, possibly to limit virulence under certain conditions.

While these experiments yielded a diversity of novel substrates to be characterised and explored further, we focused on the glycosylation of TRADD given the well-described

consequences of this modification during EPEC infection and previous reports that show SseK1 and SseK3 can inhibit NF-κB signaling following TNF stimulation (276). Using parallel reaction monitoring (PRM) mass spectrometry, we successfully observed modification of TRADD at endogenous levels of SseK1 expression using an Δ*sseK2sseK3* mutant strain (Fig 4.5). These data suggest glycosylation of TRADD is a genuine substrate of SseK1 and not an artefact of over-expressing SseK1, as possible in previous experiments (Fig 4.3, Fig 4.4). Due to the specific nature of PRM, we cannot determine if the other identified substrates are glycosylated under endogenous conditions, and so this remains a priority of future research. Interestingly, we observed glycosylation of mTRADD at Arg233 under endogenous conditions, while during overexpression we observed glycosylation at Arg243. To reconcile these findings with previous reports describing glycosylation of recombinant hTRADD at Arg235, we performed site-directed mutagenesis and demonstrated that both Arg233 and Arg245 of hTRADD appear to be primary sites of glycosylation *in vitro* (Fig 4.6, Fig 4.7). Both residues lie within the death domain region of TRADD, and we speculate that glycosylation of either residue would disrupt binding of TRADD to other adaptor proteins and interfere with immune signaling. However, in preliminary experiments we found no impact of SseK1 expression on caspase 8 cleavage or IL-8 secretion during infection, and so the contribution of TRADD glycosylation to *Salmonella* virulence remains to be fully characterised.

Our initial strategies for detecting the glycosylated substrates of SseK1 relied on over-expression of this effector protein, and these experiments identified a broad range of mammalian and bacterial substrates (Fig 4.3, Fig 4.4). In subsequent experiments, we attempted to identify the substrates of endogenous levels of SseK1, but were unable to detect glycosylation of host proteins. Subsequently, we applied a targeted parallel reaction monitoring (PRM) approach, and were able to demonstrate that TRADD is indeed

glycosylated by endogenous levels of SseK1 (Fig 4.5). Thus, while TRADD appears to be a preferred target of SseK1 during *S.* Typhimurium infection, it remains possible that endogenous SseK1 may glycosylate substrates other than TRADD, and future experiments are needed to further explore the true range of proteins that are targeted by SseK1.

While this study was in progress, another study used anti-Arg-GlcNAC antibodies to explore the function of the SseK effectors. This study confirmed many findings reported here, demonstrating that SseK1 and SseK3 were indeed arginine glycosyltransferases, and that glycosylated protein was co-localised with SseK1 and SseK3 by immunofluorescence (314). Similarly, the authors used single mutants to demonstrate glycosylation profiles for SseK1 and SseK3 by western blot, and in co-transfection experiments showed SseK1-mediated glycosylation of both TRADD and FADD (314), similar to data presented here (Fig 4.6). However, these findings are in conflict with the PRM mass spectrometry approach described in this chapter (Fig 4.5), in which TRADD but not FADD was glycosylated during endogenous expression of SseK1 during infection. Thus the modification of FADD may be dependent on over-expression of SseK1 or be an artefact of *in vitro* ectopic expression of these proteins. Finally, the authors demonstrate a co-operative impact of SseK1 and SseK3 on cell death during infection, and demonstrate inhibition of MLKL phosphorylation during infection, indicating the SseKs appear to inhibit necroptotic cell death (314). Separately, another study reported SseK1- and SseK3-dependent inhibition of IκBα degradation and subsequent suppression of p65 nuclear translocation, while also demonstrating SseK1-mediated inhibition of TRAF2 poly-ubiquitylation (315). Finally, another study showed no SseK-mediated inhibition of IL-8 secretion during infection (280), consistent with the findings reported here (Fig 4.8). Collectively, these studies contribute to an emerging model of SseK-dependent inhibition of host cell death and innate immune signaling. However, further work is needed to better elucidate the contributions of each SseK family member, and

to explore how the three SseK effectors act cooperatively or redundantly to impact the host response.

Previous reports have implicated both TRADD and FADD as substrates of SseK1 (245, 314, 315), yet our data suggests that TRADD is the preferred substrate of endogenous SseK1 during *S.* Typhimurium infection (Fig 4.5). TRADD plays a number of key roles in immune signaling, and therefore represents an attractive target for inhibition by a bacterial effector. Following stimulation of TNFR1 by the extracellular ligand TNF, TRADD participates in the formation of complex I, a signaling platform that also involves RIPK1, TRAF2, and the E3 ligases cIAP1 and cIAP2 (257, 258). The eventual outcome of these signaling events is induction of the canonical NF-κB pathway, resulting in pro-inflammatory cytokine secretion. Alternatively, TNF stimulation can induce the formation of complex II, which involves both TRADD and FADD along with RIPK1, RIPK3 and MLKL (259). Complex II signaling can result in programmed cell death via apoptosis or necroptosis (260). The death domain region of TRADD is critical for the protein-protein interactions that enable the formation of both complexes I and II (261), and here we show that SseK1 glycosylates arginine residues within the death domain of TRADD (Fig 4.3, Fig 4.4, Fig 4.5). Previous work suggests SseK1 plays a role in inhibiting both NF-κB activation and necroptotic cell death in infected macrophages (314), and so it is likely that *S.* Typhimurium employs SseK1 to inhibit both of these pathways as required. Single deletion mutants have not clearly demonstrated a requirement for SseK1 *in vivo* in mouse infection models (242, 246, 248), so it is possible that SseK1 acts in concert with other effectors to achieve significant inhibition of cell signaling during *S.* Typhimurium infection.

Ultimately, the data presented in this chapter established that SseK1 and SseK3 function as arginine glycosyltransferases during *Salmonella* infection, while SseK2 appears to catalyse a different reaction. We developed a mass spectrometry based approach to

specifically enrich for the uniquely arginine-glycosylated host substrates of SseK1 from infected cell lysate, and showed that an array of both host and bacterial proteins were glycosylated. Overexpression of SseK1 appeared to greatly expand the range of potential substrates, while highly specific PRM mass spectrometry confirmed TRADD was modified at endogenous levels but FADD was not modified under these conditions. These data provide strong evidence that SseK1 indeed modifies TRADD during infection, though future work remains to fully describe how this modification impacts bacterial virulence. The approaches described here demonstrate the importance of studying bacterial effectors at endogenous levels and in experiments better reflecting natural infection conditions. Conceivably, these approaches could be applied to bacterial infections *in vivo*, providing new understanding of how effectors function in the natural context of infection. Future work will explore how the SseK effectors co-operate to antagonise host cell signaling, and provide evidence for the different host substrates that are targeted by the different SseK effectors.

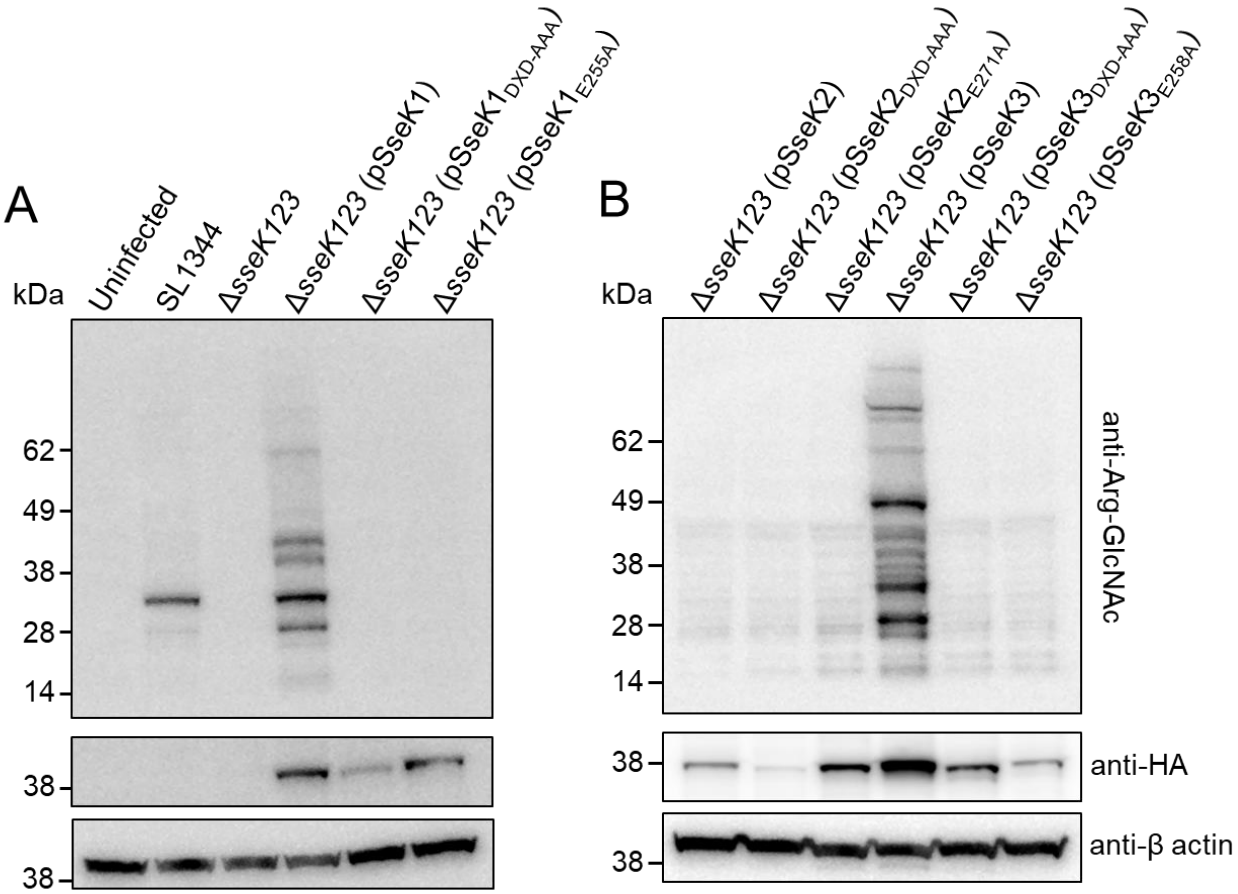

Figure 4.1. Immunoblot of RAW264.7 cells infected with derivatives of *S.* Typhimurium SL1344.

Wild type *S.* Typhimurium, a triple Δ*sseK1sseK2sseK3* mutant and triple mutant complemented with plasmids encoding one of HA-tagged SseK1, SseK2 or SseK3, or with catalytically-inactive effector derivatives were used to infect RAW264.7 for 20 h, as indicated (A and B). Overexpression of the effectors was induced during host cell infection by the addition of 1 mM IPTG. RAW264.7 cells were lysed and proteins detected by immunoblot with anti-ArgGlcNAc and anti-HA antibodies as indicated. Anti-β-actin was used as a loading control. Representative immunoblot of at least three independent experiments.

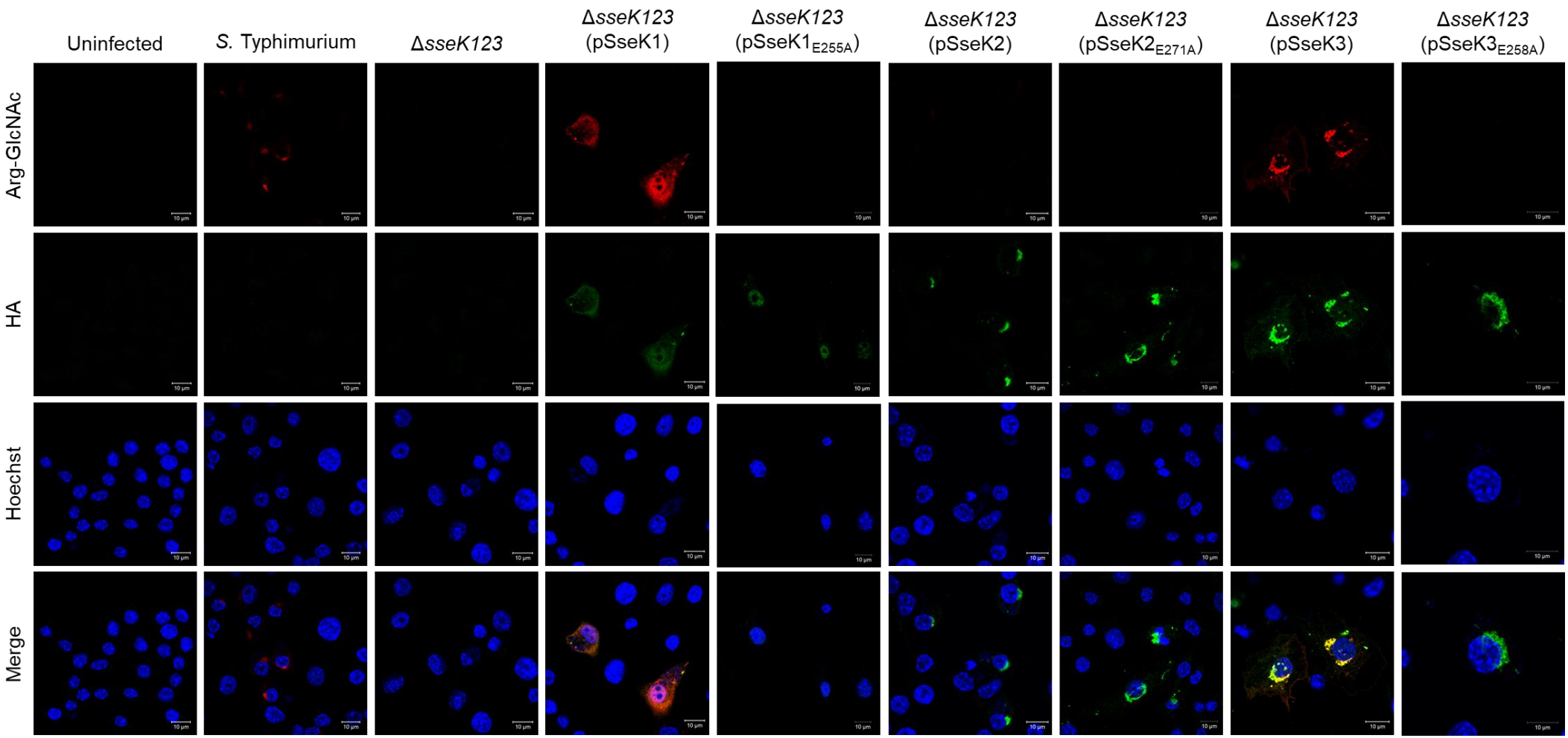
Uninfected
S. Typhimurium
ΔsseK123
ΔsseK123 (pSseK1)
ΔsseK123 (pSseK1E255A)
ΔsseK123 (pSseK2)
ΔsseK123 (pSseK2E271A)
ΔsseK123 (pSseK3)
ΔsseK123 (pSseK3E258A)
Arg-GlcNAc
HA
Hoechst
Merge

Figure 4.2. Sub-cellular localisation of arginine-glycosylated host substrates during *S.* Typhimurium infection.

Representative immunofluorescence fields of RAW264.7 cells infected with complemented *S.* Typhimurium strains. Wild type *S.* Typhimurium, a triple Δ*sseK1sseK2sseK3* mutant and triple mutant complemented with plasmids encoding one of HA-tagged SseK1, SseK2 or SseK3, or with catalytically-inactive effector derivatives were used to infect RAW264.7 for 20 h, as indicated. Overexpression of the effectors was induced during host cell infection by the addition of 1 mM IPTG. Cells were fixed and permeabilized at 20 hours post infection. Arginine glycosylation was visualised using anti-ArgGlcNAc antibody (red). HA-tagged effector proteins were visualised using anti-HA antibody (green). Cell nuclei were visualised with Hoechst stain (blue).

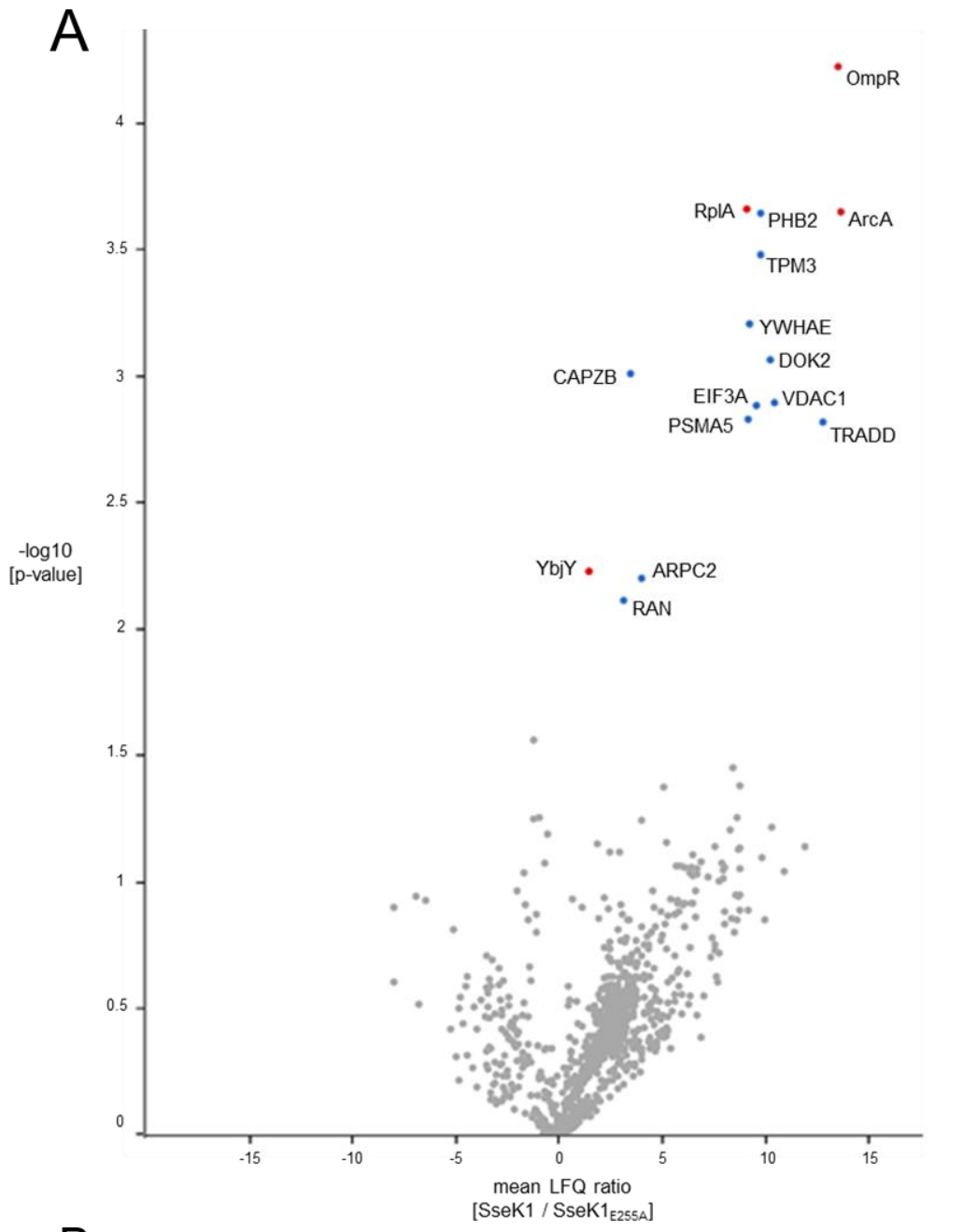
A
OmpR
RplA
PHB2
ArcA
TPM3
YWHAE
DOK2
CAPZB
EIF3A
VDAC1
PSMA5
TRADD
YbjY
ARPC2
RAN
-log10
[p-value]
mean LFQ ratio
[SseK1 / SseK1E255A]

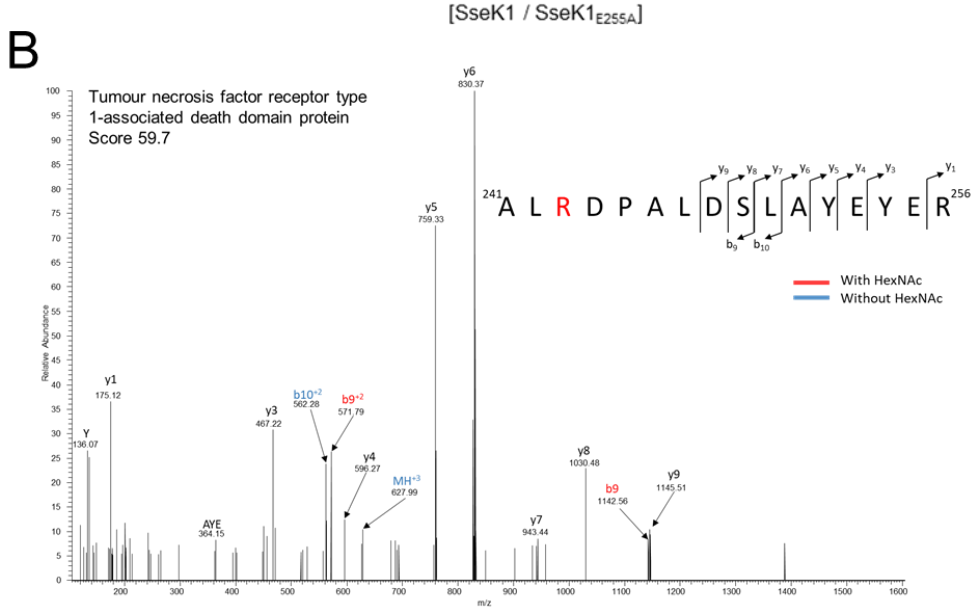
B
Tumour necrosis factor receptor type
1-associated death domain protein
Score 59.7
241A L R D P A L D S L A Y E Y E R256
With HexNAc
Without HexNAc
Relative Abundance
m/z

Figure 4.3. Enrichment of arginine-glycosylated proteins modified by overexpressed SseK1.

(A) Label-free quantification of ArgGlcNAc modified proteins immunoprecipitated from RAW264.7 cells infected with *S.* Typhimurium Δ*sseK1sseK2sseK3* complemented with either SseK1-HA or SseK1E$_{255A}$-HA. Arginine-glycosylated proteins are presented as a volcano plot depicting mean ion intensity peptide ratios of SseK1-HA versus SseK1E$_{255A}$-HA plotted against logarithmic *t* test *p* values from biological triplicate experiments. Arginine glycosylated peptides with corresponding *t* test *p* values below 0.01 are annotated by gene game, with human peptides shaded blue and bacterial peptides shaded red. (B) Manually curated spectra showing glycosylation of Arg^{243} within the death domain of mouse TRADD, Andromeda score 59.7.

A

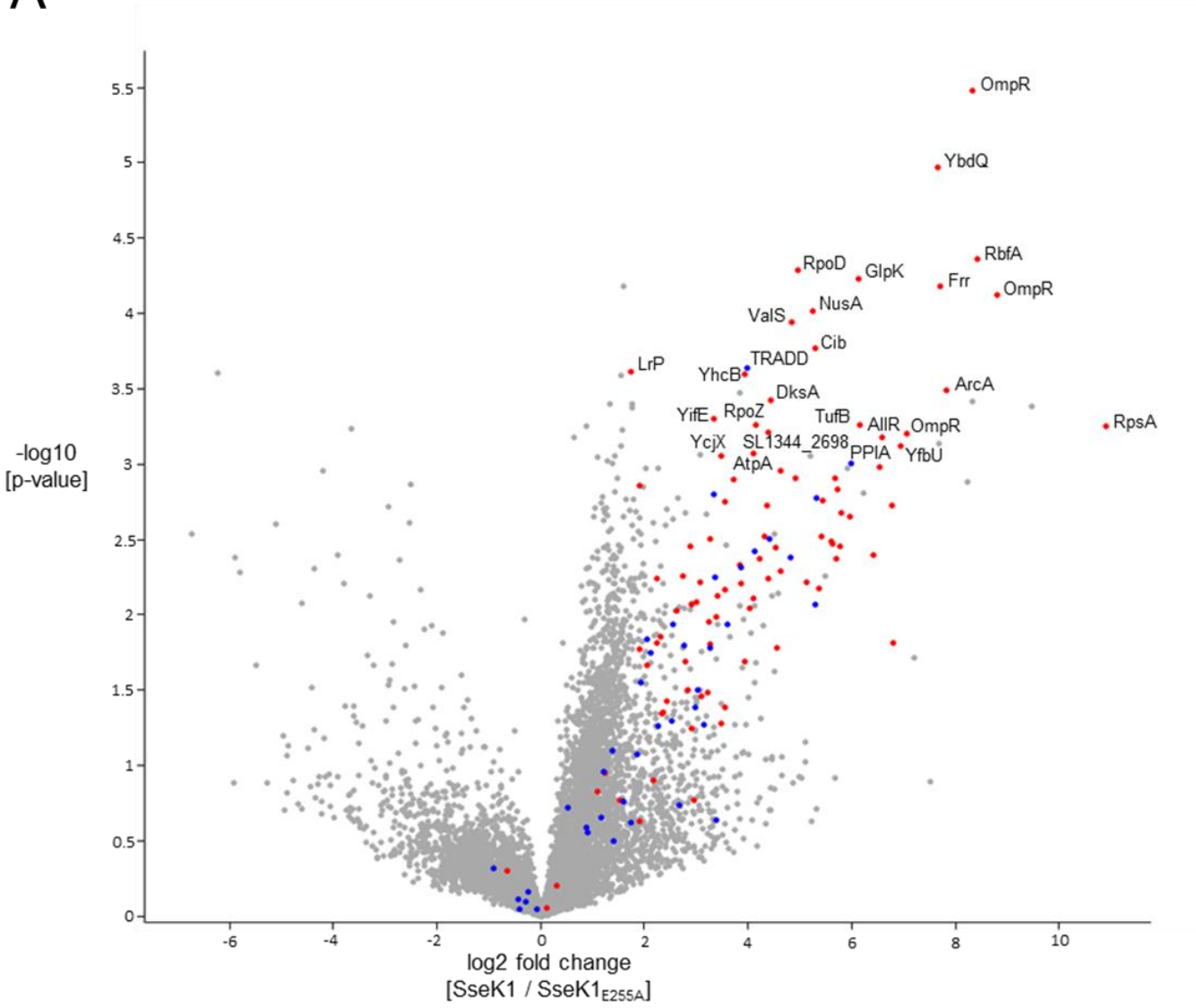
OmpR
YbdQ
RbfA
RpoD
GlpK
Frr
OmpR
NusA
ValS
Cib
TRADD
LrP
YhcB
ArcA
DksA
YifE
RpoZ
TufB
AllR
OmpR
RpsA
YcjX
SL1344_2698
PPIA
YfbU
AtpA
-log10 [p-value]
log2 fold change [SseK1 / SseK1E255A]

B

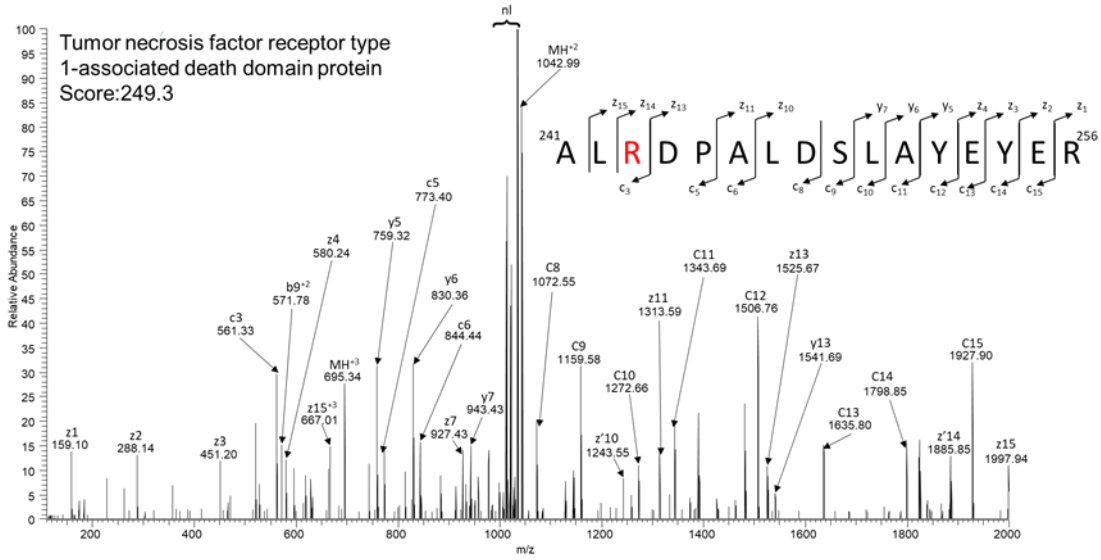
Tumor necrosis factor receptor type 1-associated death domain protein
Score:249.3
241 A L R D P A L D S L A Y E Y E R 256
Relative Abundance
m/z

Figure 4.4. Enrichment of arginine-glycosylated peptides modified by overexpressed SseK1.

(A) Label-free quantification of ArgGlcNAc peptide immunoprecipitated from RAW264.7 cells infected with *S.* Typhimurium Δ*sseK1sseK2sseK3* complemented with either SseK1-HA or SseK1E$_{255A}$-HA. Arginine-glycosylated peptides are presented as a volcano plot depicting mean ion intensity peptide ratios of SseK1-HA versus SseK1E$_{255A}$-HA plotted against logarithmic *t* test *p* values from biological triplicate experiments. Arginine glycosylated peptides with corresponding *t* test *p* values below 0.001 are annotated by gene name, with human peptides shaded blue and bacterial peptides shaded red. (B) Manually curated EThcD spectra showing glycosylation of Arg^{243} within the death domain of mouse TRADD, Andromeda score 249.3. Within MS/MS spectra nl denote neutral loss associated ions.

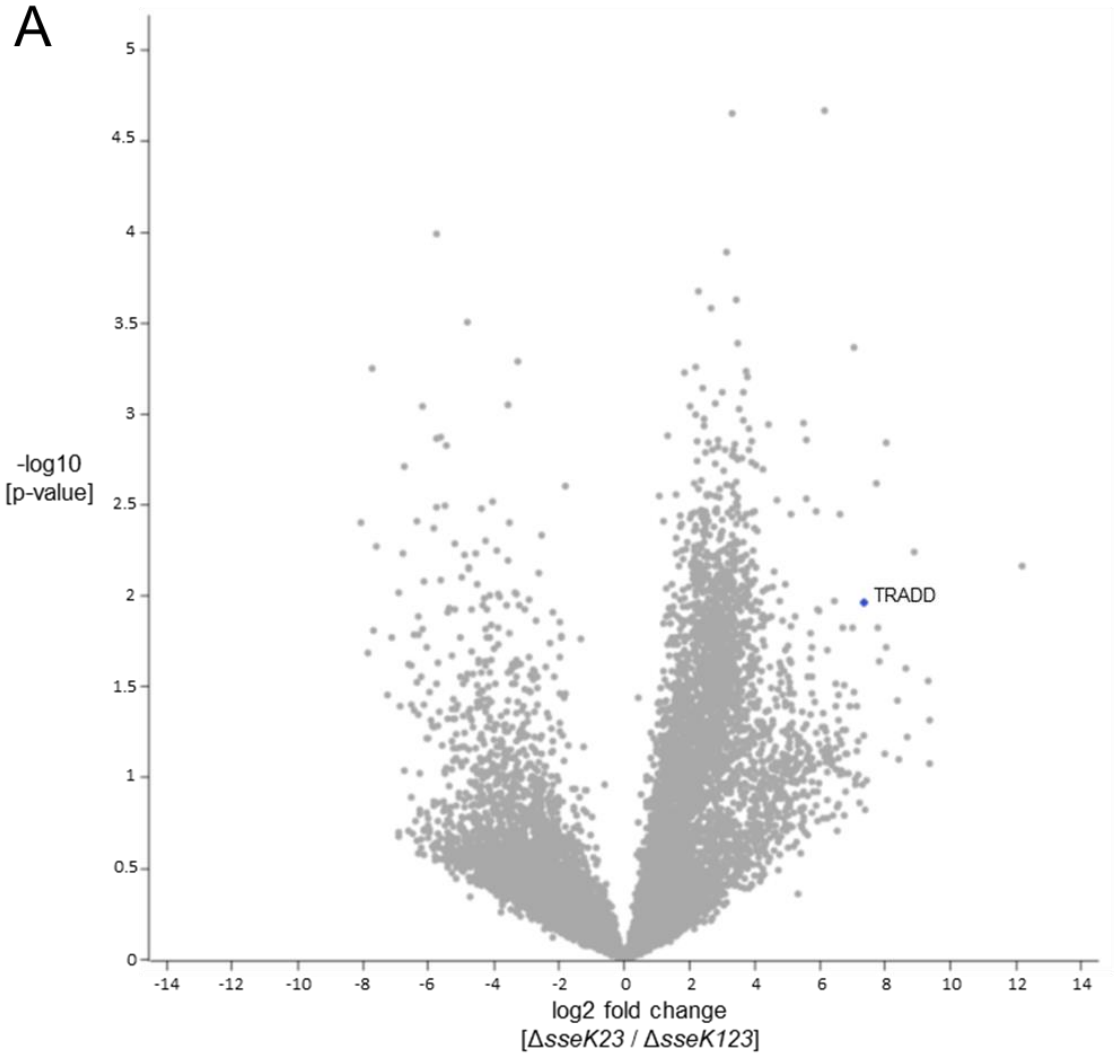
A
-log10
[p-value]
TRADD
log2 fold change
[ΔsseK23 / ΔsseK123]

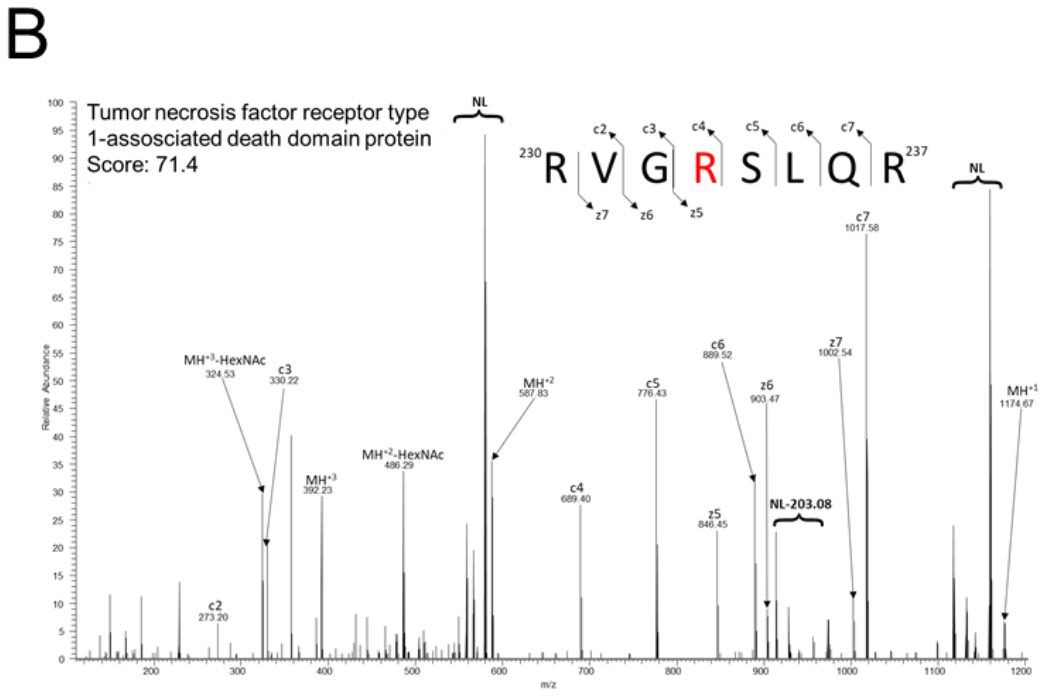
B
Tumor necrosis factor receptor type
1-assosciated death domain protein
Score: 71.4
NL
230 R V G R S L Q R 237
NL-203.08
Relative Abundance
m/z

Figure 4.5. Enrichment of arginine-glycosylated peptides modified by endogenous SseK1.

(A) Parallel reaction monitoring of ArgGlcNAc peptide immunoprecipitated from RAW264.7 cells infected with *S.* Typhimurium Δ*sseK1sseK2sseK3* or *S.* Typhimurium Δ*sseK2sseK3*. Arginine-glycosylated peptides are presented as a volcano plot depicting mean log2 ion intensity peptide ratios of Δ*sseK1sseK2sseK3* versus Δ*sseK2sseK3* plotted against logarithmic *t* test *p* values from biological triplicate experiments. Arginine-glycosylated peptides are annotated by gene name and shaded blue. (B) Manually curated EThcD spectra showing glycosylation of Arg^{233} within the death domain of mouse TRADD, Andromeda score 71.4. Within MS/MS spectra NL denote neutral loss associated ions.

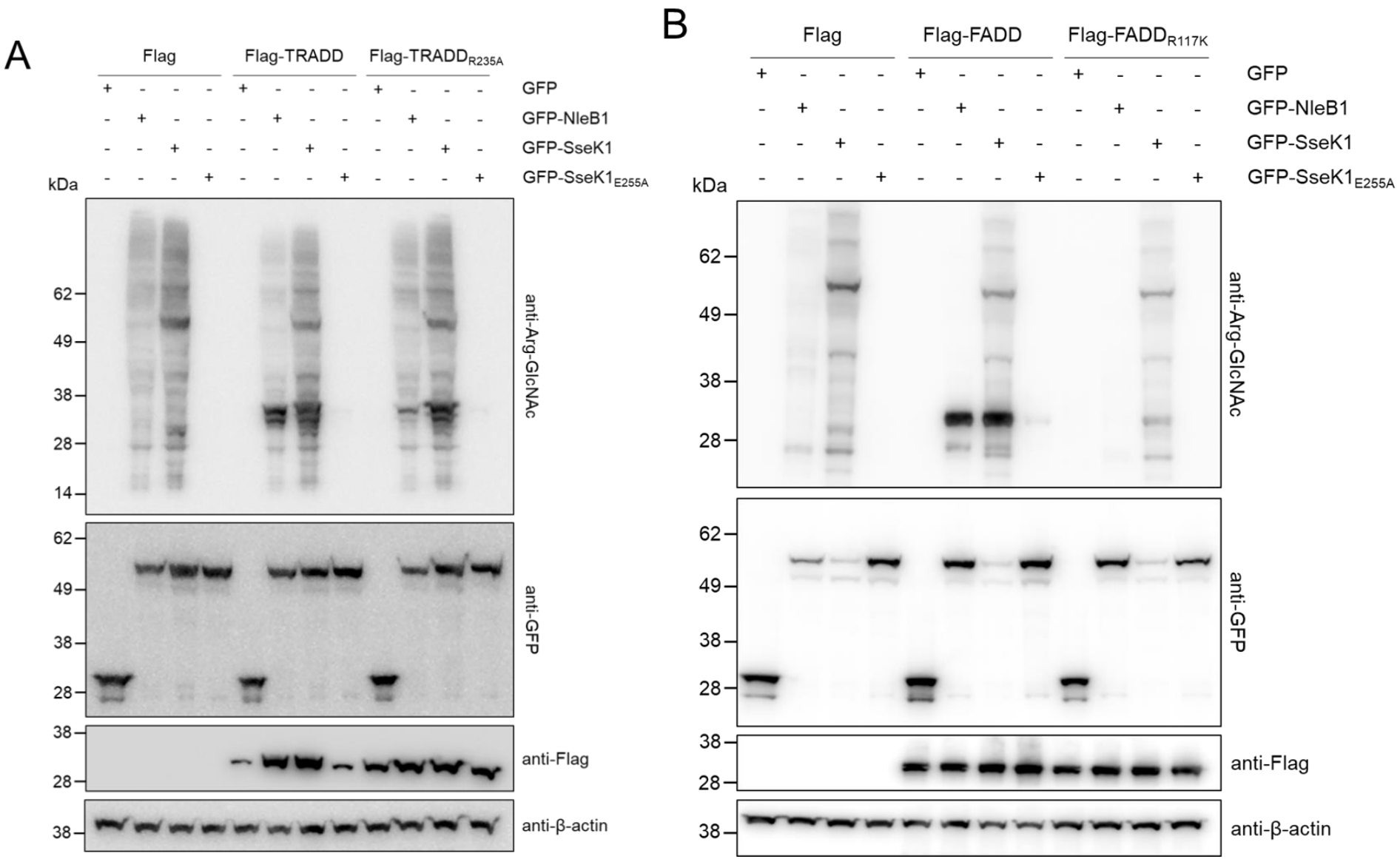
A
Flag
Flag-TRADD
Flag-TRADD$_{R235A}$
GFP
GFP-NleB1
GFP-SseK1
GFP-SseK1$_{E255A}$
kDa
62
49
38
28
14
anti-Arg-GlcNAc
anti-GFP
anti-Flag
anti-β-actin
B
Flag
Flag-FADD
Flag-FADD$_{R117K}$
GFP
GFP-NleB1
GFP-SseK1
GFP-SseK1$_{E255A}$
kDa
anti-Arg-GlcNAc
anti-GFP
anti-Flag
anti-β-actin

Figure 4.6. Validation of SseK1-mediated glycosylation of host death-domain proteins.

Immunoblots of HEK293T cells co-transfected with GFP-fusions of indicated effector proteins or catalytic mutants and Flag-tagged putative host substrates (A) TRADD and (B) FADD. Proteins were detected with anti-ArgGlcNAc, anti-GFP, and anti-Flag, as indicated. Anti-β-actin was used as a loading control. Representative immunoblot of at least three independent experiments.

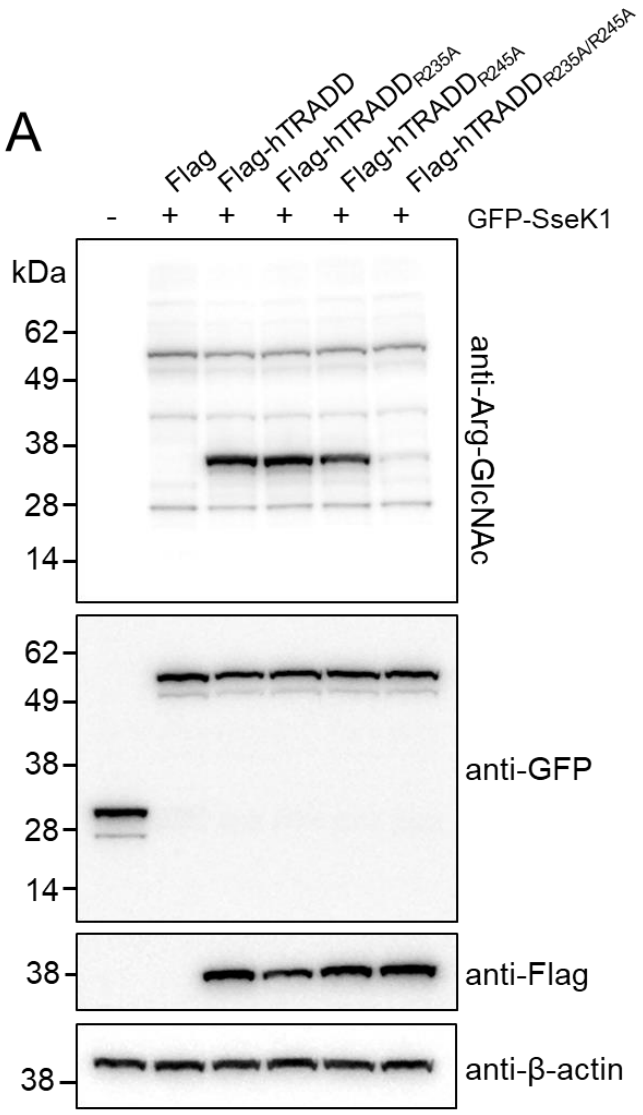
A
Flag
Flag-hTRADD
Flag-hTRADD$_{R235A}$
Flag-hTRADD$_{R245A}$
Flag-hTRADD$_{R235A/R245A}$
- + + + + +
GFP-SseK1
kDa
62
49
38
28
14
anti-Arg-GlcNAc
62
49
38
28
14
anti-GFP
38
anti-Flag
38
anti-β-actin

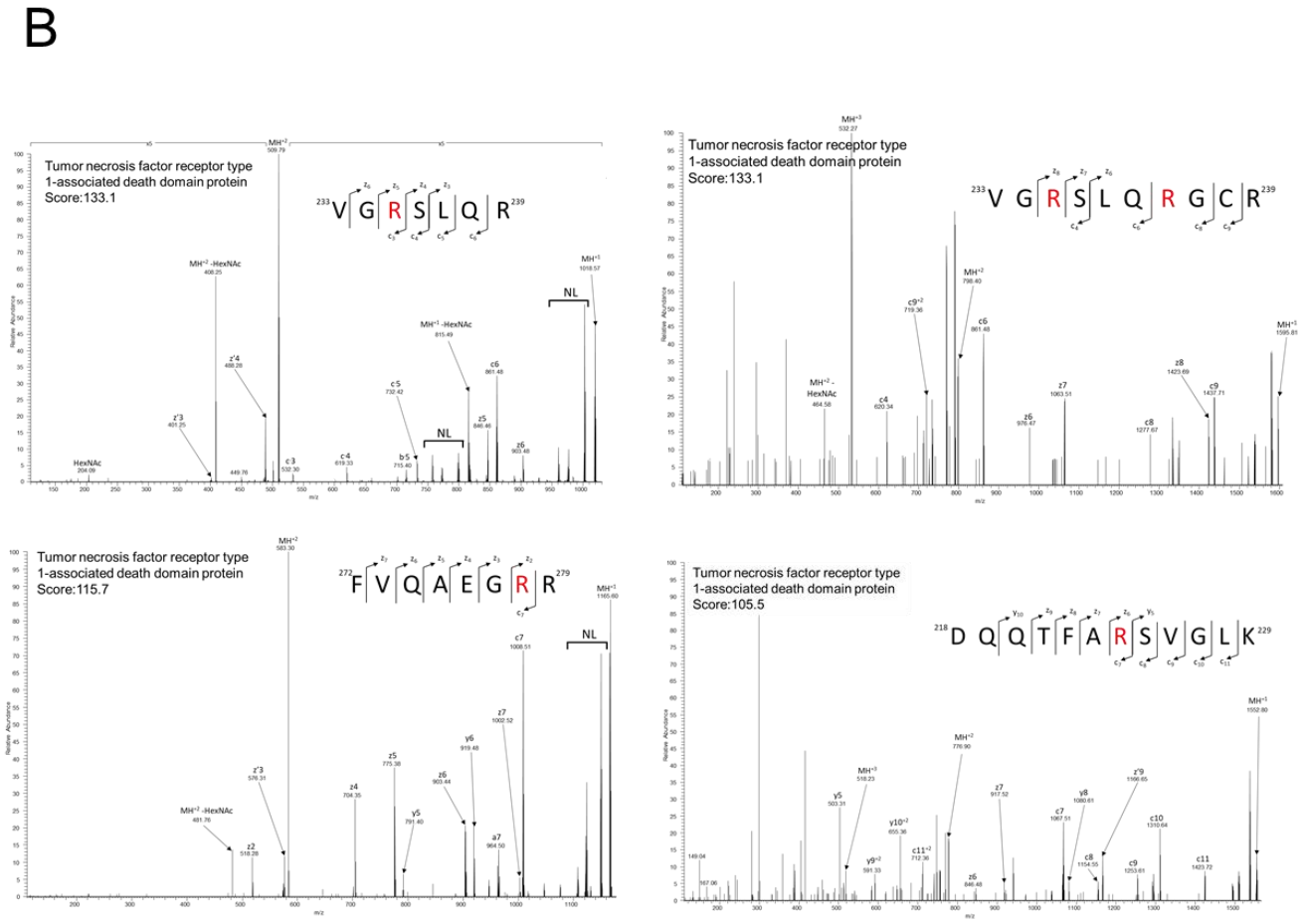
B
Tumor necrosis factor receptor type 1-associated death domain protein
Score:133.1
233 V G R S L Q R 239
Tumor necrosis factor receptor type 1-associated death domain protein
Score:133.1
233 V G R S L Q R G C R 239
Tumor necrosis factor receptor type 1-associated death domain protein
Score:115.7
272 F V Q A E G R R 279
Tumor necrosis factor receptor type 1-associated death domain protein
Score:105.5
218 D Q Q T F A R S V G L K 229

Figure 4.7. Mutagenesis of putative glycosylation sites of TRADD.

(A) Immunoblot showing arginine glycosylation of ectopically expressed FLAG-hTRADD or FLAG-hTRADD mutants in HEK293T cells co-transfected with pEGFP-SseK1. Cells were harvested for immunoblotting and detected with anti-ArgGlcNAc, anti-GFP, and anti-FLAG antibodies. Antibodies to β-actin were used as a loading control. Representative immunoblot of at least three independent experiments. (B) Manually curated EThcD spectra of arginine-glycosylated FLAG-hTRADD enriched by anti-FLAG immunoprecipitation following ectopic expression in HEK293T cells, co-transfected with pEGFP-SseK1. Various observed sites of arginine-glycosylation are highlighted in red, and presented alongside corresponding M/Z values and observed Andromeda scores. Within MS/MS spectra NL denote neutral loss associated ions.

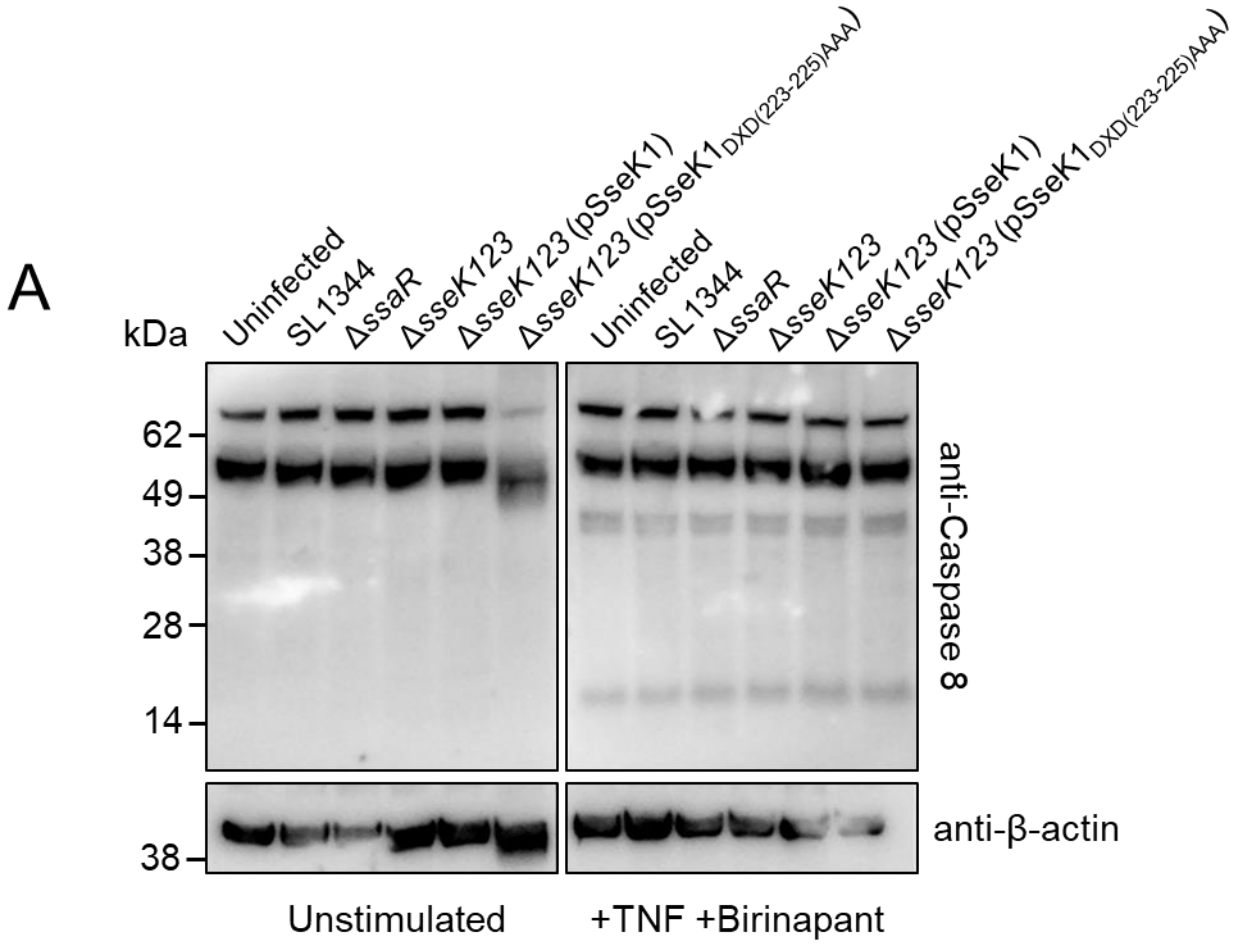
A
kDa
Uninfected
SL1344
ΔssaR
ΔsseK123
ΔsseK123 (pSseK1)
ΔsseK123 (pSseK1DXD(223-225)AAA)
62
49
38
28
14
anti-Caspase 8
anti-β-actin
Unstimulated
+TNF +Birinapant

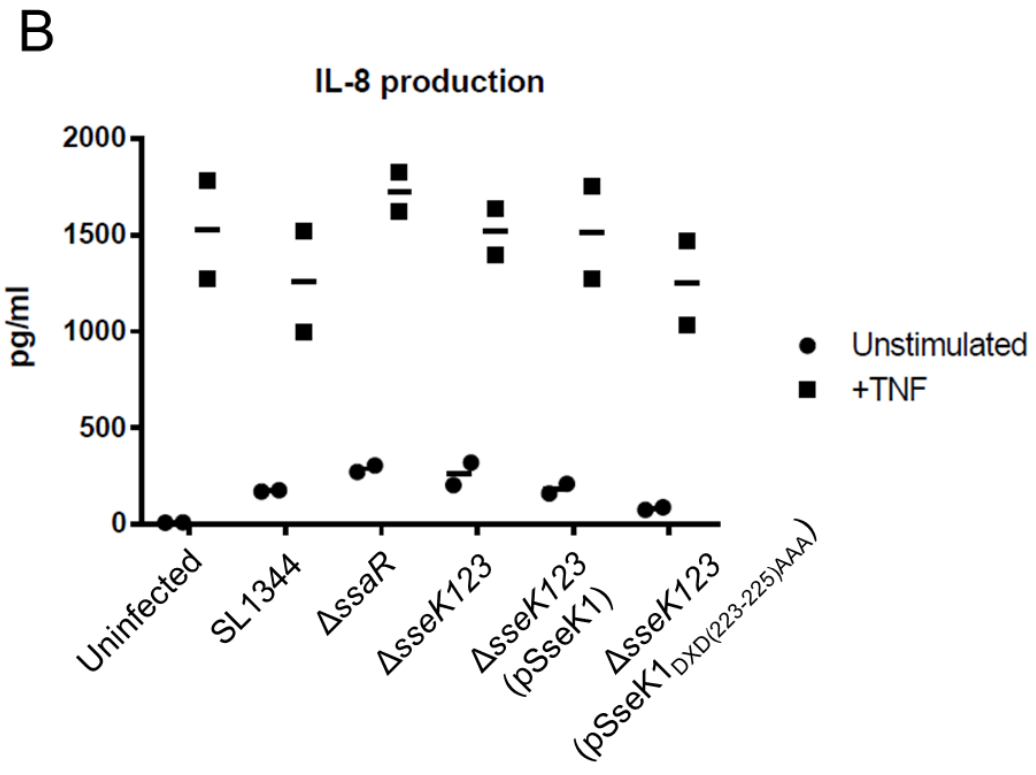
B
IL-8 production
pg/ml
2000
1500
1000
500
0
Unstimulated
+TNF
Uninfected
SL1344
ΔssaR
ΔsseK123
ΔsseK123 (pSseK1)
ΔsseK123 (pSseK1DXD(223-225)AAA)

Figure 4.8. Functional consequences of SseK1-mediated glycosylation of TRADD. (A) Immunoblot of lysate of RAW264.7 cells infected with *S.* Typhimurium derivatives. Cells were infected for 3 hours then either left unstimulated (left) or treated with TNF and Birinapant (right). Cells were lysed 5.5 hours post-stimulation. Proteins were detected with anti-caspase 8, and anti-β-actin was used as a loading control. (B) Quantification of IL-8 production by ELISA. RAW264.7 cells were infected with indicated *S.* Typhimurium strains. Cells were infected for 3 hours then either left unstimulated or treated with TNF. Supernatant was collected 6 hours post-stimulation and IL-8 production quantified via ELISA.

Chapter Five

Identifying and validating the host substrates of SseK3

CHAPTER 5. Identifying and validating the host substrates of SseK3.

5.1. Introduction

Several reports describing the function of the SseK effectors have contributed to an emerging understanding that these effectors may antagonise cell signaling in a manner similar to the homologous effector NleB1 from enteropathogenic *E. coli* (EPEC). NleB1 is known to inhibit apoptotic cell death and NF-κB signaling through glycosylation of the host adaptors TRADD and FADD (244, 245). Based on sequence homology between NleB1 and the SseK effectors (276), most investigations have hypothesised that these effectors similarly inhibit immune signaling. However, few studies have identified the specific host proteins that are targeted by these effectors, and among these studies there is little consensus. In the previous chapter, we showed that SseK1 translocated during *S.* Typhimurium infection functions as an arginine glycosyltransferase that predominantly targets Arg235 in the death domain of TRADD (Fig 4.5), confirming and extending previous reports that observed this interaction during ectopic expression and in *in vitro* glycosylation experiments (245).

However, relatively few reports have suggested host targets for SseK2 and SseK3. One study reported binding of SseK3 to TRIM32 but further showed SseK3 did not glycosylate TRIM32 nor influence the ubiquitination of TRIM32 (280). A later study confirmed the binding of SseK3 to TRIM32, but further used TRIM32 knockout macrophages to show the translocation and localisation of SseK3 was not changed in the absence of TRIM32 (314). Separately, another study reported SseK2-mediated glycosylation of FADD during *in vitro* glycosylation assays, while SseK1 and SseK3 did not glycosylate FADD in this same experiment (315). In conflict with this finding, another report showed that FADD was glycosylated by SseK1 but not by SseK2 or SseK3 (314). This same report also showed weak glycosylation of TRADD in the presence of SseK3 (314). Collectively, these

reports provide conflicting data regarding the host targets of SseK2 and SseK3, and so identifying the genuine host targets remains a priority.

Functional analyses of the activity of SseK2 and SseK3 have been more revealing. One report showed that SseK3 inhibited NF-κB activation following TNF stimulation via a luciferase reporter assay, and that SseK3 also prevented the degradation of IκB in a manner dependent on the catalytic activity of SseK3 (280). A later report demonstrated that both SseK1 and SseK3, but not SseK2, were capable of preventing nuclear translocation of p65, and these effectors also prevented IκBα degradation (315). This study also showed that SseK1 inhibited the polyubiquitination of TRAF2, while SseK2 and SseK3 had no impact on this activity (315). Separately, another study reported that SseK1 and SseK3 additively contributed to inhibition of NF-κB activation during infection, again using a luciferase reporter assay. Further, the authors showed a reduction in IL-6 mRNA levels during infection with strains expressing SseK1 or SseK3. Finally, this study used a range of assays to demonstrate that SseK1 and SseK3 inhibit cell death following TNF stimulation, and provided preliminary evidence to suggest these effectors inhibit necroptotic cell death during *S.* Typhimurium infection (314). Together, these studies suggest overlapping functions for SseK1 and SseK3. However, in this thesis we showed the glycosylation pattern of overexpressed SseK3 appeared to be much broader than that of SseK1 (Fig 4.1), while the subcellular localisation patterns of these effectors were distinct (Fig 3.2). This suggests SseK1 and SseK3 may have different host targets and play different roles during infection. Ultimately, identifying the host proteins that are targeted by these effectors will greatly contribute to understanding how these effectors function during infection.

Thus, the aim of this chapter was to identify the host targets of SseK3 and characterise the contribution of SseK3 to virulence in animal models. We applied our method for the enrichment of arginine glycosylated peptides to cells infected with *sseK12* deletion mutants,

and by mass spectrometry we observed glycosylation of the host signaling receptors TNFR1 and TRAILR. These proteins had not been identified as targets of the SseK effectors previously, and so represented novel substrates. We proceeded to validate SseK3-dependent glycosylation of TNFR1 and TRAILR through a range of *in vitro* approaches, and conducted preliminary investigations into the contribution of SseK3 in two different animal models. Collectively this work suggested the SseK effectors target different components of death receptor signaling during infection of host cells.

5.2. Results

5.2.1. SseK3 glycosylates a conserved arginine residue in the mammalian death receptors TNFR1 and TRAILR.

Previously, we observed that the glycosylation profile of SseK1 increased during over-expression compared to endogenous levels of expression (Fig 4.1), and that over-expression greatly increased the range of glycosylated substrates (Fig 4.3, Fig 4.4) when compared to the activity of endogenous levels of SseK1 (Fig 4.5). Similarly, we found that overexpression of SseK3 greatly increased arginine glycosylation activity relative to the levels generated by wild type *S.* Typhimurium during infection (Fig. 1B). Therefore, we aimed to identify the substrates of SseK3 during endogenous levels of expression, given that overexpression would likely lead to non-authentic glycosylation of other substrates. Here, we applied our peptide enrichment strategy to identify Arg-GlcNAcylated substrates in the presence of native levels of SseK3. Arg-GlcNAcylated peptides were enriched from RAW264.7 cells infected with either a double *ΔsseK12* mutant or a triple Δ*sseK1sseK2sseK3* mutant, and we applied label free MS based quantification to screen for glycosylation events in a non-biased manner (Fig 5.1A). Under these conditions, we detected SseK3-dependent arginine glycosylation of mouse TNFR1 (mTNFR1) and TRAILR (mTRAILR), both death

domain-containing receptors of the TNF superfamily (316). Arg-GlcNAcylation was observed in all three biological replicates of cells infected with the *ΔsseK12* deletion mutant, while no Arg-GlcNAcylation was detected in cells infected with the Δ*sseK1sseK2sseK3* deletion mutant (Fig 5.1B). Glycosylation of mTRAILR occurred at Arg^{293} while mTNFR1 was glycosylated at Arg^{376}. An alignment of protein sequences demonstrated that these sites corresponded to a conserved arginine in the death domains of both proteins (Figs. 5.1C and 5.1D) that also corresponds to the conserved arginine from other death domain-containing proteins targeted by NleB1 (244, 245). No other Arg-GlcNAcylated peptides were detected under these conditions, suggesting that TRAILR and TNFR1 were the preferred substrates of SseK3.

5.2.2. SseK3 glycosylates a range of insoluble membrane-associated host proteins.

Previously, we showed that SseK3 co-localises with the host Golgi during infection (Fig 3.2), and that the arginine-glycosylated substrates of SseK3 have a similar localisation phenotype (Fig 4.2). Given that the host substrates of SseK3 are likely associated with the Golgi, we speculated that using cellular fractionation to isolate insoluble proteins might improve the detection of glycosylated substrates. To explore this, we isolated various fractions of cell lysate by centrifugation and treatment with digitonin, and immunoblotted for arginine glycosylation to observe the fractionation of glycosylated protein (Fig 5.2A). We observed that the majority of arginine glycosylated proteins remained in the insoluble fraction. Therefore, we repeated our experiment to enrich for arginine glycosylated peptides and focused exclusively on the digitonin-insoluble fraction. Again we used label free MS quantification to detect arginine glycosylation, and in this experiment we observed glycosylation of a range of mammalian proteins (Fig 5.2B). We again detected glycosylation

of TNFR1 and TRAILR but additionally observed modification of several Rab-family proteins including Rab1, Rab5, and Rab11 (Fig 5.2B, Fig 5.2C). Additionally, we observed glycosylation of TRADD among a range of other mammalian proteins, and we also detected glycosylation of several bacterial proteins including Rho, RstA, YjjK, and NanK. Collectively, this experiment demonstrated that endogenous levels of SseK3 appeared to glycosylate a range of mammalian and bacterial proteins, which suggests a diversity of possible roles for SseK3 in *S.* Typhimurium virulence.

5.2.3. Validation of the interaction between SseK3 and TRAILR

Our findings identified novel substrates of endogenous levels of SseK3 during *S.* Typhimurium infection, both from whole cell lysates (Fig 5.1) and from enriched cellular fractions (Fig 5.2). In validating the interaction between SseK3 and these novel substrates, and in exploring the contribution of these interactions to virulence, we chose to focus on TRAILR and TNFR1 given that these substrates were detected in both experiments and are among the most highly enriched GlcNAcylated peptides.

Previously, we observed glycosylation of mouse TRAILR during infection of RAW264.7 cells (Fig 5.1, Fig 5.2). Here, we confirmed glycosylation of the human homologue of mTRAILR. Humans express four isoforms of TRAILR, and so we focused on hTRAILR2 as it shows the strongest sequence similarity to mTRAILR (266). First, we used the yeast two-hybrid system to validate the protein-protein interaction between SseK3 and hTRAILR2. Auxotrophic yeast strains were co-transformed to express SseK3 and the death domain of hTRAILR2 ($hTRAILR2_{DD}$). However, yeast co-transformed to express SseK3 and $hTRAILR2_{DD}$ did not grow on selective media (Fig 5.3A), suggesting that the interaction may be transient or otherwise not detectable in this system.

Next, we attempted to validate SseK3-dependent glycosylation of TRAILR2. To achieve this, the Flag-tagged death domain of hTRAILR2 (Flag-hTRAILR2$_{DD}$) was enriched by anti-Flag immunoprecipitation from HEK293T cells co-transfected with pEGFP-SseK3. Using anti-Arg-GlcNAc antibody, we detected Arg-GlcNAcylation of Flag-hTRAILR2$_{DD}$ by GFP-SseK3 but not GFP-SseK3$_{E258A}$ (Fig 5.3B), thus confirming the interaction and demonstrating that the catalytic activity of SseK3 was required to mediate glycosylation. To validate the specific site of modification, recombinant GST-SseK3 was incubated with His-hTRAILR2$_{DD}$ in the presence of the sugar donor UDP-GlcNAc, subjected to tryptic digestion and analysed by LC-MS. We detected hTRAILR2$_{DD}$ modified at Arg359 (Fig 5.3C, Fig 5.3D), equivalent to the modification of mTRAILR at Arg293 described above (Fig 5.1D). In the absence of UDP-GlcNAc, the modification of hTRAILR2$_{DD}$ was not observed (Fig 5.3E). For both experiments the unmodified peptide ^{396}DASVHTLLDALETGER^{412} derived from mTRAILR was monitored as an internal control and showed comparable ion intensity within the sample input which was consistent with the total observed protein levels between samples (data not shown). To further validate glycosylation of hTRAILR2$_{DD}$, we again incubated recombinant GST-SseK3 and His-hTRAILR2$_{DD}$ with UDP-GlcNAc, then immunoblotted using anti-ArgGlcNAc antibody. This approach confirmed glycosylation of hTRAILR2$_{DD}$ by SseK3 in a manner dependent on UDP-GlcNAc (Fig 5.3F), but we also detected UDP-GlcNAc-independent glycosylation of free GST and GST-SseK3, possibly as an artefact of expressing recombinant SseK3. Collectively, these data confirm SseK3 catalyses arginine glycosylation of human TRAILR2, specifically at Arg293 within the conserved death domain region.

5.2.4. Validation of the interaction between SseK3 and TNFR1

Next, we focused on confirming the interaction between SseK3 and TNFR1. As above, though we previously identified glycosylation of mouse TNFR1 (Fig 5.1A, Fig 5.2B), here we validated the glycosylation of human TNFR1. In yeast two-hybrid experiments, auxotrophic yeast strains were co-transformed to express SseK3 and the death domain of human TNFR1 ($hTNFR1_{DD}$). Yeast expressing SseK3 and $hTNFR1_{DD}$ grew when plated on selective media, indicating a stable interaction between SseK3 and $hTNFR1_{DD}$ (Fig 5.4A). Here, we validated glycosylation of $hTNFR1_{DD}$ by co-transfecting HEK293T cells with pFlag-hTNFR1DD and pEGFP-SseK3, then enriching for hTNFR1DD by anti-Flag immunoprecipitation. Immunoblotting of cell lysates with anti-Arg-GlcNAc antibody showed glycosylation of Flag-$hTNFR1_{DD}$ by GFP-SseK3 but not GFP-$SseK3_{E258A}$ (Fig 5.4B), confirming the modification seen during infection (Fig 5.1) and again demonstrating that the catalytic activity of SseK3 was required for this modification.

Further validation of arginine glycosylation of hTNFR1 by *in vitro* glycosylation assays as above was complicated by the insoluble nature of recombinant His-$hTNFR1_{DD}$. Instead, Flag-$hTNFR1_{DD}$ was enriched from HEK293T cells by anti-Flag immunoprecipitation following co-transfection with pEGFP-SseK3. Immunoprecipitated protein samples were subjected to tryptic digestion ahead of analysis by LC-MS, and using this approach we observed glycosylation of $hTNFR1_{DD}$ at Arg376 (Fig 5.4C), consistent with the site observed in the primary screen (Fig 5.1). Together, these data supported our findings that SseK3 mediates arginine glycosylation of TNFR1 at Arg376 within the death domain.

5.2.5. Functional consequences of SseK-mediated glycosylation on TRAIL signaling.

We observed the glycosylation of the signaling receptor TRAILR during infection of murine RAW264.7 cells (Fig 5.1, Fig 5.2), and confirmed that SseK3 also glycosylates the human homologue hTRAILR2 *in vitro* (Fig 5.3). Next, we attempted to determine the physiological consequence of this modification during *S.* Typhimurium infection of RAW264.7 cells. TRAIL signaling is reported to potentiate a range of signaling outcomes, including cell death via caspase 8 mediated apoptosis or alternatively via necroptosis, but TRAIL can also stimulate production of anti-apoptotic proteins and inflammatory cytokines through NF-κB signaling pathways (269, 317). We initially focused on apoptotic signaling, given the well-reported ability of the homologous effector NleB1 to impede caspase 8 dependent apoptosis during infection (244, 245). To explore inhibition of apoptotic signaling, we infected RAW264.7 cells with various *S.* Typhimurium mutants and stimulated with TRAIL ligand to potentiate cell death. Immunoblotting for the initiator caspase 8 (Fig 5.5A) and the executioner caspase 3 was used as an indicator of cell death (Fig 5.5B). We noted that cleavage of caspase 8 appeared to be decreased in cells infected with the Δ*sseK1sseK2sseK3* mutant relative to cells infected with wild-type SL1344, suggesting that these effectors may promote cleavage of caspase 8 and cell death. Consistent with this, immunoblotting for caspase 3 showed greater cleavage of caspase 3 during wild-type infection and reduced cleavage during infection with the Δ*sseK1sseK2sseK3* mutant. The panel of single and double mutants may suggest additive or redundant functions for these effectors, though future experiments are needed to better elucidate these contributions.

5.2.6. The SseK effectors do not impede formation of the TNFR1 signaling complex.

Binding of extracellular TNF to the cognate receptor TNFR1 potentiates the recruitment of various adaptor and signaling proteins to the nascent signaling complex, and assembly of this complex is required for cell signaling outcomes including cell death and inflammatory cytokine production (316, 318). Hence, we explored whether the SseK effectors antagonised assembly of the TNFR1 signaling complex during *S.* Typhimurium infection. Infected cells were stimulated with Fcγ-conjugated TNF to potentiate complex formation, then protein G beads were used to enrich for the Fcγ-TNFR1 complex. Cell lysates and immunoprecipitates were then immunoblotted to detect a range of TNFR1 complex proteins and to determine if the SseK effectors influenced TNFR1 complex assembly (Fig 5.6). First, we probed cell lysates with anti-TNFR1 and observed the formation of bands between 38 and 49 kDa in cells that had been stimulated with TNFR1 (Fig 5.6A, upper panel). This is lower than the expected 50 kDa for TNFR1, however these same bands appeared to be stronger when we probed Fcγ-TNFR1 immunoprecipitates (Fig 5.6A, lower panel), suggesting that these bands may correspond to enriched TNFR1. We noted the intensity of these bands appeared stronger in infected cells relative to uninfected, though there was no apparent difference between wild type and Δ*sseK1sseK2sseK3* infected cells.

Next, we probed for RIPK1 and again detected bands lower than the expected weight (74.8 kDa) in whole cell lysates (Fig 5.6B, upper panel). In immunoprecipitates we detected apparent poly-ubiquitination of RIPK1 in uninfected cells following TNF stimulation, and strikingly this modification was not present in infected cells, suggesting that *S.* Typhimurium engages in inhibition of RIPK1 polyubiquitination during infection (Fig 5.6B, lower panel). However, this activity appeared to be SseK-independent, suggesting other bacterial factors and perhaps other effector proteins mediate this activity.

Anti-TRADD immunoblots were less revealing, as we only detected faint bands below the expected size of 34.5 kDa in whole cell lysates (Fig 5.6C, upper panel). Probing of immunoprecipitates was confounded by the appearance of strong bands between 38 and 49 kDa (Fig 5.6C, lower panel), similar to those observed during anti-TNFR1 immunoblotting (Fig 5.6A, lower panel). However, faint bands were detected around 34 kDa in infected cells following longer stimulation with TNF, corresponding to the expected size of TRADD, though there was no clear difference between cells infected with wild type and Δ*sseK1sseK2sseK3* infected cells.

Next we probed for the adaptor protein TRAF2, a well-described positive regulator of NF-κB signaling (319). In whole cell lysates, TRAF2 was detected slightly below the expected size of 56 kDa, and bands corresponding to TRAF2 appeared weaker in both wild type and Δ*sseK1sseK2sseK3* infected cells (Fig 5.6D, upper panel). Again, probing immunoprecipitates with anti-TRAF2 was confounded by the presence of strong bands between 38 kDa and 49 kDa (Fig 5.6D, lower panel), as seen previously.

We then probed for the presence of cIAP, an E3 ligase which plays a crucial role in skewing TNF signaling from pro-cell survival to programmed cell death (269). Interestingly, we noted a marked reduction of cIAP1 in infected cell lysates, relative to uninfected cells (Fig 5.6E, upper panel). There was no apparent contribution of the SseK effectors, but we did note the formation of a large molecular weight band in Δ*sseK1sseK2sseK3* infected cells after 90 minutes of TNF stimulation (Fig 5.6E, upper panel). Probing immunoprecipitates with anti-cIAP1 antibody did not reveal the presence of cIAP1 bound to the TNFR1 complex in any condition (Fig 5.6E, lower panel).

Lastly, we probed cell lysates for arginine glycosylation and observed strong bands between 28 and 38 kDa (Fig 5.6F, upper panel), corresponding to TRADD at the reported size of 34.5 kDa. Fainter bands were observed around 28 kDa, while we again noted weaker

bands between 38 and 49 kDa similar to those seen on the anti-TNFR1 lysate blot (Fig 5.6A, upper panel). Probing immunoprecipitates with anti-ArgGlcNAc failed to detect glycosylated substrates (Fig 5.6F, lower panel), potentially suggesting that modified TRADD is not co-enriched with the TNFR1 complex. However, these blots were again confounded by the presence of non-specific bands similar those seen on other blots.

Collectively, our strategy to enrich the TNFR1 complex from infected cells revealed apparent inhibition of RIPK1 ubiquitination and a reduction of both TRAF2 and cIAP1 during *S.* Typhimurium infection. While these results appeared to be independent of the SseK effectors, these findings warrant future investigation to uncover the mechanisms involved.

5.2.7. The SseK effectors do not contribute to virulence during infection of C57BL/6 mice.

Next, we attempted to further explore the contribution of the SseK effectors to virulence in an animal model, and in particular characterise the contribution of SseK3 given we previously observed the novel modification of the immune signaling receptors TNFR1 and TRAILR2 (Fig 5.1, Fig 5.2) . To this end, we orally infected C57BL/6 mice with *S.* Typhimurium wild type, Δ*sseK1sseK2sseK3*, or Δ*sseK3*, and collected various organs after 5 days of infection to determine bacterial load. We observed no significant difference between bacterial load in the spleen, liver, colon, or cecum of infected animals (Figure 5.7A), suggesting neither SseK3 nor the SseK effectors collectively contributed to bacterial replication in these organs under these conditions. Next, we quantified the levels of a selected panel of cytokines in the infected mouse colon via cytokine bead array. Detectable levels of TNFα, IFNγ, MCP-1, and IL-6 did not vary to a significant degree between wild type and mutant strains (Fig 5.7B). Collectively, these data suggest that the SseK effectors do not have a major effect on virulence in this model of infection.

5.2.8. Response of TRAIL$^{-/-}$ mice to attenuated *Salmonella* infection.

While a number of previous studies have attempted to characterise the *in vivo* activity of the SseK effectors, none have utilised transgenic mouse lines to explore the contribution of host factors during infection. In this chapter, we observed that TRAILR was the most highly enriched glycosylated protein observed across multiple experiments (Fig 5.1, Fig 5.2). Here, we utilised TRAILR$^{-/-}$ mice to test the contribution of TRAILR to controlling *S.* Typhimurium infection. We used a Δ*aroA* mutant strain of *S.* Typhimurium, which is deficient for aromatic amino acid synthesis and is attenuated for replication. For this reason, infection of standard laboratory mice (e.g. C57BL/6) can be conducted for much longer periods than for non-attenuated bacteria, allowing for the observation of subtle phenotypes that may be overlooked in shorter infections. First, we infected C57BL/6 or TRAILR$^{-/-}$ mice intravenously with *S.* Typhimurium Δ*aroA* and quantified bacterial replication in the spleen and liver after 21 days of infection (Fig 5.8A). We detected a slight but statistically significant difference between bacterial loads in the spleen of C57BL/6 and TRAILR$^{-/-}$ mice, suggesting a contribution of TRAILR in controlling *S.* Typhimurium infection. In contrast, we detected no significant difference in bacterial loads recovered from the liver of these animals. Further, we quantified the detectable levels of a panel of cytokines in the spleen, liver, and serum of these animals via cytokine bead array (Fig 5.8B). In this experiment, we observed no significant difference in the levels of IL-6, IL-10, MCP-1, IFNγ, TNFα or IL-12p70, suggesting TRAILR$^{-/-}$ mice were equally competent at cytokine secretion under these conditions.

Next, we repeated this experiment but instead infected animals orally to determine if the route of infection influenced bacterial loads and cytokine levels. As previously, we collected organs after 21 days of infection, but here we collected the spleen, liver, colon, and

cecum to determine bacterial loads. We observed no significant differences in bacterial loads in these organs when comparing C57BL/6 and TRAILR$^{-/-}$ mice (Fig 5.8C). Again, we determined cytokine levels in these organs as well as the serum (Fig 5.8D), and here we observed a significant difference in levels of IL-6 secretion in the liver when comparing C57BL/6 and TRAILR$^{-/-}$ mice. This result requires further validation in future to better establish a deficiency in IL-6 secretion in these animals, but this may suggest a dependency on TRAILR signaling to stimulate IL-6 secretion in response to *S.* Typhimurium infection. Collectively, these data suggest TRAIL signaling may be important to control bacterial loads in the infected spleen and may also influence IL-6 secretion in the liver, and further work should explore the contribution of the SseK effectors in this model.

5.3. Discussion

Evasion of the host immune response represents a core focus for bacterial pathogens, and selective pressures have produced a variety of evasion mechanisms for not only preventing clearance of the bacteria but also promoting the replication and dissemination of invading pathogens (320). Several pathogens achieve these goals by manipulating immune signaling pathways, which involve complex signaling cascades that are initiated following the detection of pathogens (269, 316, 319). The T3SS effector YopM from *Yersinia* spp. prevents caspase 1 from participating in inflammasome formation, and thus inhibits pyroptosis (321). Similarly, *Shigella* spp. utilise the T3SS effector OspC3 to inhibit caspase 4 and promote cell survival (322). A variety of *Salmonella* SPI-1 T3SS effectors manipulate immune signaling during invasion of host cells, including SipB which binds and activates the caspase 1 inflammasome (180), SspH1 which inhibits NF-κB signaling through E3 ligase activity (182, 183), and AvrA which functions as an acetyltransferase and targets MAPK kinases to inhibit NF-κB and JNK signaling (188). During intracellular infection, a range of SPI-2 T3SS

effectors also manipulate immune signaling, including the metalloproteases PipA, GogA, and GtgG which coordinate to cleave various NF-κB proteins and prevent inflammation (221, 222), while SseL and GogB prevent the degradation of IκBα through different mechanisms in order to prevent NF-κB activation (223, 237). An emerging body of evidence suggests SseK1 predominantly targets the signaling adaptor TRADD (Chapter 4) (245, 314), which likely contributes to the inhibition of NF-κB signaling and necroptotic cell death during infection (314). While SseK3 shows strong homology to SseK1 (276), its function and contribution to virulence has remained relatively unexplored. In this chapter, we identified the preferred host targets of SseK3 utilising a label free mass spectrometry approach to identify arginine glycosylated peptides during *S.* Typhimurium infection. Although SseK3 had been reported to interact with TRADD and TRIM32 (280, 314), here we found that the preferred substrates of SseK3 were TNFR1 and TRAILR, both members of the mammalian TNF receptor superfamily.

TNFR1 responds to stimulation by extracellular TNF and initiates a signaling cascade culminating in either inflammatory cytokine production or programmed cell death, as described in the previous chapter (Section 4.3) (258, 323). Similarly, extracellular TRAIL binds the membrane-associated receptors TRAIL-R1 (262), TRAIL-R2 (263), TRAIL-R3 (264), and TRAIL-R4 (265). Only TRAIL-R1 and TRAIL-R2 contain full-length death domains and are capable of stimulating a range of signaling events, while TRAIL-R3 lacks an intracellular domain and TRAIL-R4 has a truncated death domain (269). Stimulation of TRAIL-R1 and TRAIL-R2 can induce formation of the signaling platform complex I that includes FADD, TRAF2, RIPK1, and caspase 8 (267, 268). This TRAIL-induced complex I, distinct from the TNF-induced complex I in composition, can potentiate a range of signaling outcomes, including inflammatory cytokine production, stimulation of apoptotic cell death via caspase 8 and caspase 3, or the promotion of cell survival via anti-apoptotic functions

mediated by TRAF2 ubiquitination of capase-8 (266-270). Separately, TRAIL stimulation can induce the formation of complex II, which is similar in composition to complex I and also participates in cytokine production and apoptosis, but has further been implicated in necroptosis (270). This diversity of signaling outcomes complicates the interrogation of bacterial manipulation of TRAIL signaling. Previous work suggests SseK3 can inhibit necroptosis during infection (314) and our data provide a possible mechanism for this activity, however it is conceivable that *Salmonella* would benefit from manipulation of a range of TRAIL-mediated outcomes. Thus, the true contribution of the glycosyltransferase activity of SseK3 to *Salmonella* infection requires further exploration, in parallel with the current advances in understanding fundamental aspects of TRAIL signaling.

There are few reports of pathogenic bacteria that directly target TRAIL receptors to promote infection. To our knowledge, the only described example is CADD, a protein of *Chlamydia* that interacts with TNFR1, FasR, TRAIL-R1 and TRAIL-R2 to induce apoptosis *in vitro* (324, 325). Interestingly, a domain of CADD shows sequence similarity to mammalian death domain proteins, and CADD binds directly to death domains of these mammalian TNF family receptors. Despite this potential role in *Chlamydia* pathogenesis, CADD remains a putative virulence factor and has not been established as a translocated effector. In other reports, *Helicobacter pylori* enhances TRAIL-induced, caspase 8 mediated apoptosis in gastric epithelial cells that are otherwise TRAIL resistant (326). While the specific mechanism is not described, *H. pylori* appears to inhibit FLIP recruitment to the TRAIL-induced signaling complex, and thus enhances caspase 8 recruitment and apoptotic cell death. Ultimately, bacterial manipulation of TRAIL signaling remains an underappreciated aspect of host-pathogen research, and it is likely that other pathogenic bacteria engage in inhibition of the TRAIL pathway. We found that TRAIL deficient mice showed a slightly increased susceptibility to infection with *S.* Typhimurium (Fig 5.8A), while

a previous report suggested TRAIL-R$^{-/-}$ mice showed no difference in survival compared to wild type littermate controls during *S.* Typhimurium infection (327). Separately, a number of studies have demonstrated an increased susceptibility to *S.* Typhimurium infection in chickens that display TRAIL polymorphisms (328, 329), possibly suggesting that control of TRAIL signaling is important in species other than inbred mice tested here and elsewhere. Further research characterising the importance of TRAIL signaling to immune defence in other species is required.

Concurrently, *in vivo* studies characterising the effect of SseK3-mediated glycosylation of TNFR1 are recommended. Early reports demonstrated that TNFR1 deficient mice are highly susceptible to *S.* Typhimurium infection (330) and that administration of anti-TNFα antibodies similarly enhances infection in animal models (331, 332). A later study showed that while SPI-2 T3SS-deficient *S.* Typhimurium are attenuated during infection of C57BL/6 mice, this same mutant was significantly more virulent during infection of congenic TNFR1 knockout mice, further demonstrating the importance of TNFR1 to controlling infection (333). Another report supports this observation, as TNFR1 deficient C57BL/6 mice were susceptible to both a SPI-2 T3SS mutant and a virulence plasmid-cured strain of *S.* Typhimurium (334). Elsewhere, TNFR1 has been reported to be required for the killing of CD8α^{+} dendritic cells during infection of C57BL/6 mice, in a manner that is also dependent on the adaptor protein MyD88 (335). Macrophages isolated from TNFR1 knockout mice were deficient in killing of *S.* Typhimurium, which the authors linked to a deficiency in vesicular NADPH oxidase trafficking (333). In another report, *S.* Typhimurium was shown to avoid killing by NADPH oxidase in a SPI-2 dependent manner (336), and so targeting of TNFR1 by SseK3 may provide the mechanism for this phenotype. Further research will more fully elucidate the impact of TNFR1 glycosylation during infection, and determine whether

this modification is important for interfering with inflammatory signaling, programmed cell death, or avoidance of vesicular NADPH oxidase.

TNFR1 and TRAILR were the most highly enriched targets when we examined glycosylated peptides derived from insoluble membrane fractions (Figure 5.2). However, we also detected glycosylation of a range of other mammalian proteins, including several members of the Rab family of small GTPases. Rab proteins are regulators of intracellular vesicular trafficking, and coordinate the appropriate delivery of vesicular cargo to various organelles in eukaryotic cells (337). Rab GTPases function as molecular switches by undergoing conformational changes in conserved switch regions, and these regions are recognised by cognate guanine nucleotide exchange factors (GEFs) that catalyse the exchange of GDP to GTP and thus activate the Rab GTPase (338). A range of bacterial pathogens have evolved mechanisms for manipulating Rab GTPases (339), and the manipulation of intracellular trafficking is a common goal for intracellular pathogens (340). Here we detected glycosylation of Rab1 at Arg114 (Figure 5.2C), providing the first suggestion that *S.* Typhimurium may utilise SseK3 to manipulate intracellular trafficking. Rab1 is a key regulator of trafficking between the endoplasmic reticulum and the Golgi, and several effectors from *Legionella pneumophila* target Rab1 to alter the surface of the *Legionella*-containing vacuole (341, 342). During *S.* Typhimurium infection, Rab1 is recruited to cytoplasmic *Salmonella* and is important for the autophagy-mediated clearance of bacteria (343). The T3SS effectors SseF and SseG bind directly to Rab1 and inhibit the initiation of autophagy (344), and so it is possible that SseK3 plays a complementary or redundant role in impeding autophagy. Alternatively, given that Rab1 plays a critical role in vesicular trafficking and Golgi homeostasis, and that SseK3 co-localises with the Golgi (Figure 3.2), it is possible that SseK3 targets Rab1 to impede intracellular trafficking or disrupt the Golgi membrane. Further research will elucidate the impact of SseK3-mediated

glycosylation of Rab1. Concurrently, we also observed glycosylation of Rab5 at Arg121 (Figure 5.2C). Rab5 is recruited to the nascent SCV and is required for vacuole maturation, and this activity is promoted by the T3SS effector SopB (193). The recruitment of Rab5 to the vacuole leads to remodelling of the SCV membrane, which acquires phosphatidylinositol (PI) 3-phosphate (PI(3)P) and influences the membrane surface charge , and these activities are required for the normal maturation of the SCV (193, 195, 345). Thus *Salmonella* relies on Rab5 activity to facilitate intracellular replication, though our data provide a new mechanism by which Rab5 activity might instead be inhibited. During infection, *L. pneumophila* uses the T4SS effector VipD to inhibit the binding of Rab5 to its downstream effectors and thus block endosomal trafficking (346), and so it is possible that SseK3 targets Rab5 to achieve impede trafficking. Ultimately, our data suggest a new mechanism by which *S.* Typhimurium may influence vesicular trafficking, autophagy-mediated killing, or SCV membrane dynamics, and future work will further characterise the influence of SseK3 on these events.

Together, the data presented in this chapter describe novel host substrates of SseK3 during *in vitro S.* Typhimurium infection, and suggests that the preferred targets are TNFR1 and TRAILR. Alongside the glycosylation of TRADD by SseK1, these observations lend support to the emerging hypothesis that *Salmonella* employs the SseK effectors to antagonise immune signaling during infection. These findings may provide the mechanism for several unexplained phenotypes reported in the literature including inhibition of NF-κB signaling and impairment of necroptotic cell death, while also providing a possible means for manipulating vesicular trafficking with consequences for SCV dynamics and evasion of bacterial killing by macrophages. Further research will elucidate the impact of SseK3 on these events and explore the complementarity or redundancy with the SseK family and other SPI-2 T3SS effectors.

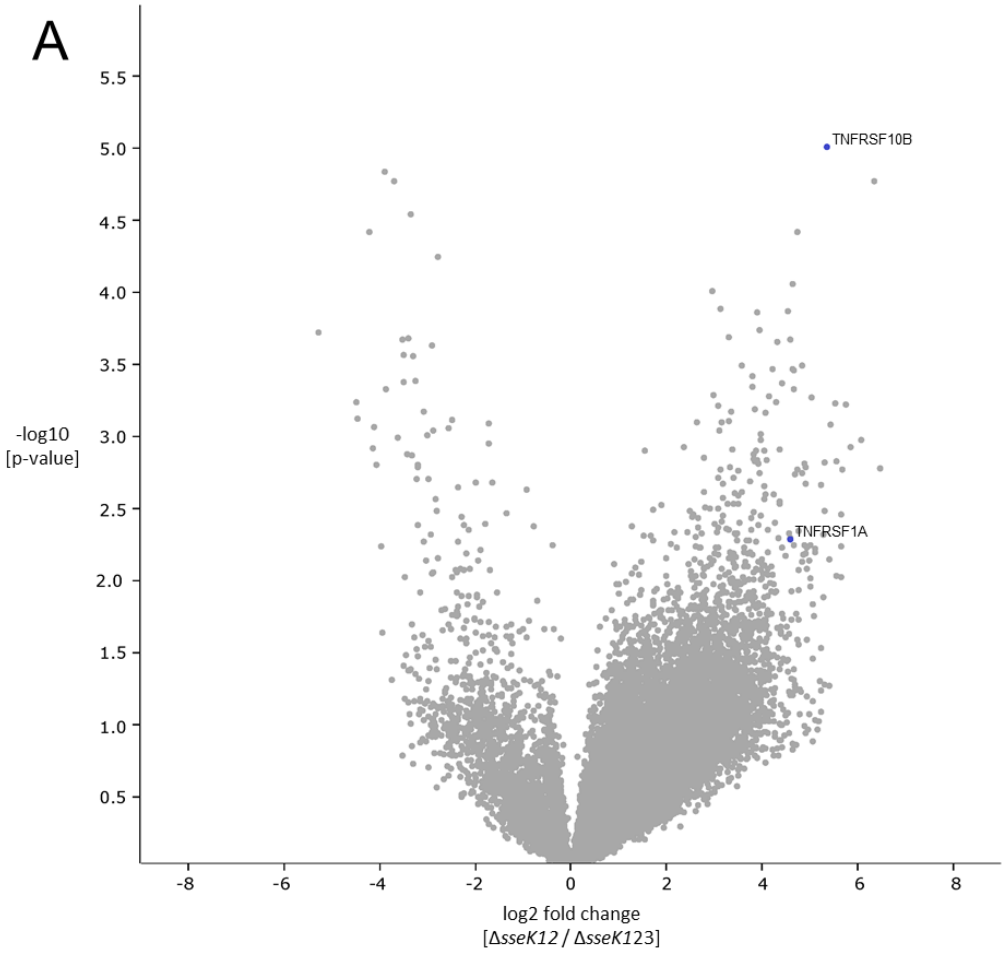

B

```
Tnfrsf10b DIVPFDSWNRLMRQLGLTDNQIQMVKAET
          D VP    W    MR +GL++ +I+ ++ +
Tnfrsf1a  DGVPPARWKEFMRFMGLSEHEIERLEMQN
```

C

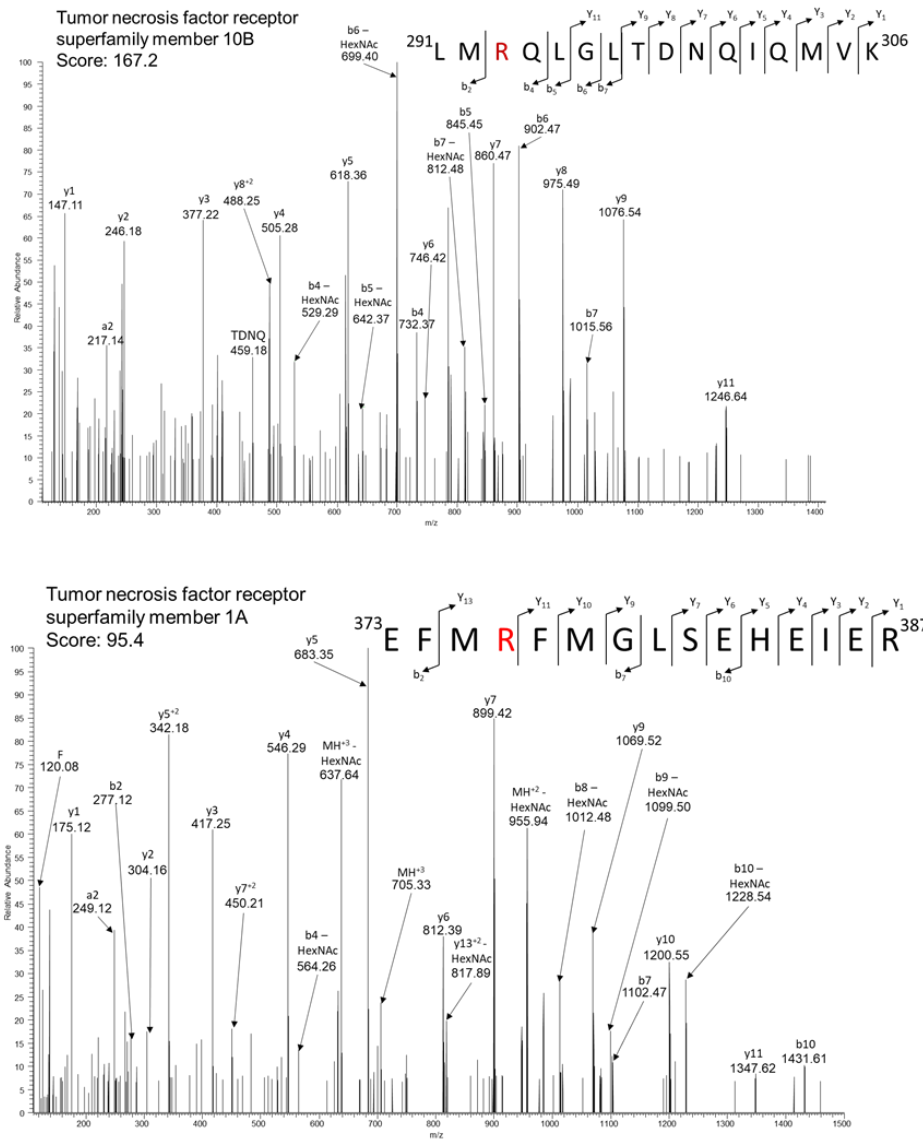

Figure 5.1. Enrichment of arginine-glycosylated peptides modified by endogenous SseK3.

(A) Label-free quantification of ArgGlcNAc peptide immunoprecipitated from RAW264.7 cells infected with *S.* Typhimurium Δ*sseK1sseK2sseK3* or Δ*sseK1sseK2*. Arginine-glycosylated peptides are presented as a volcano plot depicting mean log2 ion intensity peptide ratios of Δ*sseK1sseK2sseK3* versus Δ*sseK1sseK2* plotted against logarithmic *t* test *p* values from biological triplicate experiments. Arginine-glycosylated peptides are annotated by gene name and shaded blue. (B) Partial sequence alignment showing observed glycosylated arginine residue is conserved between identified substrates. (C). Manually curated HCD spectra of arginine glycosylated TNFRSF10B (upper) and TNFRSF1A (lower). Observed sites of arginine-glycosylation are highlighted in red, and presented alongside corresponding M/Z values and observed Andromeda scores.

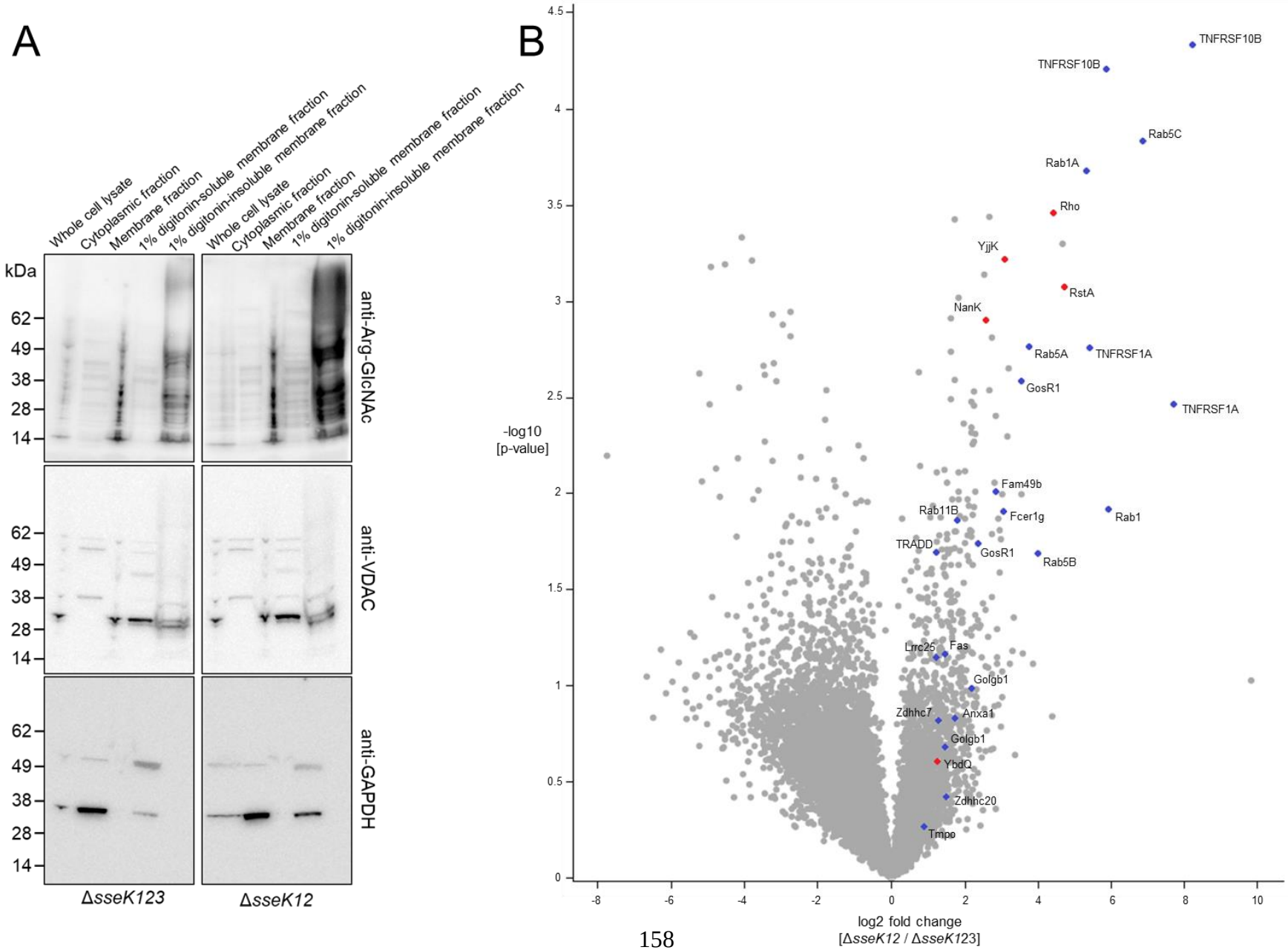
A
Whole cell lysate
Cytoplasmic fraction
Membrane fraction
1% digitonin-soluble membrane fraction
1% digitonin-insoluble membrane fraction
Whole cell lysate
Cytoplasmic fraction
Membrane fraction
1% digitonin-soluble membrane fraction
1% digitonin-insoluble membrane fraction
kDa
62
49
38
28
14
anti-Arg-GlcNAc
anti-VDAC
anti-GAPDH
ΔsseK123
ΔsseK12
B
-log10 [p-value]
log2 fold change [ΔsseK12 / ΔsseK123]
TNFRSF10B
TNFRSF10B
Rab5C
Rab1A
Rho
YjjK
RstA
NanK
Rab5A
TNFRSF1A
GosR1
TNFRSF1A
Fam49b
Rab11B
Fcer1g
Rab1
TRADD
GosR1
Rab5B
Lrrc25
Fas
Golgb1
Zdhhc7
Anxa1
Golgb1
YbdQ
Zdhhc20
Tmpo

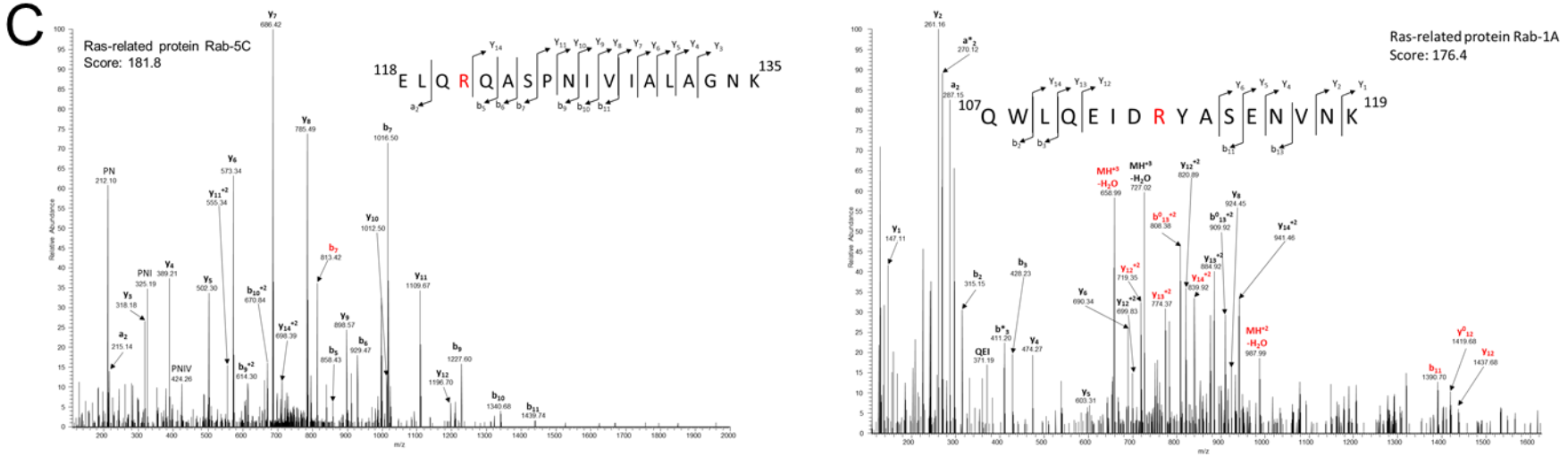

Figure 5.2. Enrichment of insoluble arginine-glycosylated peptides modified by endogenous SseK3.

(A) Immunoblot of RAW264.7 cells infected with Δ*sseK1sseK2sseK3* (left) or Δ*sseK1sseK2* (right). Cells were infected for 18 hours, then lysed and fractionated via centrifugation and treatment with 1% digitonin. Proteins were detected with anti-Arg-GlcNAc, while anti-VDAC and anti-GAPDH antibodies were used as loading controls for cellular fractionation. (B) Label-free quantification of ArgGlcNAc peptide immunoprecipitated from the 1% digitonin-insoluble membrane fractions of infected cell lysates. Arginine-glycosylated peptides are presented as a volcano plot depicting mean log2 ion intensity peptide ratios of Δ*sseK1sseK2sseK3* versus Δ*sseK1sseK2* plotted against logarithmic *t* test *p* values from biological triplicate experiments. Arginine-glycosylated peptides are annotated by gene name, with human peptides shaded blue and bacterial peptides shaded red. (C) Manually curated spectra showing glycosylation of Rab-5C and Rab-1A at Arg^{121} and Arg^{114} respectively, with corresponding Andromeda scores 181.8 and 176.4.

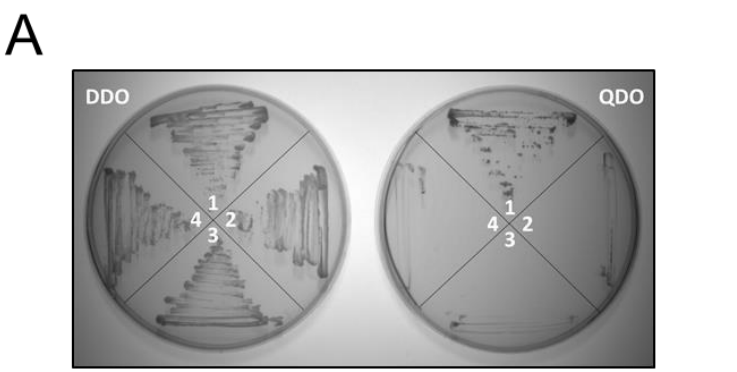
A
DDO
QDO
1
2
3
4
1 – pGBKT7-NleB1 + pGADT7-FADD DD
2 – pGBKT7-SseK3 + pGADT7
3 – pGBKT7 + pGADT7-hTRAILR2 DD
4 – pGBKT7-SseK3 + pGADT7-hTRAILR2 DD

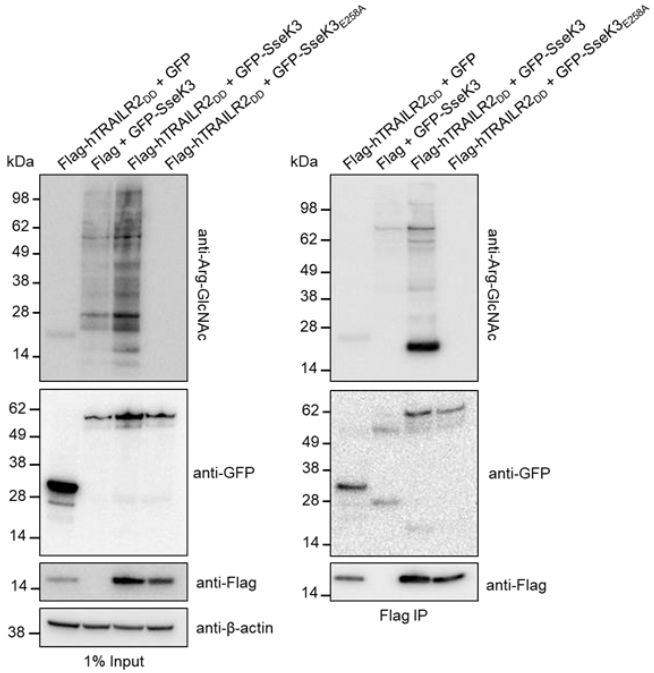
B
kDa
Flag-hTRAILR2DD + GFP
Flag + GFP-SseK3
Flag-hTRAILR2DD + GFP-SseK3
Flag-hTRAILR2DD + GFP-SseK3E258A
anti-Arg-GlcNAc
anti-GFP
anti-Flag
anti-β-actin
1% Input
Flag IP

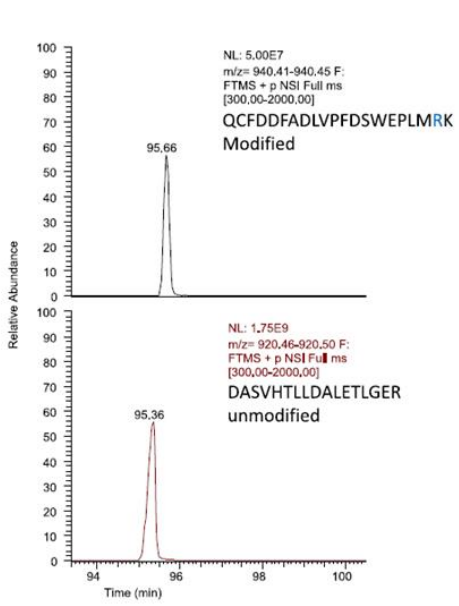
C
NL: 5.00E7
m/z= 940,41-940,45 F:
FTMS + p NSI Full ms
[300,00-2000,00]
QCFDDFADLVPFDSWEPLMRK
Modified
95,66
NL: 1,75E9
m/z= 920,46-920,50 F:
FTMS + p NSI Full ms
[300,00-2000,00]
DASVHTLLDALETLGER
unmodified
95,36
Relative Abundance
Time (min)

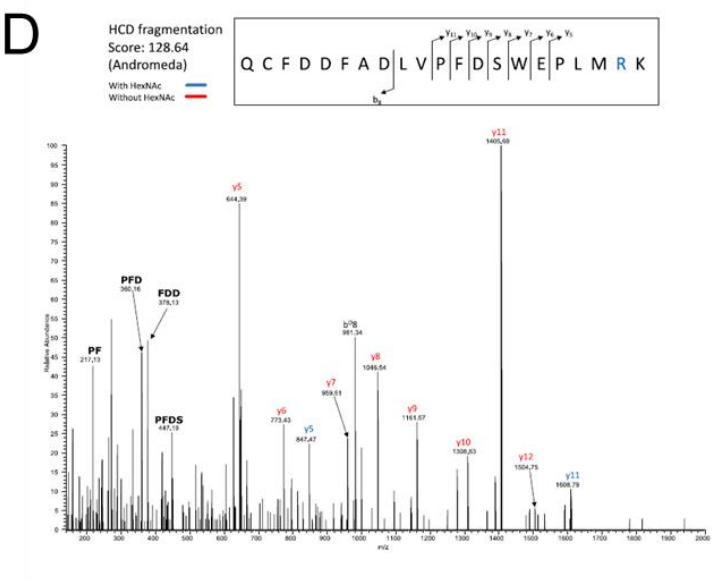
D
HCD fragmentation
Score: 128.64
(Andromeda)
With HexNAc
Without HexNAc
Q C F D D F A D L V P F D S W E P L M R K
PFD
FDD
PF
PFDS

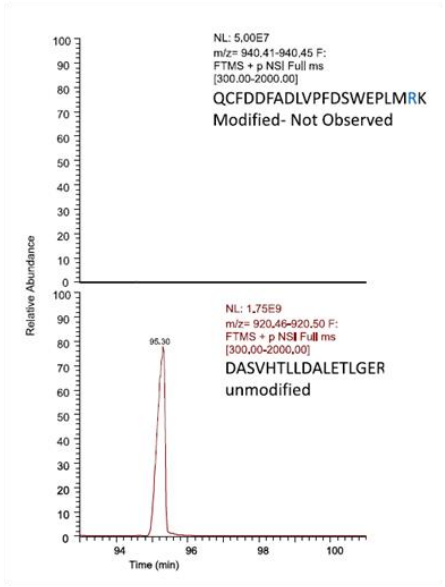
E
NL: 5.00E7
m/z= 940,41-940,45 F:
FTMS + p NSI Full ms
[300,00-2000,00]
QCFDDFADLVPFDSWEPLMRK
Modified- Not Observed
NL: 1,75E9
m/z= 920,46-920,50 F:
FTMS + p NSI Full ms
[300,00-2000,00]
DASVHTLLDALETLGER
unmodified
95,30
Relative Abundance
Time (min)

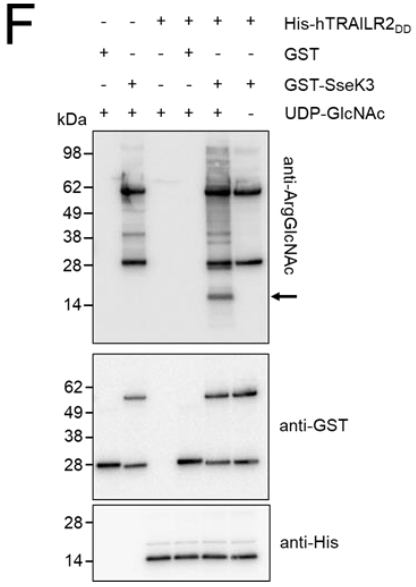
F
His-hTRAILR2DD
GST
GST-SseK3
UDP-GlcNAc
kDa
anti-ArgGlcNAc
anti-GST
anti-His

Figure 5.3. Validation of SseK3-mediated arginine-glycosylation of TRAIL-R2.

(A) *S. cerevisiae* Y2HGold co-transformed with pGBKT7-SseK3 and pGADT7-hTRAILR2 and plated to selective media to observe correct transformation (left) and validate protein-protein interactions (right). (B) Immunoblot of inputs and immunoprecipitates (IP) of anti-FLAG immunoprecipitations performed on lysates of HEK293T cells co-transfected with pFLAG-hTRAILR2$_{DD}$ and pEGFP-SseK3 or pEGFP-SseK3$_{E258A}$. (C) LC-MS analysis of tryptic digest derived from co-incubation of recombinant His-hTRAILR2$_{DD}$ and GST-SseK3 in the presence of UDP-GlcNAc. (D) LC-MS analysis of tryptic digest fractions derived from co-incubation of recombinant His-hTRAILR2$_{DD}$ and GST-SseK3 with no sugar donor. (E) HCD fragmentation of recombinant His-hTRAILR2$_{DD}$ incubated with GST-SseK3 and UDP-GlcNAc, Andromeda score 167.28. (F) Immunoblot of recombinant His-hTRAILR2$_{DD}$ and GST-SseK3 following co-incubation at 37°C for 5 hours. Proteins were detected with anti-ArgGlcNAc, anti-GST, and anti-His antibodies as indicated. Arrow indicates arginine-glycosylated His-hTRAILR2$_{DD}$. Representative immunoblot of at least three independent experiments.

A

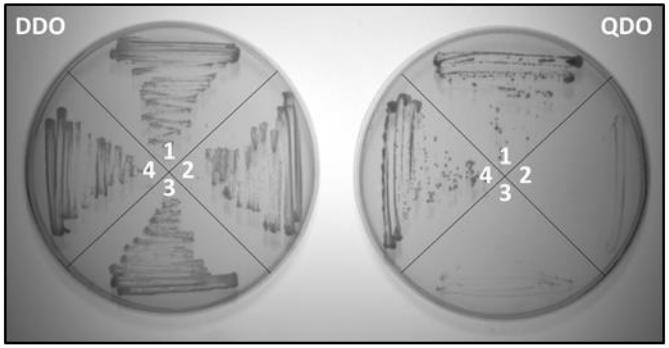

1 – pGBKT7-NleB1 + pGADT7-FADD DD
2 – pGBKT7-SseK3 + pGADT7
3 – pGBKT7 + pGADT7-TNFR1 DD
4 – pGBKT7-SseK3 + pGADT7-TNFR1 DD

B

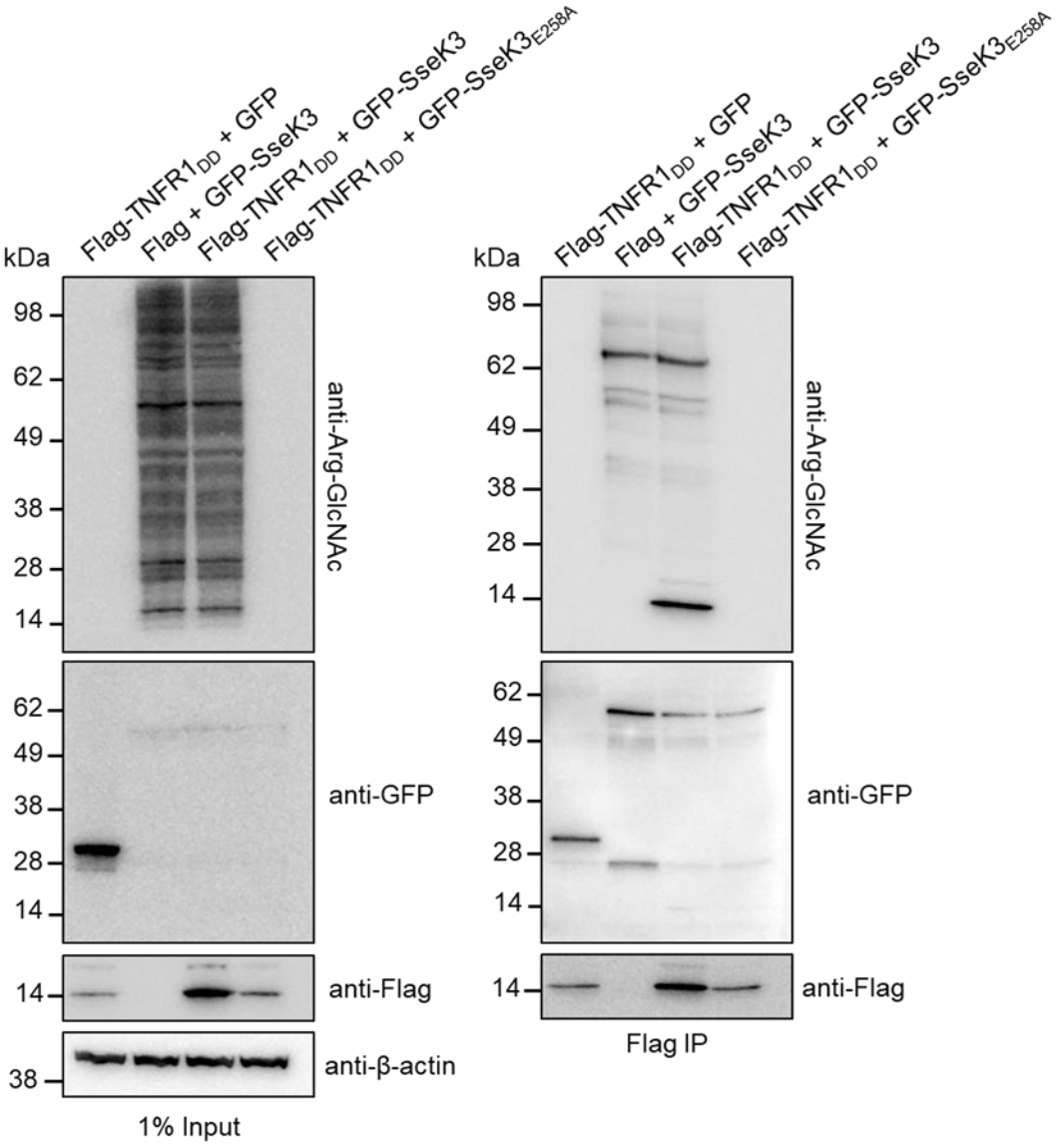

C

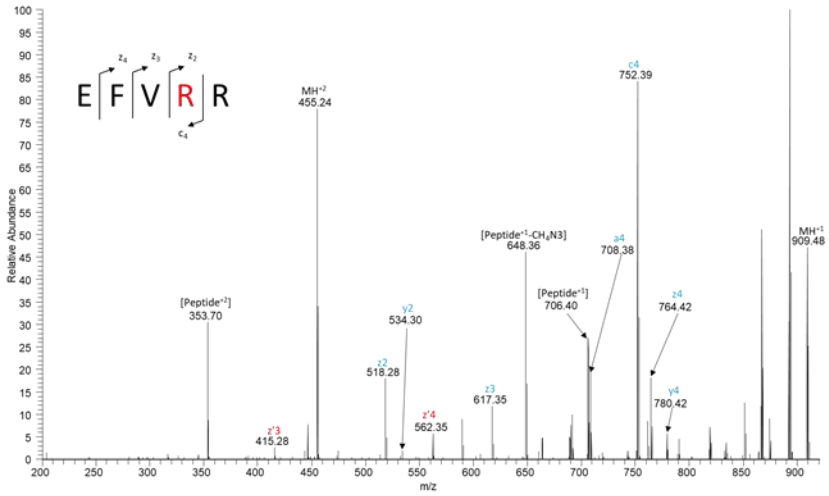

Figure 5.4. Validation of SseK3-mediated arginine-glycosylation of TNFR1

(A) *S. cerevisiae* Y2HGold co-transformed with pGBKT7-SseK3 and pGADT7-TNFR1 and plated to selective media to observe correct transformation (left) and validate protein-protein interactions (right). (B) Immunoblot of inputs and immunoprecipitates (IP) of anti-FLAG immunoprecipitations performed on lysates of HEK293T cells co-transfected with pFLAG-TNFR1$_{DD}$ and pEGFP-SseK3 or pEGFP-SseK3$_{E258A}$. (C) EThcD fragmentation of FLAG-hTNFR1$_{DD}$ enriched from HEK293T cells by anti-FLAG immunoprecipitation following co-transfection with pEGFP-SseK3, peptide confirmed by manual annotation.

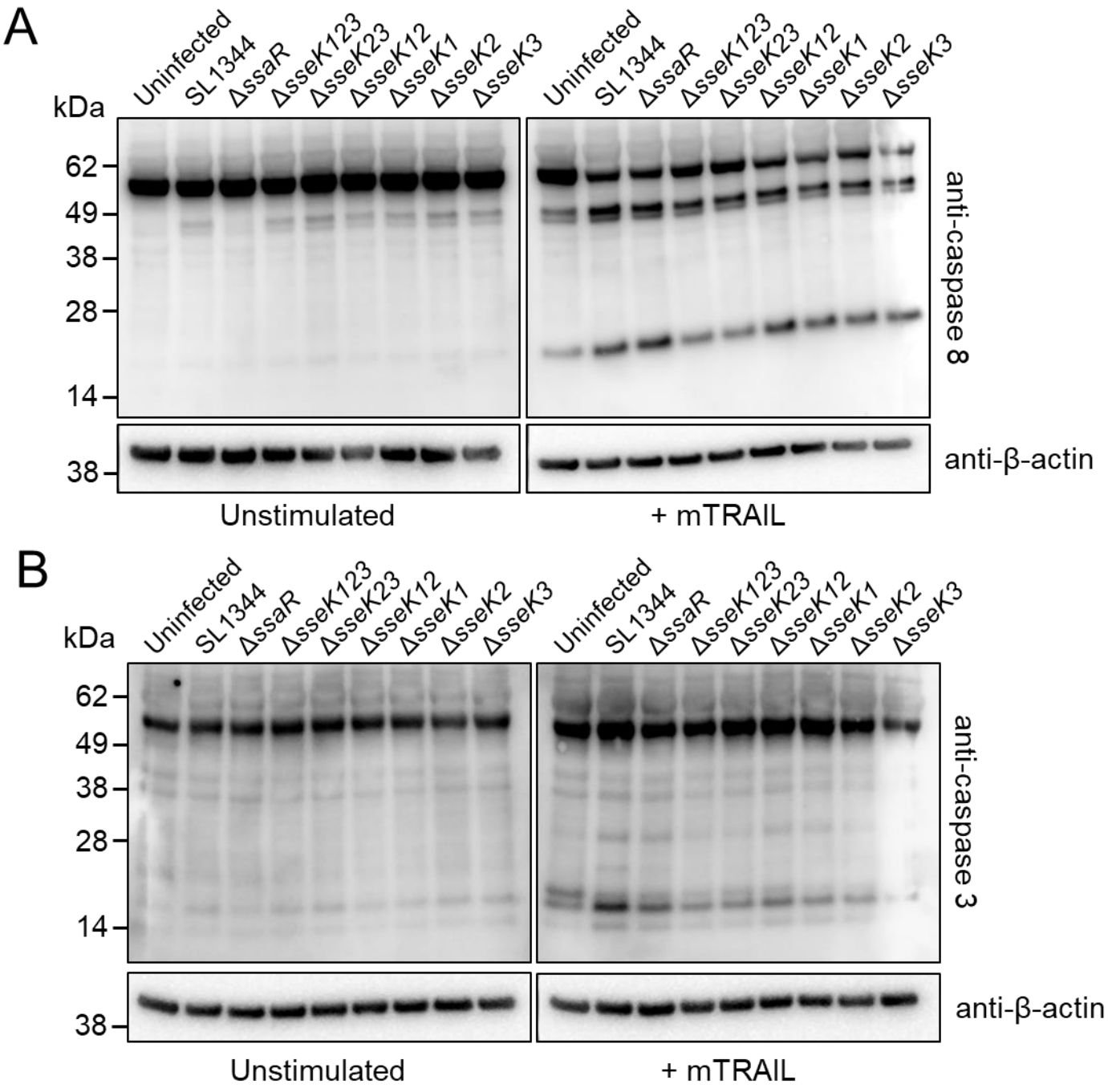

Figure 5.5. TRAIL-induced cleavage of caspase 8 and caspase 3 during *S.* Typhimurium infection

Immunoblots of lysate of HeLa229 cells infected with *S.* Typhimurium derivatives. Cells were infected for 20 hours then either left unstimulated (left) or treated with mTRAIL. Cells were lysed 5 hours post-stimulation. Proteins were detected with (A) anti-caspase 8 and (B) anti-caspase 3 as indicated. Anti-β-actin was used as a loading control.

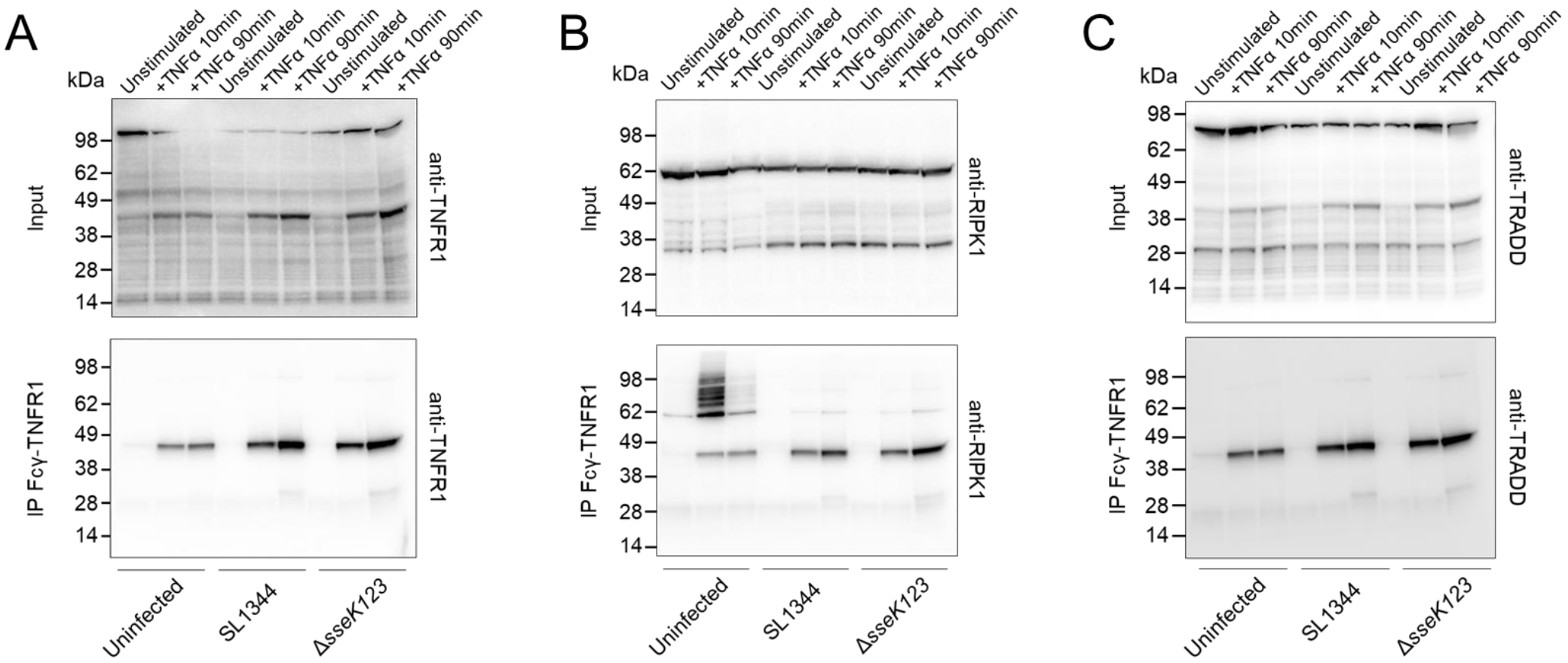
A
B
C
kDa
Unstimulated
+TNFα 10min
+TNFα 90min
Unstimulated
+TNFα 10min
+TNFα 90min
Unstimulated
+TNFα 10min
+TNFα 90min
98
62
49
38
28
14
Input
IP Fcγ-TNFR1
anti-TNFR1
anti-RIPK1
anti-TRADD
Uninfected
SL1344
ΔsseK123

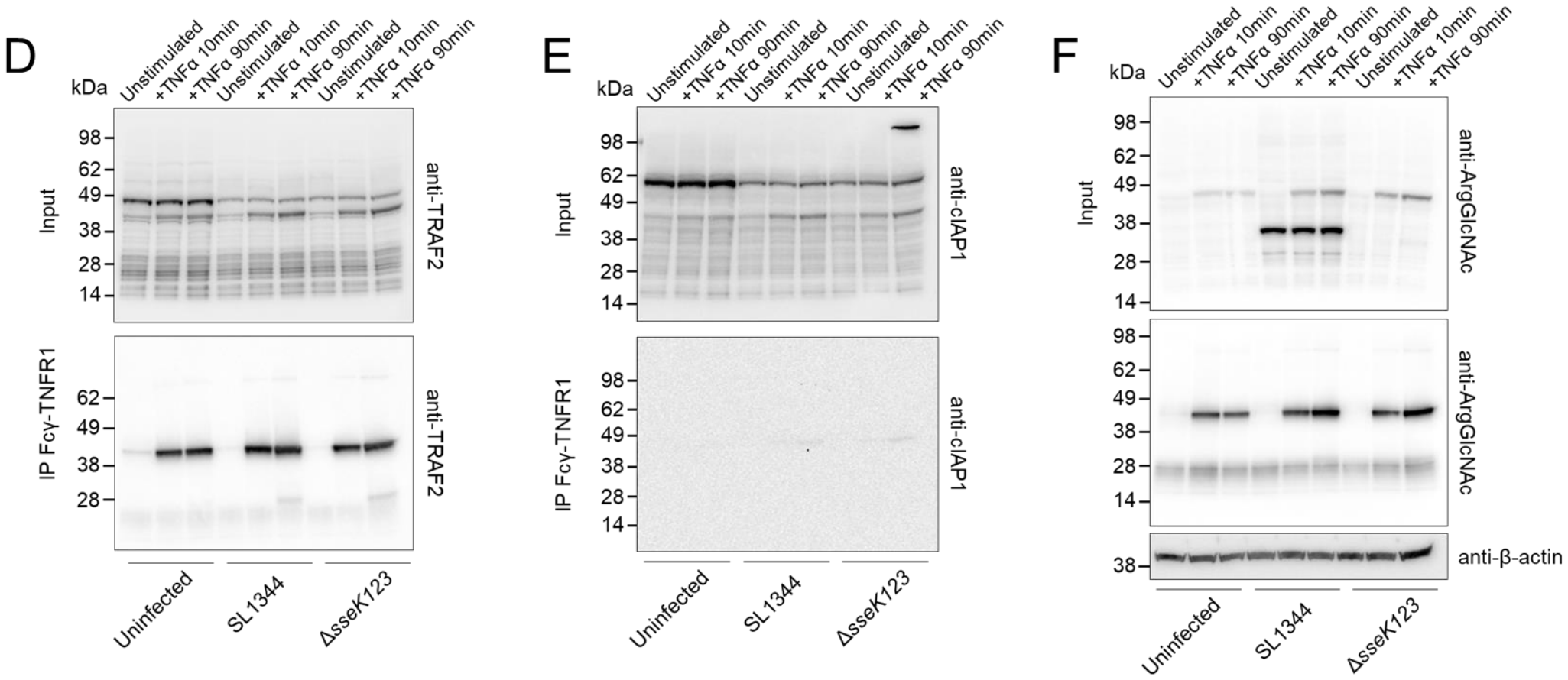

Figure 5.6. Immunoprecipitation of the TNFR1 complex in *S.* Typhimurium infection

Immunoblots of inputs and immunoprecipitates (IP) of Fcγ-TNFR1 immunoprecipitations performed on lysates of RAW264.7 cells infected with *S.* Typhimurium. Cells were infected with derivatives of *S.* Typhimurium for 24 hours. Cells were stimulated with Fcγ-TNF for indicated times then lysed and incubated with Protein G beads to enrich for the Fcγ-TNF complex. Proteins were detected with (A) anti-TNFR1, (B) anti-RIPK1, (C) anti-TRADD, (D) anti-TRAF2, (E) anti-cIAP1, (F) anti-Arg-GlcNAc, and anti-β-actin, as indicated.

A

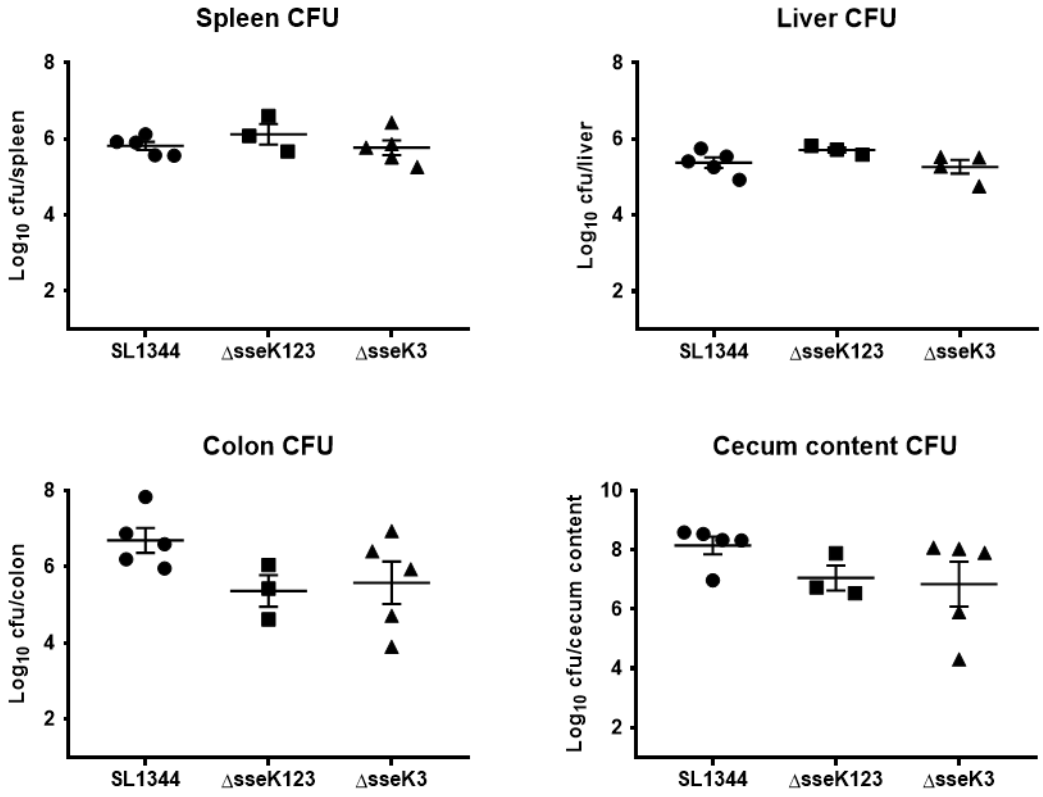
Spleen CFU
Log10 cfu/spleen
Liver CFU
Log10 cfu/liver
Colon CFU
Log10 cfu/colon
Cecum content CFU
Log10 cfu/cecum content
SL1344
ΔsseK123
ΔsseK3

B

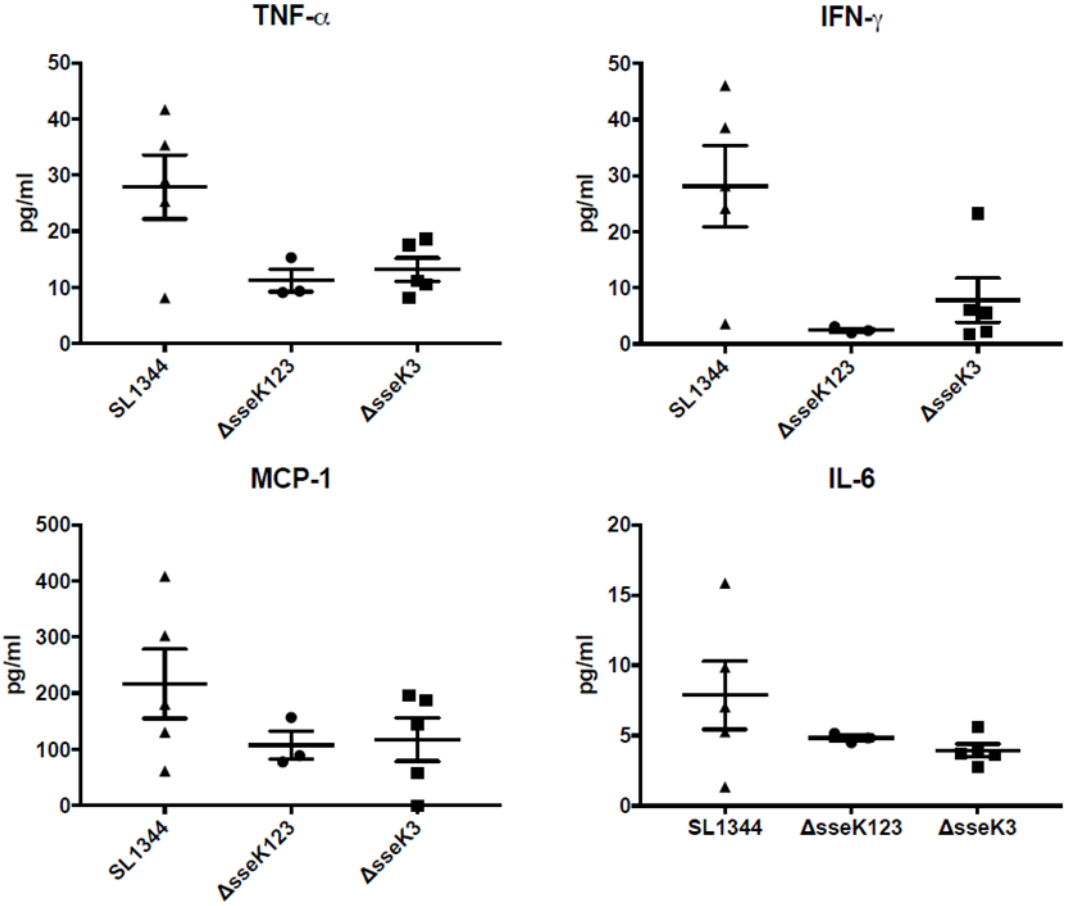
TNF-α
IFN-γ
MCP-1
IL-6
pg/ml
SL1344
ΔsseK123
ΔsseK3

Figure 5.7. Effect of SseK effectors during infection of C57BL/6 mice.

(A) Colonisation of C57BL/6 mice in various organs with *S.* Typhimurium derivatives. Mice were orally infected with 5x10^7 cfu *S.* Typhimurium. At day 5 post infection, tissues were collected and homogenised, and serial dilutions were plated on LB+50ug/ml streptomycin plates. Each data point represents log10 CFU per organ per individual animal on day 5 post infection. Mean ± SEM are indicated. (B) Quantification of indicated cytokines isolated from homogenised colon and measured by cytometric bead array. Mice were infected with indicated *S.* Typhimurium derivatives and colons were extracted on day 5 post infection. Colons were homogenised and cell debris centrifuged, and concentration of cytokines determined by cytometric bead array. Means ± SEM are indicated. *P* values from Mann-Whitney test.

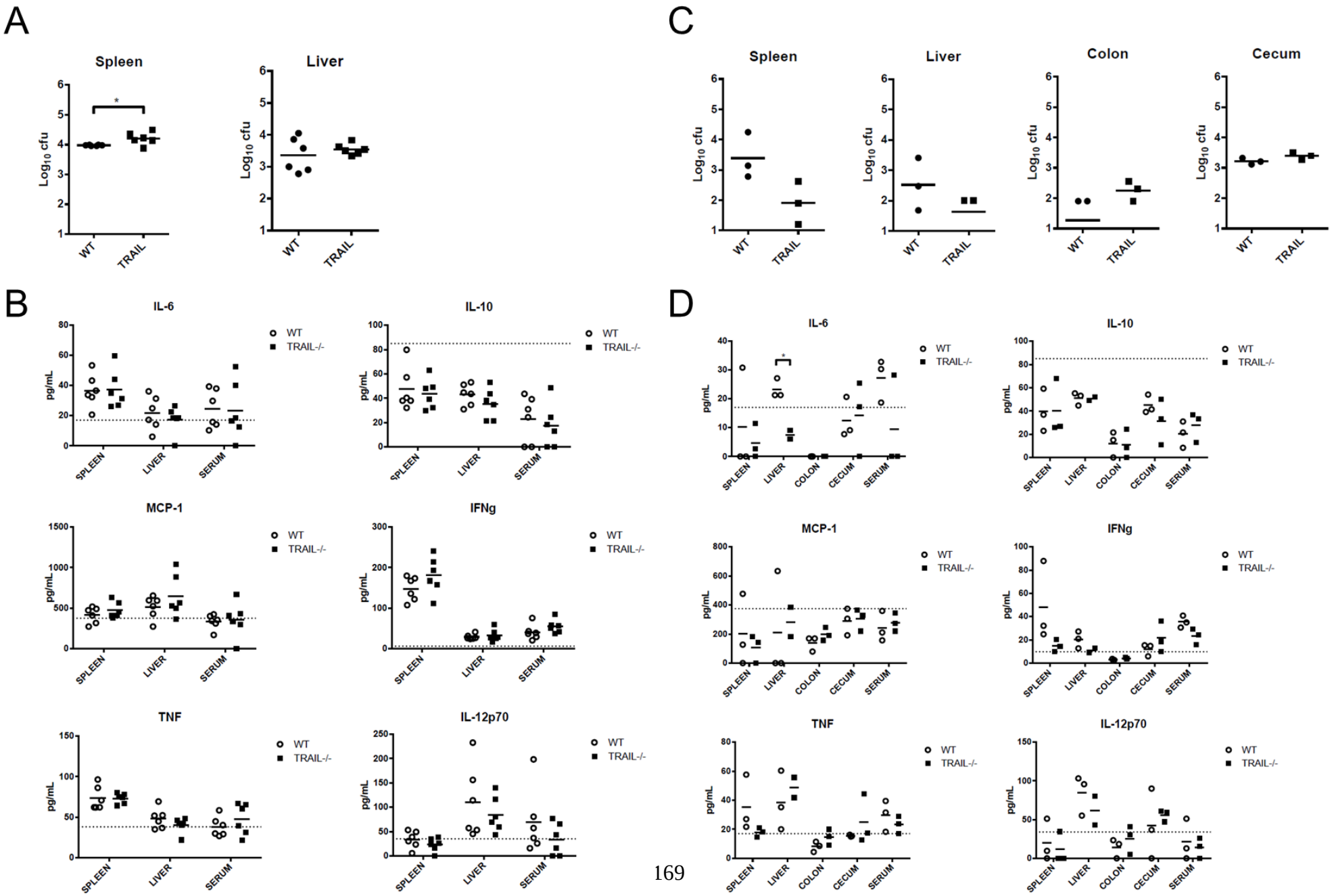
A
Spleen
Liver
Log10 cfu
WT
TRAIL
C
Spleen
Liver
Colon
Cecum
B
IL-6
IL-10
MCP-1
IFNg
TNF
IL-12p70
pg/mL
WT
TRAIL-/-
SPLEEN
LIVER
SERUM
D
IL-6
IL-10
MCP-1
IFNg
TNF
IL-12p70
SPLEEN
LIVER
COLON
CECUM
SERUM

Figure 5.8. Response of TRAIL$^{-/-}$ mice to attenuated *Salmonella* infection.

(A) Colonisation of C57BL/6 WT and TRAIL$^{-/-}$ mice spleen and liver with *S.* Typhimurium *ΔaroA.* Mice were infected intravenously with *S.* Typhimurium *ΔaroA* and culled after 21 days. Organs were extracted and homogenised and serial dilutions were plated for quantification of CFU. Mean ± SEM are indicated. *P* value from unpaired *t* test, * denotes *p* value <0.05. (B) Quantification of various cytokines isolated from indicated organs measured by cytometric bead array. Mean ± SEM are indicated. Dotted lines denote thresholds of detection. (C) Colonisation of C57BL/6 WT and TRAIL$^{-/-}$ mice in spleen and liver with *S.* Typhimurium *ΔaroA.* Mice were infected orally with *S.* Typhimurium *ΔaroA* and culled after 21 days. Organs were extracted and homogenised and serial dilutions were plated for quantification of cfu. Mean ± SEM are indicated. (D) Quantification of indicated cytokines isolated from indicated organs measured by cytometric bead array. Mean ± SEM are indicated. *P* values from Mann-Whitney test, * denotes *p* value <0.05. Dotted lines denote thresholds of detection

Chapter Six

Perspective

CHAPTER 6. Perspective

All bacterial pathogens face the central challenge of evading the host immune response in order to facilitate their colonisation, replication, and dissemination. In particular, intracellular pathogens must develop strategies for evading the complex suite of signaling and trafficking events that are engaged following the detection of pathogen associated molecular patterns (320, 347). While different pathogens have acquired various mechanisms for achieving this evasion, perhaps the most striking and programmable is the evolution of specialised secretion systems that allow the translocation of bacterial effector proteins directly into the cytoplasm of host cells (116, 120). The acquisition or loss of effector proteins over evolutionary time allows a bacterial pathogen to adapt to new niches, exert greater control over infected host cells, and outcompete rival microorganisms (50, 64, 348, 349). Thus, the study of effector proteins enables a deeper understanding of how bacterial pathogens achieve infection, and given the highly conserved and typically indispensable nature of secretion systems, it is possible that antagonising these activities will provide the foundation for novel anti-virulence therapeutics.

The acquisition of type three secretion systems (T3SS) represent defining points in the evolution of *Salmonella* spp, as it is speculated that the acquisition of the SPI-1 T3SS is linked to the divergence of *Salmonella* from *Escherichia coli* (8, 97), and that the later acquisition of the SPI-2 T3SS permitted dissemination of *Salmonella* from the gastrointestinal tract to systemic sites within an infected host (8, 96, 97). Given that mutants deficient for the SPI-1 and SPI-2 T3SS are severely attenuated in animal models of infection (98, 99, 101), it follows that *Salmonella* relies heavily on the activity of effector proteins to achieve and maintain infection. Since the discovery of the SPI-1 and SPI-2 T3SS, more than 40 effector proteins have been described across various serovars of *Salmonella* spp., and these effectors collectively contribute to invasion of host cells, suppression or activation of

innate immune signaling, formation and maturation of the *Salmonella*-containing vacuole (SCV), and interference with adaptive immunity (50, 64, 105, 106, 156). The function of many effector proteins remains undescribed, particularly those translocated by the SPI-2 T3SS, and so discovering how these effectors contribute to *Salmonella* infection remains a priority.

Since the first discovery of SseK1 and SseK2 (242) and the later report describing SseK3 (243), there have been only incremental advances in understanding the function of these effector proteins. Some reports suggest a contribution of the SseK family to virulence *in vivo* (243, 247), while other reports suggest these effectors are dispensable for virulence in murine models (242, 246, 248). Similarly, a range of studies have attempted to describe the host targets of the SseK effectors, but these findings have often not been supported or indeed have been contradicted by later studies (245, 280, 314, 315). Most studies have explored the possibility that these effectors function in a manner similar to the homologous effector NleB1, which impedes NF-κB signaling and apoptotic cell death during enteropathogenic *E. coli* (EPEC) infection of enterocytes (244, 245). Despite the extracellular nature of EPEC infections, there are many similarities between the strategies employed by *S.* Typhimurium and EPEC in order to subvert the host response, and it is logical that *S.* Typhimurium would similarly benefit from dampening host immune signaling at various stages of infection. Arguably, the clearest means of discovering the function of an enzymatic effector is to identify the host substrate and the modification mediated by the effector, followed by a thorough analysis of how the enzymatic activity of the effector shapes the outcome of infection. Thus, the aim of this thesis was to identify the preferred host targets of the SseK effectors and explore their contribution to virulence during *S.* Typhimurium infection.

SseK1 has received considerable attention and has emerged as perhaps the best characterised effector of this family, partly because it shows the strongest sequence

homology to NleB1 (276), it appears to be generally well conserved between serovars (105), and it was the first to be discovered and characterised alongside SseK2 (242). Various reports have described putative substrates of SseK1, though all have relied heavily on *in vitro* approaches removed from the natural context of infection, including ectopic expression in mammalian cells and purification of recombinant protein for glycosylation assays. An early report showed TRADD was glycosylated by SseK1 (245), while a later report did not observe binding between SseK1 and TRADD (276). Other studies have described interactions with both FADD (314) and GAPDH (315). In this thesis, we described the enzymatic activity of endogenous, bacterially-translocated SseK1 during *in vitro* infection of RAW264.7 cells. We showed that TRADD was the preferred substrate of SseK1 under these conditions, but that overexpressing SseK1 greatly broadened the range of potential substrates. The broader activity of overexpressed SseK1 may explain the modification of other substrates reported previously, which were observed under non-physiological conditions. TRADD participates as an adaptor protein in TNF signaling pathways, which can lead to pro-inflammatory cytokine production via NF-κB signaling or programmed cell death via apoptosis or necroptosis (258, 323). Conceivably, *S.* Typhimurium benefits from antagonising these pathways at various points during the intracellular stage of infection, in a manner similar to the inhibition of TRADD by NleB1 during EPEC infection (244, 245). A recent report provided some evidence that SseK1 may inhibit necroptotic cell death (314), while previous data suggests SseK1 inhibits NF-κB signaling (276), and so this data may provide the mechanism for these phenotypes. Further research will explore how the modification of TRADD by SseK1 influences immune signaling, and how this activity overlaps with that of the other SseK effectors and with other SPI-1 and SPI-2 T3SS effectors that target other components of these pathways (64, 105). Further, while this study described the glycosylation of TRADD in

immortalised RAW264.7 cells, the influence of this modification on immune signaling may be better explored in primary macrophages or other cells isolated *ex vivo*.

Various reports have suggested that SseK1 may function in a similar manner to NleB1, but the function of SseK3 has remained less clear. While the E3 ligase TRIM32 was identified as a binding partner of SseK3 (280), there are now several reports suggesting this interaction does not contribute to virulence (280, 314). Another study demonstrated relatively weak glycosylation of TRADD by ectopically expressed SseK3 (314), while several studies have shown that FADD is not glycosylated by SseK3 (314, 315). In a departure to the current literature, we showed here that the preferred substrates of SseK3 are the signaling receptors TNFR1 and TRAILR. These receptors respond to stimulation by the cognate ligands TNF and TRAIL and potentiate an array of immune signaling outcomes ranging from NF-κB-mediated inflammatory cytokine production, programmed cell death via apoptosis or necroptosis, promotion of cell survival, and cellular migration and proliferation (266, 269, 316, 319, 323). Thus, our work provides the mechanism by which intracellular *S.* Typhimurium manipulates a broader array of cellular functions during infection. However, it seems most conservative to suggest that SseK3 functions to inhibit inflammatory signaling or cell death signaling pathways that are dependent on TNF and TRAIL stimulation. Further research should initially focus on exploring the impact on cell death and cytokine production, while *in vivo* infection of host species that are deficient for these receptors may be of interest.

Still, the function of SseK2 remains poorly described. Based on very strong sequence homology between SseK2 and SseK3 (276), it seems likely that these effectors share a similar function. SseK3 is encoded on the ST64B prophage within the *S.* Typhimurium genome (243), so it is possible that the phage-mediated transfer of SseK2 resulted in the acquisition and stable incorporation of SseK3, and that the evolutionary benefit of two copies of this effector favoured retention of SseK3. Data presented in this thesis and elsewhere (314)

suggest that SseK2 does not function as an arginine glycosyltransferase, though these findings are based entirely on the use of an antibody raised against glycosylated arginine species (299). Based on structural similarities (350) and sequence homology (276), it seems highly likely that SseK2 functions as a glycosyltransferase that utilises a different host sugar or catalyses a different glycosidic bond. Discovering the nature of the glycosyltransferase activity of SseK2 will assist in identifying the glycosylated host proteins that are targeted by this effector, and collectively this information will permit a deeper understanding of how the SseK effectors act cooperatively during infection.

In this thesis, we showed that the overexpression of bacterially-translocated SseK1 greatly broadened the range of potential substrates, and while TRADD was among the most highly enriched mammalian substrates, we also detected a range of bacterial proteins that were glycosylated during infection. Of particular interest were the two-component response regulators OmpR and ArcA, which contribute to the complex regulatory network that controls appropriate transcriptional responses to environmental cues. The EnvZ-OmpR two-component system is indirectly involved in SPI-2 T3SS expression (149-151), while the ArcA-ArcB system involved in responding to reactive oxygen species (313). Arginine glycosylation of TRADD and FADD by NleB1 is deleterious to the function of those proteins (244, 245), and so our data may provide a mechanism by which *S.* Typhimurium can inhibit the function of selected two-component systems. The functional consequences of this remain unclear, as these systems are required for appropriate transcriptional regulation during infection. Unpublished work from our laboratory suggests that SseK1 and SseK3 are translocated between 10 and 18 hours post-infection, so it is tempting to speculate that these effectors inhibit two-component function in order to impede SPI-2 T3SS activity at later time-points. Much work is required to interrogate this hypothesis, but the later stages of intracellular infection are not well understood, and it is not clear how *Salmonella* alter their

virulence strategies during egress from the infected cell and upon exposure to the extracellular environment.

Much of the literature concerning the SseK effectors has relied on studying these effectors in experimental approaches and methodology that are removed from the natural context of infection (245, 280, 314, 315). Indeed, the study of bacterial effector proteins generally relies on these approaches, including ectopic expression of bacterial proteins in mammalian cells, purification of recombinant protein for use in *in vitro* assays, or binding assays performed using yeast two-hybrid systems. We found that the activity of bacterially-translocated SseK1 in particular was greatly influenced by the level of expression, and further that ectopic expression of SseK1 and TRADD expanded the range of potential sites of glycosylation. These data provide an example of how common strategies for studying effectors and their substrates can be misleading if removed from physiologically relevant conditions. While these approaches are often necessary for validation purposes, we provide here an example of the necessity of interrogating bacterial effectors under conditions that are as natural as is practicable.

Data presented in this thesis have demonstrated that *S.* Typhimurium interacts with various components of host innate immune signaling pathways in a manner that is more complex than previously anticipated. We observed that SseK1 predominantly targets the adaptor protein TRADD while SseK3 targets the signaling receptors TNFR1 and TRAILR (Fig 6.1). However, several other SPI-1 and SPI-2 T3SS effectors also target these pathways. Several SPI-1 T3SS effectors including SopE, SopE2, SopB, and SipB contribute to a potent, localised inflammation while several other SPI-1 effectors including SptP, SpvC, AvrA and SspH1 have an anti-inflammatory role (50, 64, 156). During the intracellular stage of infection, the SPI-2 T3SS effectors PipA, GogA, GtgA, SseL, SpvD, SarA, and GogB all participate through various mechanisms to inhibit innate immune signaling, while SspH2

reportedly enhances cytokine secretion (50, 64, 105, 106, 156). A priority of future research should be to reconcile how these effectors act hierarchically and temporally to manipulate immune signaling appropriately. Clearly, manipulation of immune signaling pathways is a primary function of the *S.* Typhimurium SPI-1 and SPI-2 T3SS, and a considerable challenge for the field is the reconciliation of these activities into a coherent description of the bacterial strategy for subverting the host response. The role of the SseK effectors in the context of this strategy remains to be defined, though considering data presented in this thesis and elsewhere it seems most probable that these effectors function to impede various stages of cell death signaling pathways, and it is possible that this activity is unique to certain cell types or host species.

In conclusion, this thesis has identified novel host targets of the *S.* Typhimurium effectors SseK1 and SseK3. Here, we demonstrated that SseK1 and SseK3 function as arginine glycosyltransferases that recognise different host targets. We developed an approach combining immunoprecipitation and mass spectrometry to identify arginine glycosylated peptides during *S.* Typhimurium infection *in vitro*. We show that the preferred host target of SseK1 is the signaling adaptor protein TRADD, while SseK3 targets the signaling receptors TNFR1 and TRAILR. Future research will elucidate how these glycosylation events impact virulence and immunity, providing new avenues for the development of anti-virulence interventions and a deeper understanding of how intracellular bacteria evade the host immune response.

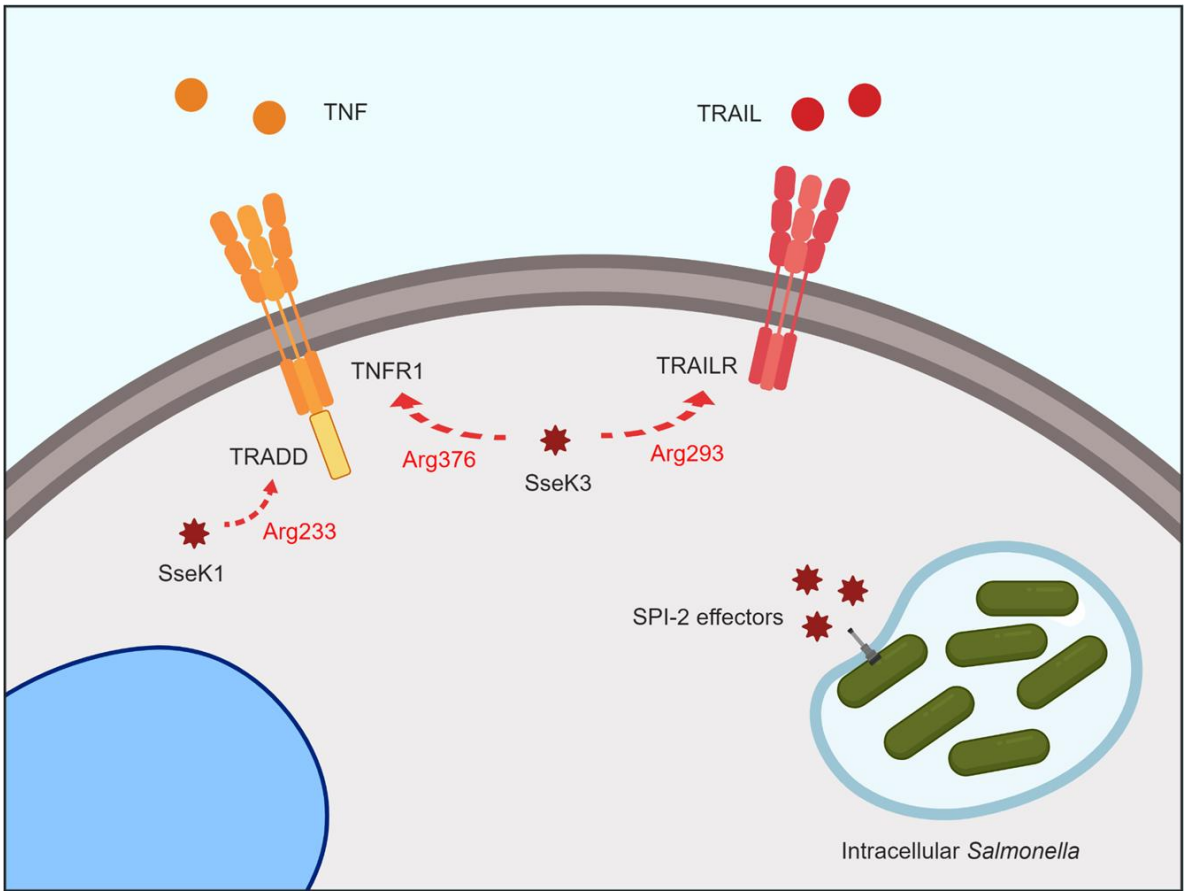

Figure 6.1. SseK1 and SseK3 mediate arginine glycosylation of host immune signaling proteins.

Intracellular *Salmonella* reside within the host-derived *Salmonella*-containing vacuole, which after bacterial remodeling serves as a replicative niche. The *Salmonella* SPI-2 T3SS translocates effectors into the host cytoplasm, which function in various ways to subvert the host response. In this thesis, we demonstrated that SseK1 and SseK3 function as arginine glycosyltransferases with different preferred host targets. SseK1 targets the signaling adaptor TRADD at Arg233 while SseK3 targets the signaling receptors TNFR1 and TRAILR at Arg376 and Arg293, respectively. TNFR1 and TRAILR respond to stimulation by the extracellular ligands TNF and TRAIL, respectively, and potentiate a range of innate immune signaling outcomes. Thus, these data provide new mechanisms by which *Salmonella* may manipulate innate immunity during infection.

REFERENCES

1. **Ochman H, Wilson AC.** 1987. Evolution in bacteria: evidence for a universal substitution rate in cellular genomes. J Mol Evol **26:**74-86.
2. **Doolittle RF, Feng DF, Tsang S, Cho G, Little E.** 1996. Determining divergence times of the major kingdoms of living organisms with a protein clock. Science **271:**470-477.
3. **Fookes M, Schroeder GN, Langridge GC, Blondel CJ, Mammina C, Connor TR, Seth-Smith H, Vernikos GS, Robinson KS, Sanders M, Petty NK, Kingsley RA, Baumler AJ, Nuccio SP, Contreras I, Santiviago CA, Maskell D, Barrow P, Humphrey T, Nastasi A, Roberts M, Frankel G, Parkhill J, Dougan G, Thomson NR.** 2011. Salmonella bongori provides insights into the evolution of the Salmonellae. PLoS Pathog **7:**e1002191.
4. **Grimont PA, Weill F-X.** 2007. Antigenic formulae of the Salmonella serovars. WHO collaborating centre for reference and research on Salmonella **9:**1-166.
5. **Achtman M, Wain J, Weill FX, Nair S, Zhou Z, Sangal V, Krauland MG, Hale JL, Harbottle H, Uesbeck A, Dougan G, Harrison LH, Brisse S, Group SEMS.** 2012. Multilocus sequence typing as a replacement for serotyping in Salmonella enterica. PLoS Pathog **8:**e1002776.
6. **Klemm E, Dougan G.** 2016. Advances in Understanding Bacterial Pathogenesis Gained from Whole-Genome Sequencing and Phylogenetics. Cell Host Microbe **19:**599-610.
7. **Lamas A, Miranda JM, Regal P, Vazquez B, Franco CM, Cepeda A.** 2018. A comprehensive review of non-enterica subspecies of Salmonella enterica. Microbiol Res **206:**60-73.
8. **Baumler AJ, Tsolis RM, Ficht TA, Adams LG.** 1998. Evolution of host adaptation in Salmonella enterica. Infect Immun **66:**4579-4587.
9. **Gal-Mor O, Boyle EC, Grassl GA.** 2014. Same species, different diseases: how and why typhoidal and non-typhoidal Salmonella enterica serovars differ. Front Microbiol **5:**391.
10. **Budd W.** 1873. Typhoid Fever: Its Nature, Mode of Spreading, and Prevention.
11. **Eberth C.** 1880. Die Organismen in den Organen bei Typhus abdominalis. Archiv für pathologische Anatomie und Physiologie und für klinische Medicin **81:**58–74.
12. **Gaffky G.** 1884. On the etiology of enteric fever. Recent Essays by Various Authors on Bacteria in Relation to Disease (London: New Sydenham Society, 1886)**:**205-257.
13. **Stuart BM, Pullen RL.** 1946. Typhoid: clinical analysis of three hundred and sixty cases. Archives of Internal Medicine **78:**629-661.
14. **Parry CM, Hien TT, Dougan G, White NJ, Farrar JJ.** 2002. Typhoid fever. N Engl J Med **347:**1770-1782.
15. **Crump JA, Luby SP, Mintz ED.** 2004. The global burden of typhoid fever. Bull World Health Organ **82:**346-353.
16. **Buckle GC, Walker CL, Black RE.** 2012. Typhoid fever and paratyphoid fever: Systematic review to estimate global morbidity and mortality for 2010. J Glob Health **2:**010401.
17. **Crump JA, Mintz ED.** 2010. Global trends in typhoid and paratyphoid Fever. Clin Infect Dis **50:**241-246.
18. **Parkhill J, Dougan G, James KD, Thomson NR, Pickard D, Wain J, Churcher C, Mungall KL, Bentley SD, Holden MT, Sebaihia M, Baker S, Basham D, Brooks K, Chillingworth T, Connerton P, Cronin A, Davis P, Davies RM, Dowd L, White N, Farrar J, Feltwell T, Hamlin N, Haque A, Hien TT, Holroyd S, Jagels**

K, Krogh A, Larsen TS, Leather S, Moule S, O'Gaora P, Parry C, Quail M, Rutherford K, Simmonds M, Skelton J, Stevens K, Whitehead S, Barrell BG. 2001. Complete genome sequence of a multiple drug resistant Salmonella enterica serovar Typhi CT18. Nature **413:**848-852.

19. **Dougan G, Baker S.** 2014. Salmonella enterica serovar Typhi and the pathogenesis of typhoid fever. Annu Rev Microbiol **68:**317-336.
20. **Sabbagh SC, Forest CG, Lepage C, Leclerc JM, Daigle F.** 2010. So similar, yet so different: uncovering distinctive features in the genomes of Salmonella enterica serovars Typhimurium and Typhi. FEMS Microbiol Lett **305:**1-13.
21. **Feng Y, Johnston RN, Liu GR, Liu SL.** 2013. Genomic comparison between Salmonella Gallinarum and Pullorum: differential pseudogene formation under common host restriction. PLoS One **8:**e59427.
22. **Sprinz H, Gangarosa EJ, Williams M, Hornick RB, Woodward TE.** 1966. Histopathology of the upper small intestines in typhoid fever. Biopsy study of experimental disease in man. Am J Dig Dis **11:**615-624.
23. **Coburn B, Grassl GA, Finlay BB.** 2007. Salmonella, the host and disease: a brief review. Immunol Cell Biol **85:**112-118.
24. **Broz P, Ohlson MB, Monack DM.** 2012. Innate immune response to Salmonella typhimurium, a model enteric pathogen. Gut Microbes **3:**62-70.
25. **Crawford RW, Gibson DL, Kay WW, Gunn JS.** 2008. Identification of a bile-induced exopolysaccharide required for Salmonella biofilm formation on gallstone surfaces. Infect Immun **76:**5341-5349.
26. **Felix A, Pitt RM.** 1936. The Vi antigens of various Salmonella types. British journal of experimental pathology **17:**81.
27. **Wilson RP, Winter SE, Spees AM, Winter MG, Nishimori JH, Sanchez JF, Nuccio SP, Crawford RW, Tukel C, Baumler AJ.** 2011. The Vi capsular polysaccharide prevents complement receptor 3-mediated clearance of Salmonella enterica serotype Typhi. Infect Immun **79:**830-837.
28. **Wangdi T, Lee CY, Spees AM, Yu C, Kingsbury DD, Winter SE, Hastey CJ, Wilson RP, Heinrich V, Baumler AJ.** 2014. The Vi capsular polysaccharide enables Salmonella enterica serovar typhi to evade microbe-guided neutrophil chemotaxis. PLoS Pathog **10:**e1004306.
29. **Haghjoo E, Galan JE.** 2004. Salmonella typhi encodes a functional cytolethal distending toxin that is delivered into host cells by a bacterial-internalization pathway. Proc Natl Acad Sci U S A **101:**4614-4619.
30. **Spano S, Ugalde JE, Galan JE.** 2008. Delivery of a Salmonella Typhi exotoxin from a host intracellular compartment. Cell Host Microbe **3:**30-38.
31. **Song J, Gao X, Galan JE.** 2013. Structure and function of the Salmonella Typhi chimaeric A(2)B(5) typhoid toxin. Nature **499:**350-354.
32. **Liang L, Juarez S, Nga TV, Dunstan S, Nakajima-Sasaki R, Davies DH, McSorley S, Baker S, Felgner PL.** 2013. Immune profiling with a Salmonella Typhi antigen microarray identifies new diagnostic biomarkers of human typhoid. Sci Rep **3:**1043.
33. **Waddington CS, Darton TC, Woodward WE, Angus B, Levine MM, Pollard AJ.** 2014. Advancing the management and control of typhoid fever: a review of the historical role of human challenge studies. J Infect **68:**405-418.
34. **World Health Organization.** 2008. Typhoid vaccines: WHO position paper. Wkly Epidemiol Rec **83:**49-59.
35. **Lin FY, Ho VA, Khiem HB, Trach DD, Bay PV, Thanh TC, Kossaczka Z, Bryla DA, Shiloach J, Robbins JB, Schneerson R, Szu SC.** 2001. The efficacy of a

Salmonella typhi Vi conjugate vaccine in two-to-five-year-old children. N Engl J Med **344:**1263-1269.

36. **Majowicz SE, Musto J, Scallan E, Angulo FJ, Kirk M, O'Brien SJ, Jones TF, Fazil A, Hoekstra RM, International Collaboration on Enteric Disease 'Burden of Illness S.** 2010. The global burden of nontyphoidal Salmonella gastroenteritis. Clin Infect Dis **50:**882-889.
37. **Salmon D, Smith T.** 1886. The bacterium of swine plague. Am Month Micr J **7:**204.
38. **Su LH, Chiu CH.** 2007. Salmonella: clinical importance and evolution of nomenclature. Chang Gung Med J **30:**210-219.
39. **Velge P, Cloeckaert A, Barrow P.** 2005. Emergence of Salmonella epidemics: the problems related to Salmonella enterica serotype Enteritidis and multiple antibiotic resistance in other major serotypes. Vet Res **36:**267-288.
40. **Galanis E, Lo Fo Wong DM, Patrick ME, Binsztein N, Cieslik A, Chalermchikit T, Aidara-Kane A, Ellis A, Angulo FJ, Wegener HC.** 2006. Web-based surveillance and global Salmonella distribution, 2000-2002. Emerg Infect Dis **12:**381-388.
41. **Crump JA, Sjolund-Karlsson M, Gordon MA, Parry CM.** 2015. Epidemiology, Clinical Presentation, Laboratory Diagnosis, Antimicrobial Resistance, and Antimicrobial Management of Invasive Salmonella Infections. Clin Microbiol Rev **28:**901-937.
42. **Feasey NA, Hadfield J, Keddy KH, Dallman TJ, Jacobs J, Deng X, Wigley P, Barquist Barquist L, Langridge GC, Feltwell T, Harris SR, Mather AE, Fookes M, Aslett M, Msefula C, Kariuki S, Maclennan CA, Onsare RS, Weill FX, Le Hello S, Smith AM, McClelland M, Desai P, Parry CM, Cheesbrough J, French N, Campos J, Chabalgoity JA, Betancor L, Hopkins KL, Nair S, Humphrey TJ, Lunguya O, Cogan TA, Tapia MD, Sow SO, Tennant SM, Bornstein K, Levine MM, Lacharme-Lora L, Everett DB, Kingsley RA, Parkhill J, Heyderman RS, Dougan G, Gordon MA, Thomson NR.** 2016. Distinct Salmonella Enteritidis lineages associated with enterocolitis in high-income settings and invasive disease in low-income settings. Nat Genet **48:**1211-1217.
43. **Stevens MP, Humphrey TJ, Maskell DJ.** 2009. Molecular insights into farm animal and zoonotic Salmonella infections. Philos Trans R Soc Lond B Biol Sci **364:**2709-2723.
44. **Acheson D, Hohmann EL.** 2001. Nontyphoidal salmonellosis. Clinical Infectious Diseases **32:**263-269.
45. **Buchwald DS, Blaser MJ.** 1984. A review of human salmonellosis: II. Duration of excretion following infection with nontyphi Salmonella. Rev Infect Dis **6:**345-356.
46. **Shimoni Z, Pitlik S, Leibovici L, Samra Z, Konigsberger H, Drucker M, Agmon V, Ashkenazi S, Weinberger M.** 1999. Nontyphoid Salmonella bacteremia: age-related differences in clinical presentation, bacteriology, and outcome. Clin Infect Dis **28:**822-827.
47. **Kankwatira AM, Mwafulirwa GA, Gordon MA.** 2004. Non-typhoidal salmonella bacteraemia--an under-recognized feature of AIDS in African adults. Trop Doct **34:**198-200.
48. **Sanchez-Vargas FM, Abu-El-Haija MA, Gomez-Duarte OG.** 2011. Salmonella infections: an update on epidemiology, management, and prevention. Travel Med Infect Dis **9:**263-277.
49. **Parry CM, Threlfall EJ.** 2008. Antimicrobial resistance in typhoidal and nontyphoidal salmonellae. Curr Opin Infect Dis **21:**531-538.

50. **Haraga A, Ohlson MB, Miller SI.** 2008. Salmonellae interplay with host cells. Nat Rev Microbiol **6:**53-66.
51. **Lupp C, Robertson ML, Wickham ME, Sekirov I, Champion OL, Gaynor EC, Finlay BB.** 2007. Host-mediated inflammation disrupts the intestinal microbiota and promotes the overgrowth of Enterobacteriaceae. Cell Host Microbe **2:**119-129.
52. **Stecher B, Robbiani R, Walker AW, Westendorf AM, Barthel M, Kremer M, Chaffron S, Macpherson AJ, Buer J, Parkhill J, Dougan G, von Mering C, Hardt WD.** 2007. Salmonella enterica serovar typhimurium exploits inflammation to compete with the intestinal microbiota. PLoS Biol **5:**2177-2189.
53. **Raffatellu M, George MD, Akiyama Y, Hornsby MJ, Nuccio SP, Paixao TA, Butler BP, Chu H, Santos RL, Berger T, Mak TW, Tsolis RM, Bevins CL, Solnick JV, Dandekar S, Baumler AJ.** 2009. Lipocalin-2 resistance confers an advantage to Salmonella enterica serotype Typhimurium for growth and survival in the inflamed intestine. Cell Host Microbe **5:**476-486.
54. **Liu JZ, Jellbauer S, Poe AJ, Ton V, Pesciaroli M, Kehl-Fie TE, Restrepo NA, Hosking MP, Edwards RA, Battistoni A, Pasquali P, Lane TE, Chazin WJ, Vogl T, Roth J, Skaar EP, Raffatellu M.** 2012. Zinc sequestration by the neutrophil protein calprotectin enhances Salmonella growth in the inflamed gut. Cell Host Microbe **11:**227-239.
55. **Winter SE, Thiennimitr P, Winter MG, Butler BP, Huseby DL, Crawford RW, Russell JM, Bevins CL, Adams LG, Tsolis RM, Roth JR, Baumler AJ.** 2010. Gut inflammation provides a respiratory electron acceptor for Salmonella. Nature **467:**426-429.
56. **Heffernan EJ, Reed S, Hackett J, Fierer J, Roudier C, Guiney D.** 1992. Mechanism of resistance to complement-mediated killing of bacteria encoded by the Salmonella typhimurium virulence plasmid gene rck. J Clin Invest **90:**953-964.
57. **Rosselin M, Virlogeux-Payant I, Roy C, Bottreau E, Sizaret PY, Mijouin L, Germon P, Caron E, Velge P, Wiedemann A.** 2010. Rck of Salmonella enterica, subspecies enterica serovar enteritidis, mediates zipper-like internalization. Cell Res **20:**647-664.
58. **Francis CL, Starnbach MN, Falkow S.** 1992. Morphological and cytoskeletal changes in epithelial cells occur immediately upon interaction with Salmonella typhimurium grown under low-oxygen conditions. Mol Microbiol **6:**3077-3087.
59. **Velge P, Wiedemann A, Rosselin M, Abed N, Boumart Z, Chausse AM, Grepinet O, Namdari F, Roche SM, Rossignol A, Virlogeux-Payant I.** 2012. Multiplicity of Salmonella entry mechanisms, a new paradigm for Salmonella pathogenesis. Microbiologyopen **1:**243-258.
60. **Jones BD, Ghori N, Falkow S.** 1994. Salmonella typhimurium initiates murine infection by penetrating and destroying the specialized epithelial M cells of the Peyer's patches. J Exp Med **180:**15-23.
61. **Rescigno M, Urbano M, Valzasina B, Francolini M, Rotta G, Bonasio R, Granucci F, Kraehenbuhl JP, Ricciardi-Castagnoli P.** 2001. Dendritic cells express tight junction proteins and penetrate gut epithelial monolayers to sample bacteria. Nat Immunol **2:**361-367.
62. **Lahiri A, Lahiri A, Iyer N, Das P, Chakravortty D.** 2010. Visiting the cell biology of Salmonella infection. Microbes Infect **12:**809-818.
63. **Müller AJ, Kaiser P, Dittmar KE, Weber TC, Haueter S, Endt K, Songhet P, Zellweger C, Kremer M, Fehling H-J.** 2012. Salmonella gut invasion involves TTSS-2-dependent epithelial traversal, basolateral exit, and uptake by epithelium-sampling lamina propria phagocytes. Cell host & microbe **11:**19-32.

64. **LaRock DL, Chaudhary A, Miller SI.** 2015. Salmonellae interactions with host processes. Nat Rev Microbiol **13:**191-205.
65. **Takeuchi A.** 1967. Electron microscope studies of experimental Salmonella infection. I. Penetration into the intestinal epithelium by Salmonella typhimurium. The American journal of pathology **50:**109.
66. **Takeuchi A, Sprinz H.** 1967. Electron-microscope studies of experimental salmonella infection in the preconditioned guinea pig: ii. response of the intestinal mucosa to the invasion by Salmonella typhimurium. The American journal of pathology **51:**137.
67. **Kihlström E, Latkovic S.** 1978. Ultrastructural studies on the interaction between Salmonella typhimurium 395 M and HeLa cells. Infection and immunity **22:**804-809.
68. **Finlay BB, Falkow S.** 1989. Common themes in microbial pathogenicity. Microbiological reviews **53:**210-230.
69. **Steele-Mortimer O, Méresse S, Gorvel JP, Toh BH, Finlay BB.** 1999. Biogenesis of Salmonella typhimurium-containing vacuoles in epithelial cells involves interactions with the early endocytic pathway. Cellular microbiology **1:**33-49.
70. **Garcia-del Portillo F, Zwick MB, Leung KY, Finlay BB.** 1993. Salmonella induces the formation of filamentous structures containing lysosomal membrane glycoproteins in epithelial cells. Proceedings of the National Academy of Sciences **90:**10544-10548.
71. **Liss V, Swart AL, Kehl A, Hermanns N, Zhang Y, Chikkaballi D, Bohles N, Deiwick J, Hensel M.** 2017. Salmonella enterica Remodels the Host Cell Endosomal System for Efficient Intravacuolar Nutrition. Cell Host Microbe **21:**390-402.
72. **Brumell JH.** 2002. Disruption of the Salmonella-Containing Vacuole Leads to Increased Replication of Salmonella enterica Serovar Typhimurium in the Cytosol of Epithelial Cells. Infection and Immunity **70:**3264-3270.
73. **Birmingham CL, Smith AC, Bakowski MA, Yoshimori T, Brumell JH.** 2006. Autophagy controls Salmonella infection in response to damage to the Salmonella-containing vacuole. Journal of Biological Chemistry **281:**11374-11383.
74. **Birmingham CL, Brumell JH.** 2006. Autophagy recognizes intracellular Salmonella enterica serovar Typhimurium in damaged vacuoles. Autophagy **2:**156-158.
75. **Thurston TL, Wandel MP, von Muhlinen N, Foeglein Á, Randow F.** 2012. Galectin 8 targets damaged vesicles for autophagy to defend cells against bacterial invasion. Nature **482:**414.
76. **Ferreira RB, Valdez Y, Coombes BK, Sad S, Gouw JW, Brown EM, Li Y, Grassl GA, Antunes LC, Gill N, Truong M, Scholz R, Reynolds LA, Krishnan L, Zafer AA, Sal-Man N, Lowden MJ, Auweter SD, Foster LJ, Finlay BB.** 2015. A Highly Effective Component Vaccine against Nontyphoidal Salmonella enterica Infections. MBio **6:**e01421-01415.
77. **Maki DG.** 2009. Coming to grips with foodborne infection--peanut butter, peppers, and nationwide salmonella outbreaks. N Engl J Med **360:**949-953.
78. **Gordon MA.** 2008. Salmonella infections in immunocompromised adults. J Infect **56:**413-422.
79. **Feasey NA, Dougan G, Kingsley RA, Heyderman RS, Gordon MA.** 2012. Invasive non-typhoidal salmonella disease: an emerging and neglected tropical disease in Africa. Lancet **379:**2489-2499.
80. **Ao TT, Feasey NA, Gordon MA, Keddy KH, Angulo FJ, Crump JA.** 2015. Global burden of invasive nontyphoidal Salmonella disease, 2010(1). Emerg Infect Dis **21**.
81. **Gordon MA, Banda HT, Gondwe M, Gordon SB, Boeree MJ, Walsh AL, Corkill JE, Hart CA, Gilks CF, Molyneux ME.** 2002. Non-typhoidal salmonella

bacteraemia among HIV-infected Malawian adults: high mortality and frequent recrudescence. Aids **16:**1633-1641.

82. **Peters RP, Zijlstra EE, Schijffelen MJ, Walsh AL, Joaki G, Kumwenda JJ, Kublin JG, Molyneux ME, Lewis DK.** 2004. A prospective study of bloodstream infections as cause of fever in Malawi: clinical predictors and implications for management. Trop Med Int Health **9:**928-934.
83. **Brent AJ, Oundo JO, Mwangi I, Ochola L, Lowe B, Berkley JA.** 2006. Salmonella bacteremia in Kenyan children. Pediatr Infect Dis J **25:**230-236.
84. **MacLennan CA, Gilchrist JJ, Gordon MA, Cunningham AF, Cobbold M, Goodall M, Kingsley RA, van Oosterhout JJ, Msefula CL, Mandala WL, Leyton DL, Marshall JL, Gondwe EN, Bobat S, Lopez-Macias C, Doffinger R, Henderson IR, Zijlstra EE, Dougan G, Drayson MT, MacLennan IC, Molyneux ME.** 2010. Dysregulated humoral immunity to nontyphoidal Salmonella in HIV-infected African adults. Science **328:**508-512.
85. **Gordon MA, Gordon SB, Musaya L, Zijlstra EE, Molyneux ME, Read RC.** 2007. Primary macrophages from HIV-infected adults show dysregulated cytokine responses to Salmonella, but normal internalization and killing. Aids **21:**2399-2408.
86. **Kariuki S, Gordon MA, Feasey N, Parry CM.** 2015. Antimicrobial resistance and management of invasive Salmonella disease. Vaccine **33 Suppl 3:**C21-29.
87. **Kingsley RA, Msefula CL, Thomson NR, Kariuki S, Holt KE, Gordon MA, Harris D, Clarke L, Whitehead S, Sangal V, Marsh K, Achtman M, Molyneux ME, Cormican M, Parkhill J, MacLennan CA, Heyderman RS, Dougan G.** 2009. Epidemic multiple drug resistant Salmonella Typhimurium causing invasive disease in sub-Saharan Africa have a distinct genotype. Genome Res **19:**2279-2287.
88. **Gilchrist JJ, MacLennan CA.** 2019. Invasive Nontyphoidal Salmonella Disease in Africa. EcoSal Plus **8**.
89. **Ashton PM, Owen SV, Kaindama L, Rowe WPM, Lane CR, Larkin L, Nair S, Jenkins C, de Pinna EM, Feasey NA, Hinton JCD, Dallman TJ.** 2017. Public health surveillance in the UK revolutionises our understanding of the invasive Salmonella Typhimurium epidemic in Africa. Genome Med **9:**92.
90. **Marcus SL, Brumell JH, Pfeifer CG, Finlay BB.** 2000. Salmonella pathogenicity islands: big virulence in small packages. Microbes Infect **2:**145-156.
91. **Hensel M.** 2004. Evolution of pathogenicity islands of Salmonella enterica. Int J Med Microbiol **294:**95-102.
92. **Mills DM, Bajaj V, Lee CA.** 1995. A 40 kb chromosomal fragment encoding Salmonella typhimurium invasion genes is absent from the corresponding region of the Escherichia coli K-12 chromosome. Mol Microbiol **15:**749-759.
93. **Collazo CM, Galan JE.** 1997. The invasion-associated type-III protein secretion system in Salmonella--a review. Gene **192:**51-59.
94. **Lostroh CP, Lee CA.** 2001. The Salmonella pathogenicity island-1 type III secretion system. Microbes Infect **3:**1281-1291.
95. **Galan JE.** 2001. Salmonella interactions with host cells: type III secretion at work. Annu Rev Cell Dev Biol **17:**53-86.
96. **Ochman H, Groisman EA.** 1996. Distribution of pathogenicity islands in Salmonella spp. Infect Immun **64:**5410-5412.
97. **Baumler AJ.** 1997. The record of horizontal gene transfer in Salmonella. Trends Microbiol **5:**318-322.
98. **Galan JE, Curtiss R, 3rd.** 1989. Cloning and molecular characterization of genes whose products allow Salmonella typhimurium to penetrate tissue culture cells. Proc Natl Acad Sci U S A **86:**6383-6387.

99. **Hensel M, Shea JE, Gleeson C, Jones MD, Dalton E, Holden DW.** 1995. Simultaneous identification of bacterial virulence genes by negative selection. Science **269:**400-403.
100. **Shea JE, Hensel M, Gleeson C, Holden DW.** 1996. Identification of a virulence locus encoding a second type III secretion system in Salmonella typhimurium. Proc Natl Acad Sci U S A **93:**2593-2597.
101. **Ochman H, Soncini FC, Solomon F, Groisman EA.** 1996. Identification of a pathogenicity island required for Salmonella survival in host cells. Proc Natl Acad Sci U S A **93:**7800-7804.
102. **Hensel M, Nikolaus T, Egelseer C.** 1999. Molecular and functional analysis indicates a mosaic structure of Salmonella pathogenicity island 2. Mol Microbiol **31:**489-498.
103. **Hensel M, Hinsley AP, Nikolaus T, Sawers G, Berks BC.** 1999. The genetic basis of tetrathionate respiration in Salmonella typhimurium. Mol Microbiol **32:**275-287.
104. **Hensel M, Shea JE, Raupach B, Monack D, Falkow S, Gleeson C, Kubo T, Holden DW.** 1997. Functional analysis of ssaJ and the ssaK/U operon, 13 genes encoding components of the type III secretion apparatus of Salmonella Pathogenicity Island 2. Mol Microbiol **24:**155-167.
105. **Jennings E, Thurston TLM, Holden DW.** 2017. Salmonella SPI-2 Type III Secretion System Effectors: Molecular Mechanisms And Physiological Consequences. Cell Host Microbe **22:**217-231.
106. **Figueira R, Holden DW.** 2012. Functions of the Salmonella pathogenicity island 2 (SPI-2) type III secretion system effectors. Microbiology **158:**1147-1161.
107. **Hensel M, Shea JE, Baumler AJ, Gleeson C, Blattner F, Holden DW.** 1997. Analysis of the boundaries of Salmonella pathogenicity island 2 and the corresponding chromosomal region of Escherichia coli K-12. J Bacteriol **179:**1105-1111.
108. **Blanc-Potard AB, Solomon F, Kayser J, Groisman EA.** 1999. The SPI-3 pathogenicity island of Salmonella enterica. J Bacteriol **181:**998-1004.
109. **Gerlach RG, Jackel D, Stecher B, Wagner C, Lupas A, Hardt WD, Hensel M.** 2007. Salmonella Pathogenicity Island 4 encodes a giant non-fimbrial adhesin and the cognate type 1 secretion system. Cell Microbiol **9:**1834-1850.
110. **Barlag B, Hensel M.** 2015. The giant adhesin SiiE of Salmonella enterica. Molecules **20:**1134-1150.
111. **Knodler LA, Celli J, Hardt WD, Vallance BA, Yip C, Finlay BB.** 2002. Salmonella effectors within a single pathogenicity island are differentially expressed and translocated by separate type III secretion systems. Mol Microbiol **43:**1089-1103.
112. **Folkesson A, Lofdahl S, Normark S.** 2002. The Salmonella enterica subspecies I specific centisome 7 genomic island encodes novel protein families present in bacteria living in close contact with eukaryotic cells. Res Microbiol **153:**537-545.
113. **Sana TG, Flaugnatti N, Lugo KA, Lam LH, Jacobson A, Baylot V, Durand E, Journet L, Cascales E, Monack DM.** 2016. Salmonella Typhimurium utilizes a T6SS-mediated antibacterial weapon to establish in the host gut. Proc Natl Acad Sci U S A **113:**E5044-5051.
114. **Galan JE, Lara-Tejero M, Marlovits TC, Wagner S.** 2014. Bacterial type III secretion systems: specialized nanomachines for protein delivery into target cells. Annu Rev Microbiol **68:**415-438.
115. **Hu Y, Huang H, Cheng X, Shu X, White AP, Stavrinides J, Koster W, Zhu G, Zhao Z, Wang Y.** 2017. A global survey of bacterial type III secretion systems and their effectors. Environ Microbiol **19:**3879-3895.

116. **Deng W, Marshall NC, Rowland JL, McCoy JM, Worrall LJ, Santos AS, Strynadka NCJ, Finlay BB.** 2017. Assembly, structure, function and regulation of type III secretion systems. Nat Rev Microbiol **15:**323-337.
117. **Abby SS, Rocha EP.** 2012. The non-flagellar type III secretion system evolved from the bacterial flagellum and diversified into host-cell adapted systems. PLoS Genet **8:**e1002983.
118. **Galan JE, Wolf-Watz H.** 2006. Protein delivery into eukaryotic cells by type III secretion machines. Nature **444:**567-573.
119. **Kuhle V, Hensel M.** 2004. Cellular microbiology of intracellular Salmonella enterica: functions of the type III secretion system encoded by Salmonella pathogenicity island 2. Cell Mol Life Sci **61:**2812-2826.
120. **Galan JE, Waksman G.** 2018. Protein-Injection Machines in Bacteria. Cell **172:**1306-1318.
121. **Schraidt O, Marlovits TC.** 2011. Three-dimensional model of Salmonella's needle complex at subnanometer resolution. Science **331:**1192-1195.
122. **Worrall LJ, Hong C, Vuckovic M, Deng W, Bergeron JR, Majewski DD, Huang RK, Spreter T, Finlay BB, Yu Z, Strynadka NC.** 2016. Near-atomic-resolution cryo-EM analysis of the Salmonella T3S injectisome basal body. Nature doi:10.1038/nature20576.
123. **Makino F, Shen D, Kajimura N, Kawamoto A, Pissaridou P, Oswin H, Pain M, Murillo I, Namba K, Blocker AJ.** 2016. The Architecture of the Cytoplasmic Region of Type III Secretion Systems. Sci Rep **6:**33341.
124. **Lara-Tejero M, Kato J, Wagner S, Liu X, Galan JE.** 2011. A sorting platform determines the order of protein secretion in bacterial type III systems. Science **331:**1188-1191.
125. **Lara-Tejero M, Galan JE.** 2009. Salmonella enterica serovar typhimurium pathogenicity island 1-encoded type III secretion system translocases mediate intimate attachment to nonphagocytic cells. Infect Immun **77:**2635-2642.
126. **Schlumberger MC, Hardt WD.** 2006. Salmonella type III secretion effectors: pulling the host cell's strings. Curr Opin Microbiol **9:**46-54.
127. **Abrahams GL, Hensel M.** 2006. Manipulating cellular transport and immune responses: dynamic interactions between intracellular Salmonella enterica and its host cells. Cell Microbiol **8:**728-737.
128. **Ilyas B, Tsai CN, Coombes BK.** 2017. Evolution of Salmonella-Host Cell Interactions through a Dynamic Bacterial Genome. Front Cell Infect Microbiol **7:**428.
129. **Navarre WW, Porwollik S, Wang Y, McClelland M, Rosen H, Libby SJ, Fang FC.** 2006. Selective silencing of foreign DNA with low GC content by the H-NS protein in Salmonella. Science **313:**236-238.
130. **Ali SS, Xia B, Liu J, Navarre WW.** 2012. Silencing of foreign DNA in bacteria. Curr Opin Microbiol **15:**175-181.
131. **Dorman CJ.** 2007. H-NS, the genome sentinel. Nat Rev Microbiol **5:**157-161.
132. **Schechter LM, Jain S, Akbar S, Lee CA.** 2003. The small nucleoid-binding proteins H-NS, HU, and Fis affect hilA expression in Salmonella enterica serovar Typhimurium. Infect Immun **71:**5432-5435.
133. **Olekhnovich IN, Kadner RJ.** 2007. Role of nucleoid-associated proteins Hha and H-NS in expression of Salmonella enterica activators HilD, HilC, and RtsA required for cell invasion. J Bacteriol **189:**6882-6890.
134. **Bajaj V, Hwang C, Lee CA.** 1995. hilA is a novel ompR/toxR family member that activates the expression of Salmonella typhimurium invasion genes. Mol Microbiol **18:**715-727.

135. **Bajaj V, Lucas RL, Hwang C, Lee CA.** 1996. Co-ordinate regulation of Salmonella typhimurium invasion genes by environmental and regulatory factors is mediated by control of hilA expression. Mol Microbiol **22:**703-714.
136. **Darwin KH, Miller VL.** 2001. Type III secretion chaperone-dependent regulation: activation of virulence genes by SicA and InvF in Salmonella typhimurium. Embo j **20:**1850-1862.
137. **Ellermeier CD, Ellermeier JR, Slauch JM.** 2005. HilD, HilC and RtsA constitute a feed forward loop that controls expression of the SPI1 type three secretion system regulator hilA in Salmonella enterica serovar Typhimurium. Mol Microbiol **57:**691-705.
138. **Saini S, Ellermeier JR, Slauch JM, Rao CV.** 2010. The role of coupled positive feedback in the expression of the SPI1 type three secretion system in Salmonella. PLoS Pathog **6:**e1001025.
139. **Walthers D, Carroll RK, Navarre WW, Libby SJ, Fang FC, Kenney LJ.** 2007. The response regulator SsrB activates expression of diverse Salmonella pathogenicity island 2 promoters and counters silencing by the nucleoid-associated protein H-NS. Mol Microbiol **65:**477-493.
140. **Gao R, Stock AM.** 2009. Biological insights from structures of two-component proteins. Annu Rev Microbiol **63:**133-154.
141. **Capra EJ, Laub MT.** 2012. Evolution of two-component signal transduction systems. Annu Rev Microbiol **66:**325-347.
142. **Bearson S, Bearson B, Foster JW.** 1997. Acid stress responses in enterobacteria. FEMS Microbiol Lett **147:**173-180.
143. **Garcia Vescovi E, Soncini FC, Groisman EA.** 1996. Mg2+ as an extracellular signal: environmental regulation of Salmonella virulence. Cell **84:**165-174.
144. **Bader MW, Sanowar S, Daley ME, Schneider AR, Cho U, Xu W, Klevit RE, Le Moual H, Miller SI.** 2005. Recognition of antimicrobial peptides by a bacterial sensor kinase. Cell **122:**461-472.
145. **Fabrega A, Vila J.** 2013. Salmonella enterica serovar Typhimurium skills to succeed in the host: virulence and regulation. Clin Microbiol Rev **26:**308-341.
146. **Gunn JS, Miller SI.** 1996. PhoP-PhoQ activates transcription of pmrAB, encoding a two-component regulatory system involved in Salmonella typhimurium antimicrobial peptide resistance. J Bacteriol **178:**6857-6864.
147. **Deiwick J, Nikolaus T, Erdogan S, Hensel M.** 1999. Environmental regulation of Salmonella pathogenicity island 2 gene expression. Mol Microbiol **31:**1759-1773.
148. **Chen HD, Groisman EA.** 2013. The biology of the PmrA/PmrB two-component system: the major regulator of lipopolysaccharide modifications. Annu Rev Microbiol **67:**83-112.
149. **Feng X, Oropeza R, Kenney LJ.** 2003. Dual regulation by phospho-OmpR of ssrA/B gene expression in Salmonella pathogenicity island 2. Mol Microbiol **48:**1131-1143.
150. **Lee AK, Detweiler CS, Falkow S.** 2000. OmpR regulates the two-component system SsrA-ssrB in Salmonella pathogenicity island 2. J Bacteriol **182:**771-781.
151. **Fass E, Groisman EA.** 2009. Control of Salmonella pathogenicity island-2 gene expression. Curr Opin Microbiol **12:**199-204.
152. **Bustamante VH, Martinez LC, Santana FJ, Knodler LA, Steele-Mortimer O, Puente JL.** 2008. HilD-mediated transcriptional cross-talk between SPI-1 and SPI-2. Proc Natl Acad Sci U S A **105:**14591-14596.
153. **Perez-Morales D, Banda MM, Chau NYE, Salgado H, Martinez-Flores I, Ibarra JA, Ilyas B, Coombes BK, Bustamante VH.** 2017. The transcriptional regulator

SsrB is involved in a molecular switch controlling virulence lifestyles of Salmonella. PLoS Pathog **13:**e1006497.

154. **Geddes K, Worley M, Niemann G, Heffron F.** 2005. Identification of new secreted effectors in Salmonella enterica serovar Typhimurium. Infect Immun **73:**6260-6271.
155. **Miao EA, Scherer CA, Tsolis RM, Kingsley RA, Adams LG, Baumler AJ, Miller SI.** 1999. Salmonella typhimurium leucine-rich repeat proteins are targeted to the SPI1 and SPI2 type III secretion systems. Mol Microbiol **34:**850-864.
156. **McGhie EJ, Brawn LC, Hume PJ, Humphreys D, Koronakis V.** 2009. Salmonella takes control: effector-driven manipulation of the host. Curr Opin Microbiol **12:**117-124.
157. **Hayward RD, McGhie EJ, Koronakis V.** 2000. Membrane fusion activity of purified SipB, a Salmonella surface protein essential for mammalian cell invasion. Mol Microbiol **37:**727-739.
158. **Scherer CA, Cooper E, Miller SI.** 2000. The Salmonella type III secretion translocon protein SspC is inserted into the epithelial cell plasma membrane upon infection. Mol Microbiol **37:**1133-1145.
159. **Collazo CM, Galan JE.** 1997. The invasion-associated type III system of Salmonella typhimurium directs the translocation of Sip proteins into the host cell. Mol Microbiol **24:**747-756.
160. **Hayward RD, Koronakis V.** 1999. Direct nucleation and bundling of actin by the SipC protein of invasive Salmonella. Embo j **18:**4926-4934.
161. **Zhou D, Mooseker MS, Galan JE.** 1999. Role of the S. typhimurium actin-binding protein SipA in bacterial internalization. Science **283:**2092-2095.
162. **McGhie EJ, Hayward RD, Koronakis V.** 2001. Cooperation between actin-binding proteins of invasive Salmonella: SipA potentiates SipC nucleation and bundling of actin. Embo j **20:**2131-2139.
163. **Patel JC, Galan JE.** 2006. Differential activation and function of Rho GTPases during Salmonella-host cell interactions. J Cell Biol **175:**453-463.
164. **Bakowski MA, Cirulis JT, Brown NF, Finlay BB, Brumell JH.** 2007. SopD acts cooperatively with SopB during Salmonella enterica serovar Typhimurium invasion. Cell Microbiol **9:**2839-2855.
165. **Stender S, Friebel A, Linder S, Rohde M, Mirold S, Hardt WD.** 2000. Identification of SopE2 from Salmonella typhimurium, a conserved guanine nucleotide exchange factor for Cdc42 of the host cell. Mol Microbiol **36:**1206-1221.
166. **Friebel A, Ilchmann H, Aepfelbacher M, Ehrbar K, Machleidt W, Hardt WD.** 2001. SopE and SopE2 from Salmonella typhimurium activate different sets of RhoGTPases of the host cell. J Biol Chem **276:**34035-34040.
167. **Criss AK, Casanova JE.** 2003. Coordinate Regulation of Salmonella enterica Serovar Typhimurium Invasion of Epithelial Cells by the Arp2/3 Complex and Rho GTPases. Infection and Immunity **71:**2885-2891.
168. **Shi J, Scita G, Casanova JE.** 2005. WAVE2 signaling mediates invasion of polarized epithelial cells by Salmonella typhimurium. J Biol Chem **280:**29849-29855.
169. **Zhou D, Chen LM, Hernandez L, Shears SB, Galan JE.** 2001. A Salmonella inositol polyphosphatase acts in conjunction with other bacterial effectors to promote host cell actin cytoskeleton rearrangements and bacterial internalization. Mol Microbiol **39:**248-259.
170. **Fu Y, Galan JE.** 1999. A salmonella protein antagonizes Rac-1 and Cdc42 to mediate host-cell recovery after bacterial invasion. Nature **401:**293-297.
171. **Kubori T, Galan JE.** 2003. Temporal regulation of salmonella virulence effector function by proteasome-dependent protein degradation. Cell **115:**333-342.

172. **Hobbie S, Chen LM, Davis RJ, Galan JE.** 1997. Involvement of mitogen-activated protein kinase pathways in the nuclear responses and cytokine production induced by Salmonella typhimurium in cultured intestinal epithelial cells. J Immunol **159:**5550-5559.
173. **Harada A, Sekido N, Akahoshi T, Wada T, Mukaida N, Matsushima K.** 1994. Essential involvement of interleukin-8 (IL-8) in acute inflammation. J Leukoc Biol **56:**559-564.
174. **Patel S, McCormick BA.** 2014. Mucosal Inflammatory Response to Salmonella typhimurium Infection. Front Immunol **5:**311.
175. **Boyle EC, Brown NF, Finlay BB.** 2006. Salmonella enterica serovar Typhimurium effectors SopB, SopE, SopE2 and SipA disrupt tight junction structure and function. Cell Microbiol **8:**1946-1957.
176. **Criss AK, Silva M, Casanova JE, McCormick BA.** 2001. Regulation of Salmonella-induced neutrophil transmigration by epithelial ADP-ribosylation factor 6. J Biol Chem **276:**48431-48439.
177. **Silva M, Song C, Nadeau WJ, Matthews JB, McCormick BA.** 2004. Salmonella typhimurium SipA-induced neutrophil transepithelial migration: involvement of a PKC-alpha-dependent signal transduction pathway. Am J Physiol Gastrointest Liver Physiol **286:**G1024-1031.
178. **Mrsny RJ, Gewirtz AT, Siccardi D, Savidge T, Hurley BP, Madara JL, McCormick BA.** 2004. Identification of hepoxilin A3 in inflammatory events: a required role in neutrophil migration across intestinal epithelia. Proc Natl Acad Sci U S A **101:**7421-7426.
179. **Zhang Y, Higashide WM, McCormick BA, Chen J, Zhou D.** 2006. The inflammation-associated Salmonella SopA is a HECT-like E3 ubiquitin ligase. Mol Microbiol **62:**786-793.
180. **Hersh D, Monack DM, Smith MR, Ghori N, Falkow S, Zychlinsky A.** 1999. The Salmonella invasin SipB induces macrophage apoptosis by binding to caspase-1. Proc Natl Acad Sci U S A **96:**2396-2401.
181. **Norris FA, Wilson MP, Wallis TS, Galyov EE, Majerus PW.** 1998. SopB, a protein required for virulence of Salmonella dublin, is an inositol phosphate phosphatase. Proc Natl Acad Sci U S A **95:**14057-14059.
182. **Haraga A, Miller SI.** 2006. A Salmonella type III secretion effector interacts with the mammalian serine/threonine protein kinase PKN1. Cell Microbiol **8:**837-846.
183. **Haraga A, Miller SI.** 2003. A Salmonella enterica serovar typhimurium translocated leucine-rich repeat effector protein inhibits NF-kappa B-dependent gene expression. Infect Immun **71:**4052-4058.
184. **Lin SL, Le TX, Cowen DS.** 2003. SptP, a Salmonella typhimurium type III-secreted protein, inhibits the mitogen-activated protein kinase pathway by inhibiting Raf activation. Cell Microbiol **5:**267-275.
185. **Murli S, Watson RO, Galan JE.** 2001. Role of tyrosine kinases and the tyrosine phosphatase SptP in the interaction of Salmonella with host cells. Cell Microbiol **3:**795-810.
186. **Li H, Xu H, Zhou Y, Zhang J, Long C, Li S, Chen S, Zhou JM, Shao F.** 2007. The phosphothreonine lyase activity of a bacterial type III effector family. Science **315:**1000-1003.
187. **Mazurkiewicz P, Thomas J, Thompson JA, Liu M, Arbibe L, Sansonetti P, Holden DW.** 2008. SpvC is a Salmonella effector with phosphothreonine lyase activity on host mitogen-activated protein kinases. Mol Microbiol **67:**1371-1383.

188. **Jones RM, Wu H, Wentworth C, Luo L, Collier-Hyams L, Neish AS.** 2008. Salmonella AvrA Coordinates Suppression of Host Immune and Apoptotic Defenses via JNK Pathway Blockade. Cell Host Microbe **3:**233-244.
189. **Liao AP, Petrof EO, Kuppireddi S, Zhao Y, Xia Y, Claud EC, Sun J.** 2008. Salmonella type III effector AvrA stabilizes cell tight junctions to inhibit inflammation in intestinal epithelial cells. PLoS One **3:**e2369.
190. **Lin Z, Zhang YG, Xia Y, Xu X, Jiao X, Sun J.** 2016. Salmonella enteritidis Effector AvrA Stabilizes Intestinal Tight Junctions via the JNK Pathway. J Biol Chem **291:**26837-26849.
191. **Steele-Mortimer O, Meresse S, Gorvel JP, Toh BH, Finlay BB.** 1999. Biogenesis of Salmonella typhimurium-containing vacuoles in epithelial cells involves interactions with the early endocytic pathway. Cell Microbiol **1:**33-49.
192. **Smith AC, Cirulis JT, Casanova JE, Scidmore MA, Brumell JH.** 2005. Interaction of the Salmonella-containing vacuole with the endocytic recycling system. J Biol Chem **280:**24634-24641.
193. **Hernandez LD, Hueffer K, Wenk MR, Galan JE.** 2004. Salmonella modulates vesicular traffic by altering phosphoinositide metabolism. Science **304:**1805-1807.
194. **Mukherjee K, Parashuraman S, Raje M, Mukhopadhyay A.** 2001. SopE acts as an Rab5-specific nucleotide exchange factor and recruits non-prenylated Rab5 on Salmonella-containing phagosomes to promote fusion with early endosomes. J Biol Chem **276:**23607-23615.
195. **Mallo GV, Espina M, Smith AC, Terebiznik MR, Aleman A, Finlay BB, Rameh LE, Grinstein S, Brumell JH.** 2008. SopB promotes phosphatidylinositol 3-phosphate formation on Salmonella vacuoles by recruiting Rab5 and Vps34. J Cell Biol **182:**741-752.
196. **Bujny MV, Ewels PA, Humphrey S, Attar N, Jepson MA, Cullen PJ.** 2008. Sorting nexin-1 defines an early phase of Salmonella-containing vacuole-remodeling during Salmonella infection. J Cell Sci **121:**2027-2036.
197. **Brawn LC, Hayward RD, Koronakis V.** 2007. Salmonella SPI1 effector SipA persists after entry and cooperates with a SPI2 effector to regulate phagosome maturation and intracellular replication. Cell Host Microbe **1:**63-75.
198. **Spano S, Galan JE.** 2012. A Rab32-dependent pathway contributes to Salmonella typhi host restriction. Science **338:**960-963.
199. **Spano S, Liu X, Galan JE.** 2011. Proteolytic targeting of Rab29 by an effector protein distinguishes the intracellular compartments of human-adapted and broad-host Salmonella. Proc Natl Acad Sci U S A **108:**18418-18423.
200. **Brown NF, Rogers LD, Sanderson KL, Gouw JW, Hartland EL, Foster LJ.** 2014. A horizontally acquired transcription factor coordinates Salmonella adaptations to host microenvironments. MBio **5:**e01727-01714.
201. **Garcia-del Portillo F, Finlay BB.** 1995. Targeting of Salmonella typhimurium to vesicles containing lysosomal membrane glycoproteins bypasses compartments with mannose 6-phosphate receptors. J Cell Biol **129:**81-97.
202. **Meresse S, Steele-Mortimer O, Finlay BB, Gorvel JP.** 1999. The rab7 GTPase controls the maturation of Salmonella typhimurium-containing vacuoles in HeLa cells. Embo j **18:**4394-4403.
203. **Brumell JH, Tang P, Mills SD, Finlay BB.** 2001. Characterization of Salmonella-induced filaments (Sifs) reveals a delayed interaction between Salmonella-containing vacuoles and late endocytic compartments. Traffic **2:**643-653.
204. **Catron DM, Sylvester MD, Lange Y, Kadekoppala M, Jones BD, Monack DM, Falkow S, Haldar K.** 2002. The Salmonella-containing vacuole is a major site of

intracellular cholesterol accumulation and recruits the GPI-anchored protein CD55. Cell Microbiol **4:**315-328.

205. **Cirillo DM, Valdivia RH, Monack DM, Falkow S.** 1998. Macrophage-dependent induction of the Salmonella pathogenicity island 2 type III secretion system and its role in intracellular survival. Mol Microbiol **30:**175-188.
206. **Chakravortty D, Rohde M, Jager L, Deiwick J, Hensel M.** 2005. Formation of a novel surface structure encoded by Salmonella Pathogenicity Island 2. Embo j **24:**2043-2052.
207. **Ohlson MB, Huang Z, Alto NM, Blanc MP, Dixon JE, Chai J, Miller SI.** 2008. Structure and function of Salmonella SifA indicate that its interactions with SKIP, SseJ, and RhoA family GTPases induce endosomal tubulation. Cell Host Microbe **4:**434-446.
208. **Henry T, Couillault C, Rockenfeller P, Boucrot E, Dumont A, Schroeder N, Hermant A, Knodler LA, Lecine P, Steele-Mortimer O, Borg JP, Gorvel JP, Meresse S.** 2006. The Salmonella effector protein PipB2 is a linker for kinesin-1. Proc Natl Acad Sci U S A **103:**13497-13502.
209. **Deiwick J, Salcedo SP, Boucrot E, Gilliland SM, Henry T, Petermann N, Waterman SR, Gorvel JP, Holden DW, Meresse S.** 2006. The translocated Salmonella effector proteins SseF and SseG interact and are required to establish an intracellular replication niche. Infect Immun **74:**6965-6972.
210. **Ramsden AE, Mota LJ, Munter S, Shorte SL, Holden DW.** 2007. The SPI-2 type III secretion system restricts motility of Salmonella-containing vacuoles. Cell Microbiol **9:**2517-2529.
211. **Kuhle V, Abrahams GL, Hensel M.** 2006. Intracellular Salmonella enterica redirect exocytic transport processes in a Salmonella pathogenicity island 2-dependent manner. Traffic **7:**716-730.
212. **Miao EA, Brittnacher M, Haraga A, Jeng RL, Welch MD, Miller SI.** 2003. Salmonella effectors translocated across the vacuolar membrane interact with the actin cytoskeleton. Mol Microbiol **48:**401-415.
213. **Poh J, Odendall C, Spanos A, Boyle C, Liu M, Freemont P, Holden DW.** 2008. SteC is a Salmonella kinase required for SPI-2-dependent F-actin remodelling. Cell Microbiol **10:**20-30.
214. **Domingues L, Holden DW, Mota LJ.** 2014. The Salmonella effector SteA contributes to the control of membrane dynamics of Salmonella-containing vacuoles. Infect Immun **82:**2923-2934.
215. **Nawabi P, Catron DM, Haldar K.** 2008. Esterification of cholesterol by a type III secretion effector during intracellular Salmonella infection. Mol Microbiol **68:**173-185.
216. **Stein MA, Leung KY, Zwick M, Garcia-del Portillo F, Finlay BB.** 1996. Identification of a Salmonella virulence gene required for formation of filamentous structures containing lysosomal membrane glycoproteins within epithelial cells. Mol Microbiol **20:**151-164.
217. **Knodler LA, Steele-Mortimer O.** 2005. The Salmonella effector PipB2 affects late endosome/lysosome distribution to mediate Sif extension. Mol Biol Cell **16:**4108-4123.
218. **Jiang X, Rossanese OW, Brown NF, Kujat-Choy S, Galan JE, Finlay BB, Brumell JH.** 2004. The related effector proteins SopD and SopD2 from Salmonella enterica serovar Typhimurium contribute to virulence during systemic infection of mice. Mol Microbiol **54:**1186-1198.

219. **Ruiz-Albert J, Yu XJ, Beuzon CR, Blakey AN, Galyov EE, Holden DW.** 2002. Complementary activities of SseJ and SifA regulate dynamics of the Salmonella typhimurium vacuolar membrane. Mol Microbiol **44:**645-661.
220. **Freeman JA, Ohl ME, Miller SI.** 2003. The Salmonella enterica serovar typhimurium translocated effectors SseJ and SifB are targeted to the Salmonella-containing vacuole. Infect Immun **71:**418-427.
221. **Sun H, Kamanova J, Lara-Tejero M, Galan JE.** 2016. A Family of Salmonella Type III Secretion Effector Proteins Selectively Targets the NF-kappaB Signaling Pathway to Preserve Host Homeostasis. PLoS Pathog **12:**e1005484.
222. **Jennings E, Esposito D, Rittinger K, Thurston TLM.** 2018. Structure-function analyses of the bacterial zinc metalloprotease effector protein GtgA uncover key residues required for deactivating NF-kappaB. J Biol Chem **293:**15316-15329.
223. **Le Negrate G, Faustin B, Welsh K, Loeffler M, Krajewska M, Hasegawa P, Mukherjee S, Orth K, Krajewski S, Godzik A, Guiney DG, Reed JC.** 2008. Salmonella Secreted Factor L Deubiquitinase of Salmonella typhimurium Inhibits NF- B, Suppresses I B Ubiquitination and Modulates Innate Immune Responses. The Journal of Immunology **180:**5045-5056.
224. **Rolhion N, Furniss RC, Grabe G, Ryan A, Liu M, Matthews SA, Holden DW.** 2016. Inhibition of Nuclear Transport of NF-kB p65 by the Salmonella Type III Secretion System Effector SpvD. PLoS Pathog **12:**e1005653.
225. **Grabe GJ, Zhang Y, Przydacz M, Rolhion N, Yang Y, Pruneda JN, Komander D, Holden DW, Hare SA.** 2016. The Salmonella Effector SpvD Is a Cysteine Hydrolase with a Serovar-specific Polymorphism Influencing Catalytic Activity, Suppression of Immune Responses, and Bacterial Virulence. J Biol Chem **291:**25853-25863.
226. **Jaslow SL, Gibbs KD, Fricke WF, Wang L, Pittman KJ, Mammel MK, Thaden JT, Fowler VG, Jr., Hammer GE, Elfenbein JR, Ko DC.** 2018. Salmonella Activation of STAT3 Signaling by SarA Effector Promotes Intracellular Replication and Production of IL-10. Cell Rep **23:**3525-3536.
227. **Pilar AV, Reid-Yu SA, Cooper CA, Mulder DT, Coombes BK.** 2012. GogB is an anti-inflammatory effector that limits tissue damage during Salmonella infection through interaction with human FBXO22 and Skp1. PLoS Pathog **8:**e1002773.
228. **Bhavsar AP, Brown NF, Stoepel J, Wiermer M, Martin DD, Hsu KJ, Imami K, Ross CJ, Hayden MR, Foster LJ, Li X, Hieter P, Finlay BB.** 2013. The Salmonella type III effector SspH2 specifically exploits the NLR co-chaperone activity of SGT1 to subvert immunity. PLoS Pathog **9:**e1003518.
229. **Rao S, Schieber AM, O'Connor CP, Leblanc M, Michel D, Ayres JS.** 2017. Pathogen-Mediated Inhibition of Anorexia Promotes Host Survival and Transmission. Cell **168:**503-516 e512.
230. **McLaughlin LM, Xu H, Carden SE, Fisher S, Reyes M, Heilshorn SC, Monack DM.** 2014. A microfluidic-based genetic screen to identify microbial virulence factors that inhibit dendritic cell migration. Integr Biol (Camb) **6:**438-449.
231. **McLaughlin LM, Govoni GR, Gerke C, Gopinath S, Peng K, Laidlaw G, Chien YH, Jeong HW, Li Z, Brown MD, Sacks DB, Monack D.** 2009. The Salmonella SPI2 effector SseI mediates long-term systemic infection by modulating host cell migration. PLoS Pathog **5:**e1000671.
232. **Halici S, Zenk SF, Jantsch J, Hensel M.** 2008. Functional analysis of the Salmonella pathogenicity island 2-mediated inhibition of antigen presentation in dendritic cells. Infect Immun **76:**4924-4933.

233. **Lapaque N, Hutchinson JL, Jones DC, Meresse S, Holden DW, Trowsdale J, Kelly AP.** 2009. Salmonella regulates polyubiquitination and surface expression of MHC class II antigens. Proc Natl Acad Sci U S A **106:**14052-14057.
234. **Bayer-Santos E, Durkin CH, Rigano LA, Kupz A, Alix E, Cerny O, Jennings E, Liu M, Ryan AS, Lapaque N, Kaufmann SH, Holden DW.** 2016. The Salmonella Effector SteD Mediates MARCH8-Dependent Ubiquitination of MHC II Molecules and Inhibits T Cell Activation. Cell Host Microbe **20:**584-595.
235. **Niemann GS, Brown RN, Gustin JK, Stufkens A, Shaikh-Kidwai AS, Li J, McDermott JE, Brewer HM, Schepmoes A, Smith RD, Adkins JN, Heffron F.** 2011. Discovery of novel secreted virulence factors from Salmonella enterica serovar Typhimurium by proteomic analysis of culture supernatants. Infect Immun **79:**33-43.
236. **Uchiya K, Barbieri MA, Funato K, Shah AH, Stahl PD, Groisman EA.** 1999. A Salmonella virulence protein that inhibits cellular trafficking. Embo j **18:**3924-3933.
237. **Shotland Y, Kramer H, Groisman EA.** 2003. The Salmonella SpiC protein targets the mammalian Hook3 protein function to alter cellular trafficking. Mol Microbiol **49:**1565-1576.
238. **Freeman JA, Rappl C, Kuhle V, Hensel M, Miller SI.** 2002. SpiC Is Required for Translocation of Salmonella Pathogenicity Island 2 Effectors and Secretion of Translocon Proteins SseB and SseC. Journal of Bacteriology **184:**4971-4980.
239. **Habyarimana F, Sabag-Daigle A, Ahmer BM.** 2014. The SdiA-regulated gene srgE encodes a type III secreted effector. J Bacteriol **196:**2301-2312.
240. **Cordero-Alba M, Bernal-Bayard J, Ramos-Morales F.** 2012. SrfJ, a Salmonella type III secretion system effector regulated by PhoP, RcsB, and IolR. J Bacteriol **194:**4226-4236.
241. **Knodler LA, Vallance BA, Hensel M, Jäckel D, Finlay BB, Steele-Mortimer O.** 2003. Salmonella type III effectors PipB and PipB2 are targeted to detergent-resistant microdomains on internal host cell membranes. Molecular microbiology **49:**685-704.
242. **Kujat Choy SL, Boyle EC, Gal-Mor O, Goode DL, Valdez Y, Vallance BA, Finlay BB.** 2004. SseK1 and SseK2 are novel translocated proteins of Salmonella enterica serovar typhimurium. Infect Immun **72:**5115-5125.
243. **Brown NF, Coombes BK, Bishop JL, Wickham ME, Lowden MJ, Gal-Mor O, Goode DL, Boyle EC, Sanderson KL, Finlay BB.** 2011. Salmonella phage ST64B encodes a member of the SseK/NleB effector family. PLoS One **6:**e17824.
244. **Pearson JS, Giogha C, Ong SY, Kennedy CL, Kelly M, Robinson KS, Lung TW, Mansell A, Riedmaier P, Oates CV, Zaid A, Muhlen S, Crepin VF, Marches O, Ang CS, Williamson NA, O'Reilly LA, Bankovacki A, Nachbur U, Infusini G, Webb AI, Silke J, Strasser A, Frankel G, Hartland EL.** 2013. A type III effector antagonizes death receptor signalling during bacterial gut infection. Nature **501:**247-251.
245. **Li S, Zhang L, Yao Q, Li L, Dong N, Rong J, Gao W, Ding X, Sun L, Chen X, Chen S, Shao F.** 2013. Pathogen blocks host death receptor signalling by arginine GlcNAcylation of death domains. Nature **501:**242-246.
246. **Kidwai AS, Mushamiri I, Niemann GS, Brown RN, Adkins JN, Heffron F.** 2013. Diverse secreted effectors are required for Salmonella persistence in a mouse infection model. PLoS One **8:**e70753.
247. **Lawley TD, Chan K, Thompson LJ, Kim CC, Govoni GR, Monack DM.** 2006. Genome-wide screen for Salmonella genes required for long-term systemic infection of the mouse. PLoS Pathog **2:**e11.
248. **Buckner MMC, Croxen M, Arena ET, Finlay BB.** 2014. A comprehensive study of the contribution ofSalmonella entericaserovar Typhimurium SPI2 effectors to

bacterial colonization, survival, and replication in typhoid fever, macrophage, and epithelial cell infection models. Virulence **2:**208-216.

249. **Frankel G, Phillips AD, Rosenshine I, Dougan G, Kaper JB, Knutton S.** 1998. Enteropathogenic and enterohaemorrhagic Escherichia coli: more subversive elements. Mol Microbiol **30:**911-921.
250. **Wong AR, Pearson JS, Bright MD, Munera D, Robinson KS, Lee SF, Frankel G, Hartland EL.** 2011. Enteropathogenic and enterohaemorrhagic Escherichia coli: even more subversive elements. Mol Microbiol **80:**1420-1438.
251. **Chinnaiyan AM, O'Rourke K, Tewari M, Dixit VM.** 1995. FADD, a novel death domain-containing protein, interacts with the death domain of Fas and initiates apoptosis. Cell **81:**505-512.
252. **Nadler C, Baruch K, Kobi S, Mills E, Haviv G, Farago M, Alkalay I, Bartfeld S, Meyer TF, Ben-Neriah Y, Rosenshine I.** 2010. The type III secretion effector NleE inhibits NF-kappaB activation. PLoS Pathog **6:**e1000743.
253. **Newton HJ, Pearson JS, Badea L, Kelly M, Lucas M, Holloway G, Wagstaff KM, Dunstone MA, Sloan J, Whisstock JC, Kaper JB, Robins-Browne RM, Jans DA, Frankel G, Phillips AD, Coulson BS, Hartland EL.** 2010. The type III effectors NleE and NleB from enteropathogenic E. coli and OspZ from Shigella block nuclear translocation of NF-kappaB p65. PLoS Pathog **6:**e1000898.
254. **Ruchaud-Sparagano MH, Muhlen S, Dean P, Kenny B.** 2011. The enteropathogenic E. coli (EPEC) Tir effector inhibits NF-kappaB activity by targeting TNFalpha receptor-associated factors. PLoS Pathog **7:**e1002414.
255. **Liu J, Mushegian A.** 2003. Three monophyletic superfamilies account for the majority of the known glycosyltransferases. Protein Sci **12:**1418-1431.
256. **Gao X, Wang X, Pham TH, Feuerbacher LA, Lubos ML, Huang M, Olsen R, Mushegian A, Slawson C, Hardwidge PR.** 2013. NleB, a bacterial effector with glycosyltransferase activity, targets GAPDH function to inhibit NF-kappaB activation. Cell Host Microbe **13:**87-99.
257. **Wertz IE, Dixit VM.** 2010. Regulation of death receptor signaling by the ubiquitin system. Cell Death Differ **17:**14-24.
258. **Silke J.** 2011. The regulation of TNF signalling: what a tangled web we weave. Curr Opin Immunol **23:**620-626.
259. **Micheau O, Tschopp J.** 2003. Induction of TNF Receptor I-Mediated Apoptosis via Two Sequential Signaling Complexes. Cell **114:**181-190.
260. **Vandenabeele P, Galluzzi L, Vanden Berghe T, Kroemer G.** 2010. Molecular mechanisms of necroptosis: an ordered cellular explosion. Nat Rev Mol Cell Biol **11:**700-714.
261. **Hsu H, Xiong J, Goeddel DV.** 1995. The TNF receptor 1-associated protein TRADD signals cell death and NF-kappa B activation. Cell **81:**495-504.
262. **Pan G, O'Rourke K, Chinnaiyan AM, Gentz R, Ebner R, Ni J, Dixit VM.** 1997. The receptor for the cytotoxic ligand TRAIL. Science **276:**111-113.
263. **Walczak H, Degli-Esposti MA, Johnson RS, Smolak PJ, Waugh JY, Boiani N, Timour MS, Gerhart MJ, Schooley KA, Smith CA, Goodwin RG, Rauch CT.** 1997. TRAIL-R2: a novel apoptosis-mediating receptor for TRAIL. Embo j **16:**5386-5397.
264. **Sheridan JP, Marsters SA, Pitti RM, Gurney A, Skubatch M, Baldwin D, Ramakrishnan L, Gray CL, Baker K, Wood WI, Goddard AD, Godowski P, Ashkenazi A.** 1997. Control of TRAIL-induced apoptosis by a family of signaling and decoy receptors. Science **277:**818-821.

265. **Marsters SA, Sheridan JP, Pitti RM, Huang A, Skubatch M, Baldwin D, Yuan J, Gurney A, Goddard AD, Godowski P, Ashkenazi A.** 1997. A novel receptor for Apo2L/TRAIL contains a truncated death domain. Curr Biol **7:**1003-1006.
266. **von Karstedt S, Montinaro A, Walczak H.** 2017. Exploring the TRAILs less travelled: TRAIL in cancer biology and therapy. Nat Rev Cancer **17:**352-366.
267. **Kischkel FC, Lawrence DA, Chuntharapai A, Schow P, Kim KJ, Ashkenazi A.** 2000. Apo2L/TRAIL-dependent recruitment of endogenous FADD and caspase-8 to death receptors 4 and 5. Immunity **12:**611-620.
268. **Sprick MR, Weigand MA, Rieser E, Rauch CT, Juo P, Blenis J, Krammer PH, Walczak H.** 2000. FADD/MORT1 and caspase-8 are recruited to TRAIL receptors 1 and 2 and are essential for apoptosis mediated by TRAIL receptor 2. Immunity **12:**599-609.
269. **Lafont E, Hartwig T, Walczak H.** 2018. Paving TRAIL's Path with Ubiquitin. Trends Biochem Sci **43:**44-60.
270. **Jouan-Lanhouet S, Arshad MI, Piquet-Pellorce C, Martin-Chouly C, Le Moigne-Muller G, Van Herreweghe F, Takahashi N, Sergent O, Lagadic-Gossmann D, Vandenabeele P, Samson M, Dimanche-Boitrel MT.** 2012. TRAIL induces necroptosis involving RIPK1/RIPK3-dependent PARP-1 activation. Cell Death Differ **19:**2003-2014.
271. **Hoiseth SK, Stocker BAD.** 1981. Aromatic-dependent Salmonella typhimurium are non-virulent and effective as live vaccines. Nature **291:**238-239.
272. **Strugnell R, Dougan G, Chatfield S, Charles I, Fairweather N, Tite J, Li JL, Beesley J, Roberts M.** 1992. Characterization of a Salmonella typhimurium aro vaccine strain expressing the P.69 antigen of Bordetella pertussis. Infection and Immunity **60:**3994-4002.
273. **Hanahan D.** 1983. Studies on transformation of Escherichia coli with plasmids. J Mol Biol **166:**557-580.
274. **Hoiseth SK, Stocker BA.** 1981. Aromatic-dependent Salmonella typhimurium are non-virulent and effective as live vaccines. Nature **291:**238-239.
275. **Strugnell R, Dougan G, Chatfield S, Charles I, Fairweather N, Tite J, Li JL, Beesley J, Roberts M.** 1992. Characterization of a Salmonella typhimurium aro vaccine strain expressing the P.69 antigen of Bordetella pertussis. Infect Immun **60:**3994-4002.
276. **Wong Fok Lung T.** 2015. Characterisation of a family of novel glycosyltransferases from enteropathogenic Escherichia coli and SalmonellaUniversity of Melbourne.
277. **Nordgard O, Dahle O, Andersen TO, Gabrielsen OS.** 2001. JAB1/CSN5 interacts with the GAL4 DNA binding domain: a note of caution about two-hybrid interactions. Biochimie **83:**969-971.
278. **Domingues L, Ismail A, Charro N, Rodriguez-Escudero I, Holden DW, Molina M, Cid VJ, Mota LJ.** 2016. The Salmonella effector SteA binds phosphatidylinositol 4-phosphate for subcellular targeting within host cells. Cell Microbiol **18:**949-969.
279. **Myeni S, Child R, Ng TW, Kupko JJ, 3rd, Wehrly TD, Porcella SF, Knodler LA, Celli J.** 2013. Brucella modulates secretory trafficking via multiple type IV secretion effector proteins. PLoS Pathog **9:**e1003556.
280. **Yang Z, Soderholm A, Lung TW, Giogha C, Hill MM, Brown NF, Hartland E, Teasdale RD.** 2015. SseK3 Is a Salmonella Effector That Binds TRIM32 and Modulates the Host's NF-kappaB Signalling Activity. PLoS One **10:**e0138529.
281. **Alto NM, Shao F, Lazar CS, Brost RL, Chua G, Mattoo S, McMahon SA, Ghosh P, Hughes TR, Boone C, Dixon JE.** 2006. Identification of a bacterial type III effector family with G protein mimicry functions. Cell **124:**133-145.

282. **Bhattacharjee RN, Park KS, Kumagai Y, Okada K, Yamamoto M, Uematsu S, Matsui K, Kumar H, Kawai T, Iida T, Honda T, Takeuchi O, Akira S.** 2006. VP1686, a Vibrio type III secretion protein, induces toll-like receptor-independent apoptosis in macrophage through NF-kappaB inhibition. J Biol Chem **281:**36897-36904.
283. **Ilardi JM, Mochida S, Sheng ZH.** 1999. Snapin: a SNARE-associated protein implicated in synaptic transmission. Nat Neurosci **2:**119-124.
284. **Starcevic M, Dell'Angelica EC.** 2004. Identification of snapin and three novel proteins (BLOS1, BLOS2, and BLOS3/reduced pigmentation) as subunits of biogenesis of lysosome-related organelles complex-1 (BLOC-1). J Biol Chem **279:**28393-28401.
285. **Shi B, Huang QQ, Birkett R, Doyle R, Dorfleutner A, Stehlik C, He C, Pope RM.** 2017. SNAPIN is critical for lysosomal acidification and autophagosome maturation in macrophages. Autophagy **13:**285-301.
286. **Oakley AJ.** 2005. Glutathione transferases: new functions. Curr Opin Struct Biol **15:**716-723.
287. **Vasieva O.** 2011. The many faces of glutathione transferase pi. Curr Mol Med **11:**129-139.
288. **Frova C.** 2006. Glutathione transferases in the genomics era: new insights and perspectives. Biomol Eng **23:**149-169.
289. **Gurioli G, Martignano F, Salvi S, Costantini M, Gunelli R, Casadio V.** 2018. GSTP1 methylation in cancer: a liquid biopsy biomarker? Clin Chem Lab Med **56:**702-717.
290. **Akhtar S, Mahjabeen I, Akram Z, Kayani MA.** 2016. CYP1A1 and GSTP1 gene variations in breast cancer: a systematic review and case-control study. Fam Cancer **15:**201-214.
291. **Singh S.** 2015. Cytoprotective and regulatory functions of glutathione S-transferases in cancer cell proliferation and cell death. Cancer Chemother Pharmacol **75:**1-15.
292. **Adler V, Yin Z, Fuchs SY, Benezra M, Rosario L, Tew KD, Pincus MR, Sardana M, Henderson CJ, Wolf CR, Davis RJ, Ronai Z.** 1999. Regulation of JNK signaling by GSTp. Embo j **18:**1321-1334.
293. **Wu Y, Fan Y, Xue B, Luo L, Shen J, Zhang S, Jiang Y, Yin Z.** 2006. Human glutathione S-transferase P1-1 interacts with TRAF2 and regulates TRAF2-ASK1 signals. Oncogene **25:**5787-5800.
294. **Smith CD, Carson M, Friedman AM, Skinner MM, Delucas L, Chantalat L, Weise L, Shirasawa T, Chattopadhyay D.** 2002. Crystal structure of human L-isoaspartyl-O-methyl-transferase with S-adenosyl homocysteine at 1.6-A resolution and modeling of an isoaspartyl-containing peptide at the active site. Protein Sci **11:**625-635.
295. **Johnson BA, Murray ED, Jr., Clarke S, Glass DB, Aswad DW.** 1987. Protein carboxyl methyltransferase facilitates conversion of atypical L-isoaspartyl peptides to normal L-aspartyl peptides. J Biol Chem **262:**5622-5629.
296. **Wong Fok Lung T, Giogha C, Creuzburg K, Ong SY, Pollock GL, Zhang Y, Fung KY, Pearson JS, Hartland EL.** 2016. Mutagenesis and Functional Analysis of the Bacterial Arginine Glycosyltransferase Effector NleB1 from Enteropathogenic Escherichia coli. Infect Immun **84:**1346-1360.
297. **Lairson LL, Henrissat B, Davies GJ, Withers SG.** 2008. Glycosyltransferases: structures, functions, and mechanisms. Annu Rev Biochem **77:**521-555.
298. **Breton C, Snajdrova L, Jeanneau C, Koca J, Imberty A.** 2006. Structures and mechanisms of glycosyltransferases. Glycobiology **16:**29r-37r.

299. **Pan M, Li S, Li X, Shao F, Liu L, Hu HG.** 2014. Synthesis of and specific antibody generation for glycopeptides with arginine N-GlcNAcylation. Angew Chem Int Ed Engl **53:**14517-14521.
300. **Peterson AC, Russell JD, Bailey DJ, Westphall MS, Coon JJ.** 2012. Parallel reaction monitoring for high resolution and high mass accuracy quantitative, targeted proteomics. Mol Cell Proteomics **11:**1475-1488.
301. **Benetatos CA, Mitsuuchi Y, Burns JM, Neiman EM, Condon SM, Yu G, Seipel ME, Kapoor GS, Laporte MG, Rippin SR, Deng Y, Hendi MS, Tirunahari PK, Lee YH, Haimowitz T, Alexander MD, Graham MA, Weng D, Shi Y, McKinlay MA, Chunduru SK.** 2014. Birinapant (TL32711), a bivalent SMAC mimetic, targets TRAF2-associated cIAPs, abrogates TNF-induced NF-kappaB activation, and is active in patient-derived xenograft models. Mol Cancer Ther **13:**867-879.
302. **Allensworth JL, Sauer SJ, Lyerly HK, Morse MA, Devi GR.** 2013. Smac mimetic Birinapant induces apoptosis and enhances TRAIL potency in inflammatory breast cancer cells in an IAP-dependent and TNF-alpha-independent mechanism. Breast Cancer Res Treat **137:**359-371.
303. **Belyi Y, Aktories K.** 2010. Bacterial toxin and effector glycosyltransferases. Biochim Biophys Acta **1800:**134-143.
304. **Carter GP, Rood JI, Lyras D.** 2012. The role of toxin A and toxin B in the virulence of Clostridium difficile. Trends Microbiol **20:**21-29.
305. **Voth DE, Ballard JD.** 2005. Clostridium difficile toxins: mechanism of action and role in disease. Clin Microbiol Rev **18:**247-263.
306. **Belyi Y, Jank T, Aktories K.** 2013. Cytotoxic glucosyltransferases of Legionella pneumophila. Curr Top Microbiol Immunol **376:**211-226.
307. **Wang Z, McCloskey A, Cheng S, Wu M, Xue C, Yu Z, Fu J, Liu Y, Luo ZQ, Liu X.** 2018. Regulation of the small GTPase Rab1 function by a bacterial glucosyltransferase. Cell Discov **4:**53.
308. **Bavelloni A, Piazzi M, Raffini M, Faenza I, Blalock WL.** 2015. Prohibitin 2: At a communications crossroads. IUBMB Life **67:**239-254.
309. **Sharma A, Qadri A.** 2004. Vi polysaccharide of Salmonella typhi targets the prohibitin family of molecules in intestinal epithelial cells and suppresses early inflammatory responses. Proc Natl Acad Sci U S A **101:**17492-17497.
310. **Santhanam SK, Dutta D, Parween F, Qadri A.** 2014. The virulence polysaccharide Vi released by Salmonella Typhi targets membrane prohibitin to inhibit T-cell activation. J Infect Dis **210:**79-88.
311. **Gunning PW, Schevzov G, Kee AJ, Hardeman EC.** 2005. Tropomyosin isoforms: divining rods for actin cytoskeleton function. Trends Cell Biol **15:**333-341.
312. **Aitken A.** 2006. 14-3-3 proteins: a historic overview. Semin Cancer Biol **16:**162-172.
313. **Lu S, Killoran PB, Fang FC, Riley LW.** 2002. The global regulator ArcA controls resistance to reactive nitrogen and oxygen intermediates in Salmonella enterica serovar Enteritidis. Infect Immun **70:**451-461.
314. **Gunster RA, Matthews SA, Holden DW, Thurston TL.** 2017. SseK1 and SseK3 Type III Secretion System Effectors Inhibit NF-kappaB Signaling and Necroptotic Cell Death in Salmonella-Infected Macrophages. Infect Immun **85**.
315. **El Qaidi S, Chen K, Halim A, Siukstaite L, Rueter C, Hurtado-Guerrero R, Clausen H, Hardwidge PR.** 2017. NleB/SseK effectors from Citrobacter rodentium, Escherichia coli, and Salmonella enterica display distinct differences in host substrate specificity. J Biol Chem **292:**11423-11430.
316. **Aggarwal BB.** 2003. Signalling pathways of the TNF superfamily: a double-edged sword. Nat Rev Immunol **3:**745-756.

317. **Hartwig T, Montinaro A, von Karstedt S, Sevko A, Surinova S, Chakravarthy A, Taraborrelli L, Draber P, Lafont E, Arce Vargas F, El-Bahrawy MA, Quezada SA, Walczak H.** 2017. The TRAIL-Induced Cancer Secretome Promotes a Tumor-Supportive Immune Microenvironment via CCR2. Mol Cell **65:**730-742 e735.
318. **Ting AT, Bertrand MJM.** 2016. More to Life than NF-kappaB in TNFR1 Signaling. Trends Immunol **37:**535-545.
319. **Hayden MS, Ghosh S.** 2008. Shared principles in NF-kappaB signaling. Cell **132:**344-362.
320. **Stewart MK, Cookson BT.** 2016. Evasion and interference: intracellular pathogens modulate caspase-dependent inflammatory responses. Nat Rev Microbiol **14:**346-359.
321. **LaRock CN, Cookson BT.** 2012. The Yersinia virulence effector YopM binds caspase-1 to arrest inflammasome assembly and processing. Cell Host Microbe **12:**799-805.
322. **Kobayashi T, Ogawa M, Sanada T, Mimuro H, Kim M, Ashida H, Akakura R, Yoshida M, Kawalec M, Reichhart JM, Mizushima T, Sasakawa C.** 2013. The Shigella OspC3 effector inhibits caspase-4, antagonizes inflammatory cell death, and promotes epithelial infection. Cell Host Microbe **13:**570-583.
323. **Wertz IE, Dixit VM.** 2008. Ubiquitin-mediated regulation of TNFR1 signaling. Cytokine Growth Factor Rev **19:**313-324.
324. **Stenner-Liewen F, Liewen H, Zapata JM, Pawlowski K, Godzik A, Reed JC.** 2002. CADD, a Chlamydia protein that interacts with death receptors. J Biol Chem **277:**9633-9636.
325. **Schwarzenbacher R, Stenner-Liewen F, Liewen H, Robinson H, Yuan H, Bossy-Wetzel E, Reed JC, Liddington RC.** 2004. Structure of the Chlamydia protein CADD reveals a redox enzyme that modulates host cell apoptosis. J Biol Chem **279:**29320-29324.
326. **Lin WC, Tsai HF, Liao HJ, Tang CH, Wu YY, Hsu PI, Cheng AL, Hsu PN.** 2014. Helicobacter pylori sensitizes TNF-related apoptosis-inducing ligand (TRAIL)-mediated apoptosis in human gastric epithelial cells through regulation of FLIP. Cell Death Dis **5:**e1109.
327. **Diehl GE, Yue HH, Hsieh K, Kuang AA, Ho M, Morici LA, Lenz LL, Cado D, Riley LW, Winoto A.** 2004. TRAIL-R as a negative regulator of innate immune cell responses. Immunity **21:**877-889.
328. **Malek M, Lamont SJ.** 2003. Association of INOS, TRAIL, TGF-beta2, TGF-beta3, and IgL genes with response to Salmonella enteritidis in poultry. Genet Sel Evol **35 Suppl 1:**S99-111.
329. **Tohidi R, Idris IB, Malar Panandam J, Hair Bejo M.** 2013. The effects of polymorphisms in 7 candidate genes on resistance to Salmonella Enteritidis in native chickens. Poult Sci **92:**900-909.
330. **Everest P, Roberts M, Dougan G.** 1998. Susceptibility to Salmonella typhimurium infection and effectiveness of vaccination in mice deficient in the tumor necrosis factor alpha p55 receptor. Infect Immun **66:**3355-3364.
331. **Mastroeni P, Arena A, Costa GB, Liberto MC, Bonina L, Hormaeche CE.** 1991. Serum TNF alpha in mouse typhoid and enhancement of a Salmonella infection by anti-TNF alpha antibodies. Microb Pathog **11:**33-38.
332. **Mastroeni P, Villarreal-Ramos B, Hormaeche CE.** 1992. Role of T cells, TNF alpha and IFN gamma in recall of immunity to oral challenge with virulent salmonellae in mice vaccinated with live attenuated aro- Salmonella vaccines. Microb Pathog **13:**477-491.

333. **Vazquez-Torres A, Fantuzzi G, Edwards CK, 3rd, Dinarello CA, Fang FC.** 2001. Defective localization of the NADPH phagocyte oxidase to Salmonella-containing phagosomes in tumor necrosis factor p55 receptor-deficient macrophages. Proc Natl Acad Sci U S A **98:**2561-2565.
334. **Raupach B, Kurth N, Pfeffer K, Kaufmann SH.** 2003. Salmonella typhimurium strains carrying independent mutations display similar virulence phenotypes yet are controlled by distinct host defense mechanisms. J Immunol **170:**6133-6140.
335. **Sundquist M, Wick MJ.** 2009. Salmonella induces death of CD8alpha(+) dendritic cells but not CD11c(int)CD11b(+) inflammatory cells in vivo via MyD88 and TNFR1. J Leukoc Biol **85:**225-234.
336. **Vazquez-Torres A, Xu Y, Jones-Carson J, Holden DW, Lucia SM, Dinauer MC, Mastroeni P, Fang FC.** 2000. Salmonella pathogenicity island 2-dependent evasion of the phagocyte NADPH oxidase. Science **287:**1655-1658.
337. **Stenmark H.** 2009. Rab GTPases as coordinators of vesicle traffic. Nat Rev Mol Cell Biol **10:**513-525.
338. **Hutagalung AH, Novick PJ.** 2011. Role of Rab GTPases in membrane traffic and cell physiology. Physiol Rev **91:**119-149.
339. **Spano S, Galan JE.** 2017. Taking control: Hijacking of Rab GTPases by intracellular bacterial pathogens. Small GTPases doi:10.1080/21541248.2017.1336192**:**1-10.
340. **Weber MM, Faris R.** 2018. Subversion of the Endocytic and Secretory Pathways by Bacterial Effector Proteins. Front Cell Dev Biol **6:**1.
341. **Kagan JC, Stein MP, Pypaert M, Roy CR.** 2004. Legionella subvert the functions of Rab1 and Sec22b to create a replicative organelle. J Exp Med **199:**1201-1211.
342. **Derre I, Isberg RR.** 2004. Legionella pneumophila replication vacuole formation involves rapid recruitment of proteins of the early secretory system. Infect Immun **72:**3048-3053.
343. **Huang J, Birmingham CL, Shahnazari S, Shiu J, Zheng YT, Smith AC, Campellone KG, Heo WD, Gruenheid S, Meyer T, Welch MD, Ktistakis NT, Kim PK, Klionsky DJ, Brumell JH.** 2011. Antibacterial autophagy occurs at PI(3)P-enriched domains of the endoplasmic reticulum and requires Rab1 GTPase. Autophagy **7:**17-26.
344. **Feng ZZ, Jiang AJ, Mao AW, Feng Y, Wang W, Li J, Zhang X, Xing K, Peng X.** 2018. The Salmonella effectors SseF and SseG inhibit Rab1A-mediated autophagy to facilitate intracellular bacterial survival and replication. J Biol Chem **293:**9662-9673.
345. **Bakowski MA, Braun V, Lam GY, Yeung T, Heo WD, Meyer T, Finlay BB, Grinstein S, Brumell JH.** 2010. The phosphoinositide phosphatase SopB manipulates membrane surface charge and trafficking of the Salmonella-containing vacuole. Cell Host Microbe **7:**453-462.
346. **Ku B, Lee KH, Park WS, Yang CS, Ge J, Lee SG, Cha SS, Shao F, Heo WD, Jung JU, Oh BH.** 2012. VipD of Legionella pneumophila targets activated Rab5 and Rab22 to interfere with endosomal trafficking in macrophages. PLoS Pathog **8:**e1003082.
347. **Broz P, Dixit VM.** 2016. Inflammasomes: mechanism of assembly, regulation and signalling. Nat Rev Immunol **16:**407-420.
348. **Ruby T, McLaughlin L, Gopinath S, Monack D.** 2012. Salmonella's long-term relationship with its host. FEMS Microbiol Rev **36:**600-615.
349. **Baumler AJ, Sperandio V.** 2016. Interactions between the microbiota and pathogenic bacteria in the gut. Nature **535:**85-93.
350. **Park JB, Kim YH, Yoo Y, Kim J, Jun SH, Cho JW, El Qaidi S, Walpole S, Monaco S, Garcia-Garcia AA, Wu M, Hays MP, Hurtado-Guerrero R, Angulo J,**

Hardwidge PR, Shin JS, Cho HS. 2018. Structural basis for arginine glycosylation of host substrates by bacterial effector proteins. Nat Commun **9:**4283.